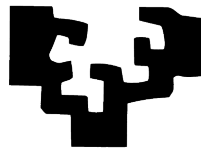


eman ta zabal zazu



Universidad
del País Vasco Euskal Herriko
Unibertsitatea

Universidad del País Vasco
Facultad de Medicina y Odontología
Departamento de Fisiología

New Oncogenic Drivers in Hepatocellular Carcinoma: Role of the RNA Binding Protein Hu antigen R

Tesis doctoral para optar al grado de Doctor, presentada por:

David Fernández Ramos

2012

Directores de tesis:

María Luz Martínez Chantar

José M. Mato



CIC bioGUNE
Unidad de Metabolómica



CIBERehd Centro de Investigación
Biomédica en Red de Enfermedades
Hepáticas y Digestivas



Portada: Paraffin sections of formalin-fixed paraffin-embedded human hepatocarcinomas from different etiologies were stained to measure Mdm2 and HuR protein levels. The patients presented alcoholic steatohepatitis (ASH), non-alcoholic steatohepatitis (NASH) and Hepatitis C.

Esta tesis doctoral ha sido realizada gracias al disfrute de una beca Predoctoral de Formación en Investigación en Salud (PFIS) del Instituto de Salud Carlos III (Orden SCO/523/2008) durante el periodo 2008-2012.

El trabajo experimental ha sido financiado por los siguientes proyectos: NIH grants: AT-1576 y AT004896; Plan Nacional de I+D: SAF 2005-00855 and SAF 2008-04800; HEPADIP-EULSHM-CT-205; ETORTEK 2008, 2009 and 2011; Fundación “La Caixa”; CIBERehd del fondo de Investigación Sanitaria del Instituto de Salud Carlos III; Sanidad del Gobierno Vasco 2009; Educación del Gobierno Vasco 2011; FIS PI11/01588.

ACKNOWLEDGEMENTS/AGRADECIMIENTOS

Dijo John Lennon que “La vida es aquello que te va sucediendo mientras estás ocupado haciendo otros planes”, y creo que expresa bastante bien cómo he llegado hasta aquí.

Cuando decidí hacer un Máster tras acabar la carrera, sin tener muy claro qué hacer con mi vida después, no sabía que una de las clases, la que impartieron José María Mato y Juanma, me haría interesarme por hacer las prácticas en el laboratorio de Malu. Y allí me presenté, por sorpresa, sólo una semana antes de empezar. Afortunadamente Malu me aceptó en su grupo sin mucho problema (siempre hacen falta manos), y tan a gusto estuve esos cuatro meses que al final decidí hacer la tesis. No me arrepiento, Malu ha sido una directora estupenda, durilla pero siempre cercana y comprensiva.

Recuerdo perfectamente que en mi primer día Mercedes me abrió la puerta, a pesar de que con el despiste que llevaba no fui capaz de encontrar el timbre. Más adelante me enseñaría algunas de las técnicas estrella del laboratorio, que yo he intentado transmitir lo mejor que he podido. Y no me olvido de su amistad y de esas empanadas de chocos que traía de vez en cuando.

Nuria fue quien me enseñó a dar los primeros pasos por el laboratorio. Trabajadora nata y con muy buena cabeza para la ciencia. Siempre con su humor absurdo, muy de Muchachada Nui (las pastillacas de Hulk Hogan), y dando vidilla al laboratorio.

Empecé a trabajar con Marta recién llegada de Londres. Aprendí muchísimo con ella mientras nos volvíamos un poco locos con el paper de regeneración. Eso sí, parecía que llegaba un huracán cuando entraba a cultivos directa del animalario. Además, con ella tuvimos en el laboratorio el primer capítulo de la “Aproximación a la maternidad”, jeje.

Con Marta nos llegó también Ashwin con sus células de Schwann, en un mundo de hígados. Siempre transmitiendo tranquilidad, y, yo creo que no muy lejos del niño feliz de la foto de la puerta. Ahora todo un padrazo, quien lo diría después de haberle visto en la fiesta de Navidad en Doností.

El grupo de Malu siguió creciendo, y recibimos a Naiara, la “princesita de Alemania” como diría Nuria. Amante de la Becks y el chocolate Lindt, aun siendo giputxi tuvo que soportar que la envolvíramos con la bandera del Athletic. Con ella pudimos disfrutar de la “Aproximación a la maternidad II”, que nos sirvió de recordatorio y ampliación de conocimientos...

En la última recta de mi tesis estuve trabajando con Nieves, a veces un poco nerviosa, pero muy comprensiva. Aprendí mucho con ella, y lo que nos costó acabar el artículo con tantos experimentos de histidinas... Además, con una paciencia infinita para aguantarnos las bromas de UCLA (IU SI EL EI).

Cargado de choricillos y cecina vino Juan desde León. Aunque al principio parecía timidillo, eso le duró poco, y enseguida empezó a tocar el organillo de Camelà en el laboratorio. Quién se iba a imaginar que siendo leonés supiera todas las canciones de BTX. Una cosa que me ha quedado clara con él es que “Toooooos somos de Leooooón, contentos de ser de aquí...”. Un muy buen amigo.

Cuando Ashwin buscó estudiante apareció Marta Txiki (era raro que Nuria no cambiara el nombre de alguien). Nada que ver con lo que se podía esperar de la MD. Trabajadora, lista y muy alegre. Lo que no sé es dónde mete todo lo que come... Últimamente se nos ha vuelto un poco churfer, pero se lo perdonaremos.

Sara entró a hacer las prácticas de técnico con nosotros, y nos ganó a todos a base de trabajo... y empanadas. También nos hizo de guía en fiestas de Basauri... Sigo sin saber si sabía muy bien en qué lío se estaba metiendo cuando vino al labo, pero parece que no lo lleva nada mal.

Una de las últimas incorporaciones fue Lucía, aunque ahora pensándolo parece que lleva toda la vida con nosotros. Siempre feliz y dando buen rollo al laboratorio. Poca gente se integra tan fácil como ella, que a los 5 días estaba tomando algo por ahí con nosotros y a los pocos meses intentando que aprendiera a girar con esquís (no hubo manera).

De las más antiguas en el labo, pero de las más jóvenes de corazón, Gotxi es el pilar fundamental del laboratorio. Difícil imaginar estos años sin ella, tantos buenos momentos, fiestas, también despedidas. Toda una vida, incluidos los momentos de la adopción. Además, es la responsable del hilo musical del laboratorio, que se ha convertido en la banda sonora de esta tesis.

Aunque suene raro, gracias a la crisis tuvimos la suerte de que Vir acabara en nuestro laboratorio. Con las miles de tinciones que nos tiene que hacer, no me extraña que tenga un cierto humor negro. Muchas gracias por la camiseta de Duff, la uso siempre que puedo.

Fer lleva poco con nosotros pero es un viejo conocido. Se ha encargado de mantener caliente algún proyecto que yo empecé, y hace lo que puede por nuestros derechos en el comité. Además es muy buena gente, para ser de Sestao...

Compartiendo el espacio (cada vez más escaso) del laboratorio tenemos a la gente del grupo de Juanma, no tan grande en cantidad como el de Malu, pero de una gran calidad:

El primero de todos Javi, que entró a hacer la tesis al mismo tiempo que yo. Catalán pero nada agarrado, rompiendo los estereotípos, compartimos el espacio vital durante mucho tiempo. Un amigo con el que hablar de lo que sea, menos de los Athletic-Barça, que siempre teníamos bronca.

La serenidad personificada en Espe, con su aura un poco Zen ayudando a que no se nos vaya de las manos la locura que a veces es el laboratorio. Siempre con un buen consejo en los labios, y, además, aficionada a la música de Extremoduro.

Para llenar el hueco que dejó Javi cuando marchó a Texas vino Laura. Recuerdo que Javi se desesperaba al principio enseñándole técnicas, pero ha demostrado que está a la altura. No sé si las centrífugas opinarán lo mismo... Un lujo poder darme la vuelta en el labo y hablar con ella, aunque ese gusto por Camela...

Con su buen gusto musical, Félix sabe lo que son las semanas 5J. Un tipo tranquilo y con muy buenos puntos cómicos. No se me olvidará la historia de cómo inundó completamente un laboratorio (derribaron el edificio).

Más tarde apareció el Servicio de Metabolómica. Sebastiaan vino desde Holanda para encargarse de todas esas máquinas. Un tío divertido, y muy buenos los productos de su país (me refiero a la anguila ahumada).

Diana acompaña a Sebastiaan en el Servicio de Metabolómica, aunque a veces pasa más tiempo en nuestro laboratorio que en el suyo... Tiene que aguantar que siempre le ocupemos el -80, pero lo lleva bien, con paciencia... y un poco de mala leche al final.

Alguien que ha estado ahí todas las mañanas para darme los buenos días ha sido Alfonso, que me encontraba siempre en el ordenador mirando el correo e intentando despertarme un poco para poder empezar. Una persona con la que siempre se puede tener una conversación interesante, de ciencia o de cualquier tema, lástima que sea del Real Madrid (es broma).

Guardo un recuerdo especial de Laura, Usue, Aroa, Marcella y Karolíne, que coincidieron conmigo durante un tiempo en el laboratorio y después siguieron su camino. Os deseo lo mejor, y sobre todo que seáis muy felices.

Una ayuda importante desde la universidad me vino con Begoña Ochoa cuando empecé y con Patricia Aspichuela ahora que acabo. Gracias a su buena disposición se me hizo más fácil lo que para mí es un mundo desconocido: los papeleos universitarios. Creo que sin su orientación seguiría rellenando impresos...

Por supuesto buena culpa de todo este lío la tienen mis padres, que me animaron siempre a ser feliz y a estudiar lo que a mí me gustara, estando siempre a mi lado en muchos momentos malos, y apoyándome en todo.

Y qué decir de Shere, media vida juntos y todavía me aguanta. Quién más ha sufrido mi tesis, a quien más me he quejado y quién más me ha apoyado, animado y comprendido. Siempre haciéndome olvidar los problemas del trabajo y dándome fuerzas para seguir.

Por eso, a todas esas personas que habéis ido moldeando mi vida, os doy las gracias de corazón.

TABLE OF CONTENTS

TABLE OF CONTENTS

ABBREVIATIONS	25
1. RESUMEN/SUMMARY.....	31
2. INTRODUCTION.....	37
2.1. CHRONIC LIVER DISEASE.....	37
2.1.1. Nonalcoholic fatty liver disease (NAFLD) as cause of chronic liver disease.....	37
2.1.2. HCC, a liver pathology with poor prognosis	38
2.1.2.1. Epidemiology, etiology and treatment of HCC.....	38
2.1.2.2. HCC derived from Hepatitis virus infection.....	38
2.1.2.3. HCC derived from NAFLD	39
a) Oxidative stress	39
b) Methionine metabolism.....	39
c) p53.....	39
2.1.2.4. Therapeutic approaches in hepatocarcinogenesis	40
a) Surgical therapy.....	40
b) Non-surgical therapy	41
2.2. METHIONINE METABOLISM AND LIVER DISEASE.....	42
2.2.1. Molecular and biological aspects of SAMe.....	42
2.2.2. Hepatic SAMe metabolism	43
2.2.3. Methionine adenosyltransferase enzymes	44
2.2.3.1. MAT regulation	45
a) Regulation of <i>MAT1A</i> and <i>MAT2A</i> expression	45
b) Regulation of MAT enzymatic activity.....	46
2.2.4. Glycine N-methyltransferase enzyme.....	46
2.2.5. Biological functions of SAMe in the liver	47
2.2.5.1. SAMe regulation of hepatocyte growth.....	47
a) SAMe blocks hepatocyte growth factor-induced hepatocyte growth	47
b) Liver regeneration.....	48
2.2.5.2. SAMe regulation of hepatocyte and hepatoma cells apoptosis	50
2.2.6. SAMe treatment in liver disease.....	50
2.2.7. Mouse models of liver disease with altered hepatic SAMe levels	51
2.2.7.1. Chronic deficiency in SAMe: <i>MAT1A</i>-KO mouse model.....	51
2.2.7.2. Chronic excess in SAMe: <i>GNMT</i>-KO mouse model	51
2.3. RNA BINDING PROTEINS IN RELATION WITH LIVER DISEASE, HCC AND LIVER PROLIFERATION	52
2.3.1. The RNA-binding protein HuR: functions, implications in cancer and regulation	53
2.3.1.1. HuR general structure.....	53
2.3.1.2. HuR function	53
a) Stabilization of target mRNAs.....	53
b) Upregulation of mRNAs translation	54

c)	Repression of mRNAs translation	54
2.3.1.3.	Regulation of HuR function	55
a)	Regulation of HuR abundance	55
b)	Regulation of HuR localization	56
c)	Phosphorylation and methylation	56
2.3.1.4.	HuR and cancer traits	57
a)	Enhanced cell proliferation	57
b)	Enhanced cell survival	57
c)	Elevation of local angiogenesis	58
d)	Evasion of immune response	58
e)	Invasion and metastasis	58
2.3.1.5.	Implication of HuR in specific cancer types	58
2.3.2.	The RNA-binding protein AUF1: functions, regulation and implications in cancer	59
2.3.2.1.	AUF1 general structure	59
2.3.2.2.	AUF1 function	59
a)	Promoting of mRNA decay	59
b)	mRNA stabilization	60
c)	Increase of mRNA translation	60
2.3.2.3.	AUF1 function regulation	60
a)	Regulation by different AUF1 isoforms expression	60
b)	Regulation of AUF1 expression via alternatively spliced 3'UTR	60
c)	Regulation by AUF1 nuclear import and export	60
d)	Post-translational modifications	60
2.3.2.4.	AUF1 in cancer	61
2.4.	NEDDYLATION: PROTEIN-STABILIZING POST-TRANSLATIONAL MODIFICATION	61
2.4.1.	NEDD8 conjugating cascade	61
2.4.2.	NEDD8 substrates	62
2.4.2.1.	Cullin family	62
2.4.2.2.	Mdm2 and p53	62
2.4.3.	NEDD8 relation with cancer	63
3.	OBJECTIVES	67
4.	EXPERIMENTAL PROCEDURES	71
4.1.	HUMAN SAMPLES	71
4.2.	ANIMAL EXPERIMENTS	71
4.3.	PARTIAL HEPATECTOMY (PH) EXPERIMENTS	71
4.4.	CELL EXPERIMENTS	71
4.4.1.	Primary rat and mouse hepatocytes	71
4.4.2.	MLP29 cell line	72
4.4.3.	SAMe-D cell line	72
4.4.4.	Commercial cell lines	72
4.4.5.	Cell treatments	72

4.5.	RIBONUCLEIC ACIDS (RNA) EXTRACTION AND PROCESSING	73
4.5.1.	RNA isolation.....	73
4.5.2.	Retrotranscription and Real Time quantitative PCR (RT-qPCR).....	73
4.6.	PROTEIN EXTRACTION AND ANALYSIS	74
4.6.1.	Total protein extraction.....	74
4.6.2.	Subcellular protein extraction	74
4.6.3.	Western blotting.....	74
4.7.	GENE SILENCING.....	74
4.8.	PLASMID CONSTRUCTS.....	77
4.8.1.	Cloning of 3'UTR of mouse MAT2A cDNA and plasmid construct.....	77
4.8.2.	Subcloning of HuR-V5, and HuR mutants production	77
4.9.	CELL TRANSFECTION	77
4.10.	IMMUNOPRECIPITATION (IP) ASSAYS	78
4.10.1.	Protein immunoprecipitation assays	78
4.10.2.	Ribonucleoprotein immunoprecipitation (RNP-IP) assay	78
4.11.	PURIFICATION ASSAYS	79
4.11.1.	Biotin pull down assay	79
4.11.2.	Protein-Histidine affinity purification using nickel-nitriolotriacetic acid (Ni^{2+} -NTA) beads.....	80
4.12.	POLYSOME ANALYSIS	80
4.13.	IMMUNOSTAINING ASSAYS.....	80
4.13.1.	Histology, immunohistochemistry and immunohistofluorescence.....	80
4.13.2.	Immunocytofluorescence	81
4.14.	SAME MEASUREMENT	81
4.15.	CASPASE-3 ACTIVITY MEASUREMENT.....	82
4.16.	CELL CYCLE ANALYSIS	82
4.17.	INVASIVENESS ASSAY (SOFT-AGAR)	82
4.18.	STATISTICAL ANALYSIS.....	82
5.	RESULTS.....	85
5.1.	HuR/METHYL-HuR AND AUF1 REGULATE THE MAT EXPRESSED DURING LIVER PROLIFERATION, DIFFERENTIATION, AND CARCINOGENESIS	85
5.1.1.	<i>MAT1A</i> and <i>MAT2A</i> mRNA levels are regulated by HuR and AUF1, respectively	85
5.1.2.	Coordinated expression of <i>MAT2A</i> and <i>MAT1A</i> , and their respective regulators, HuR and AUF1, during de-differentiation of cultured hepatocytes	87
5.1.3.	Role of HuR, methyl-HuR and AUF1 during liver development	90
5.1.4.	Regulation of <i>MAT2A</i> in an <i>in vivo</i> model of chronic excess of hepatic SAME	91
5.1.5.	HuR and AUF1 levels in human HCC	92
5.2.	IMPAIRED LIVER REGENERATION IN MICE LACKING GLYCINE N-METHYLTRANSFERASE.....	93
5.2.1.	Increased mortality in GNMT knockout mice during liver regeneration	93
5.2.2.	GNMT-KO mice are able to progress into cell cycle S phase	94
5.2.3.	LKB1/AMPK/eNOS pathway and HuR cytoplasmic translocation are inhibited during liver regeneration in GNMT-KO mice.....	94
5.2.4.	Inhibition of AMPK induces NF κ B activation in hepatocytes	97

5.3. MURINE DOUBLE MINUTE 2 REGULATES HU ANTIGEN R STABILITY IN HUMAN LIVER AND COLON CANCER THROUGH NEDDYLATION.....	100
5.3.1. HuR and Mdm2 are overexpressed in hepatoma and colon cancer cells and in human HCC and colon carcinoma	101
5.3.2. NEDDylation is linked to HuR stability.....	101
5.3.3. Lysines 283, 313 and 326 are important sites for HuR NEDDylation and stability.....	104
5.3.4. Cytoplasmic NEDDylation of HuR is mediated by Mdm2.....	107
5.3.5. NEDDylation controls nuclear localization of HuR.....	108
5.4. SUPPLEMENTAL FIGURES.....	109
6. DISCUSSION.....	115
6.1. HuR/METHYL-HuR AND AUF1 REGULATE THE MAT EXPRESSED DURING LIVER PROLIFERATION, DIFFERENTIATION, AND CARCINOGENESIS.....	117
6.2. IMPAIRED LIVER REGENERATION IN MICE LACKING GLYCINE N-METHYLTRANSFERASE.....	121
6.3. MURINE DOUBLE MINUTE 2 REGULATES HU ANTIGEN R STABILITY IN HUMAN LIVER AND COLON CANCER THROUGH NEDDYLATION.....	124
7. CONCLUSIONS.....	131
7.1. HuR/METHYL-HuR AND AUF1 REGULATE THE MAT EXPRESSED DURING LIVER PROLIFERATION, DIFFERENTIATION, AND CARCINOGENESIS.....	131
7.2. IMPAIRED LIVER REGENERATION IN MICE LACKING GLYCINE N-METHYLTRANSFERASE.....	131
7.3. MURINE DOUBLE MINUTE 2 REGULATES HU ANTIGEN R STABILITY IN HUMAN LIVER AND COLON CANCER THROUGH NEDDYLATION.....	132
8. BIBLIOGRAPHY.....	135
9. SUPPORT.....	155

ABBREVIATIONS

ABBREVIATIONS

AAALAC	Association for Assessment and Accreditation of Laboratory Animal Care
AdoMet	S-adenosylmethionine
AFP	α -fetoprotein
AICAR	Aminoimidazol carboxamide ribonucleotide
ALD	Alcoholic liver disease
AMP	Adenosine-5'-monophosphate
AMPK	AMP-activated protein kinase
APP-BP1	Amyloid beta precursor protein-binding protein 1
APRIL	Acidic protein rich in leucine
ARE	AU-rich element
ATM	Ataxia telangiectasia mutated kinase
ATP	Adenosine-5'-triphosphate
AUF1	AU-rich RNA binding factor 1
BCA3	Breast-cancer-associated protein 3
Bcl2	B-cell lymphoma-2
BHMT	Betaine homocysteine methyltransferase
BrdU	Bromodeoxyuridine
BRF1	Butyrate response factor 1
CaMKK	Calcium/calmodulin-dependent protein kinase kinase
CARM1	Coactivator-associated arginine methyltransferase 1
CBS	Cystathionine β -synthase
CC	Compound C
Cdk1	Cyclin dependent kinase 1
CHC	Carcinoma hepatocellular
Chk2	Checkpoint kinase 2
CHX	Cycloheximide
CIS	Cytokine-induced STAT inhibitor
γ-CTL	Cystathionase
c-Kit	v-kit Hardy-Zuckerman 4 feline sarcoma viral oncogene homolog
c-Myc	v-myc myelocytomatisis viral oncogene homolog (avian)
COX-2	Cyclooxygenase-2
Crk	v-crk sarcoma virus CT10 oncogene homolog (avian)
CRM1	Chromosome region maintenance 1
CYP2E1	Cytochrome P450 2E1
DEN1	Deneddylylase-1
DNS	hnRNP D nucleocytoplasmic shuttling sequence
EGF	Epidermal growth factor
EHGNA	Enfermedad del hígado graso no alcohólica
EHNA	Esteatohepatitis no alcohólica
eIF4E	Eukaryotic translation initiation factor 4E
ELAVL1	Embrionic lethal abnormal vision like 1
EMT	Epithelial-to-mesenchymal transition
eNOS	Endothelial nitric oxide synthase
ERK	Extracellular signal-regulated kinases
FADD	Fas (TNFRSF6)-associated via death domain
FBS	Fetal bovine serum
GAPDH	Glyceraldehyde-3-phosphate dehydrogenase
γ-GCSH	γ -glutamylcysteine synthetase heavy subunit
GFP	Green fluorescent protein
GMCSF	Granulocyte / macrophage colony-stimulating factor
GNMT	Glycine N-methyltransferase
GSH	Glutathione
HAUSP	Herpes virus-associated ubiquitin-specific protease
HBV	Hepatitis B virus
HBx	Hepatitis B virus x interacting protein

HCC	Hepatocellular carcinoma
HCV	Hepatitis C virus
Hcy	Homocysteine
HGF	Hepatocyte growth factor
HIF-1α	Hypoxia inducible factor 1 α
HSC	Hepatic stellate cell
Hu/elav	Human embryonic lethal abnormal vision
HuR	Hu antigen R
IGF-1	Insulin like growth factor 1
IGF-I	Insulin growth factor I
IGF-IR	Type I insulin-like growth factor receptor
IL	Interleukin
IMP-2	Inner mitochondrial membrane peptidase, subunit 2
iNOS	Inducible nitric oxide synthase
IκBα	NF-kappa-B inhibitor alpha
JAK	Janus kinase
KO	Knockout
KSRP	KH-type splicing regulatory protein
LKB1	Liver kinase B1
LPS	Lipopolysaccharide
MAPK	Mitogen-activated protein kinase
MAT	Methionine adenosyltransferase
MAT1A	Methionine adenosyltransferase 1A
MAT2A	Methionine adenosyltransferase 2A
MAT2B	Methionine adenosyltransferase 2B
MCD	Methionine and choline deficient
Mcl1	Myeloid cell leukemia-1
Mdm2	Murine double minute 2
MEK	Mitogen-associated/extracellular regulated kinase
MKP-1	MAP kinase phosphatase 1
MLP29	Mouse liver progenitor 29
MMP-9	Matrix metalloproteinase-9
MTA	5'-methylthioadenosine
MTHFR	5,10-methylenetetrahydrofolate reductase
MTHFS	Methylenetetrahydrofolate synthase
mTOR	Mamalian target of rapamycin
MTR	5'-methylthioribose
NAE	NEDD8-activating enzyme
NAFLD	Non-alcoholic fatty liver disease
NAM	Nicotinamide
NASH	Non-alcoholic steatohepatitis
NEDD8	Neural precursor cell-expressed developmentally downregulated-8
NEDP1	NEDD8 protease 1
NES	Nuclear export sequence
NFkB	Nuclear factor κ B
NLS	Nuclear localization signal
nNOS	Neuronal nitric oxide synthase
NO	Nitric oxide
NOS	Nitric oxide synthase
NSAP-1	NS1-associated protein 1
NSEP-1	Nuclease-sensitive element-binding protein 1
NUB1	NEDD8 ultimate buster 1
Pak	p21-activated kinase
PAR-CLIP	Photoactivatable ribonucleoside enhanced crosslinking and immunoprecipitation
PCNA	Proliferation cell nuclear antigen
PDGF	Platelet-derived growth factor
PH	Partial hepatectomy
PHAP-I	Putative human HLA class II-associated protein

PI3K	Phosphoinositide-3 kinase
PKC	Protein kinase C
PP1	Protein phosphatase 1
PP2A	Protein phosphatase 2A
PTMA	Prothymosin α
PTH	Parathyroid hormone
qPCR	Quantitative PCR
RASSF	Ras-association domain family
Rac	ras-related C3 botulinum toxin substrate 3
Rap1	Repressor/activator protein 1
RBD	RNA binding domain
RBP	RNA binding protein
RFA	Radiofrequency ablation
RIP-chip	RNA-binding protein immunopurification-microarray
RISC	RNA-induced silencing complex
RNP-IP	Ribonucleoprotein immunoprecipitation
ROS	Reactive oxygen species
RRM	RNA recognition motif
RT-PCR	Real time PCR
RT-qPCR	Real Time quantitative PCR
SAH	S-adenosylhomocysteine
SAM	S-adenosylmethionine
SAME	S-adenosylmethionine
SDS-PAGE	sodium dodecyl sulphate-polyacrylamide gel electrophoresis
SENP8	SUMO/sentrin specific peptidase family member 8
SIRT1	Sirtuin 1
SOCS	Supressor of cytokine signaling
STAT3	Sinal transducer and activator of transcription 3
TACE	Transcatheter arterial chemoembolization
TAK1	TGF β -activated kinase 1
TGFα	Transforming growth factor α
TGFβ	Transforming growth factor β
TIA-1	T-cell intracellular antigen 1
TIAR	TIA-1-related
TNFα	Tumor necrosis factor α
Tsp1	Thrombospondin 1
TTP	Tristetraprolin
Ub	Ubiquitin-like
Uba3	ubiquitin-like modifier activating enzyme 3
UBL	Ubiquitin-like
UCH-L3	Ubiquitin carboxyl-terminal hydrolase L3
UCP2	Uncoupling protein 2
uPA	urokinase-type plasminogen activator
uPAR	uPA receptor
VEGF	Vascular endothelial growth factor
Wnt5a	Wingless-type MMTV integration site family, member 5A

1. RESUMEN/SUMMARY

1. RESUMEN/SUMMARY

RESUMEN

La enfermedad hepática crónica es una de las principales causas de mortalidad en humanos. Comprende enfermedades con diferentes etiologías como la infección por los virus de la hepatitis B y C, toxinas, consumo de alcohol y drogas, enfermedades autoinmunes y hereditarias y la enfermedad del hígado graso no alcohólica (EHGNA). La EHGNA es una de las principales enfermedades hepáticas crónicas en los países desarrollados, asociada con los factores de riesgo del síndrome metabólico (obesidad, resistencia a la insulina, dislipidemia e hipertensión), e incluyendo alteraciones que van desde la esteatosis hasta la esteatohepatitis no alcohólica (EHNA), que en algunos casos puede ir acompañada de fibrosis. Los pacientes de EHNA con presencia de fibrosis pueden llegar a desarrollar carcinoma hepatocelular (CHC).

El CHC representa la tercera causa de muerte por cáncer, y la primera causa de muerte en pacientes cirróticos. El CHC es el cáncer más prevalente en la población, con mal pronóstico incluso en los países desarrollados. Su etiología es diversa, con los virus de la hepatitis B y C, el alcoholismo, la aflatoxina B1 y el EHGNA como principales factores de riesgo. Entre los factores moleculares involucrados en la progresión desde EHGNA a CHC podemos encontrar el estrés oxidativo, el metabolismo de la metionina y la disfunción de p53. Numerosos estudios han mostrado que los pacientes cirróticos con alto riesgo de desarrollar CHC presentan una desregulación del metabolismo de la metionina y unos niveles anormales de S-adenosilmetionina (SAMe).

La S-adenosilmetionina es el principal donador biológico de grupos metilo, y el hígado aparece como el principal responsable de su homeostasis. SAMe juega un papel fundamental en la proliferación de los hepatocitos y su diferenciación, y en la apoptosis de células tumorales. En el hígado SAMe es capaz de inhibir la activación de la ruta LKB1/AMPK/eNOS y evitar la translocación al citoplasma de HuR, una proteína de unión al ARN, siendo ambos mecanismos importantes para la proliferación de los hepatocitos y la regeneración hepática. Por tanto, los niveles de SAMe deben estar estrechamente regulados. Las dos principales enzimas responsables de la síntesis y el catabolismo de SAMe son la metionina adenosiltransferasa (MAT) y la glicina N-metiltransferasa (GNMT), respectivamente. La enzima MAT está codificada por dos genes, *MAT1A* y *MAT2A*. *MAT1A* codifica para la formación de las enzimas MAT I y MAT III, y *MAT2A* codifica para MAT II. *MAT1A* se expresa en el hígado adulto y diferenciado, mientras que *MAT2A* se expresa en el hígado fetal y en proliferación. Durante el desarrollo del hígado hay un cambio en la expresión desde *MAT2A* hasta *MAT1A*, y durante la proliferación y la desdiferenciación hepáticas y durante la transformación maligna, los niveles de expresión de *MAT1A* se reducen junto con un aumento en la expresión de *MAT2A*. La regulación de la expresión de *MAT1A* y *MAT2A* se ha relacionado con la metilación de los promotores y la acetilación de las histonas asociadas a ellos.

Por otra parte, la enzima GNMT, responsable de la catabolización de SAMe, está presente en grandes cantidades en el hígado, y muy reducida en tumores hepáticos y prostáticos. Se han encontrado individuos con mutaciones en *GNMT* que espontáneamente desarrollan enfermedad hepática. La enzima GNMT regula el ratio SAMe a SAH, el cual es considerado como el índice del potencial de transmetilación de la célula. La desregulación de este ratio puede resultar en metilaciones aberrantes.

Con el fin de estudiar las implicaciones de la desregulación del nivel de SAMe en el hígado, se generaron dos modelos de ratones knockout, *MAT1A-KO* y *GNMT-KO*, caracterizados por niveles de SAMe crónicamente disminuidos y elevados, respectivamente. El ratón *MAT1A-KO* presenta estrés oxidativo y desarrolla esteatosis y EHNA a los 8 meses, y finalmente CHC. El ratón *GNMT-KO* desarrolla esteatosis, fibrosis y CHC. La observación de que tanto los altos como los bajos niveles de SAMe provocan una patología similar subrayan la importancia del mantenimiento de la homeostasis de SAMe.

La regulación de los niveles de SAMe está relacionada con la regulación de la expresión de los ARNm de *MAT1A* y *MAT2A*. La explicación de dicha regulación por la metilación de los promotores y la acetilación

de las histonas no explica por completo los cambios entre *MAT1A* y *MAT2A*. Además, la conversión de la metionina en SAMe es capaz de regular la tasa de recambio del ARNm de *MAT2A*.

El principal objetivo de este estudio es la identificación de nuevos mecanismos implicados en la proliferación, diferenciación y desdiferenciación de los hepatocitos, la regeneración hepática y la transformación maligna, en relación con SAMe. Nuestra hipótesis consiste en la existencia de una regulación post-transcripcional de los ARNm de *MAT1A* y *MAT2A* mediante proteínas de unión al ARN, estabilizando y desestabilizando dichos ARNm. Nuestros datos indican que la proteína de unión al ARN HuR se une al ARNm de *MAT2A* estabilizándolo, y la proteína de unión al ARN AUF1 se une al ARNm de *MAT1A* desestabilizándolo. Asimismo, la metilación de HuR por SAMe cambia su funcionalidad, de forma que se une al ARNm de *MAT2A* desestabilizándolo o inhibiendo su traducción. Los niveles de metil-HuR/HuR y AUF1 varían durante el desarrollo del hígado, la desdiferenciación de los hepatocitos y la transformación maligna, regulando los niveles de los ARNm de *MAT2A* y *MAT1A*. Asimismo, el modelo de ratón GNMT-KO, con un nivel de SAMe elevado crónicamente, presenta una desregulación de *MAT2A* por metil-HuR/HuR.

Como el ratón GNMT-KO presenta desregulación de *MAT2A* y se caracteriza por altos niveles de SAMe, estudiamos su respuesta regenerativa tras hepatectomía parcial. Encontramos que el ratón GNMT-KO presenta una alta mortalidad tras la hepatectomía parcial, junto con la inhibición de la ruta LKB1/AMPK/eNOS y de la translocación de HuR al citoplasma, procesos fundamentales para la normal proliferación y regeneración hepática. Además, el bloqueo de la fosforilación de AMPK promueve la activación basal del factor de transcripción NFκB junto con la pérdida de la capacidad de activación de NFκB en respuesta a TNFα, así como el bloqueo de la expresión de iNOS tras la hepatectomía parcial.

De acuerdo con nuestros resultados, la proteína de unión al ARN HuR es fundamental para la proliferación de los hepatocitos, la diferenciación hepática y la transformación maligna. La regulación de su función está relacionada con la localización subcelular, la fosforilación, la metilación y su abundancia proteica. En concreto, su abundancia está regulada por ubiquitinización, pero los mecanismos responsables de la estabilización de la proteína son desconocidos. El estudio de la regulación de la estabilidad de la proteína HuR en CHC y cáncer de colon nos llevó a descubrir la existencia de una estabilización mediante la neddilización de HuR. Mediante el análisis de la abundancia de HuR en líneas celulares de CHC y cáncer de colon y en muestras humanas de CHC y metástasis de colon al hígado, concluimos que Mdm2 neddiliza HuR en el citoplasma, promoviendo su localización nuclear y protegiéndolo de la degradación por el proerasoma. El análisis mutacional de la proteína HuR nos permitió localizar las lisinas en las que tiene lugar esta modificación post-traduccional.

En conclusión, nuestros resultados descubren un nuevo mecanismo de regulación post-transcripcional de *MAT1A* y *MAT2A*, subrayando la importancia de la homeostasis de SAMe en la proliferación, diferenciación y transformación maligna en el hígado. Además, el descubrimiento de un nuevo mecanismo de regulación de la abundancia de HuR en CHC y cáncer de colon a través de la neddilización mediada por Mdm2, abre nuevas vías para el tratamiento de estas enfermedades.

SUMMARY

The chronic liver disease is one of the main causes of mortality in humans. It comprises illnesses with etiologies such as hepatitis B and C virus infection, toxins, alcohol and drugs consumption, autoimmune and hereditary diseases and non-alcoholic fatty liver disease (NAFLD). NAFLD is one of the main chronic liver diseases in developed countries, associated with the metabolic syndrome risk factors (obesity, insulin resistance, dyslipidemia and hypertension), and including alterations from steatosis to non-alcoholic steatohepatitis (NASH), in some cases accompanied by fibrosis. NAFLD patients of NASH with fibrosis can finally develop hepatocellular carcinoma (HCC).

HCC represents the third leading cause of cancer death globally, and the first cause of death in cirrhotic patients. HCC is the most prevalent cancer in the population, with a poor prognosis even in the developed countries. The etiology is diverse, with hepatitis B and C virus, alcoholism, aflatoxin B1 and NAFLD as the main risk factors. Among the molecular factors involved in NAFLD progression to HCC we can find the oxidative stress, the methionine metabolism and the impairment of p53. In particular, several studies have shown that human patients with liver cirrhosis at a high risk of HCC development present impairment in methionine metabolism and abnormal S-adenosylmethionine (SAMe) levels.

SAMe is the main methyl donor in the cell, being the liver the principal responsible of its homeostasis. SAMe plays a critical role in hepatocyte proliferation, differentiation and tumoral cells apoptosis. In the liver SAMe is able to inhibit the activation of the LKB1/AMPK/eNOS pathway, and avoid the translocation of the RNA binding protein (RBP) HuR, which are important mechanisms for hepatocyte proliferation and liver regeneration. Therefore, SAMe levels must be tightly regulated. The two main enzymes in SAMe synthesis and catabolism are methionine adenosyltransferase (MAT) and glycine N-methyltransferase (GNMT), respectively. The MAT enzymes are codified by two genes, *MAT1A* and *MAT2A*. *MAT1A* encodes for MAT I and MAT III enzymes, and *MAT2A* codifies for MAT II. *MAT1A* is expressed in the adult and differentiated liver, whereas *MAT2A* is expressed in fetal and proliferating liver. During liver development, there is a switch from *MAT2A* to *MAT1A* expression, and during liver de-differentiation, proliferation and malignant transformation, *MAT1A* levels decrease together with an increase of *MAT2A* levels. This regulation of *MAT1A* and *MAT2A* expression is related with promoter methylation and histone acetylation.

On the other hand, the SAMe catabolizing enzyme GNMT, is present in large amounts in the liver, and highly reduced in liver and prostate tumors. Individuals with *GNMT* mutations spontaneously develop liver disease. GNMT enzyme regulates the SAMe to SAH ratio, which is considered the index of the transmethylation potential of the cell. The impairment of this ratio can result into aberrant methylation patterns.

In order to study the implications of the impairment of SAMe regulation in the liver, two knockout models were developed, *MAT1A*-KO and *GNMT*-KO, characterized by chronic deficiency and excess of SAMe levels, respectively. The *MAT1A*-KO mice present oxidative stress, and develop steatosis and NASH at 8 month, and HCC. The *GNMT*-KO mice develop steatosis, fibrosis and finally HCC. The observations that both low and high SAMe levels lead to similar pathology highlight the importance of the SAMe homeostasis.

The regulation of SAMe levels involves *MAT1A* and *MAT2A* mRNA expression regulation. The regulation of their expression based on the promoter methylation and histone acetylation does not completely explain the changes between *MAT1A* and *MAT2A*. In addition, methionine conversion into SAMe regulates *MAT2A* mRNA turnover.

The main objective of this study is to identify new mechanisms implicated in the hepatocyte proliferation, differentiation and dedifferentiation, liver regeneration and malignant transformation, in relation with SAMe. We hypothesize that there is a post-transcriptional regulation of *MAT1A* and *MAT2A* mRNAs that involve RBPs, which bind to mRNAs stabilizing or destabilizing them. Our data indicate that the RBP HuR binds to *MAT2A* mRNA stabilizing it, and the RBP AUF1 binds to and destabilizes *MAT1A* mRNA. Importantly, SAMe methylates HuR promoting *MAT2A* mRNA destabilization or inhibition of the translation. The levels of methyl-HuR/HuR and AUF1 vary during liver development, hepatocyte de-differentiation and malignant

transformation, thus regulating the levels of *MAT2A* and *MAT1A* mRNAs. The knockout mouse model GNMT-KO, with chronically elevated SAMe levels, also presents an impairment in *MAT2A* mRNA regulation by methyl-HuR/HuR.

As the GNMT-KO mice presents dysregulation of *MAT2A* and is characterized by high SAMe levels, we studied its regenerative response after partial hepatectomy (PH). We found that GNMT-KO mice present high mortality after PH, together with the inhibition of the LKB1/AMPK/eNOS pathway and the translocation of HuR to the cytoplasm, processes fundamental for the normal liver proliferation and regeneration. In addition, the blockade of AMPK phosphorylation promotes NF κ B basal activation and lack of TNF α -induced NF κ B activation and iNOS expression after PH. All these results show the impairment in the liver regeneration of the GNMT-KO mice.

The RBP HuR appears, according with our results, as fundamental in the hepatocyte proliferation, liver differentiation and malignant transformation processes. The regulation of its function is related with HuR subcellular localization, phosphorylation, methylation and protein abundance. In particular, HuR abundance is regulated by ubiquitination, but the mechanisms leading to HuR stability are not known. We studied the regulation of HuR protein stability in HCC and colon cancer, and we found that HuR is stabilized by neddylation. By studying HuR abundance in HCC and colon cancer cell lines, and in human HCC and metastatic colon cancer samples, we conclude that Mdm2 neddylates HuR in the cytosol, promoting its nuclear localization and protecting it from the proteasomal degradation. The mutational analysis of HuR protein allowed us to map the lysines involved in this post-translational modification.

In conclusion, our results uncover a new regulatory post-transcriptional mechanism for *MAT1A* and *MAT2A*, highlighting the importance of SAMe homeostasis in the proliferation, differentiation and malignant transformation of the liver. In addition, the finding of a new mechanism for the regulation of HuR abundance in HCC and colon cancer through Mdm2-mediated neddylation opens a new field in the treatment of these malignancies.

2. INTRODUCTION

2. INTRODUCTION

2.1. CHRONIC LIVER DISEASE

The “chronic liver disease” includes a large number of conditions with different etiologies, and corresponding with different illnesses [1]. The chronic liver disease is one of the main causes of mortality in Europe and United States [2, 3], and between the conditions included on this category, we can find Hepatitis B and C virus (HBV, HCV) infection, toxins (e.g. aflatoxin B1), alcohol and drugs consumption, autoimmune diseases (primary sclerosing cholangitis, primary biliary cirrhosis and autoimmune hepatitis), hereditary diseases (e.g., hemochromatosis, alpha1-antitrypsin deficiency, Wilson’s disease) and nonalcoholic fatty liver disease (NAFLD) [1]. Most of these forms can slowly progress, often over 20 to 40 years, from hepatitis to cirrhosis and hepatocellular carcinoma (HCC) [4].

2.1.1. Nonalcoholic fatty liver disease (NAFLD) as cause of chronic liver disease

NAFLD is one of the most common causes of chronic liver disease worldwide [5], and particularly, the main chronic liver disease condition in the Western world [6, 7]. NAFLD is a clinical pathological term that includes a spectrum of alterations that range from simple triglyceride accumulation in the hepatocytes (steatosis) to hepatic steatosis with inflammation (nonalcoholic steatohepatitis or NASH), which may or not have associated fibrosis [8–10].

NAFLD is tightly linked to obesity, insulin resistance, type 2 diabetes, dyslipidemia and hypertension [5–7, 9, 11], all of them risk factors to the metabolic syndrome [11]. Metabolic syndrome is a clustering of different conditions that collectively increases the probability of developing cardiovascular disease and diabetes [12]. NAFLD can be considered the hepatic manifestation of the metabolic syndrome, being a key factor predisposing to it [11, 13].

The prevalence of NAFLD in developed countries is 20% to 30% of adults. [5, 6, 14, 15]. It is more frequent among people with diabetes (30-50%) and obesity (80-90%), and almost universal when combining both factors [16, 17]. In the case of children, there is a prevalence of 3-10% rising up to 40-70% among obese children [18, 19]

The progression of NAFLD comprises a series of steps: starting from the liver steatosis, usually associated with a benign prognosis, about 10% of the people can develop NASH by mechanisms not well understood, but related with the metabolic syndrome [9, 11, 20]. At this point, liver steatosis is reversible, and also NASH can be reversed. When maintained in the time, NASH can lead into fibrosis and cirrhosis in about 25% of patients [11, 21, 22], and after this, it can culminate with liver failure or even HCC (10-25% of cirrhotic patients) [5, 20, 22, 23] (Figure 1).

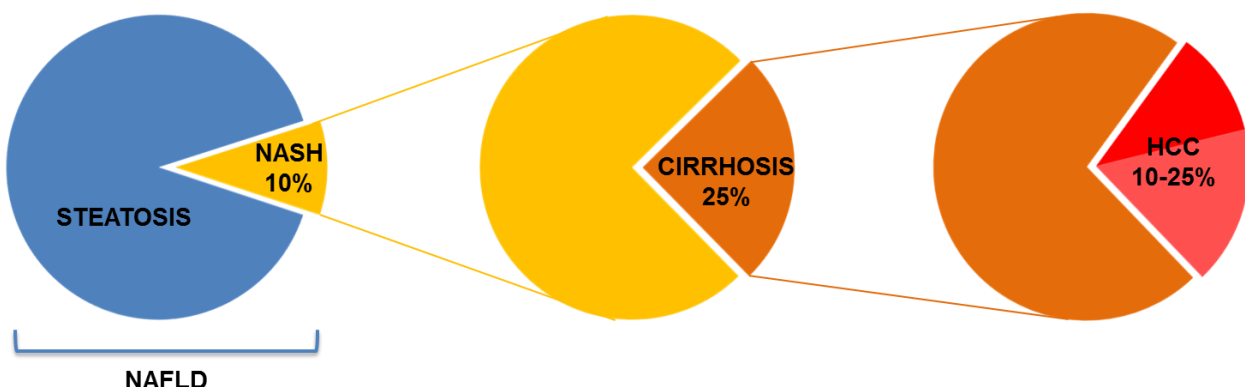


Figure 1. Sequential progression from NAFLD to HCC. 10% of liver steatosis develops inflammation, transforming into NASH. 25% of NASH can progress through cirrhosis by replacement of liver tissue by fibrous scar and regenerative nodules. Finally, 10-25% of cirrhosis can lead into HCC, a primary malignancy of the liver.

2.1.2. HCC, a liver pathology with poor prognosis

Liver tumors are an important cause of morbidity and mortality worldwide. In men, liver cancer is the fifth most frequently diagnosed cancer, and the second cause of cancer death. In women, the seventh diagnosed and the sixth cause of cancer death [24]. The most common injuries are hepatic adenoma, focal nodular hyperplasia and hemangioma. The rest of the liver neoplasms include hemangiosarcoma, hepatoblastoma, cholangiocarcinoma and HCC [24, 25].

2.1.2.1. Epidemiology, etiology and treatment of HCC

HCC represents, among primary liver cancers, the major histological subtype, accounting for 70% to 85% of total liver cancer worldwide [26]. HCC is the fifth most common malignancy worldwide and the third leading cause of cancer-related deaths after lung and gastric cancer [27], and the most frequent primary epithelial tumor developed from hepatocytes, with a poor prognosis.

The etiology is heterogeneous, being the main causes the infection with HBV and HCV, alcoholism and aflatoxin B1. NAFLD, NASH and the metabolic syndrome appear as relevant and emerging risk factors [23, 26], because of the increasing prevalence particularly in the developed countries. A more detailed description of the HCC with hepatitis virus and NAFLD etiology will be provided in sections 2.1.2.2. and 2.1.2.3., respectively.

HCC is often asymptomatic at the early stage of the pathology. As consequence, the pathology is detected at an advanced stage, making only 15% of patients eligible for curative therapies such as liver transplantation or tumor resection [28, 29]. When surgical management is possible, 1 year survival rates in 10-70% of the patients can be achieved, and 2 years survival in 8-50% of cases [30]. In patients with advanced disease, the median survival rate is less than 1 year, in part due to the absence of effective systemic therapies [29]. In many cases recurrences are inevitable. Systemic therapy, including chemotherapy, hormonal therapy, biologic and biochemical therapy, and molecularly targeted therapy, has

been shown to be ineffective, as evidenced by poor response rates and no demonstrated improved survival rates. That is due to the heterogeneity of signaling pathways converging to the same malignant transformation, together with the usually underlying cirrhosis that limits the use of cytotoxic agents and the chemotherapy resistance of the HCC [31]. In section 2.1.2.4., a description of the main therapeutic approaches will be presented.

2.1.2.2. HCC derived from Hepatitis virus infection

The majority of cases of HCC occur in individuals with a subjacent HBV or HCV chronic infection [32].

HBV infection causes acute and chronic liver disease, and has been shown to increase 100-fold the risk of developing liver cancer in chronic carriers. Approximately 340000 cases of liver cancer are attributable to HBV infection, the majority in Africa, Asia and western Pacific region [26]. The infection with HBV is thought to cause HCC via direct and indirect pathways. First, HBV infection causes hepatocyte injury and chronic inflammation, with hepatocyte proliferation, fibrosis, and cirrhosis. The continuous regeneration leads to the accumulation of mutations in the hepatic proliferating cells. This can result in the activation of oncogenes, inactivation of tumor suppressor genes, etc. [33]. Second, HBV is able to integrate its DNA into host cells, acting as a mutagenic agent [34]. In addition, the viral protein HBx is able to stimulate protein kinase C (PKC) and nuclear factor kappa B (NFkB) pathways, as well as deregulation of cell cycle control and interference with cellular DNA repair and apoptosis [35].

HCV infection produces cirrhosis, chronic inflammation, cell death and proliferation in the liver, increasing 17-fold the risk of liver cancer in patients. HCV-related HCC is found almost exclusively in cirrhotic patients. HCV causes cirrhosis by various indirect mechanisms: HCV core protein enters the host cells and localizes in the outer mitochondrial membrane and the endoplasmic reticulum, producing oxidative stress. This promotes the activation of p38 MAPK and NFkB pathways, what upregulates cytokine production and inflammation, alters the apoptotic

and proliferative pathways and, finally, leads to tumor formation. Alcohol consumption importantly increases HCC development in patients infected with HVC, probably because of the increase in the oxidative stress [26].

2.1.2.3. HCC derived from NAFLD

As described before, when maintained over time, some patients progress from NAFLD to NASH, cirrhosis and finally HCC. 99% of NAFLD-associated HCCs present at least one type of metabolic disease, and 76% have two or more. Among them, obesity and diabetes mellitus are the most common. The HCC associated to NAFLD develops at a more advanced age than in the case of hepatitis virus infection, what means that this HCC develops later or more slowly [23].

Many molecular factors have been linked to the progression of NAFLD to HCC. Between these factors, p53 impairment, the oxidative stress and the methionine metabolism have been shown to play an essential role in the molecular bases of NAFLD-related HCC:

a) Oxidative stress

In NAFLD, the impairment of the fatty acid metabolism leads to the production of oxidative stress. Reactive oxygen species (ROS) in the liver can be generated by mechanisms involving mitochondria, peroxisomes, cytochrome P450 (CYP), reduced nicotinamide adenine dinucleotide oxidase, cyclooxygenase and lipoxygenase [36]. In NAFLD, the ROS imbalance triggers steatohepatitis by lipid peroxidation. Hepatocytes are the major site for lipid peroxidation, due to the generation of pro-oxidants by mitochondria and CYP [36]. In NASH patients, about 40% of mitochondria present abnormalities associated with uncoupling oxidation from phosphorylation, leading to ROS formation [37]. The decreased activities of mitochondrial respiratory complexes leads to decrease in ATP production and reduction of the antioxidant glutathione (GSH) [38], and increase of TNF α expression, which augments lipid peroxidation of mitochondrial membranes, worsening the mitochondrial function, and producing hepatotoxicity and cell death [39]. The lipid peroxidation products act as chemoattractants for inflammatory cells, and are also able to activate hepatic stellate cells, stimulating hepatic fibrosis [40, 41].

In murine models of NASH, CYP2E1 and CYP4A have been found induced. Both CYPs are responsible of the formation of lipid peroxides, associating the hepatic microsomal lipid peroxidation with NASH progression [42].

b) Methionine metabolism

It has been demonstrated that a diet deficient in methionine and choline produces steatosis, NASH and finally HCC in rats [43]. The methionine and choline deficient (MCD) diet model produces also inflammation (NASH) and lipid peroxidation [42], providing evidences of the importance of the methionine metabolism in the liver.

Also in humans, liver cirrhosis patients show hypermethioninemia [44, 45]. This is due to the decrease in the hepatic metabolism of methionine to produce S-adenosylmethionine (SAMe) [46, 47]. As a consequence, a reduction in SAMe levels has been detected in many types of liver diseases. SAMe is the main biological methyl donor, and its functions are related with processes such as hepatocyte proliferation, liver regeneration, differentiation, cell death and apoptosis.

The levels of SAMe in the liver are tightly regulated, and their impairment results in liver disease. This has been demonstrated by two knockout mouse models. The MAT1A-KO mouse model lacks the *MAT1A* (methionine adenosyltransferase 1A) gene, responsible of the synthesis of SAMe from methionine in the liver. This mouse present chronic hepatic SAMe deficiency, and spontaneously develops steatosis, NASH and HCC [48]. The second mouse model lacks the *GNMT* (glycine N-methyltransferase) gene, responsible of the catabolism of SAMe. The deficiency in *GNMT* leads to chronic SAMe excess, developing spontaneously steatosis, fibrosis and HCC [49].

A detailed description of the methionine metabolism in relation with liver disease and HCC will be provided in section 2.2.

c) p53

Discovered 30 years ago, p53 is considered as the "guardian of the genome" due to its crucial tumor suppression role. p53 prevents abnormal proliferation of the cell and protects against cellular stresses and genotoxic damage [50]. As result of these stresses and damages, p53 enhances the

transactivation of many target genes involved in cell cycle arrest, apoptosis and DNA repair, thus preventing the proliferation of the genetically altered cells (reviewed in [51]). In the case of NAFLD to HCC progression, p53 impairment has been shown to be linked to the development of the disease in experimental models.

Two animal models of steatosis, ob/ob and SREBP-1 transgenic mouse model, show an increased nuclear expression of p53, which results in increased p21. The reasons why p53 levels are elevated in these mice are not clear, but it is probably due to the oxidative stress and liver peroxidation, stimulus that, in fact, are able to activate p53. In these models, p53 signaling contributed to liver damage, a crucial step for the development of fatty liver disease, but the subsequent mechanisms are not known [52]. Similar results were found in the liver of patients with NAFLD, where p53 was found elevated with the intensification of liver inflammation [53].

The methionine and choline deficient (MCD) diet model, has also demonstrated an impairment of p53. In this model, liver of MCD-fed mice show a high increase in p53 expression levels. The increase in p53 was linked to the fall in levels of Insulin-like growth factor 1 (IGF-1), which exerts negative regulation on p53 expression. p53 overexpression in these model leads to continued apoptosis, which in turn produced liver damage [54]. In other study, MCD was also found to promote p53 overexpression, showing a role for p53 in regulating steatohepatitis progression by controlling p66Shc signaling, by which p53 controls intracellular redox status, levels of oxidation-damaged DNA and oxidative stress-induced apoptosis [55].

Finally, a tumoral cell line (SAMe-D) derived from HCC of the previously mentioned MAT1A-KO mouse model was isolated. In SAMe-D cells, due to the high levels of cytoplasmic LKB1 (liver kinase B1) phosphorylation, there is an accumulation of S389-phosphorylated p53 in the cytoplasm, which avoids the apoptotic response. This mechanism appears as the way by which this HCC-derived cells can proliferate, by evading p53-dependent apoptosis [56].

In summary, both oxidative stress and methionine metabolism impairment appear as key

molecular mechanisms for progressing from NAFLD to HCC. p53 misregulation is, in many cases the effector by which oxidative stress and methionine metabolism in NASH led to progress to HCC.

After describing the main mechanisms involved in HCC development, the next section will show the therapeutic approaches that can be used in the treatment of the hepatocarcinogenesis.

2.1.2.4. Therapeutic approaches in hepatocarcinogenesis

HCC is a very heterogeneous and complex pathology, due to the numerous etiologies and the convergence of multiple signaling pathways in the same malignant transformation. No systemic therapy exists for patients with advanced HCC, due to the large variety of underlying liver diseases associated to HCC. The development of effective therapeutical approaches requires the comprehension of the molecular mechanisms contributing to the malignant transformation and the relationship between the pathways involved. The treatment options depend on the extent of the disease, the type of liver cancer (primary or metastatic) and the liver function affection. The treatment modalities can be divided into two groups [57–59]:

a) Surgical therapy

Surgery, either hepatic resection or liver transplantation, is considered the only potentially curative therapy for HCC. It is highly recommended when the tumor is localized and there is no spread outside of the liver. Surgery includes hepatic resection, liver transplantation and cryosurgery:

- **Hepatic resection.** This approach consists in the removal of the tumor together with surrounding tissue, preserving enough normal liver to maintain the hepatic function. Surgical resection has been shown to be most beneficial for solitary tumors in patients without cirrhosis, with postresection 5-year survival rates of 41–74%. Among patients with cirrhosis or multiple tumor foci, resection may not always be the most ideal treatment option. Among the factors to consider before resecting the tumor we can find liver function status, portal hypertension, risk of postresection tumor recurrence (up to 70% in 5

years). Between patients with more advanced disease, cirrhosis or impaired liver function, tumor resection can contribute to liver failure [59].

- **Liver transplantation.** It should be considered in any patient with cirrhosis and small HCC, according with the Milan criteria (<5 cm single nodule or up to 3 lesions of 3 cm or less) [58, 59]. Due to the risk of post-transplantation recurrence, HCC patients with extrahepatic disease or with disease beyond accepted criteria are not eligible [59].

- **Cryosurgery.** This technique consists on the destruction of the abnormal tissue using sub-zero temperatures. The tumor is not removed, and the destroyed cancer is left to be reabsorbed by the body. Cryosurgery involves the placement in the center of the tumor of a stainless steel probe through the end of which liquid nitrogen is circulated. It is of particular value in patients where resection is difficult because of vessels proximity or extensive infiltration. The initial results are equivalent to those of resection [60].

b) Non-surgical therapy

Non-surgical therapy should only be used in patients where surgical treatments are not possible, or in combination with surgery. The options are:

- **TACE (Transcatheter arterial chemoembolization).** Among patients with large multifocal HCC or with tumor characteristics that are not appropriate for surgery, TACE appears as the primary therapy. TACE involves the injection of intra-arterial chemotherapy (such as doxorubicin) to the affected hepatic lobe. The greatest benefits are seen in patients with preserved liver function, absence of vascular invasion and small tumors [58, 59].

- **Radiofrequency ablation (RFA).** This technique uses high frequency ultrasound to generate heat at the probe tip that can destroy the tissue. RFA has shown promising results in some studies, with 5-year survival rates of 70% in tumors smaller than 2 cm, but more studies are needed to consider RFA as a potential first-line therapy for small localized tumors [59].

- **Radioembolization.** It consists in the intrahepatic application of radioactive microspheres via hepatic artery to destroy diffuse or multifocal liver tumors. Several studies show promising efficacy and clinical safety [59].

- **Percutaneous ethanol injection (PEI).** Together with RFA, PEI appears as the most common tumor ablation modality. PEI consists in the pure alcohol injection in the tumor through the skin. It is more effective than RFA for tumors smaller than 3 cm, but significantly losses efficacy with the increase in the tumor diameter [59].

- **Molecular therapy.** Until recently, molecular treatments have failed in showing impact on overall HCC survival rates. In late 2007, the angiogenesis inhibitor sorafenib was approved for use in advanced HCC, showing promising results in HCC treatment [61]. Sorafenib is the first targeted therapeutic proven to show a survival benefit for the treatment of advanced HCC, via favorable effects on proliferation and angiogenesis (it blocks VEGF, PDGF and c-Kit receptors) [62]. Unless initial responses exist, the side effects are also important, and there is a loss of efficacy over time [29].

Everolimus is another inhibitor that has been shown to have activity against HCC in xenografts and is now being studied in phase II trials in metastatic disease [63]. Everolimus is an inhibitor of mTOR, analog of rapamycin, which has demonstrated antineoplastic activity *in vitro*, taking into account that the aberrant activation of AKT/mTOR signaling pathway has been observed in patients with HCC [64, 65]. Pre-clinical studies with analogs of rapamycin, such as Everolimus, are currently in progress. Moreover, Everolimus has also been studied in conjunction with sorafenib or EGFR/VEGF inhibitor with promising early results [66].

The next section provides a description of the methionine metabolism, as main mechanism of liver disease and HCC development when impaired in NAFLD patients.

2.2. METHIONINE METABOLISM AND LIVER DISEASE

One of the first clues involving methionine metabolism in liver disease emerged in 1932 when Best demonstrated that a diet deficient in methyl groups (methionine, choline and folates) produced liver steatosis in rats. Moreover, the prolongation of the diet could lead to the development of steatohepatitis, fibrosis and HCC [43].

In humans, the crucial role of the liver in regulating the methionine metabolism was first established by Kinsell et al. in 1947, showing hypermethioninemia and delayed plasma clearance of intravenously injected methionine in liver cirrhosis patients [44, 45]. Also patients with alcoholic liver disease (ALD) presented elevated methionine levels in plasma correlating with the prognosis of the malignancy [67].

These elevated hepatic levels of methionine are due to the decrease in the levels of the enzyme methionine adenosyltransferase (MAT I/III) and the product of its reaction, S-adenosylmethionine (SAMe), during liver disease [46, 47]. The expression of MAT I/III coding gene, *MAT1A* is also diminished in end-stage cirrhotic patients independently of the etiology (alcohol, hepatitis virus, etc.) [47]. As a consequence, a reduction in SAMe levels has been detected in many types of liver diseases.

Since SAMe is a precursor of the cell antioxidant glutathione (GSH), the decrease in SAMe levels leads to a decrease in GSH levels, as reported in many cases of liver disease [68]. Treatments with SAMe in patients with less advanced alcoholic liver cirrhosis increases GSH levels and improves survival [69, 70].

Conversely, mutations in glycine N-methyltransferase (*GNMT*) gene, which codifies for the main enzyme responsible of SAMe catabolism, produces loss of *GNMT* enzyme activity and abnormally elevated SAMe levels. This situation can lead to steatosis, hepatocyte apoptosis, fibrosis and HCC [71–73]. Also, alterations in *GNMT* gene such as *GNMT* polymorphism 1289 C → T, have been associated with early events in the development of HCC [74].

All these findings indicate that the liver needs the right amount of SAMe, and that the impairment

in SAMe levels causes liver injury. Next sections will be focused on the detailed description of SAMe, including SAMe molecular aspects, metabolism and enzymes, biological functions, SAMe as liver disease treatment and mouse models for the study of SAMe levels impairment.

2.2.1. Molecular and biological aspects of SAMe

In 1951 Cantoni demonstrated that a liver homogenate supplemented with adenosine triphosphate (ATP) and methionine converted nicotinamide to N-methylnicotinamide, in a reaction that involved the formation of an “active methionine” [75, 76]. Two years later, in 1953, Cantoni confirmed the formation of this “active methionine” as the product of the reaction between methionine and ATP, and proposed the formulation of the molecule, which he called S-adenosylmethionine (abbreviated as AdoMet, SAM or SAMe) [77].

SAMe is the main biological methyl donor, being the liver the principal responsible of its homeostasis [70]. Under normal conditions, up to 85% of the methylation reactions occur in the liver,

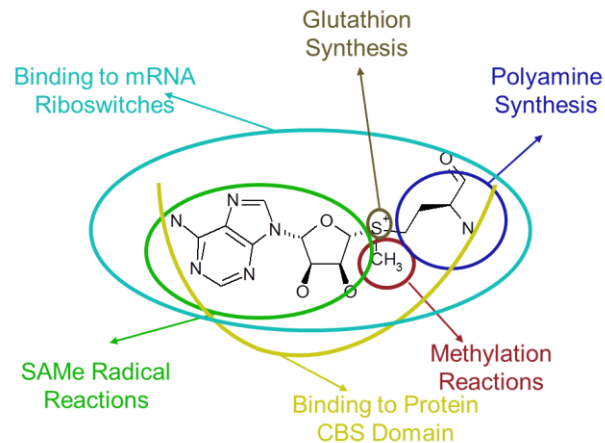


Figure 2. Molecular structure of S-adenosylmethionine. SAMe participates in multiple cellular reactions. The methyl group is donated in methylation reactions, and the propylamino group is donated in polyamine synthesis. Sulfur atom participates in glutathione synthesis. “Radical SAMe” enzymes use Fe₄S₄ and SAMe to generate 5'-deoxyadenosyl radicals. In addition SAMe can bind to CBS-domain containing proteins and to specific SAMe riboswitches, structural domains in the non-coding sequences of certain mRNA domains that serve as metabolite-responsive genetic control elements.

together with 50% of methionine metabolism [78, 79].

SAMe molecular structure confers the ability of participating in many biological reactions. The three major types of reactions are transmethylation, transsulfuration, and aminopropylation.

In transmethylation reactions, SAMe serves primarily as the universal methyl donor to a variety of acceptors including nucleic acids, proteins, phospholipids, and biologic amines. Transsulfuration reactions allow the synthesis of GSH, the main antioxidant molecule in the cell, and the aminopropyl group takes part in the polyamine synthesis [80–82]. Together with this, SAMe is able to bind proteins containing cystathione β -synthase (CBS)-domains, in bacteria can bind to genetic regulatory elements called riboswitches and it can take part in radical reactions to generate the oxidizing agents 5'-deoxyadenosyl radicals (Figure 2).

2.2.2. Hepatic SAMe metabolism

As expressed before, unless SAMe is synthesized in all the cells, its main metabolism occurs in the liver. In this organ, 50% of the daily methionine intake is converted into SAMe, and up to 85% of all methylation reactions occur [78]. Figure 3 integrates the main liver SAMe metabolism.

SAMe is synthesized from L-methionine and ATP in a two-step reaction catalyzed by the enzyme methionine adenosyltransferase (MAT) [83]. In mammals, three distinct forms of MAT have been identified: MAT I and MAT III, codified by the gene *MAT1A*, and MAT II, encoded by the gene *MAT2A* [70]. The description of these MAT enzymes and its regulation will be presented later.

SAMe participates in the polyamine biosynthesis [80–82]. Through this pathway, SAMe is decarboxylated by SAMe decarboxylase and the aminopropyl group is transferred first to putrescine for the formation of spermidine, and then to spermidine for the obtaining of spermine. During these reactions two molecules of 5'-methylthioadenosine (MTA) are produced. This

MTA powerfully inhibits polyamine synthesis, being necessary its removal by the MTA/SAH nucleosidase and 5'-methylthioribose (MTR) kinase to restore methionine levels. This process is known as the methionine salvage pathway [84]. It has been proposed that MTA can affect gene expression, proliferation, differentiation and apoptosis [85].

As the major methyl donor in the cell, SAMe participates in more than 40 transmethylation reactions. It consists in the donation of the methyl group to a variety of substrates, including DNA, RNA, histones, proteins and phospholipids [81]. As reaction product, S-adenosylhomocysteine (SAH) is obtained. The methyltransferase responsible of the larger amount of transmethylation reactions is the glycine N-methyltransferase (GNMT), comprising the 1% of the soluble protein in rat liver [70, 86]. The importance of GNMT enzyme is to maintain the ratio SAMe/SAH, which is considered the indicator of the methylation capacity of the cell [87]. To prevent SAH accumulation, SAH hydrolase catalyzes a reversible reaction in which SAH is transformed into homocysteine (Hcy) and adenine [88].

The Hcy can be metabolized by two pathways: remethylation and transsulfuration pathways. In the remethylation pathway, Hcy obtains a methyl group to form methionine, in a reaction catalyzed by two different enzymes: betaine homocysteine methyltransferase (BHMT) that requires betaine, or the methionine synthase (MS) that requires vitamin B12 and normal levels of folate. BHMT is exclusive of liver and renal tissues [89]. The remethylation by the MS is coupled to the folate cycle: 5-methyltetrahydrofolate (5-MTHF) donates the methyl group to the Hcy being converted into tetrahydrofolate (THF). THF is converted into 5,10-methyltetrahydrofolate (5,10-MTHF), and, finally, to 5-MTHF to complete the folate cycle.

Hcy can also undergo the transsulfuration pathway to form cysteine via a two-step enzymatic process catalyzed by cystathione β -synthase (CBS) and γ -Cystationase (γ -CTL), both requiring vitamin B6 as cofactor. The transsulfuration pathway is particularly active in the liver, making SAMe an important precursor of GSH [89, 90].

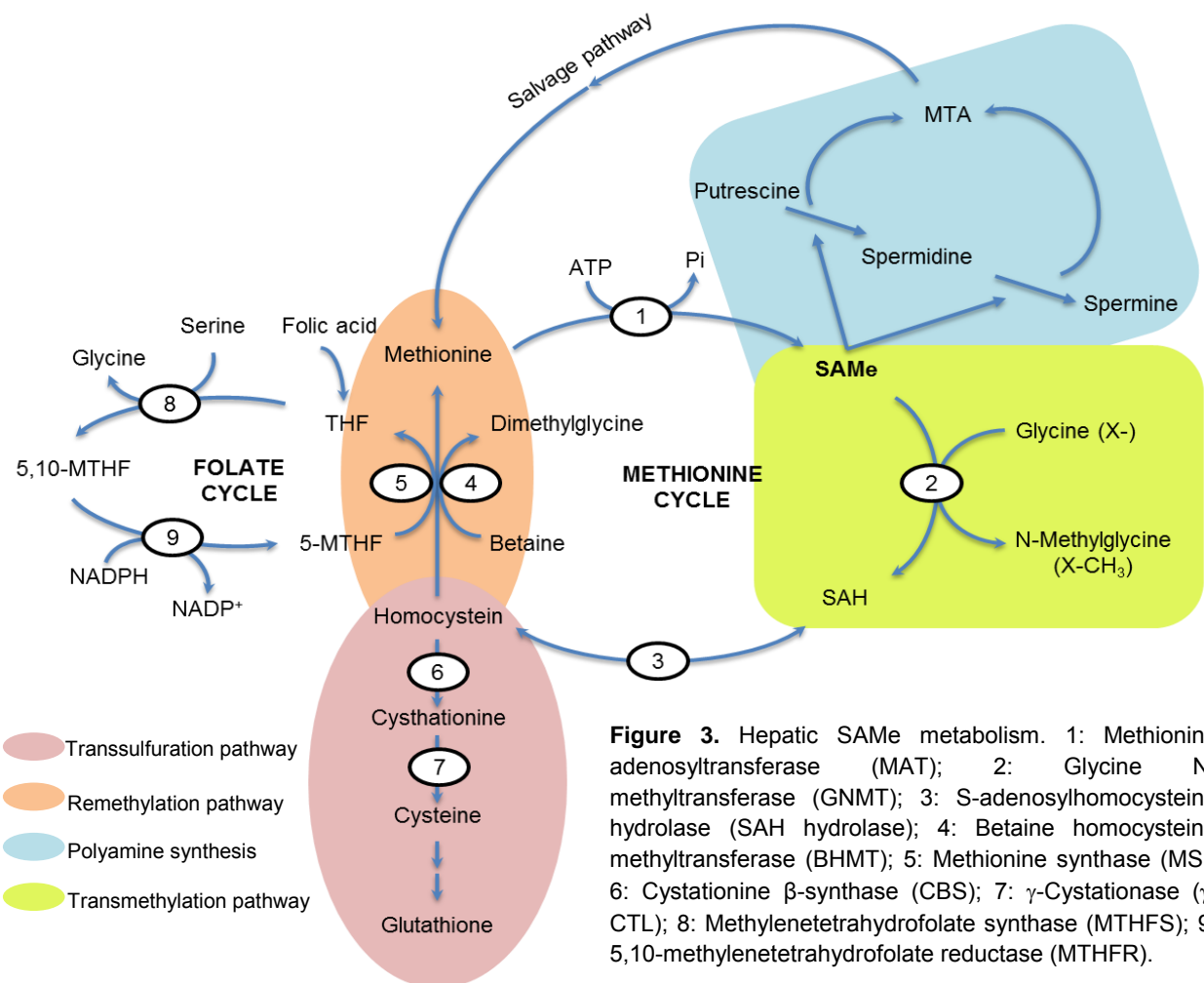


Figure 3. Hepatic SAMe metabolism. 1: Methionine adenosyltransferase (MAT); 2: Glycine N-methyltransferase (GNMT); 3: S-adenosylhomocysteine hydrolase (SAH hydrolase); 4: Betaine homocysteine methyltransferase (BHMT); 5: Methionine synthase (MS); 6: Cystathione β -synthase (CBS); 7: γ -Cystathionase (γ -CTL); 8: Methylenetetrahydrofolate synthase (MTHFS); 9: 5,10-methylenetetrahydrofolate reductase (MTHFR).

In the liver, SAMe inhibits MTHFR and MS, and activates CBS. When SAMe is depleted, homocysteine is channeled to remethylation to regenerate SAMe, whereas when SAMe level is high, homocysteine is directed to the transsulfuration pathway [81, 91].

In the next sections, the enzymes involved in SAMe biosynthesis (methionine adenosyl-transferases) and catabolism (GNMT) will be described in detail.

2.2.3. Methionine adenosyltransferase enzymes

As previously mentioned, SAMe is synthesized by MAT enzymes, being the *MAT* gene one of the 482 genes required for the survival of an organism [83].

In mammals, MAT catalytic subunit is codified by two genes: *MAT1A* and *MAT2A*, encoding for two homologous MAT catalytic subunit, $\alpha 1$ and $\alpha 2$ respectively [83]. *MAT1A* is expressed only in the adult and differentiated liver [92]. The $\alpha 1$ subunit produced by *MAT1A* organizes both into dimers (MAT III) and into tetramers (MAT I) [81, 83]. *MAT2A* gene is expressed in extrahepatic tissues, in the fetal and proliferating liver, and in liver disease [92]. These $\alpha 2$ subunits adopt a tetrameric disposition (MAT II). The $\alpha 1$ and $\alpha 2$ subunits share an amino acid identity of the 84% [83]. Together with these catalytic subunits, there also exists a β regulatory subunit, codified by the gene *MAT2B*, which associates only with MATII enzyme and is expressed in the extrahepatic tissues and during liver development and disease [93, 94] (Figure 4).

2.2.3.1. MAT regulation

As the enzyme responsible for the biosynthesis of SAMe, MAT must be tightly regulated.

a) Regulation of *MAT1A* and *MAT2A* expression

In the developing rat liver, *MAT1A* expression increases progressively from day 20 of gestation, increases 10 fold immediately after birth, and reaches a peak at 10 days of age. Conversely, *MAT2A* expression decreases towards birth, increases threefold in the newborn and decreases further in the postnatal life, reaching a minimum in the adulthood [92]. In consequence, adult liver is characterized by low *MAT2A* expression together with high levels of *MAT1A* and SAMe.

MAT1A can serve as a marker of differentiated hepatocyte, as its developmental pattern is closely related to those of albumin and α -fetoprotein [70]. In addition, it is well established that *MAT1A* gene transcription is turned off in HCC [95], and decreased in patients with a wide spectrum of liver disease [47, 96]. In contrast, *MAT2A* expression is induced in human HCC [95], and in rodents during rapid liver growth and dedifferentiation [97, 98]. This switch from *MAT1A* to *MAT2A* expression facilitates liver cancer cell growth, as demonstrated by the decrease in liver cancer growth when overexpressing *MAT1A* [99]. Similar to *MAT2A*, *MAT2B* also increases in HCC,

which reduces SAMe cellular content, stimulating DNA synthesis [100].

In accordance with this, during liver regeneration caused by hepatotoxins or partial hepatectomy (PH), liver mass loss initiates a cellular proliferative response until original liver mass is restored. During this process SAMe levels decrease coinciding with a decrease in *MAT1A* levels and an increase in *MAT2A* levels [98].

The last scenario where regulation of MAT can be studied takes place during the de-differentiation of the cultured hepatocytes. When primary hepatocytes are isolated from the liver and *in vitro* cultured, spontaneously de-differentiate into fibroblasts [101]. This process is accompanied by a loss in the expression of certain genes [102, 103], a decrease in SAMe levels and a switch from *MAT1A* to *MAT2A* expression. The addition of SAMe to the culture medium can exert a protective effect in the reduction of *MAT1A* expression and in the maintenance of the hepatocyte differentiation [101].

It has been found that this regulation of the expression of *MAT1A* and *MAT2A* genes is related to changes in the methylation status of *MAT1A* and *MAT2A* promoters and acetylation of the histones associated to these promoters [70]. *MAT1A* promoter is methylated at two CpG sites in extrahepatic tissues and fetal liver, but unmethylated in adult liver, where the gene is actively transcribed. Accordingly, the degree of

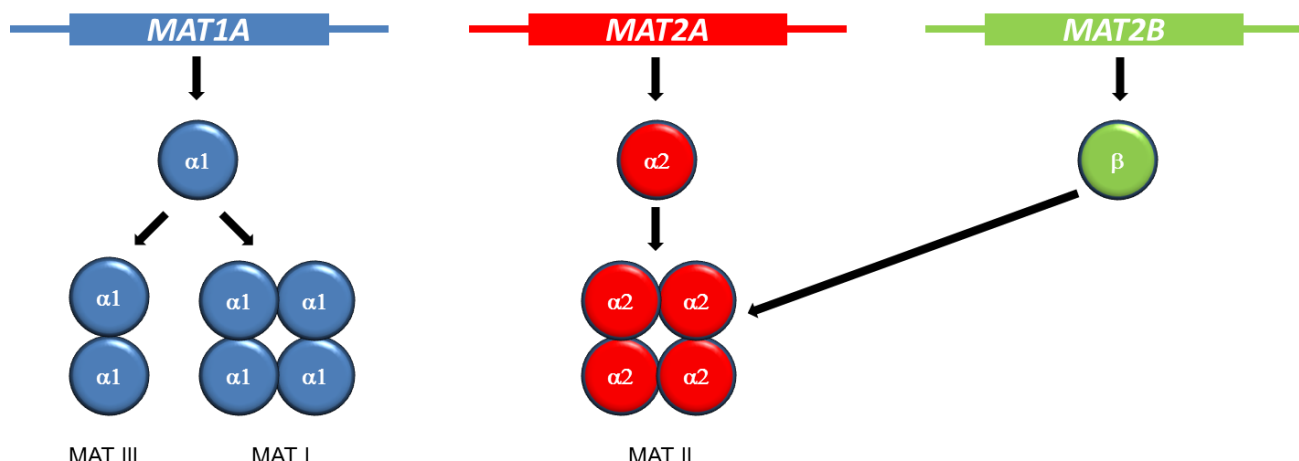


Figure 4. MAT coding genes and enzymes. The catalytic subunit of MAT is codified by *MAT1A* and *MAT2A* genes. *MAT1A* encodes for the $\alpha 1$ subunit that adopts dimeric (MAT III) or tetrameric (MAT I) conformation. The $\alpha 2$ subunit, codified by the gene *MAT2A*, adopts a tetrameric disposition (MAT II). The gene *MAT2B* encodes the regulatory β subunit that associates with MAT II enzyme.

acetylation of the H4 histones associated to the *MAT1A* promoter is approximately 15-fold higher in the liver than in the kidney [104, 105]. The same occurs in liver cancer cell lines and in human liver cirrhosis, which are hypermethylated in *MAT1A* promoter.

In the case of *MAT2A*, there are no differences in the promoter methylation between liver and other tissues, but they exist between normal liver and liver cancer, being *MAT2A* promoter hypomethylated in HCC [106]. The acetylation of the histones related to *MAT2A* promoter is also reduced in normal liver compared to other tissues and liver cancer [107].

b) Regulation of MAT enzymatic activity

Each MAT isoform possesses its own kinetic and regulatory properties, and sensitivity to different inhibitors.

MAT I and MAT II have relatively low K_m for methionine ($23\mu M$ - $1mM$ and 4 - $10\mu M$, respectively), whereas MAT III has the highest K_m ($215\mu M$ – $7mM$) [108]. The activity of MAT enzyme is also modulated by the product of the catalytic reaction, SAMe. Normal cellular concentration of SAMe is able to inhibit MAT II strongly ($IC_{50} = 60\mu M$), and minimally MAT I ($IC_{50} = 400 \mu M$) and even stimulates MAT III up to 8-fold at $500\mu M$ SAMe) [109]. Thus, in cells expressing only MAT II isoenzyme, SAMe levels should be relatively unaffected by methionine fluctuations, because of the inhibitory feedback. In contrast, SAMe synthesis and levels increase in the cells expressing MAT I/III with increasing methionine availability [79]. In the case of β regulatory subunit, its interaction with $\alpha 2$ catalytic subunit lowers MAT II K_m for methionine and increases the sensitivity of the enzyme to the feedback inhibition of SAMe. Therefore, regulation of β subunit expression may be a mechanism to regulate the intracellular content of SAMe [110, 111].

Finally, both MAT I and MAT III enzymatic activity can be regulated by nitric oxide (NO) and reactive oxygen species (ROS). The nitrosylation (formation of a $-SNO$ group) by the NO, and the oxidation (formation of $-SOH$) by ROS of a single cysteine residue on position 121, switch the enzymes to an inactive conformation [70]. Cysteine 121 is located over the active site of the

enzyme, and its nitrosylation and oxidation makes the active site less accessible to the substrates. As a consequence, there is remarkable decrease in MAT I/III activity, together with depletion of SAMe content [112–114]. This enzymatic inactivation can be reversed by the physiological concentration of GSH [113]. In MAT II this inactivation does not occur, as 121 position corresponds to a glycine residue. NO and ROS increase during processes like liver regeneration, where a transient reduction in SAMe levels is necessary.

2.2.4. Glycine N-methyltransferase enzyme

GNMT is a tetrameric protein composed by four identical subunits. It is localized in the cytosol of the cell [115] and catalyzes the transmethylation reaction in which SAMe donates the methyl group to glycine to produce sarcosine. In mammals, it is present in large amounts in liver (1–3% of cytosolic protein) and in exocrine pancreas and prostate (0.4% of cytosolic protein) as well as tissues active in secretion (proximal kidney tubules, submaxillary glands, intestinal mucosa, cortical neurons, and Purkinje cells of the brain) [116]. GNMT is not present or is present in minimal amounts in embryonic liver, but it is strongly expressed after birth [116].

GNMT expression has been observed downregulated or even completely blocked in liver and prostate tumors [117, 118], in most cells and in some preneoplastic lesions correlating with the poor prognosis. Also some individual with *GNMT* mutations have spontaneous liver disease [72, 73].

First discovered as a folate binding protein, GNMT activity is known to be inhibited by it. [119]. Upon binding, GNMT suffers a conformational change that makes less accessible the active site for SAMe [116]. Because SAH is a potent inhibitor of most methyltransferases [120], the intracellular ratio of SAM to SAH is considered to be an important index of transmethylation potential [121, 122]. GNMT is a key protein in transmethylation because it is believed to function in the regulation of the SAM:SAH ratio: under conditions of excess of methionine, SAMe content increases. SAMe is able to inhibit MTHFR, leading to a decrease in the content of 5'-MTHF. This reduction in 5-MTHF reduces its inhibition on GNMT which can convert the excess in SAMe into SAH. Conversely, methionine deficient conditions favor synthesis of

5-MTHF and inhibition of GNMT, thereby increasing SAMe levels and conserving methyl groups for important transmethylation reactions [123].

2.2.5. Biological functions of SAMe in the liver

SAMe levels are related to the growth and differentiation status of the hepatocytes. SAMe participates in essential biological processes such as hepatocyte proliferation, liver regeneration, differentiation, cell death and apoptosis. Molecular functions of SAMe in the cell will be described in this section.

2.2.5.1. SAMe regulation of hepatocyte growth

a) SAMe blocks hepatocyte growth factor-induced hepatocyte growth

Hepatocyte growth factor (HGF) is the most potent of liver mitogens that plays a role in hepatocyte proliferation [124, 125]. Through binding to c-Met receptor, HGF exerts pleiotropic effects on various mitogenic signaling cascades [126], such as: Ras/extracellular signal-regulated kinase (ERK)/mitogen activated protein kinase (MAPK), phosphatidylinositol-3 kinase (PI3K)/AKT, Rac/Pak and Crk/Rap1 [127, 128].

HGF/c-Met pathway is essential for DNA synthesis after liver injury [126] but also in cultured hepatocytes [129]. In HGF induced hepatocyte proliferation is of great importance the activation of the Ras/ERK/MAPK cascade. Downstream ERK activation, the up-regulation of D-type cyclins controls cell cycle progression by accelerating the late G₁ phase progression [130, 131].

In cultured hepatocytes, SAMe treatment has been described to block cell growth by inhibiting HGF-induced hepatocyte proliferation [129]. The molecular mechanism by which SAMe blocks both HGF-dependent expression of cyclin D1 and D2 and DNA synthesis does not affect ERK phosphorylation. In contrast, it is related with the blockade of a non-canonical signaling pathway by which HGF mediates hepatocyte proliferation. This pathway involves the liver kinase B1 (LKB1)/AMP-activated protein kinase (AMPK)/endothelial nitric oxide synthase (eNOS) axis [132].

AMPK is a highly conserved serine/threonine kinase, and the energy sensor of the cell. AMPK maintains the cellular energy homeostasis by coordinating catabolic and anabolic processes through direct effects on gene transcription and key metabolic enzymes [133].

AMPK is activated under conditions of energy stress, including glucose deprivation, hypoxia, oxidative damage and heat shock [134]. It can also be induced by exercise, hormones and the antidiabetic drug metformin [133]. Once activated, AMPK inactivates ATP-consuming enzymes (proteins, lipids and glycogen synthesis) and activates ATP generating processes (glycolysis and lipid oxidation). AMPK is regulated by changes in the ratio AMP/ATP, sensitive indicator of the energy state of the cell [135]. AMP binds to AMPK promoting a conformational change that makes threonine 172 (Thr172) less accessible to the phosphatases [135, 136]. Phosphorylation of Thr172 is absolutely necessary for AMPK different upstream kinases [137] (Figure 5).

The major upstream kinase of AMPK is LKB1. LKB1 phosphorylates AMPK at Thr172 after change in AMP/ATP ratio, regulating AMPK glucose and lipid metabolism in the liver [138, 139]. Other kinases phosphorylate AMPK in an AMP/ATP ratio independent manner such as Ca⁺⁺-calmodulin dependent protein kinase kinase (CaMKK) that phosphorylates AMPK Thr172 in response to an increase in Ca⁺⁺ content [140, 141]. Other kinases able to phosphorylate AMPK Thr172 are transforming growth factor-β (TGFβ) activated kinase 1 (TAK1) [142, 143], and ataxia

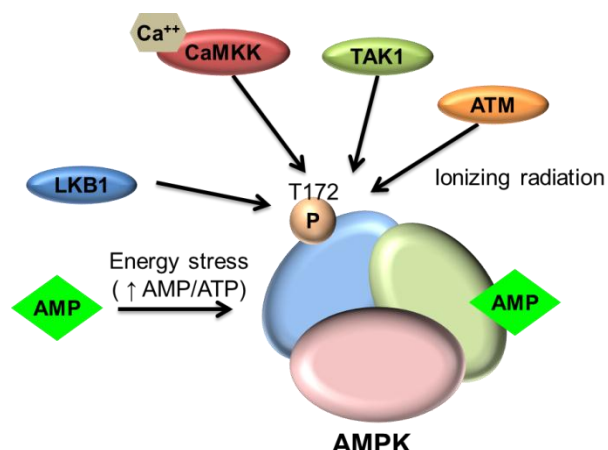


Figure 5. Regulation of AMPK by energy stress and upstream kinases.

telangiectasia mutated (ATM) kinase in response to double-stranded DNA breaks [144].

eNOS is the last member of the LKB1/AMPK/eNOS pathway. There are three nitric oxide synthases (NOS): neuronal (nNOS), inducible (iNOS) and endothelial (eNOS). Both iNOS and eNOS are present in hepatocytes and are related with liver diseases [145, 146]. Nitric oxide (NO) plays a crucial role in hepatocyte proliferation, and the induction of NO blocks the cytotoxic effect of TNF α during the priming of the liver proliferation [147]. AMPK-mediated HGF induction of NO production by eNOS results into iNOS induction [148–151], obtaining a higher amount of NO that, as commented before, is able to inactivate MAT I/III, decreasing SAMe levels [114, 129].

In hepatocytes, it has been found that HGF-induced AMPK activation promotes the nucleo-cytoplasmic shuttling of the RNA binding protein HuR (Human antigen R). HuR is a RNA binding protein that increases the half-life of target mRNAs related with cell cycle progression, proliferation, stress and apoptosis. SAMe can prevent the AMPK dependent translocation of HuR from the nucleus to the cytosol in response to proliferative stimuli, as SAMe methylates protein phosphatase 2A (PP2A), which dephosphorylates AMPK inactivating it. As a consequence, HuR remains in the nucleus and cell cycle progression is blocked [152]. A more extensive description of HuR RNA binding protein will be provided in section 2.3.1.

In accordance with this regulation, a novel non-canonical LKB1/AMPK/eNOS pathway has been proposed in the hepatocyte proliferation [132]. According with this, when hepatocytes proliferate, HGF induces phosphorylation of LKB1, AMPK and eNOS. Phosphorylated AMPK promotes HuR translocation to the cytosol, inducing cell cycle progression and hepatocyte proliferation. eNOS activation leads to an increase in NO levels that induce iNOS, which further contributes to the increase in NO. High levels of NO inactivate MAT I/III, reducing the levels of SAMe, which in turn prevents the activation of the protein phosphatases, further increasing the activation of the LKB1/AMPK/eNOS cascade (Figure 6).

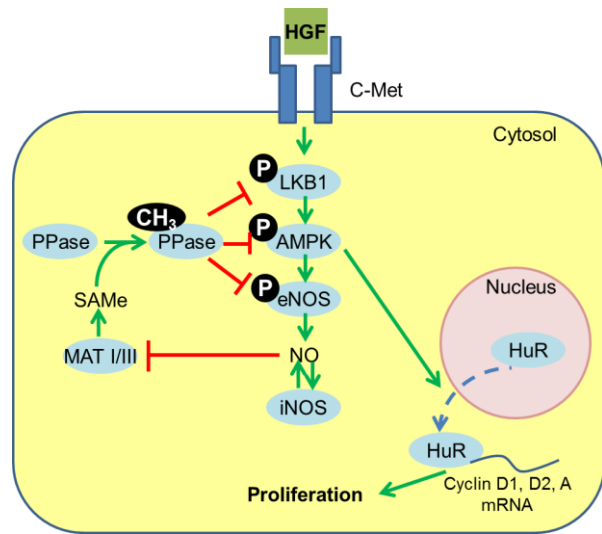


Figure 6. Model of the non-canonical LKB1/AMPK/eNOS pathway implicated in hepatocyte proliferation. Adapted from [132].

b) Liver regeneration

Liver, skin, gut and bone marrow are unique organs because they heal by regeneration as opposed to repair. In the case of the liver, the response involves not only stem cells, but also existing hepatocytes [153]. Repopulation after acute liver failure depends on the differentiation of the progenitor cells, in contrast, after CCl₄ treatment or PH removing 2/3 of liver mass, normal quiescent cells go to a series of steps leading finally to the restoration of the original liver mass [154]. Liver regeneration can be considered as a process of compensatory growth as it does not follow the same general steps in true regenerative processes [154].

Liver regeneration is a complex process coordinating several signaling networks composed by cytokines, growth factors and metabolic networks between hepatic cell populations, which links liver function with cell growth and proliferation [124, 154]. A characteristic feature of these networks is that redundancy exists among the intracellular components of each network, such that loss of an individual gene rarely leads to complete inhibition of liver regeneration [154]. The hepatic cell populations involved in liver regeneration include hepatocytes and non-parenchymal cells: kupffer cells (resident macrophages), endothelial cells (allow contact between circulation blood and hepatocytes), biliary

epithelial cells (from the bile duct), progenitor cells (repopulates in case of attenuated hepatocyte proliferation) and hepatic stellate cells (activated and differentiated into myofibroblasts after liver damage). Through a sequence of distinctive pathways that are known to vary according to circadian rhythms, liver cells proliferate until the organ recovers the original mass and architecture [124, 125, 154–156].

Experimentally, PH is the most widely extended procedure for assessing liver regeneration in animal models. PH consists in the surgical removal of the 2/3 parts of the liver tissue. The original technique was developed by Higgins and Anderson in rats, and must be modified in mice to be safely and reproducibly performed [157].

In contrast of cells of proliferative tissues, hepatocytes are resting cells in G₀ phase (quiescent), and must enter into G₁ for the regenerative process. In this direction, during the first few hours after PH, it takes place a *priming phase* (Figure 7A and 7B black arrows). In this early stage, after PH or liver injury, Kupffer cells induce nuclear factor kappa B (NFκB) signaling pathway, in response to proinflammatory mediators and tumor necrosis factor α (TNFα) [158–161]. The induction of NFκB leads to the expression of the cytokines interleukin-6 (IL6) and TNFα, which are secreted activating the neighbor hepatocytes. The activation of the hepatocytes comprises the induction of the transcription factor NFκB, JAK/STAT3 (janus kinase/signal transducer and activator of transcription 3) pathway and

intracellular signaling pathways that involve mitogen activated protein kinase (MAPK).

The activation in the hepatocytes of the NFκB pathway also stimulates IL6 production, which in turn enhances STAT3 pathway activation and the early response genes, together with the progression from quiescent to proliferative hepatocytes [124].

NO plays an important role in early stages after PH. NO is produced in kupffer cells and in hepatocytes in response to iNOS activation after cytokines effects [162]. Kupffer cells are the responsible of NO production in the beginning, but hepatocyte production is more sustained in the time. NO protects cells from the pro-apoptotic effect of TNFα via caspase-3 [163, 164]. In other hand, nitric oxide inactivates MAT I/III, blocking the ATP consuming process of SAMe production, being able to employ ATP to liver regenerative process [70]. In this moment, hepatocytes are sensitized to the proliferative effects of the growth factors.

During the *proliferative phase* (Figure 7A and 7B green arrows), the primed hepatocytes progress through the cell cycle in response to growth factors stimulus such as insulin growth factor I (IGF-I), epidermal growth factor (EGF) transforming growth factor α (TGFα) and hepatocyte growth factor (HGF). HGF is mainly synthesized by the hepatic stellate cells (HSC), and is considered the central stimulation for the hepatocyte cell cycle progression [125]. Secreted to the blood as inactive precursors, growth factor

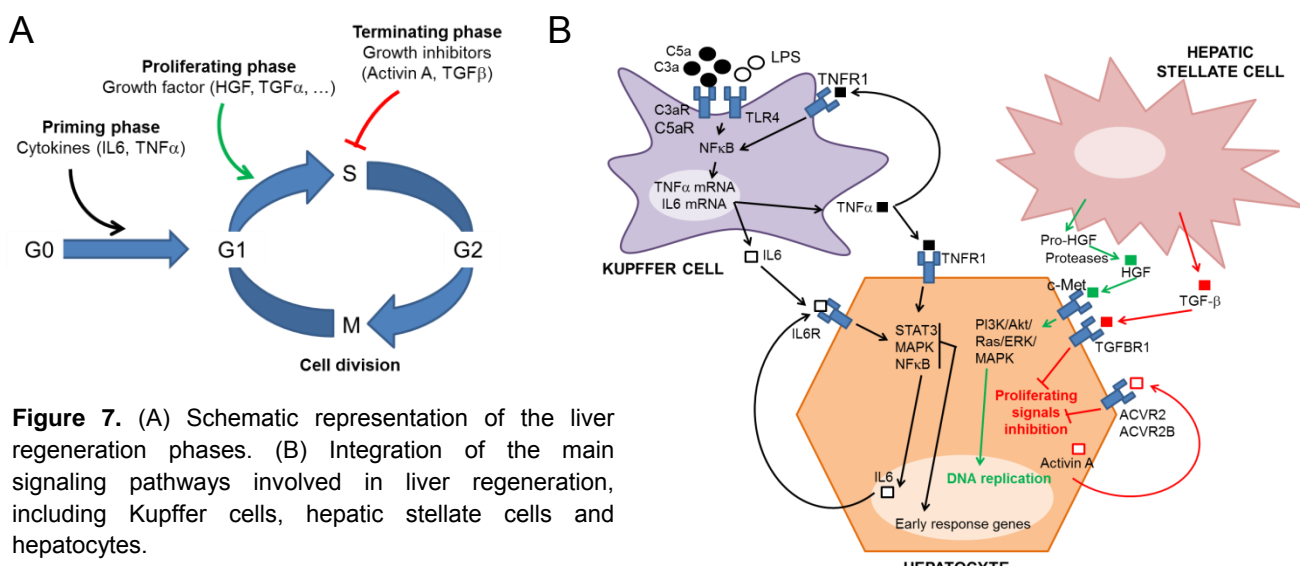


Figure 7. (A) Schematic representation of the liver regeneration phases. (B) Integration of the main signaling pathways involved in liver regeneration, including Kupffer cells, hepatic stellate cells and hepatocytes.

are cleaved and activated by proteases of the extracellular matrix within 5 minutes after PH. The binding to the corresponding receptors promotes a signaling cascade that drives hepatocytes into cell cycle transition from G₁ to S phase, DNA replication and mitosis. In hepatocytes, DNA synthesis begins 12 hours after PH, and reaches a maximum at 24 hours [124, 165].

Through a *remodeling phase*, liver recovers its architecture due to the action of the endothelial cells, the biliary epithelial cells and the synthesis of the extracellular matrix. Finally, there is a *terminating phase* (Figure 7A and 7B red arrows) by which quiescent and inhibitory factors (TGF β) produced by hepatic stellate cells, and activin A produced by hepatocytes, inhibits proliferation processes.

Cellular content of SAMe dramatically decreases after PH, coinciding with the increase in DNA synthesis and the induction of the early response genes [98]. The administration of SAMe prevents DNA synthesis in hepatocytes after PH [132, 165]. The non-canonical pathway LKB1/AMPK/eNOS is also activated within 30 minutes after PH, and maintained during 24 hours. The pretreatment with SAMe blocks this pathway, decreasing the proliferation and impairing the regenerative response [132].

2.2.5.2. SAMe regulation of hepatocyte and hepatoma cells apoptosis

In addition to the hepatocyte growth, SAMe is also able to regulate hepatocyte apoptotic response. Although SAMe protects against okadaic acid-induced apoptosis in normal hepatocytes, it induces apoptosis in hepatoma cell lines such as HepG2 and Huh7 via mitochondrial death pathway [166]. The SAMe product in the polyamine synthesis MTA also recapitulates SAMe effects on apoptosis.

There exist at least two methods by which SAMe exerts different apoptotic effects on normal versus cancerous cells. One of them is mediated by the apoptotic protein Bcl-x_S [167]. It is known that SAMe and MTA treatment upregulate Bcl-x protein in hepatoma cell lines. Bcl-x is alternatively spliced into two major mRNAs and protein: Bcl-x_S, which is proapoptotic, and Bcl-x_L, antiapoptotic. The treatment with SAMe or MTA induces selectively the levels of Bcl-x_S in HepG2 cell, but

has no effect in normal hepatocytes [167]. This alternative splicing is modulated by the protein phosphatase 1 (PP1) [168]. Both SAMe and MTA increase the steady state of the catalytic subunit of PP1, inducing Bcl-x splicing into Bcl-x_S.

Another mechanism for SAMe and MTA to exert proapoptotic effect in liver cancer cells is their ability to transcriptionally inhibit the expression of BHMT [169], the enzyme responsible of the regeneration of Hcy to methionine. Impairment in Hcy metabolism can result in endoplasmic reticulum stress, which can lead into apoptosis [170]. Importantly, SAMe and MTA have no effect on the expression of BHMT in normal hepatocytes (Lu, unpublished observations, 2007).

2.2.6. SAMe treatment in liver disease

The importance of SAMe to normal hepatic physiology, together with the depletion of SAMe in the development of liver disease, led to the study of the therapeutic effects of SAMe treatment on animal models of liver disease.

SAMe administration to animal model of alcoholic liver disease such as ethanol-fed rats and baboon, and in rat models of liver injury caused by CCl₄, has been reported to increase MAT activity and GSH concentrations, ameliorating liver injury including fibrosis [68, 81, 171].

Also treatment with SAMe has been tested for protecting rat liver from the development of HCC after hepatocarcinogen administration, exerting a protective effect [172]. In addition, the induction of MAT1A expression in liver cancer cells has been proved to increase SAMe content, reduce tumor growth and slightly increase apoptosis [173].

A variety of clinical studies indicate that SAMe treatment can be effective in liver disease, particularly in the less advanced stage of the diseases. More studies in patients with liver disease are necessary to better define SAMe role as a therapeutic agent [70].

In summary, SAMe has been shown to be fundamental in liver proliferation process and in liver disease. In order to study the direct impact of the impairment of SAMe regulation in the liver, two

knockout (KO) mouse models have been developed: MAT1A-KO and GNMT-KO mice.

2.2.7. Mouse models of liver disease with altered hepatic SAMe levels

2.2.7.1. Chronic deficiency in SAMe: MAT1A-KO mouse model

In order to study the effects in the liver of the chronic deficiency of SAMe, it was developed a mouse lacking *MAT1A* gene. These mice are deficient in MAT I/III enzymes and present a reduction in hepatic levels of SAMe (74% compared to the wild type mice). These mice also present markedly increased serum methionine levels and decreased GSH content (40%) [48].

As a compensatory response, *MAT2A* gene expression is increased, but due to the kinetic properties of the MAT II enzyme the hepatic levels of SAMe are not restored. Other genes from the methionine metabolism are also overexpressed, such as nicotinamide N-methyltransferase, *BHMT* and *CBS*, suggesting that in the liver SAMe level regulates the expression of a number of genes involved in methionine metabolism [48].

The results obtained in this mouse are in accordance with the observation that SAMe and *MAT1A* levels are related with the differentiation status of the liver, and lack of this gene can predispose to liver injury. Knockout mice present increased expression of genes related with cell proliferation, as *MAT2A*, α -fetoprotein (AFP) and proliferation cell nuclear antigen (PCNA). According with this increased expression of growth related genes, at 3 months of age mice exhibit increased liver weights [48].

These mice are also more susceptible to develop liver steatosis when fed with a choline deficient diet during 6 days, and develop fatty liver and periportal inflammation at eight month with normal diet [48]. In addition, altered expression of genes involved in acute phase response, oxidative stress and lipid and carbohydrates metabolism was detected [174]. In accordance, MAT1A-KO mice present hyperglycemia and elevated hepatic triglycerides. Together with this, there is an increase in liver peroxidation and oxidative stress, as indicated by the overexpression of CYP2E1 (cytochrome P450 2E1) and the uncoupling protein 2 (UCP2), both influencing generation of ROS

[174]. This increased oxidative stress and decrease of GSH predispose the mice to liver injury in response to treatment with CCl₄ and ethanol. All these impairments lead at 18 months of age to the spontaneous development of HCC [174].

Unless proliferative genes are increased, liver regeneration after 2/3 PH is impaired. MAT1A-KO mice are able to respond to TNF α and IL6 in the *priming phase* after PH, but after this, there is a defect in the progression in G₁ phase and in the response to growth factors. Even though MAT1A-KO mice present basal proliferative status and hyperphosphorylation of LKB1, AMPK, ERK, c-Jun and increased cyclin D1, all of them essential during the regeneration, these proteins together with eNOS fail to increase after PH [175]. When studying MAT1A-KO isolated hepatocytes, it was found a loss of responsiveness to the mitogenic stimulus HGF [175].

All of these evidences suggest that the chronic reduction in the hepatic levels of SAMe lead to liver disease, predispose to HCC and impair the capacity of the liver to regenerate.

2.2.7.2. Chronic excess in SAMe: GNMT-KO mouse model

The identification of individuals presenting natural mutations in *GNMT* gene and mild liver disease, together with the observations that GNMT enzyme is absent in HCC and downregulated in patients infected with HCV and alcohol-induced cirrhosis, supported the hypothesis that the high SAMe levels are hepatotoxic. These observations led to the development of a GNMT knockout mouse model [176].

GNMT-KO mouse present 35-fold increase in hepatic SAMe levels, and SAMe/SAH ratio increases about 100-fold [176]. The SAMe/SAH ratio is indicative of the methylation capacity of the cell, and its increase is related with aberrant methylations [49]. These mice also present elevated methionine and transaminases, and spontaneously develop steatosis, fibrosis, and HCC. This supports the concept that GNMT is a tumor susceptibility gene for liver cancer and that reduced GNMT activity may be an early event in the development of HCC [49].

The increased SAMe level in the liver makes these mice an epigenetic model characterized by global DNA hypermethylation and gene promoter methylation. Consequently, some member of the Ras-association domain family (RASSF) and suppressor of cytokine family (SOCS), inhibitors of the Ras and JAK/STAT pathways, are inactivated by methylation of their promoters. This reduction in the suppressors leads to Ras, MEK (mitogen-associated/extracellular regulated kinase), ERK, cyclin D1 and cyclin D2 hyperactivation, what provides proliferative and survival advantages [49].

The processes altered in these mice that correlate with the liver pathogenesis observed are oxidative stress, inflammation and lipid metabolism [177]. The treatment of the GNMT-KO mice with nicotinamide (NAM), the substrate of the NAM N-methyltransferase (NNMT) that uses SAMe to form N-methylnicotinamide, reduces the excess of SAMe in the liver. This reduction is accompanied by decrease in the global DNA methylation, decreased Ras pathway and decreased signs of steatosis and liver fibrosis compared to the wild type mice [177].

In conclusion, these two mouse models, characterized by increased or reduced SAMe levels, lead to liver disease and finally HCC, supporting the idea that SAMe levels in the liver must be tightly controlled.

2.3. RNA BINDING PROTEINS IN RELATION WITH LIVER DISEASE, HCC AND LIVER PROLIFERATION

As previously shown, SAMe metabolism must be tightly regulated, according to specificity of the tissue, developmental stage of the liver, proliferating status of the liver, and liver disease and malignant transformation. Specifically, *MAT1A* and *MAT2A* expression patterns are tightly regulated in the liver, but the molecular mechanisms underlying these processes are not well understood.

It is known that *MAT1A* and *MAT2A* are transcriptionally regulated by a different promoter methylation and histone acetylation pattern according with the tissue [105], but it does not completely explain the regulation in the liver during development, liver disease and malignant

transformation, and through cultured hepatocyte de-differentiation.

Moreover, methionine conversion into SAMe regulates *MAT2A* expression at the level of mRNA turnover [100]. This could point towards a regulation in which RNA binding proteins (RBPs) are involved. RBPs regulate the turnover and translation of the mRNAs by recognizing specific RNA sequences and binding to them. Between these specific sequences, we can find conserved sequences called AU-rich elements (AREs), present in the 3'UTR of the mRNAs and involved in mRNAs degradation, translation and localization [178, 179]. AREs coordinately regulate networks of chemokine, cytokine, and growth regulatory transcripts involved in cellular activation, proliferation, inflammation and disease, including malignant transformation. ARE-mediated regulation is carried out by RBPs, whose activity is regulated in a cell type and activation-dependent manner [180].

Focusing on the RBPs, some of them control one specific post-transcriptional process: for example, tristetraprolin (TTP), butyrate response factor 1 (BRF1), KH-type splicing regulatory protein (KSRP) selectively accelerate mRNA degradation [181–184]. However, most of RBPs, including AU-rich RNA binding factor 1 (AUF1), T-cell intracellular antigen 1 (TIA-1) and TIA-1-related (TIAR), participate in both mRNA turnover regulation and translation [185, 186]. In addition, RBPs usually function together, cooperating, competing or sequentially binding to target mRNAs. Actually, the RBPs, as many disease-associated factors, are encoded by mRNAs containing sites for the binding of RBPs, being regulated by themselves or other RBPs [186].

Between the RBPs, there are some that bind to mRNAs stabilizing them or enhancing their translation, and others that function as mRNA destabilizers or blocking the translation. Among the first group, we can find the human embryonic lethal abnormal vision (Hu/elav) family, which are the best known RBPs that selectively recognize and bind to AREs. HuR, the most ubiquitous member of the Hu/elav family, has been found to interact with dozens of mRNAs, many of them encoding proteins linked to specific pathologies [186]. In the liver, as explained before, AMPK-dependent HuR translocation from the nucleus to

the cytosol has been found to be essential in the cell cycle progression during hepatocyte proliferation [152].

In contrast with these mRNA stabilizing proteins, a number of other RBPs, including TTP, BRF1, KSRP, and the AU-rich RNA binding factor 1 (AUF1), bind to mRNAs destabilizing them [186]. Among these, AUF1 [187] binds to mRNAs encoding for mitogenic, immune and stress responses and cell cycle regulatory proteins, and its deregulation has been implicated in carcinogenesis [188, 189].

2.3.1. The RNA-binding protein HuR: functions, implications in cancer and regulation

First described in Drosophila as *elav*, the mammalian Hu/elav family of RBPs comprises the ubiquitous HuR, and the primarily neuronal HuB, HuC and HuD. The neuronal Hu have been implicated in neuronal development, neuronal plasticity and memory [190, 191]. HuR, also called ELAVL1 (ELAV-like 1), was identified in 1996 [192], and initially described to stabilize ARE-containing mRNAs [193]. After this, it has been also shown to modulate the translation, both enhancing and inhibiting it [185, 194].

2.3.1.1. HuR general structure

HuR protein contains three RNA recognition motifs (RRMs), in an identical arrangement to the other Hu/elav proteins [192], through which these RBPs bind to the target mRNAs, and a hinge region between RRM2 and RRM3 (Figure 8). All three RRMs are conserved among the four Hu family members, indicating to be essentials for the protein function, whereas the hinge region differs [195]. Each individual Hu member is highly conserved among vertebrates, and in the case of HuR, the human protein is 99,7% identical to mouse, 98,2% to chicken and >90% to *Xenopus* [195–197].

The HuR hinge region (amino acids 186-244) has a basic sequence similar to the classical nuclear localization signal (NLS), that was identified to possess both NLS and nuclear export sequence (NES) activities [198]. This sequence is, therefore, involved in the shuttling of HuR from the nucleus to the cytosol, and received the name of HuR Nucleocytoplasmic Shutting (HNS) domain

[198]. Although HuR is a predominantly nuclear protein, it has been shown to exert its function by translocating from the nucleus to the cytosol in response to stimulus, a process in which HNS domain and several transport mechanisms are involved (see section 2.6.1.3.b).

2.3.1.2. HuR function

HuR is predominantly nuclear, but its mRNA stabilizing function and the modulation of the translation are linked to the translocation to the cytosol [194]. Recently, by integrating the results from high-throughput technology (PAR-CLIP, RIP-chip and whole transcript expression profiling) studying HuR targets, it has been proposed that, in the nucleus, HuR also possess the ability to regulate pre-mRNA processing, including alternative splicing, regulate the export of mature mRNAs (Figure 9), and can also antagonize microRNA (miRNA)-mediated repression of miRNAs proximal to HuR binding sites [199, 200].

Focusing in the best characterized HuR functions exerted in the cytoplasm, HuR can promote three kinds of effects over the bound mRNAs: mRNA stabilization, mRNA translation upregulation and repression of mRNA translation (Figure 9).

a) Stabilization of target mRNAs

HuR-stabilized target mRNAs include those that encode p21, c-fos, VEGF, the MAPK phosphatase (MKP)-1, iNOS, granulocyte / macrophage colony-stimulating factor (GMCSF), sirtuin 1 (SIRT1), TNF α , B-cell lymphoma-2 (Bcl2), myeloid cell leukemia-1 (Mcl1), cyclooxygenase-2 (COX-2), γ -glutamylcysteine synthetase heavy subunit (γ -GCSH), urokinase-type plasminogen activator (uPA) and its receptor (uPAR), p53, interleukin (IL)-3, and cyclins A2, B1, E1, and D1 [186, 201].

The exact mechanisms by which HuR is able to stabilize labile mRNAs is not well understood, but is believed that the binding of HuR to the mRNAs block the binding of other RBPs or miRNAs that can recruit cellular structures for mRNA degradation (exosome, processing bodies or RISC complex) [202–206].

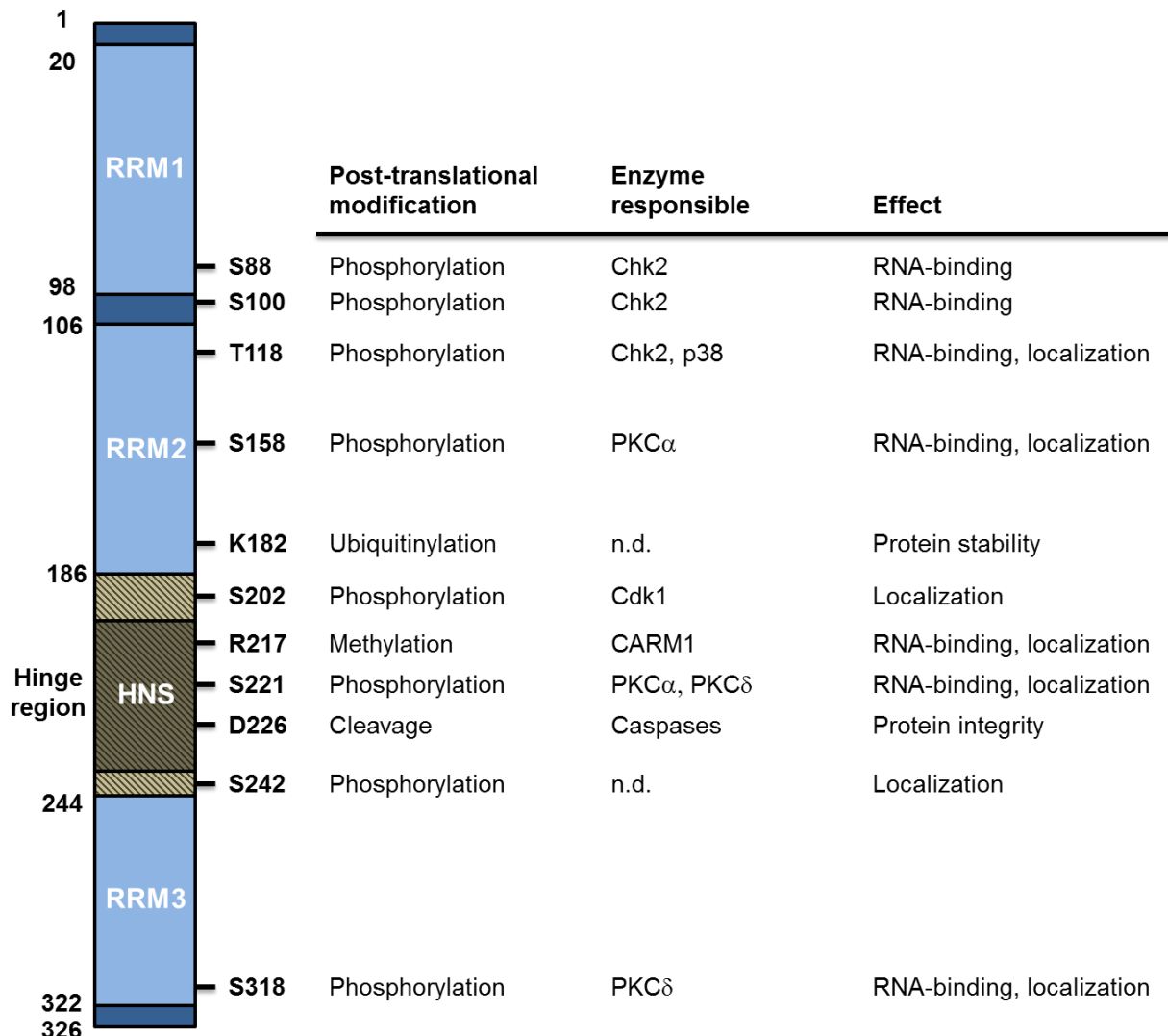


Figure 8. Schematic representation of HuR protein and its posttranslational modifications by cancer-related enzymes. The HuR RNA recognition motifs and the hinge region containing the HuR nucleocytoplasmic shuttling (HNS) domain are indicated. The posttranslational modifications, enzyme responsible and effects of the modification are listed. n.d., not determined. (Modified from [201]).

b) Upregulation of mRNAs translation

HuR also promotes the translation of several target mRNAs, many involved in disease processes, such as those that encode the hypoxia-inducible factor (HIF)-1 α , p53, prothymosin α (PTMA), MKP-1, cytochrome c, heme oxygenase-1, and cationic amino acid transporter 1 (CAT-1) [186, 201].

It is also unclear how HuR is able to promote the translation. In some cases, HuR was proposed to interfere with internal ribosome entry sites (IRESs) in the 5'UTRs of target mRNAs directly enhancing the translation (such as *XIAP*) [207]; in other cases, its effects on translation were due to

competition with repressor RBPs or with microRNAs/RISC complex (e.g., cytochrome c mRNAs) [208–210].

c) Repression of mRNAs translation

There is also a small subset of target mRNAs encoding disease-associated proteins which translation is inhibited by HuR. HuR binds to the 5'UTR of p27, the type I insulin-like growth factor receptor (IGF-IR), or the 3'UTR of Wnt5a and c-Myc, and represses their translation [186, 201]. The mechanisms seem to be the disruption of IRESs in the case of p27 and IGF-IR [211, 212], and the recruitment of let-7/RISC complex for c-Myc [213].

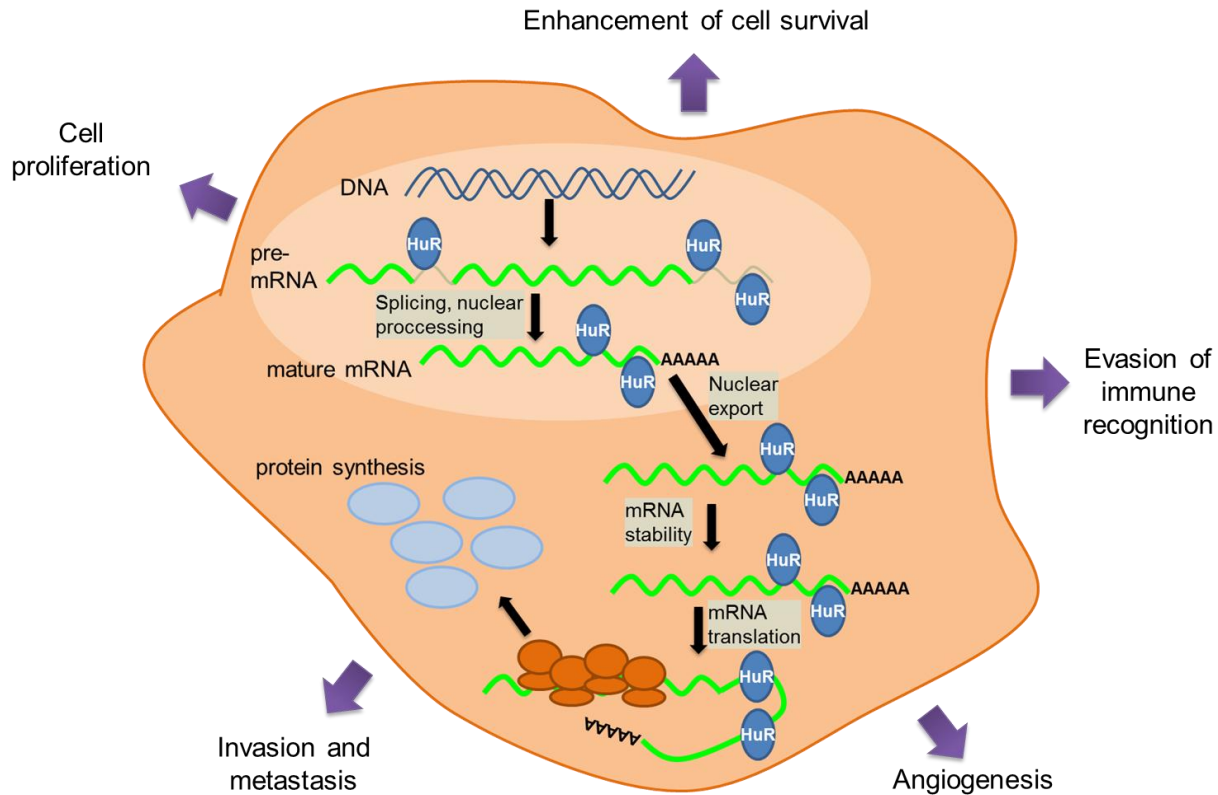


Figure 9. HuR influence on target gene expression. In the nucleus, HuR binds to the pre-mRNAs participating in their splicing and nuclear processing and collaborates with the mRNA export. In the cytosol HuR enhances mRNA stability and translation in the polysomes. In the case of malignant transformation, the effects over HuR targets enhance cell proliferation, cell survival, evasion of immune recognition, angiogenesis, invasion and metastasis. Adapted from references [200, 201].

2.3.1.3. Regulation of HuR function

According with the involvement of HuR in many important biological processes, its function must be tightly regulated at many levels: abundance and integrity of the protein, subcellular localization and post-translational modification.

a) Regulation of HuR abundance

The levels of HuR protein are regulated in many ways.

- Transcriptional regulation.** The transcriptional regulation of HuR is not well understood, but it is known to be positively regulated by the transcription factor NF κ B. In this regulation, it has been described that in gastric tumors, HuR overexpression depends on a mechanism in which PI3K/AKT signaling pathway activation increased p65/RelA binding to a putative NF κ B binding site in the HuR promoter, increasing its transcription [214].

- HuR auto-regulation.** HuR protein is able to bind to *HuR* mRNA, in the same way that many RBPs bind to their own encoding mRNAs [215]. Among the different mRNA polyadenylation variants of *HuR* mRNA, HuR is able to bind to and stabilize a long *HuR* mRNA containing a distal ARE. This is opposed by the mRNA decay of TTP [216].

In addition to this regulation, HuR was also found to associate with the 3'UTR of the *HuR* mRNA and upregulated HuR translation by promoting the nuclear export of *HuR* mRNA [217].

- Downregulation of HuR by microRNAs.** HuR mRNA is the target for two miRNAs: miR-519 and miR-125a. miR-519 binds to a sequence in the coding region (CR), repressing HuR protein biosynthesis at the translational level, but not reducing mRNA abundance. This reduction in HuR protein leads to diminished cell division, enhanced cellular senescence and suppresses tumor growth in xenograft models [218–220].

Similarly, miR-125a associates with the 3'UTR of *HuR* mRNA inhibiting *HuR* translation. In breast cancer cell lines, miR-125a overexpression reduced cell growth by dramatically suppressing cell proliferation and migration, and promoting apoptosis [221].

- ***HuR ubiquitination.*** In response to moderate heat shock, the levels of *HuR* transiently and potently decrease. This abundance reduction is linked to the ubiquitination of the K182 residue present in the RRM2 (Figure 8). This degradation leads to a proteasome-mediated degradation of *HuR* protein that, in fact, enhances cell survival to the heat shock stimulus. The phosphorylation of *HuR* by Chk2 at residues S88, S100 and T118 antagonizes heat shock dependent *HuR* decay [222]. Whereas ubiquitination is involved in *HuR* protein degradation, the machinery involved in enhancing *HuR* protein stability remains obscure.

- ***Caspase-mediated HuR cleavage.*** Recently it was described a new mechanism by which *HuR* contributes to stress-induced cell death. After lethal stress, *HuR* translocates to the cytoplasm and associates with the apoptosome activator pp32/PHAP-I. In the cytoplasm, *HuR* is caspase-mediated cleaved at aspartate 226 as a regulatory step contributing to an amplified apoptotic response [223]. In response to staurosporine apoptotic stimulus, *HuR* cleavage involves the apoptotic pathway FADD/caspase-8/caspase-3, obtaining two cleavage products (*HuR* CP-1, 24 kDa and *HuR* CP-2, 8 kDa) that are capable of promoting apoptosis [224]. In muscle cells, *HuR* CP-1 has been shown to interact with transportin 2 blocking the *HuR* nuclear import. This leads to an accumulation of *HuR* in the cytoplasm that promotes the myogenesis [225].

b) Regulation of *HuR* localization

Although *HuR* is predominantly nuclear, the best characterized *HuR* functions take place in the cytoplasm. As mentioned before, the *HuR* HNS domain present in the hinge region is required for the *HuR* nucleocytoplasmic shuttling [198]. Together with this sequence, several transport machinery components are also necessary. Transportin 1 and transportin 2 have been identified as redundant nuclear import factors for *HuR* [226, 227]. Together with this, the nuclear export factor CRM1 (chromosome region

maintenance 1) has been involved in the *HuR*-bound mRNA nuclear export, in cooperation with the *HuR* ligands pp32 and APRIL [228].

HuR nucleocytoplasmic transport is influenced by the action of kinases (Cdk1, AMPK, PKC and p38) that phosphorylate *HuR* and *HuR* transport proteins, as explained in next section.

c) Phosphorylation and methylation

Together with the ubiquitination previously explained, *HuR* is also posttranslationally modified by several kinases and by methylation. These modifications affect the subcellular localization (mainly when the modification is closed to the HNS) and the binding affinity of *HuR* (mainly if the modification occurs in the RRMs) (Figure 8) [186]. The main *HuR* modifying enzymes are the next:

- **Chk2.** After oxidative stress damage, Chk2 is activated, phosphorylating *HuR* in S88, S100 and T118. S88 and T118 are within RRM1 and RRM2 domains, and their phosphorylation seem to increase the *HuR* binding affinity, probably because of conformational changes in these regions; on the other hand, S100 is located between RRM1 and RRM2 and reduces the binding affinity, perhaps by regulating RRM1 and RRM2 relative distance. In particular, after oxidative damage Chk2-dependent phosphorylation on S100 reduces the binding to *SIRT1* and other mRNAs, lowering cell survival after oxidant treatment [229].

- **Cdk1.** The G2-phase kinase Cdk1 phosphorylates *HuR* at S202 in synchronous G2-phase cultures. The phosphorylation promotes the retention of *HuR* in the nucleus, in a process that involves the association with 14-3-3 proteins in the nucleus. Under stress conditions (UVC radiation, chemical inhibition...), Cdk1 decreases, *HuR* is unphosphorylated, and the protein can translocate to the cytosol, where it binds to mRNAs encoding proliferative and anti-apoptotic proteins [230].

- **PKC.** *HuR* is a substrate for protein kinase C. PKC α phosphorylates *HuR* at S158 and S221 in response to ATP treatment, which leads to an increase in cyclooxygenase-2 (COX-2) mRNA stability and subsequent increase in prostaglandin E2 synthesis in renal cells. This process modifies the vasoconstriction and regulates the glomerular filtration rates [231].

PKC δ also phosphorylates HuR in response to angiotensin II, in this case at S221 and S318. HuR phosphorylation allows the protein to translocate to the nucleus, binding to cyclin A, cyclin D1 and COX-2 mRNAs. In human mesangial cells, this regulation is responsible of the inhibition of cell migration [232, 233].

- **p38.** In response to DNA damage such as γ radiation, p38 MAPK phosphorylates HuR at T118. This results in HuR cytoplasmic accumulation and stabilization of the p21 mRNA. The enhancement in p21 levels lead to G1 arrest, which corresponds with a p53-independent mechanism at the G1/S checkpoint [234].

- **CARM1.** In addition to the phosphorylations, HuR can also be methylated in R217 by the methyltransferase CARM1 (coactivator-associated arginine methyltransferase 1). Lipopolysaccharide (LPS) activation of macrophages promotes the methylation of HuR in R217 within the HNS domain, which is thought to promote HuR translocation and the stabilization of *TNF α* mRNA, involved in the inflammatory response [235].

2.3.1.4. HuR and cancer traits

Hu/elav family was among the first RBPs implicated in carcinogenesis. The earliest reports of HuR elevated in cancer proceed from brain and colon cancer, correlating with enhanced expression of COX-2, VEGF, TGF β and IL8 [186]. After this, subsequent studies revealed HuR elevated levels in most malignancies: breast, colon, stomach, kidney, pancreas, esophagus, prostate, skin, lung, etc. [236]. HuR has been proposed to play a causal role in tumor development, since HuR overexpression in carcinoma cells increased the tumor formation in xenograft experiments, and HuR reduction limited the tumor size [236]. Numerous HuR-regulated mRNAs have been identified to directly contribute to the acquisition of the cancer traits, including enhanced ability to proliferate, enhanced cell survival, elevation of local angiogenesis, evasion of immune recognition, and invasion and metastasis (Figure 9) [201].

a) Enhanced cell proliferation

Cancer cells must divide actively for promoting the growth of the tumor. This trait is

accompanied by altered abundance of cell cycle regulators that decrease cell division times. HuR binds to the mRNAs of many cell cycle regulators, particularly cyclins. In addition, HuR overexpression suppresses the cellular senescence [201]. Among the cyclins stabilized by HuR, we can find cyclin D1, which elevation is related with the shortening of G1 phase; cyclin E1, critical for the progression through G1/S transition; cyclin A2, which promotes progression through the S phase; and cyclin B2, a key factor for progression through G2 phase [186, 201]. The stabilization of these cyclins by HuR has been detected in many types of cancers, such as human cervical carcinoma cells, breast cancer cells and colon cancer.

Other cell cycle regulatory proteins influenced by HuR are p27, which translation is repressed by HuR binding, allowing cell proliferation; EGF, that stimulates cell growth and division; and eukaryotic translation initiation factor 4E (eIF4E), which is related with transformation and enhancement of tumorigenesis [186, 201].

In summary, the stabilization by HuR of the mRNA of factors enhancing the cell cycle progression, and the repression of factors inhibiting it, lead to accelerate cell division and proliferation.

b) Enhanced cell survival

Tumor cells develop under stress conditions such as oxidative stress, reduced nutrients availability and reduced access to growth factors. Thus, is important for them to avoid the cell-death and apoptotic signals. HuR helps cancerous cells in the acquisition of these traits by regulating the expression of proapoptotic and antiapoptotic signals.

Between the mRNAs of antiapoptotic proteins stabilized by HuR, we can found *prothymosin α* (*PTMA*), which inhibits the formation of the apoptosome in cells committed to apoptotic death; *B-cell lymphoma-2* (*Bcl-2*) and *Myeloid cell leukemia-1* (*Mcl-1*), two similar proteins that inhibit cytochrome c release from the mitochondria; *SIRT1*, which deacetylates proapoptotic proteins such as p53, Foxo and Ku70, suppressing their activities; and *Mdm2*, that inactivates p53 targeting it to proteasome-mediated degradation [201].

On the other hand, HuR inhibits the translation of the proapoptotic c-Myc transcription factor [213].

Taken together, the repression of proapoptotic factors, together with the increase of antiapoptotic factors exerts a potent antiapoptotic influence in cancer cells.

c) Elevation of local angiogenesis

In order to expand, tumor cells need to develop vasculature to allow the arrival of nutrients and oxygen. HuR both promotes proangiogenic factors and represses antiangiogenic factors. HuR promotes translation of HIF-1 α , a transcription factor that activates several genes essential for cell adaptation to hypoxia, and also enhances the translation of VEGF and COX-2 related with proliferation, migration and angiogenesis. On the other hand, in some breast cancers, the expression of the tumor suppressor and inhibitor of angiogenesis Thrombospondin 1 (TSP1), usually enhanced by HuR, loses this regulation, leading to a decrease in TSP1 levels [186, 201].

In summary HuR develops an angiogenic program in cancer cells.

d) Evasion of immune response

The immune system is able to eliminate tumor cells. Therefore, cancer cells have developed mechanisms to avoid the recognition of the immune cells. HuR stabilizes and enhances the translation of MKP-1, which potently suppresses immune function. In addition, *TGF β* , which has been found to promote tumor growth by allowing tumor cells to escape from the immune system, is also posttranscriptionally regulated by HuR.

e) Invasion and metastasis

Cancer cells can acquire the ability to invade adjacent tissues and colonize distant tissues. This implicates interaction with its environment and with the extracellular matrix. HuR stabilizes the mRNA and increases the translation of proteins that confer these capacities. In particular, HuR stabilizes the mRNA of the transcription factor *Snail*, which promotes the epithelial-to-mesenchymal transition (EMT) associated to metastasis; HuR also stabilizes the mRNAs of *matrix metalloproteinase-9* (*MMP-9*), and

urokinase-type plasminogen activator (uPA) and *uPA receptor (uPAR)* involved in the cleaving and degradation of the extracellular matrix, affecting cell adhesion, invasion and metastasis. Thus, HuR increases invasion and angiogenesis by promoting the degradation of the extracellular matrix and the proteins that enhance the EMT [201].

2.3.1.5. Implication of HuR in specific cancer types

Taking into account the regulation of the cancer traits above described, numerous studies have examined the levels of HuR in individual cancer types.

In breast carcinomas, elevated cytoplasmic HuR level correlates with the tumor grade and the poor prognosis. In breast cancer cells, HuR increased expression of cyclin E1, IL8, estrogen receptor, TSP1, and c-fms, and repressed the translation of Wnt5a, a protein that inhibits tumor growth. HuR was identified as an important prognostic factor in a subset of breast cancers [201].

In pancreatic cancer, high HuR levels correlate with high VEGF levels and with poor prognosis, unless after treated with the chemotherapeutic gemcitabine, HuR high levels are associated with improved survival [186].

In ovarian carcinomas, HuR levels are found elevated, together with COX-2 levels. The same relation is detected in prostate cancers, together with high levels of SIRT1 and EGF. In these cancers, again high HuR levels are related with poor prognosis [186].

Increased expression of HuR in colon cancer tissues enhanced the expression of COX-2 and VEGF, while the cytoplasmic abundance of HuR was associated with advanced tumor stage. In a nude xenograft model, the overexpression of HuR increased the growth of colon cancer cells [201].

HuR was also found upregulated in oral, lung, gastric, pharyngeal and nervous system cancers.

The role of HuR in hepatocarcinogenesis has also been reported, with the finding of an increased presence of HuR in the liver of cirrhosis and HCC patients, together with a prominent increase of the cytosolic localization [236]. Also

HuR has been found highly expressed in the HCC-derived SAMe-D cell line, in which it stabilizes HAUSP mRNA. HAUSP is an ubiquitin specific protease that stabilizes p53 in the cytosol blocking the cell cycle arrest and the apoptotic response [56].

Finally, it has been recently found a relationship between HuR and cirrhosis, which highly increases the risk of HCC development. According to this study, HuR silencing in a cholestatic liver injury model (biliary duct ligation) reduces expression of proinflammatory and chemoattractant genes, leading to decreased liver damage, oxidative stress, inflammation, macrophage infiltration and liver fibrosis development [237]. Moreover, HuR has been shown to regulate hepatic stellate cells activation, by mediating the response of two of the main hepatic stellate cell activators, PDGF and TGF β . All these data suggest that HuR has a significant role in fibrosis development after liver injury by controlling hepatic stellate cells activation, in addition to liver damage and inflammation [237].

2.3.2. The RNA-binding protein AUF1: functions, regulation and implications in cancer

The AU-rich RNA binding factor 1 (AUF1, also hnRNP D) was first identified by Brewer in 1991, with the identification and characterization of a factor that selectively bound to the c-Myc ARE destabilizing its mRNA [238]. The factor was identified as two polypeptides with 37 and 40 kDa copurified with fractions of postribosomal supernatant [238]. Later, this factor, which received the name of AUF1, was purified and cloned [187]. Further studies determined that AUF1 is codified by a gene in which the alternative splicing can render four alternative transcripts, corresponding with a family of proteins designated by their molecular masses p37, p40, p42 and p45 [239]. The four isoforms present different functional and regulatory properties, but, with some exceptions, promote decay of target mRNAs. As HuR, AUF1 is ubiquitously expressed and predominantly nuclear, but its activity destabilizing target mRNAs is linked to the translocation to the cytosol [240, 241].

2.3.2.1. AUF1 general structure

AUF1 consists of two RNA binding domains (RBDs) through which it binds to target mRNAs, together with a high content of glycine in the C-domain [241]. The sequence comparison shows a highly conserved protein, with 98,9% similarity between humans and mice, which suggests the critical function of AUF1 [242].

In addition, AUF1 possesses an amino acid sequence in the C-terminal tail that acts both as NLS and NES, involved in the nucleocytoplasmic shuttling. This region receives the name of hnRNP D nucleocytoplasmic shuttling sequence (DNS). Two separate regions of the DNS, the C-terminal and the N-terminal, are essential for nuclear import by transportin 1 [241].

2.3.2.2. AUF1 function

AUF1 is predominantly nuclear, but its function is related with the cytoplasmic translocation. In the nucleus, it has been shown to bind to pre-mRNAs before alternative splicing, being proposed that AUF1 can participate in the nuclear processing (alternative splicing and maturation of 5' and 3' ends) [243]. It has also been described that the import of AUF1 to the nucleus is a prerequisite to bind to target mRNAs and control their turnover in the cytoplasm [244].

The functions AUF1 exerts in the cytoplasm can be divided in three main classes: destabilization of mRNAs, stabilization of mRNAs and enhancing of mRNA translation.

a) Promoting of mRNA decay

The first described AUF1 function was to promote the decay of target mRNAs. It is also the best characterized function. AUF1 binds to mRNAs codifying for proteins such as c-Myc, Bcl-2, c-Fos, IL10, IL3, p21, cyclin D1 and TNF α [238, 245–249].

AUF1 has no nuclease activity and is not able to degrade mRNAs by itself. For exerting its function, it has been proposed that the interaction with other proteins is necessary. Some of these proteins are factors involved in the recruitment of the mRNA degradation machinery, such as translation initiation factor eIF4G, chaperones hsp27 and hsp70, heat-shock cognate protein

hsc70, lactate dehydrogenase and poly(A)-binding protein [250]. The ubiquitin-conjugating enzyme E2I and three RNA binding proteins (NSEP-1, NSAP-1 and IMP-2) have been also identified as AUF1 interacting proteins. Between them, NSEP-1 has demonstrated endonuclease activity *in vitro* which points towards an implication of these proteins in AUF1-induced mRNA decay [251].

b) mRNA stabilization

In some cases, AUF1 is also involved in the stabilization of mRNA targets, such as parathyroid hormone (PTH) and alpha-globin [252, 253]. The exact mechanism in which AUF1 participates is not clear; in the case of alpha-globin, AUF1 has been identified as a component of a multiprotein stability complex [253].

c) Increase of mRNA translation

Finally, AUF1 is also related with the increase of the translation of Myc proto-oncogene by a mechanism in which AUF1 competitively binds to Myc mRNA avoiding the binding of TIAR, a Myc translational suppressor [254].

2.3.2.3. AUF1 function regulation

There is a regulation of AUF1 function linked with its alternative mRNA splicing, rendering four different molecular weight proteins, and also mature mRNAs with different 3'UTRs. In addition, we can find AUF1 being regulated by nucleocytoplasmic shuttling and posttranslational modifications.

a) Regulation by different AUF1 isoforms expression

The four AUF1 isoforms present a different ARE-binding affinity, with the rank order p37>p42>p45>p40. The two isoforms with higher binding affinity exert the higher effect on mRNA stability. Thus, the selective expression of the different AUF1 isoforms differentially regulates mRNA turnover [255, 256]. In relation with this, it has been proposed a model in which the isoforms with less binding affinity compete with p37 and p42 when their abundance increase; the decrease in the abundance of p45 and p40 allows the other two isoforms to gain access to the target mRNAs, regulating them. Thus, the alterations in ARE mRNA stability regulated by AUF1, might be due

to alteration in the relative abundance of the different AUF1 isoforms [257].

b) Regulation of AUF1 expression via alternatively spliced 3'UTR

The mRNA of AUF1 has been found to present alternative splicing in its 3'UTR. These splice variants are generated by selective excision of the introns 8 and 9 and the exons 8 and 9, and proposed to subject AUF1 mRNA to differential turnover regulation [258, 259].

c) Regulation by AUF1 nuclear import and export

AUF1 appears as a predominantly nuclear protein, but its functions are linked with the cytoplasmic translocation. AUF1 shuttling is linked to a mechanism involving the binding of transportin 1 to the DNS domain [241]. This process takes place in different ways depending on the AUF1 isoforms. The nuclear import sequences are only found in the two smaller isoforms, whereas nuclear export sequences are only present in the larger ones. It has been suggested that the isoforms could form heterocomplexes facilitating the translocation [260]. Thus, the regulation of the shuttling of the different isoforms can regulate the functionality of AUF1.

d) Post-translational modifications

It has been demonstrated that AUF1 is post-translationally modified by phosphorylation, affecting the binding and the turnover of target mRNAs, and by ubiquitination, controlling AUF1 protein stability.

The p40 AUF1 isoform is reversibly phosphorylated in S83 and S87 when associated to the polysomes [261]. This phosphorylation regulates the mRNA turnover by modifying ARE-binding affinity, and remodeling local RNA structures, altering the subsequent recruitment of factors involved in mRNA decay [262].

In the case of ubiquitination, p37 and p40 are ubiquitin conjugated, whereas p42 and p45 are not modified. The difference between isoforms is due to the presence in p42 and p45 of a C-terminal exon 7 that is able to block the ubiquitination. This ubiquitination controls the abundance of p37 and p42 through rapid proteasomal degradation,

regulating the amount of total AUF1 and also the relative amount of the splicing variants [263].

2.3.2.4. AUF1 in cancer

AUF1 regulates the expression of many key players in cancer, including proto-oncogenes, regulators of apoptosis and cell cycle, and pro-inflammatory cytokines. In addition, AUF1 overexpression in murine models enhances tumorigenesis, and AUF1 appears to be upregulated in some tumors [264].

In example, AUF1 has been found to allow IL10 increase in malignant melanoma cells after AUF1 reduction, protecting them from apoptosis and immune system recognition [247]; in leukemia cells exposed to UVC, AUF1 enhances the turnover of *Bcl-2*, playing a role in the apoptotic process [245]; in neoplastic lung tissue, AUF1 cytoplasmic abundance correlates with tumor growth rate [189]; finally, in thyroid carcinoma, AUF1 disturbs the stability of mRNAs encoding cyclin-dependent kinase inhibitors, leading to uncontrolled growth and progression of tumor cells [265].

As commented before, the regulation of these mRNAs is influenced by AUF1 isoform distribution, subcellular localization and post-translational modifications. In this respect, the cascades modulating AUF1 function are deregulated in some types of cancers [264].

In order to study the influence of AUF1 deregulation *in vivo*, transgenic mice overexpressing p37 isoform of AUF1 were developed. These mice spontaneously develop tumors containing high levels of *c-myc*, *c-fos*, *c-jun* and *cyclin D1*, showing that the deregulation of AUF1 leads to tumorigenesis [188].

Both HuR and AUF1 are good candidates for regulating the turnover of *MAT1A* and *MAT2A* mRNAs, and for being implicated in the processes of liver differentiation, hepatocyte proliferation, liver regeneration and hepatocyte malignant transformation. An extensive description of their regulation will be reported in the Results Section 5.1.

2.4. NEDDYLATION: PROTEIN-STABILIZING POST-TRANSLATIONAL MODIFICATION

The ubiquitin-like (UBL) molecule NEDD8 (neural precursor cell-expressed developmentally downregulated-8) is the protein involved in the NEDDylation, a post-translational modification of the proteins involved in several processes such as cell growth, viability and development. NEDD8 was identified in 1992 as a neural precursor cell-expressed, developmentally downregulated (NEDD) gene [266]. The analysis of the sequence found a 60% amino acid identity between NEDD8 and Ub, and the ability to conjugate to substrates with a conjugation pattern different from Ub [267]. NEDD8 appears as mainly nuclear, and is highly conserved in most eukaryotes and expressed in most tissues, suggesting an important function among eukaryotic cells [268].

The effects of the NEDDylation in proteins are diverse, including the induction of conformational changes, stimulation of enzymatic activity, disruption of the interaction with other proteins, competition with other modifications such as ubiquitination, recruitment of NEDD8 interacting proteins and protecting proteins from destabilization [268, 269].

2.4.1. NEDD8 conjugating cascade

Similar to Ub, NEDD8 attaches covalently to a lysine in the target protein. Analogous to Ub, the NEDD8 conjugation cascade (NEDDylation) involves E1, E2, E3 and deNEDDylating enzymes. NEDD8 is first synthesized as a precursor that is processed at the Gly76 residue by deNEDDylating enzymes. NEDP1 (NEDD8 protease 1, also known as DEN1 and SENP8) and UCH-L3 (Ubiquitin carboxyl-terminal hydrolase L3) are the NEDD8 specific deNEDDylases able to process the NEDD8 precursor. After this, the C-terminal glycine of NEDD8 is activated by the E1 NEDD8-activating enzyme (NAE), which is composed of APP-BP1 (APP binding protein 1) and Uba3 (ubiquitin-like modifier activating enzyme 3) heterodimer. Activated NEDD8 is transferred to the E2 NEDD8-conjugating enzymes, Ubc12 or Ube2f, and then, an E3 NEDD8 ligase transfers NEDD8 to the Lysine on substrates (Figure 10) [270]. NEDD8 E3s include Rbx1 and Rbx2, Mdm2, c-CBL, FBXO11 and DCN1 [271–275].

NEDD8 chains are beginning to be elucidated. Poly-NEDD8 and NEDD8-Ub chains are known to exist, but their functionality is unknown [270].

Protein NEDDylation is reversed by NEDD8 isopeptidases, in a process that is known as deNEDDylation. The best characterized NEDD8 isopeptidase is a subunit of the COP9 signalosome (CSN), CSN5, which possess the catalytic activity [268]. The cysteine protease NEDP1, involved, as commented, in the processing of the NEDD8 precursor, also functions as specific NEDD8 deNEDDylase, deNEDDylating cullins with less activity than CSN, and non-cullin proteins [276, 277].

2.4.2. NEDD8 substrates

Until recently, the only known substrates for the NEDDylation were the members of the cullin family of proteins [268].

Through direct biological approaches or proteomic techniques, it is evident that NEDD8 conjugates to a broader spectrum of proteins. The Mdm2 oncogene, the p53 tumor suppressor protein and its homologue p73, the von Hippel-Landau protein, the EGF receptor, the breast-cancer-associated protein 3 (BCA3) and a subset of ribosomal proteins have also been described as NEDD8 substrates [269, 273, 274, 278–281].

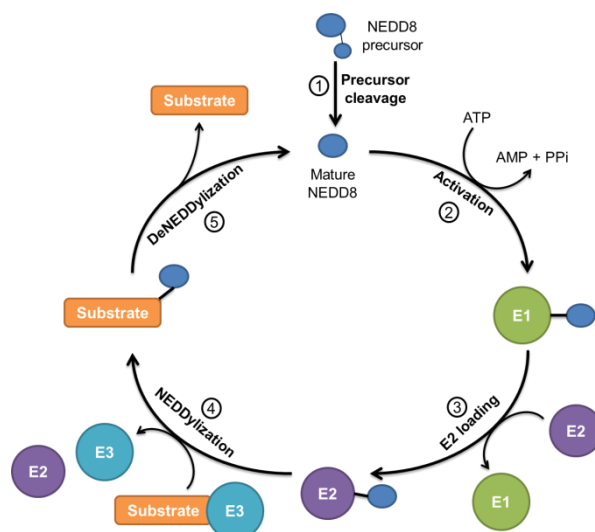


Figure 10. NEDD8 conjugation cascade. NEDD8 precursor is cleaved (1) to obtain the mature NEDD8, which is activated (2) by NAE and loaded into an E2 enzyme (3). Then, an E3 ligase conjugates NEDD8 to the substrate (4). The deNEDDylating enzymes reverse the process (5). Adapted from [268].

Interestingly, NEDDylated proteins seem to be either substrates or components of ubiquitin E3s, for example, p53 and p73 are both NEDDylated and ubiquitinated on several lysines by the RING-domain protein Mdm2, which also self-NEDDylates [274, 281].

2.4.2.1. Cullin family

Cullins function as scaffolds for the ubiquitin E3 protein ligases and interact with RING finger proteins to enable the recruitment of E2 enzymes [282]. These cullin-RING ligase complexes (CRLs) target numerous substrates for ubiquitination, which is increased by NEDDylation, and thus have an impact on cellular processes such as cell growth, development, signal transduction, transcriptional control, genomic integrity and tumor suppression [283]. The deNEDDylation by CSN has the opposite effect, inactivating the ubiquitination activity. Interestingly, the CRL NEDDylation and deNEDDylation cycles are important to maintain the ubiquitination activity, as deletion of CSN inactivates CRL activity [270].

2.4.2.2. Mdm2 and p53

Murine double minute-2 (Mdm2) is a RING finger E3 ligase amplified in many human cancers [284, 285]. Mdm2 is the specific inhibitor of p53, as Mdm2 poly-ubiquitinates p53 C-terminal region, targeting p53 for proteasomal degradation [286, 287]. At the same time, in the nucleus p53 enhances the transcription of the *Mdm2* gene, establishing a feedback regulation by which p53 levels are always under equilibrium [288]. Under stress conditions such as DNA damage, Mdm2 is phosphorylated, what promotes its self-ubiquitination and avoids the binding and degradation of p53 that translocates to the nucleus stimulating the transcription of genes involved in cell cycle arrest, apoptosis and DNA repair [289].

Xirodimas demonstrated that Mdm2 promotes the NEDDylation of p53, attenuating its transcriptional activity [274]. Unless Mdm2 is able to ubiquitinate and NEDDylate p53, these two processes are regulated by different mechanisms, as demonstrated by the evidence that Tip60 acetyltransferase, a regulator of Mdm2-p53 axis, inhibits Mdm2-mediated NEDDylation but not ubiquitination [290]. NEDD8 ultimate buster 1 (NUB1) protein, a NEDD8 interacting protein, decreases p53 NEDDylation promoting mono-

ubiquitination and p53 nuclear export, thus involving NEDDylation in the cellular localization of the proteins [291]. Also the F-box protein FBXO11 represses p53 transactivation activity by NEDDylation [271].

Mdm2 also NEDDylates itself, in a reaction with similar characteristics to the self-ubiquitination, that significantly increases its stability. Chemotherapy induced NEDP1 deNEDDylates Mdm2 promoting the activation of p53 [274, 292].

Finally, Mdm2 also NEDDylates the ribosomal protein L11, controlling its stability and localization. NEDP1 relocates L11 from the nucleus to the nucleoplasm, providing a signal for p53 activation [269, 293, 294].

2.4.3. NEDD8 relation with cancer

As commented above, the NEDDylation of many substrates (cullins, p53, Mdm2, p73, BCA3, L11 ribosomal protein, EGFR) is related with tumorigenesis [270].

Many of the substrates of the CRL have been involved in cancer; the misregulation of the CRLs NEDDylation modifies the ubiquitination of their substrates, thus producing impairment in DNA replication, cell cycle progression, stress responses, etc. As an example we can find the temperature sensitive mutation in the ts41 Chinese hamster ovary cell line that affects to the NEDD8 conjugation pathway. At the non-permissive temperature, cells pass through successive S phases without mitosis, accumulating DNA through multiple replications. This is due to the lack of NEDDylation of CRL4a^{DDB1-cdt2} and CRL1Skp2 cullins, that in normal conditions ubiquitinate the Cdt-1 replication licensing factor to ensure appropriate DNA replication only once per cell cycle [295].

Other NEDD8 substrates different from cullins are well characterized for its role in tumorigenesis when misregulated, including p53, Mdm2, BCA3 and von Hippel landau protein. Unless NEDDylation function in many of them is not well characterized, a deeper study could show the relation of their NEDDylation with cancer.

Recently, it was generated an inhibitor of the NAE, MLN4924, that blocks substrate

NEDDylation. This molecule has been shown to promote S-phase defects, DNA damage and apoptosis in colorectal tumoral cells, and also inhibited tumor growth in xenograft assays. Also, MLN4924 was shown to have tumor growth inhibiting properties in acute myeloid leukemia cells in vitro and in xenograft assays, concomitant with increases in key CRL substrates, including IκBα [270].

Due to the number of oncoproteins and tumor suppressor targets of NEDD8 conjugation cascade, and the CRLs whose activity is regulated by NEDD8, MLN4924 appears as a promising anticancer drug.

Taking in consideration the role of HuR in liver tumorigenesis and its tightly regulated levels, an approach to identify NEDDylation modification in this RBP was performed, as described in Results section.

3. OBJECTIVES

3. OBJECTIVES

The principal aim of this study consists in the identification of new mechanisms implicated in the hepatocyte proliferation, differentiation and dedifferentiation, liver regeneration and malignant transformation, in relation with SAMe.

For this purpose, our first objective will be to elucidate the existence of a post-transcriptional regulation involved in the switch from *MAT2A* to *MAT1A* mRNA during hepatocyte differentiation, and from *MAT1A* to *MAT2A* during hepatocyte dedifferentiation, proliferation and malignant transformation. Using *in silico* and *in vitro* analysis such as ribonucleoprotein immunoprecipitation, gene silencing and protein analysis by Western blotting, we will study the regulation of *MAT2A* and *MAT1A* mRNAs by the RNA binding proteins HuR and AUF1. This regulation will be studied in hepatocyte dedifferentiation and liver development, in the GNMT-KO mice model, and in human HCC. We will try to propose a model for this post-transcriptional regulation.

The second objective aims to study the effect of chronic increased SAMe levels in GNMT-KO mouse model during liver regeneration after partial hepatectomy. After 2/3 partial hepatectomy, we will study by real time PCR and Western blotting the main molecular pathways involved in liver proliferation and regeneration, together with the survival and apoptosis after PH. Particularly, we will study DNA synthesis and hepatocyte proliferation, and the LKB1/AMPK/eNOS pathway that is fundamental for the hepatocyte proliferation. We also explore the translocation of HuR to the cytoplasm after PH, and the activity of NFkB and iNOS production after PH.

Finally, our third objective is focused on the post-translational mechanisms involved in HuR protein stability in HCC and colon cancer. HuR protein is fundamental during hepatocyte proliferation, differentiation and transformation, but the mechanisms involved in the protein stability are not well known. We will study HuR post-translational modification by NEDDylation in HCC and colon cancer, and the influence on HuR protein stability and subcellular localization. The residues involved in HuR NEDDylation will be mapped and the relation over cell cycle and apoptotic response explored. As conclusion, we will propose a new mechanism for the post-translational regulation of HuR stability, which could be a new therapeutical target for HCC and colon cancer.

4. EXPERIMENTAL PROCEDURES

4. EXPERIMENTAL PROCEDURES

4.1. HUMAN SAMPLES

Surgically resected specimens of 61 patients with metastatic colon cancer to the liver included in two tissue arrays and 22 HCC (10 hepatitis C etiology, 10 alcoholic steatohepatitis [ASH], and 2 nonalcoholic steatohepatitis [NASH]) patients were examined. Healthy human liver, healthy colon mucosa and colon carcinoma primary tumors were used as controls for immunostaining. Patients gave informed consent to all clinical investigations, which were performed in accordance with the principles embodied in the Declaration of Helsinki. The data and type of biospecimen used in this project were provided by the Basque Biobank for Research.

4.2. ANIMAL EXPERIMENTS

All animal experimentation was conducted in accordance with Spanish Guide for the Care and use of Laboratory animals, and with International Animal Care and Use Committee Standards. All procedures were approved by the CIC bioGUNE Ethical Review Committee. Mice and rats were housed in a temperature-controlled animal facility (AAALAC-accredited) with 12-hour light/dark cycles, and fed a standard diet (Harlan Teklad) with water *ad libitum*.

Liver samples were harvested, snap-frozen in liquid nitrogen and stored at -80 °C for subsequent analysis. The animals used for the experimentation were:

GNMT-KO [176] and wild-type (C57BL/6J) mice: 8-month-old male were used for the protein and mRNA levels of MAT2A and HuR; 3-month-old male were subjected to partial hepatectomy experiments.

Wistar rats: livers were removed from embryonic days 16 (E16) and 18 (E18), postnatal days 1 (P1) and 5 (P5) and from 3-month-old Wistar rats for protein and mRNA study of MAT1A and MAT2A regulation during liver development.

4.3. PARTIAL HEPATECTOMY (PH) EXPERIMENTS

Two-thirds partial hepatectomy was performed in 3-month-old male WT and GNMT-KO mice. PH was done according to the method of Higgins and Andersen [296] between 8 and 11 A.M., liver specimens removed (time zero) and snap frozen in liquid nitrogen or formalin fixed for subsequent analysis. Groups of animals (n=4 to 8) were sacrificed at 0.5, 6, 24 and 48 hours. Two hours before the sacrifice, mice were injected intraperitoneally with bromodeoxyuridine (BrdU, 100 mg/kg body weight) to assess hepatocyte synthesis. At the time of sacrifice, livers were rapidly split into several pieces, some were snap frozen for subsequent RNA or protein extraction, others were formalin fixed for histology and immunohistochemistry.

4.4. CELL EXPERIMENTS

4.4.1. Primary rat and mouse hepatocytes

Hepatocytes were isolated from male Wistar rats (200 g) or 3-months old male WT mice (C57BL/6J mouse strain), by perfusion with collagenase type I (Worthington) as described previously [297]. In brief, animals were anesthetized with isofluorane (1.5% isofluorane in O₂), the abdomen was opened and a catheter was inserted into the inferior vena cava and clamped supra inferior vena cava; in the case of rats is easier to canulate the portal vein. Liver was perfused with buffer A (1x PBS, 5 mM EGTA) (37 °C, oxygenated), and portal vein was cut. Subsequently, liver was perfused with buffer B (1x PBS, 2 mM CaCl₂, collagenase type I) (37 °C, oxygenated). After the perfusion, the liver was placed in a petri dish containing buffer C (1x PBS, 2 mM CaCl₂, 0.6% bovine serum albumin) and gently disgregated with forceps. Digested liver was filtered through sterile gauze; hepatocytes were collected and washed twice in buffer C (300 rpm, 3 min, 4 °C). Supernatant was removed and pelleted hepatocytes were resuspended in fresh 10% fetal bovine serum (FBS; Gibco) Minimum Essential Medium (MEM; Gibco) containing 1% penicillin-streptomycin-glutamine (PSG; Invitrogen). In the case of mouse hepatocytes, viable cells were

purified by centrifugation in a Percoll (GE Healthcare) gradient. Cell viability was validated by tripan blue exclusion test and more than 80% were considered acceptable for the experiments.

Isolated hepatocytes were seeded over collagen-coated culture dishes at a density of 7600 cells/mm² in MEM supplemented with 10% FBS and 1% PSG, and placed at 37 °C in a humidified atmosphere of 5% CO₂-95% air. After 2 hours of attachment, the culture medium was removed and replaced with the same medium without FBS or supplemented with 5% FBS, and the treatments were performed after 2 additional hours of incubation.

4.4.2. MLP29 cell line

The Mouse Liver Progenitor 29 (MLP29) cell line was isolated by the professor E. Medico from a epithelial cell line established from mouse embryonic liver [298]. MLP29 was one of the clones isolated and characterized by their morphological behavior and expression of differentiation markers. Morphologically, MLP29 cell line featured small cells with ovoid nuclei, forming tightly packed colonies. These cells homogenously express AFP, albumin, cytokeratin 19 and tyrosine kinase receptors of the Met family conferring sensitivity to the HGF proliferative stimulus.

Cell cultures were maintained in DMEM supplemented with 10% FBS and 1% penicillin-streptomycin-glutamine at 37 °C in a humidified atmosphere of 5% CO₂-95% air.

4.4.3. SAMe-D cell line

SAMe-D (SAMe-Deficient) cell line was isolated in our laboratory from HCC spontaneously developed in MAT1A-KO mouse liver, and characterized by Dr. N. Martínez-López [56]. In brief, SAMe-D cells represent a model of NASH-derived HCC cell line, characterized for low intracellular levels of SAMe together with a hyperactivated LKB1 that activates the survival pathway through AKT activation, and inhibits the apoptotic response through p53 and HuR.

Cell cultures were maintained in DMEM supplemented with 10% FBS and 1% penicillin-streptomycin-glutamine at 37 °C in a humidified atmosphere of 5% CO₂-95% air.

4.4.4. Commercial cell lines

HepG2 human hepatoma cell line and RKO colon carcinoma cells were purchased from the American Type Culture Collection (ATCC). Cells were cultured in DMEM supplemented with 10% FBS and 1% penicillin-streptomycin-glutamine at 37 °C in a humidified atmosphere of 5% CO₂-95% air.

4.4.5. Cell treatments

Primary hepatocytes and tumor cell lines were subjected to different treatments in the present study. Reagents, concentrations and FBS percentage in the culture medium are listed in Table 1.

For ultraviolet C (UVC) light treatment, after 16 hours with 0% FBS culture medium, it was removed from the plates and they were placed in a

Table 1. Cell treatments performed in this study. Table describes concentration, solubility, biological function, manufacturer and medium condition for each specific treatment. Abbreviations: DMSO, dimethyl sulfoxide; AICAR, 5-Aminoimidazole-4-carboxamide-1-β-riboside; AMPK, AMP-activated kinase; HGF, hepatocyte growth factor; PBS, phosphate buffer saline; BSA, bovine serum albumin; SAMe, S-adenosylmethionine; TNFα, tumor necrosis factor α.

COMPOUND	DOSE	SOLUBILITY	FUNCTION/TARGET	SUPPLIER	%FBS MEDIUM
ACTINOMYCIN D	2 µg/ml	DMSO	Transcription inhibitor	Sigma-Aldrich	0%
AICAR	2 mM	Culture medium	AMPK activator	Calbiochem	0%
CYCLOHEXIMIDE	50 µg/ml	Water	Translation inhibitor	Sigma-Aldrich	5%
COMPOUND C (CC)	40 µM	DMSO	AMPK inhibitor	Calbiochem	0%
HGF	40 ng/ml	PBS >0.1% BSA	Stimulates hepatocyte proliferation	Calbiochem	0%
MG132	1 µM	DMSO	Proteasome inhibitor	Calbiochem	5%
SAMe	4 mM	Culture medium	Multiple functions	Abbott	0%
TNFα	10 ng/ml	dH ₂ O	Multiple effects. Involved in hepatocyte proliferation	Calbiochem	0%

CL-1000 Crosslinker (254 nm). Cells were subjected to 20 Joules pulse of UVC light, culture medium was returned and cells were maintained in a 5% CO₂-95% air incubator at 37 °C.

4.5. RIBONUCLEIC ACIDS (RNA) EXTRACTION AND PROCESSING

4.5.1. RNA isolation

Total liver, cultured hepatocytes or cell lines

RNA was isolated using Trizol (Invitrogen) according to manufacturer's instructions. RNA concentration was determined spectrophotometrically before use in the Nanodrop ND-1000 Spectrophotometer (Thermo Scientific). RNA integrity was checked by electrophoresis in a 1% agarose gel with ethidium bromide for visualization.

4.5.2. Retrotranscription and Real Time quantitative PCR (RT-qPCR)

2 µg of the obtained RNA were treated with

Table 2. Sequence of primers used for real-time PCR

GENE NAME	SYMBOL	SPECIES	GENE ID	SEQUENCE	
18S ribosomal RNA	Rn18S	<i>Mus musculus</i>	NR_003278.3	Forward	5'-GCACCACCAACCCACGGAATCG-3'
				Reverse	5'-TTGACCGAAGGGCACCAACAG-3'
18S ribosomal RNA	Rn18S	<i>Rattus norvegicus</i>	NR_046237.1	Forward	5'-ACGGACCAGAGCGAAAGCAT-3'
				Reverse	5'-TGTCAATCCTGTCCGTGTCC-3'
Acidic ribosomal protein	ARP	<i>Mus musculus/Rattus norvegicus</i>	NM_007475.5/NM_022402.2	Forward	5'-CGACCTGGAAAGTCCAAC-TAC-3'
				Reverse	5'-ATCTGCTGCATCTGCTTC-3'
AU-rich RNA binding factor 1	AUF1	<i>Rattus norvegicus</i>	NM_024404	Forward	5'-AACCAAGGCTATGGCAGCTA-3'
				Reverse	5'-GATGACCACCTCGTCTGGAT-3'
Cyclin A2	CCNA2	<i>Mus musculus</i>	NM_009828.2	Forward	5'-ATAGATTCCCTCTCCTCCATGTCTG-3'
				Reverse	5'-AAAGCAAGGACTTCAATACAAGG-3'
Cyclin D1	CCND1	<i>Mus musculus</i>	NM_007631.2	Forward	5'-GCCTCTAAGATGAAGGAGACCAT-3'
				Reverse	5'-ATTGGAGAGGAAGTGTTCGAT-3'
Cyclin D1	CCND1	<i>Rattus norvegicus</i>	NM_171992.4	Forward	5'-AGATGTGAAGTTCATTTCAACC-3'
				Reverse	5'-TCACACTTGATGACTCTGGAAAG-3'
Glyceraldehyde-3-phosphate-dehydrogenase	GAPDH	<i>Mus musculus</i>	NM_008084.2	Forward	5'-TGAAGCAGGCATCTGAGGG-3'
				Reverse	5'-CGAAGGTGGAAGAGTGGGAG-3'
Glyceraldehyde-3-phosphate-dehydrogenase	GAPDH	<i>Rattus norvegicus</i>	NM_017008.2	Forward	5'-AGACAGCCGCATCTCTGT-3'
				Reverse	5'-CTTGCCGTGGTAGAGTCAT-3'
Glycine N-methyltransferase	GNMT	<i>Mus musculus</i>	NM_010321.1	Forward	5'-AGTACAAGGCGTGGTTGCTT-3'
				Reverse	5'-ATCTTGTCCAGCGTCAACC-3'
Glycine N-methyltransferase	GNMT	<i>Rattus norvegicus</i>	NM_017084.1	Forward	5'-AACACAAAGCCCCACATGGT-3'
				Reverse	5'-TCTTCTTGAGCACGTGGATG-3'
Hu antigen R	HuR	<i>Rattus norvegicus</i>	NM_001108848.1	Forward	5'-AGCAATCAGCACACTGAACG-3'
				Reverse	5'-CCTCTGGACAAACCTGTGGT-3'
Nitric oxide synthase 2, inducible	iNOS	<i>Mus musculus</i>	NM_010927	Forward	5'-CACCTGGAGTTACCCAGT-3'
				Reverse	5'-ACCACTCGTACTGGGATGC-3'
Methionine adenosyltransferase I, alpha	MAT1A	<i>Mus musculus</i>	NM_133653.2	Forward	5'-GACACCATCAAGCACATTGG-3'
				Reverse	5'-ATGCATTCCCTCGGTCTCATC-3'
Methionine adenosyltransferase I, alpha	MAT1A	<i>Rattus norvegicus</i>	NM_012860.2	Forward	5'-GCTATGCCACTGACGAGACA-3'
				Reverse	5'-CAGAGATGACGATGGTGTGG-3'
Methionine adenosyltransferase II, alpha	MAT2A	<i>Mus musculus</i>	NM_145569.4	Forward	5'-CTTCCTTCAGAGAGCAGTGCT-3'
				Reverse	5'-CTTACGCCATACCCCAGAATA-3'
Methionine adenosyltransferase II, alpha	MAT2A	<i>Rattus norvegicus</i>	NM_134351.1	Forward	5'-GCTAAAGTGGCTTGTGAAACTGT-3'
				Reverse	5'-TGTAGTCAAACCCCTTGGAAAGAA-3'
Prothymosin alpha	PTMA	<i>Mus musculus</i>	NM_008972.2	Forward	5'-GCCATCTTGCATTGTTCC-3'
				Reverse	5'-TCTCTGCCTCCTCCACAAC-3'
-	V5	-	-	Forward	5'-CCTAACCCCTCCTCGGTCT-3'
				Reverse	5'-CCCGAATAAGCTTGCAGAT-3'

DNase I (Invitrogen) and cDNA was synthesized with Superscript II retrotranscriptase (Invitrogen) in the presence of random primers and RNaseOUT (Invitrogen). Resulting cDNA was diluted 1/20 in RNase free water (Sigma-Aldrich), and 5 microliter were used for PCR reaction. PCRs were performed using BioRad iCycler iQ5 Thermalcycler, with iQ SYBR Green Super Mix (Bio Rad) and specific primers, in a total reaction volume of 20 μ l, and all reactions were performed in triplicates. PCR conditions for these primers were optimized, and 40 cycles with a melting temperature of 60 °C, and 30 sec of each step, were used.

Primers were designed and synthesized by Qiagen or designed using Primer 3 Software [299] and synthesized by Sigma-Aldrich. Primer sequences are detailed in Table 2.

After checking the specificity of the PCR products with the melting curve, Ct values were extrapolated to a standard curve performed simultaneously with the samples and data was then normalized to the expression of a housekeeping gene (GAPDH, ARP and 18S).

4.6. PROTEIN EXTRACTION AND ANALYSIS

4.6.1. Total protein extraction

Extraction of total protein was performed as described before [152]. Cells were washed twice with 1x PBS buffer and resuspended in 300 μ l lysis buffer (NaH_2PO_4 1.6 mM, Na_2HPO_4 8.4 mM, 0.1% Triton X-100, NaCl 0.1 M, 0.1% SDS, 0.5% sodium azide) supplemented with protease and phosphatase inhibitor cocktail (Roche). In the case of frozen liver tissue, approximately 50 μ g of tissue was homogenized by using a Potter homogenizer in 1 ml lysis buffer for whole cell lysate. In both cases, the lysates were centrifuged (13000 rpm, 30 min, 4 °C) and the supernatant (protein extract) was quantified for total protein content by the Bio Rad protein assay, or by BCA protein assay (Pierce) when measuring proteins with high fat content.

4.6.2. Subcellular protein extraction

Cytosolic, membrane and nuclear lysates from both cells and frozen liver tissue samples

were prepared as described by the manufacturer by using the Subcellular Proteome Extraction Kit (Calbiochem). The lysates were quantified for protein content by the BCA protein assay (Pierce).

4.6.3. Western blotting

Protein extracts were boiled at 95 °C for 5 minutes in SDS-PAGE sample buffer (250 mM Tris-HCl pH 6.8, 500 mM β -mercaptoethanol, 50% glycerol, 10% SDS, bromophenol blue). Appropriate amount of protein (between 5 μ g and 30 μ g), according with specific protein abundance and antibody sensitivity, was separated by sodium dodecyl sulphate-polyacrylamide gel electrophoresis (SDS-PAGE) in 8%, 11% or 15% acrylamide gels (depending on the molecular weight of the protein), using Mini-PROTEAN Electrophoresis System (Bio Rad). Gels were transferred onto nitrocellulose membranes by electroblotting using Mini Trans-Blot cell (Bio Rad). Membranes were blocked with 5% nonfat dry milk in TBS pH 8.0 containing 0.1% Tween-20 (TBST-0.1%), for 1 hour at room temperature (RT), washed three times with TBST-0.1% and incubated overnight at 4 °C with commercial or homemade primary antibodies. Optimal incubation conditions are detailed in Table 3. Membranes were then washed three times with TBST-0.1% and incubated for 1h at RT in blocking solution containing secondary anti-rabbit or anti-mouse antibodies conjugated to horseradish peroxidase (Table 3). Immunoreactive proteins were detected by Western Lightning Enhanced Chemiluminescence reagent (ECL, Perkin Elmer) and exposed to X-ray films (Amersham) in a Curix 60 Developer (AGFA). Bands were quantified by densitometry using the free image processing software ImageJ (<http://rsbweb.nih.gov/ij>).

4.7. GENE SILENCING

Small interfering RNA (siRNA) were designed and synthesized by Qiagen or Sigma-Aldrich, and annealed according to manufacturer's instructions. For each gene, two pairs of oligonucleotides were tested and every silencing assay was performed in duplicates. Negative controls were included in each assay by using non-related siRNA (hereafter referred as siRNA Control, siCtrl). Nucleotide sequences were designed for each specific siRNA with *Mus musculus*, *Rattus norvegicus* or *Homo*

Table 3. Incubation conditions, dilution and supplier for each antibody employed in this study for Western blotting

ANTIBODY	SUPPLIER	DILUTION	INCUBATION SOLUTION
β-actin	Sigma-Aldrich	1:5000	TBS-TWEEN (0.1%)-MILK (5%)
AMPK	Upstate	1:1000	TBS-TWEEN (0.1%)-BSA (5%)
P-AMPK (Thr172)	Cell Signaling Technology	1:1000	TBS-TWEEN (0.1%)-BSA (5%)
AUF1	Millipore	1:1000	TBS-TWEEN (0.1%)-MILK (5%)
Cyclin A	ABCAM	1:1000	TBS-TWEEN (0.1%)-MILK (5%)
Cyclin D1	Cell Signaling Technology	1:1000	TBS-TWEEN (0.1%)-MILK (5%)
Cyclin E	Santa Cruz Biotechnology	1:1000	TBS-TWEEN (0.1%)-MILK (5%)
eNOS	Santa Cruz Biotechnology	1:1000	TBS-TWEEN (0.1%)-BSA (5%)
P-eNOS (Ser1177)	Cell Signaling Technology	1:1000	TBS-TWEEN (0.1%)-BSA (5%)
GAPDH	ABCAM	1:5000	TBS-TWEEN (0.1%)-BSA (5%)
GFP	Roche	1:5000	TBS-TWEEN (0.1%)-MILK (5%)
HuR	Santa Cruz Biotechnology	1:5000	TBS-TWEEN (0.1%)-MILK (5%)
IκBα	Cell Signaling Technology	1:1000	TBS-TWEEN (0.1%)-MILK (5%)
P- IκBα (Ser32)	Cell Signaling Technology	1:1000	TBS-TWEEN (0.1%)-BSA (5%)
Lamin A	Santa Cruz Biotechnology	1:5000	TBS-TWEEN (0.1%)-MILK (5%)
LKB1	ABCAM	1:1000	TBS-TWEEN (0.1%)-MILK (5%)
P-LKB1 (Ser428)	Cell Signaling Technology	1:1000	TBS-TWEEN (0.1%)-BSA (5%)
MAT I/III	Homemade	1:5000	TBS-TWEEN (0.1%)-MILK (5%)
MAT II	ABCAM	1:5000	TBS-TWEEN (0.1%)-MILK (5%)
Mdm2	Calbiochem	1:100	TBS-TWEEN (0.1%)-MILK (5%)
Methyl-HuR	Provided by Dr Laird-Offringa	1:5000	TBS-TWEEN (0.1%)-MILK (5%)
α-tubulin	Sigma-Aldrich	1:5000	TBS-TWEEN (0.1%)-MILK (5%)
NEDD8	Provided by Dr Xirodimas	1:500	TBS-TWEEN (0.1%)-MILK (5%)
NedP1	Provided by Dr Xirodimas	1:500	TBS-TWEEN (0.1%)-MILK (5%)
NPT2	ABCAM	1:5000	TBS-TWEEN (0.1%)-MILK (5%)
PARP	Cell Signaling Technology	1:1000	TBS-TWEEN (0.1%)-BSA (5%)
p27	Santa Cruz Biotechnology	1:1000	TBS-TWEEN (0.1%)-MILK (5%)
p65	Santa Cruz Biotechnology	1:1000	TBS-TWEEN (0.1%)-MILK (5%)
P-p65 (Ser536)	Cell Signaling Technology	1:1000	TBS-TWEEN (0.1%)-BSA (5%)
V5	Invitrogen	1:2500	TBS-TWEEN (0.1%)-MILK (5%)
HRP-conjugated secondary goat antibody to mouse	Santa Cruz Biotech	1:5000	TBS-TWEEN (0.1%)-MILK (5%)
HRP-conjugated secondary goat antibody to rabbit	BioRad	1:5000	TBS-TWEEN (0.1%)-MILK (5%)

sapiens origin. These are detailed in Table 4. Gene silencing efficiency was confirmed by Western blot, immunocytochemistry or mRNA expression.

We used three different protocols for the transfection:

Cell lines: MLP29, SAMeD, HepG2 and RKO cell lines were transfected with siRNA for gene knockdown using Lipofectamine 2000 (Invitrogen) with the following protocol: 5 µl of Lipofectamine 2000 were diluted in 500 µl of OptiMEM (Gibco) for 5 min and mixed with the same volume of OptiMEM containing 15 µl of siRNA (20 mM). Mix was incubated for 20 min at RT to allow the formation of siRNA-Lipofectamine complexes. Unless different conditions are explained in the Results section or Figure legends, for each transfection, cells (200000 for MLP29 and SAME-D cell lines and 300000 for RKO and HepG2 cell lines) were resuspended in 2 ml of 10%-FBS DMEM (Gibco) medium without antibiotics and plated in 60 mm tissue culture dishes containing the siRNA-Lipofectamine complexes previously formed. The final concentration of siRNA was 100

nM. The mix was left overnight and then the medium was replaced for fresh 10% FBS DMEM supplemented with antibiotics. 24 hours after the first transfection, silencing assay was repeated over the attached cells. In total, cell lines were silenced twice during a 48 hours period (once every 24 hours).

Primary cells: Rat hepatocytes isolated as described before, were transfected with siRNA for gene silencing using Amaxa Nucleofector with the following protocol. For each transfection 1,5 million hepatocytes were centrifuged (300 rpm 2 min at RT) and washed twice with 1x PBS. The pellet obtained after the second centrifugation was resuspended in 100 µl of Amaxa Rat Hepatocyte Nucleofector Solution. 5µl of 20 µM siRNA were then added to the tube containing the cells. Cells with siRNAs were immediately transferred to the Amaxa cuvette, inserted into the Nucleofector and Q-025 program (specific for rat hepatocytes) was run. After the program, cuvettes were incubated for 15 min at RT, and, then, cells were recovered from the cuvette with an Amaxa certified pipette and transferred to a 6-well plate containing 2 ml of 10% FBS MEM (Gibco) medium without antibiotics.

Table 4. si RNA sequences used for target gene silencing

GENE	SPECIES		SEQUENCE/QIAGEN PRODUCT NUMBER
siControl	<i>Rattus norvegicus</i>		Qiagen, SI1022076
siControl	<i>Mus musculus</i>	sense	5'-AAUUCUCCGAACGUGUCACGU-3'
		antisense	5'-ACGUGACACGUUCGGAGAAUU-3'
siControl	<i>Homo sapiens</i>	sense	5'-UUCUCCGAACGUGUCACAU-3'
		antisense	5'-AUGUGACACGUUCGGAGAA-3'
AUF1	<i>Rattus norvegicus</i>	sense	5'-GAGUCGGAGAGUGUAGUAU-3'
		antisense	5'-UAUCUACACUCUCCGACUC-3'
GNMT	<i>Mus musculus</i>	sense	5'-AUAUGCGCUUAAGGAGCGC-3'
		antisense	5'-GCGCUCCUUGGGCGCAUAU-3'
GNMT	<i>Rattus norvegicus</i>		Qiagen, SI00258377
HuR	<i>Mus musculus</i>	sense	5'-AAGAGGCCAAUUACCAGUUUCA-3'
		antisense	5'-UGAACUGGUAAUUGCCUCUU-3'
HuR	<i>Homo sapiens</i>	sense	5'-CAGUUUCAAUGGUCAUAATT-3'
		antisense	5'-UUUAUGACCAUUGAACUGGT-3'
Mdm2	<i>Mus musculus</i>	sense	5'-GGAUCUUGACGAUGGGCUATT-3'
		antisense	5'-UACGCCAUCGUCAAGAUCTG-3'
Mdm2	<i>Homo sapiens</i>	sense	5'-UCAUCGGACUCAGGUACAUUATT-3'
		antisense	5'-AUGUACCUGAGUCCGAUGATT-3'
NEDD8	<i>Mus musculus</i>	sense	5'-CAUCUACAGUGGCAAGCAATT-3'
		antisense	5'-UGCUUGCCACUGUAGAUGAG-3'

Medium was replaced 4 hours after the electroporation with fresh 10% FBS MEM supplemented with antibiotics and left overnight at 37 °C. Following that, the cells were subjected to a variety of treatments.

In vivo silencing of GNMT: Three month-old male WT mice were injected intravenously in the tail vein (200 µl of a 60 µM solution) with GNMT specific siRNA or control siRNA (Eurofins mwg/operon) per mice at 24 hours and 2 hours before PH. Livers were then removed during PH (time 0 hours) and 48 hours after PH, and mRNA and protein were extracted.

4.8. PLASMID CONSTRUCTS

4.8.1. Cloning of 3'UTR of mouse MAT2A cDNA and plasmid construct

cDNA obtained as described above from SAMe-D cells served as a template for polymerase chain reaction amplification of 3'UTR of MAT2A. As expected, a fragment of 1400 bp was obtained and purified by Qiaquik gel extraction (Qiagen). This PCR fragment was cloned into the pEGFP-C2 vector (CLONTECH) that contains the GFP gene, within the Xho I and Hind III restriction sites. Both restriction sites were artificially added to the cDNA extremities (Xho I site 5' and Hind III site 3') during the PCR process. The plasmid obtained after ligation and transformation was checked by restriction enzymes digestion and sequenced to exclude the presence of any mutations introduced by the procedures.

4.8.2. Subcloning of HuR-V5, and HuR mutants production

The full length cDNA of wild type (WT) mouse HuR was purchased from RZPD Deutsches Ressourcenzentrum für Genomforschung GmbH (Germany). Wild type HuR-V5 was constructed by PCR using a 5' oligonucleotide containing the V5 tag sequence and being subcloned into pcDNA 3.3 TOPO vector (Invitrogen). The HuR mutants [H(R217K)V5, H(K274R)V5, H(K283R)V5, H(K285R)V5, H(K313R)V5, H(K320R)V5, H(K323R)V5, H(K326R)V5 and H(3KR)V5] were constructed by using the QuickChange kit for site-directed mutagenesis (Stratagene), according to manufacturer's instructions, with two

complementary oligonucleotides and as template the pcDNA-V5-HuR plasmid.

4.9. CELL TRANSFECTION

MLP29, SAMe-D, RKO and HepG2 cell lines were plated (200000 for MLP29 and SAMe-D cell lines and 300000 for RKO and HepG2 cell lines) in P60 dishes with 10% FBS DMEM (Gibco) supplemented with antibiotics, and left overnight for the attachment. Then, cells were transfected in duplicates with cDNA plasmids for gene expression using Lipofectamine 2000 (Invitrogen) according to manufacturer's instructions. Plasmids used for transfection were: pEGFP-C2 (Clontech), pEGFP-C2-3'UTR (cloning described in section 4.7.), HuR-V5 (cloning described in section 4.7.), H(K313R)V5 (mutagenesis described in section 4.7.), H(K323R)V5 (mutagenesis described in section 4.7.), H(K326R)V5 (mutagenesis described in section 4.7.), Mdm2-WT (kindly provided by Dr Xirodimas), Mdm2-NLS (kindly provided by Dr Xirodimas), Mdm2(C464A) (kindly provided by Dr Xirodimas), His₆-NEDD8 (kindly provided by Dr Rodríguez), His₆-Ubiquitin (kindly provided by Dr Rodríguez), His₆-LacZ-V5 (Invitrogen), and NEDP1 (kindly provided by Dr Xirodimas). Transient transfection protocol is as follows:

DNA-Lipofectamine complex formation: Lipofectamine 2000 (2.5 µl / 1 µg DNA) was diluted in 250 µl of OptiMEM (Gibco) medium and incubated for 5 min. After the incubation, it was mixed with 250 µl of OptiMEM (Gibco) medium containing the plasmid DNA (2 µg of pEGFP-C2 and pEGFP-C2-3'UTR, 15 µg of NedP1, and 1 µg of the rest of the plasmids), and incubated during 20 min at RT to allow the formation of the DNA-Lipofectamine complexes.

Cell transfection: DNA-Lipofectamine complexes previously formed were added to P60 plates containing the attached cells and 1,5 ml of 6.5% FBS OptiMEM (Gibco) medium without antibiotics. After 4 hours, medium was replaced with fresh 10% FBS DMEM supplemented with antibiotics. 24 hours after the transfection, cells were lysed or different treatments were performed. Transfection efficiency was confirmed by Western blotting and/or RNA expression analysis.

4.10. IMMUNOPRECIPITATION (IP) ASSAYS

4.10.1. Protein immunoprecipitation assays

Protein-protein complexes were immunoprecipitated as follows:

Cell lysates preparation: MLP29 cells transfected with Mdm2 or NEDD8, or with HuR-V5 or H(K326R)V5 and Mdm2, were lysed in Nonidet P-40 (NP-40) buffer (50 mM Tris-HCl pH 8.5, 150 mM NaCl, 1% NP-40, 5 mM EDTA) supplemented with protease and phosphatase inhibitors cocktail (Roche). Whole-cell lysates were processed and quantified for protein content as described in section 4.6.

Covalent cross-linking of antibodies to beads: In order to limit the recovery of light and heavy antibody chains during immunoprecipitation, antibodies were covalently cross-linked to Protein A-Sepharose beads. 100 µl of Protein A-Sepharose beads per sample were washed four times in 1xPBS (5000 rpm 5 min 4 °C) and incubated overnight with 10 µg of the appropriate primary antibodies: HuR (Santa Cruz Biotech.) and IgG1 (BD Pharmingen) as negative control; or Mdm2 (Calbiochem) and IgG2 (BD Pharmingen) as negative control. After incubation, beads were washed three times (2500 rpm 5 min 4 °C) with Na.Borate buffer (0.2 M Borate, 3 M NaCl, pH 9), and covalently cross-linked with Na.Borate buffer containing dimethyl pimelimidate (DMP) for 30 min at RT with agitation. Beads were then washed three times with Na.Borate buffer and incubated with 0.2 M ethanolamine, pH 8.0, for 2 hours at RT with agitation. Covalent cross-link reaction was stopped by washing beads three times with fresh glycine buffer (200 mM, pH 2.5). Beads were washed three times with 1x PBS and kept at 4 °C until the incubation with the protein extract.

Immunoprecipitation assay: covalently cross-linked beads were incubated with 500 µg of protein lysate overnight at 4 °C with agitation. After incubation, beads were washed three times with NP-40 lysis buffer and bound proteins were eluted by heating at 95 °C for 5 min in 2x SDS-PAGE sample buffer. Immunoprecipitated proteins (IPs) and original cell extracts (Inputs) were analyzed by Western blotting with the appropriate antibodies.

4.10.2. Ribonucleoprotein immunoprecipitation (RNP-IP) assay

RNA-protein complexes were immunoprecipitated as described before [300].

The protein lysates for the RNP-IPs were obtained from isolated hepatocytes, cell lines or mouse and rat liver. In the case of the hepatocytes and cell lines, after the treatments they were washed twice with 1x PBS and lysed in buffer containing 100 mM KCl, 5 mM MgCl₂, 10 mM HEPES pH 7.0, 0.5% NP-40, 1 mM DTT, RNaseOUT (100 U/ml) and Complete protease inhibitor cocktail (Roche). In the case of the liver, approximately 40 mg of tissue was homogenized in a potter homogenizer with the same lysis buffer. In both cases, homogenates were centrifuged 30 min at 14000 rpm, 4 °C, and the supernatant was quantified for protein content as described above and used for IP of RNA-protein complexes.

Fresh whole-cell lysate (150 µg) or lysate from snap-frozen liver (250 µg) was first precleaned with 15 µg of IgG1 control (BD Pharmingen) and 25 µl of Protein A-Sepharose beads (Sigma-Aldrich) for 30 min, 4 °C with agitation. After spin centrifugation, the supernatant was incubated (1h, 4 °C) with 1ml of a 50% (v/v) suspension of Protein A-Sepharose beads (beads had been previously precoated overnight with 30 µg of either IgG1 or IgG2 (BD Pharmingen), HuR (Santa Cruz Biotech.), methyl-HuR [235], AUF1 (Millipore) or V5 (Invitrogen) antibodies, and washed twice using NT2 buffer (50 mM Tris-HCl pH 7.4, 150 mM NaCl, 1 mM MgCl₂, and 0.05% NP-40)). After protein lysate incubation with the beads, pellets were washed four times (5000g, 5 min) with 1 ml of ice-cold NT-2 buffer.

After last wash, for the isolation of RNA in the immunoprecipitated material, beads were incubated with 100 µl NT2 buffer containing 20U DNase I (RNase-free) (Ambion) for 15 min at 37°C, washed with NT2 buffer and further incubated in 100 µl of NT2 buffer containing 0.1% SDS and 0.5 mg/ml Proteinase K (Roche) for 15 min at 55 °C; following centrifugation, the supernatant was collected. RNA from this supernatant was extracted with acid-phenol-CHCl₃ and precipitated overnight in the presence of 5 µl glycoblue (Ambion), 25 µl sodium acetate pH 5.2 and 625 µl 100% ethanol. Next day, precipitated RNA was

Table 5. Primer sequences employed to synthesize the biotinylated probes for the biotin pull down assay

GENE	TARGET REGION		SEQUENCE
MAT2A	5'-UTR	Forward	5'-(T7)AGCCTGCTGAGAGTTGAAGC-3'
		Reverse	5'-GCTGCAGCGATGAGAGAAG-3'
	CR	Forward	5'-(T7) ATGAACGGGCAGCTAAC-3'
		Reverse	5'-TGGAGATCGACAATGGATGA-3'
	3'UTR (1)	Forward	5'-(T7)AATTGCTGAAACATGCCAAT-3'
		Reverse	5'-CAGTCCCCAACAAAAGCTAAA-3'
	3'UTR (2)	Forward	5'-(T7)CCTTCCTTATCCCTCCGT-3'
		Reverse	5'-ACACCAGCCAAGTCAGCTT-3'
MAT1A	5'-UTR	Forward	5'-(T7)GGCAGAAGTCATCTCCTTG-3'
		Reverse	5'-GTCACACAAGCCATCCACAG-3'
	CR (1)	Forward	5'-(T7)CACCTGGAGAAGTGAAGTCG-3'
		Reverse	5'-GCTTGATCACCTGCTCCTT-3'
	CR (2)	Forward	5'-(T7)TGTGCAACACAAACGAAGACA-3'
		Reverse	5'-CAGGGAGTTGAGATCTTGAGG-3'
	3'UTR (1)	Forward	5'-(T7)CCGGGAAGCTTAGCTCTGTC-3'
		Reverse	5'-TTTTGTGGAACACTGTCCA-3'
GAPDH	3'UTR	Forward	5'-(T7)TTATTTAAGGCCTGGGTTCA-3'
		Reverse	5'-ACAGGAATTTCAGCCTCTGC-3'
		Forward	5'-(T7)CACTGAGCATCTCCCTCAC-3'
		Reverse	5'-GGGTGCAGCGAACCTTATTG-3'

collected by centrifugation, the pellet washed with 70% ethanol, air dried and resuspended in 20 µl of RNase free water (Sigma-Aldrich). Finally, RNA was analyzed by real time PCR as described above.

4.11. PURIFICATION ASSAYS

4.11.1. Biotin pull down assay

HuR-MAT2A mRNA and AUF1-MAT1A mRNA complexes formation was assessed by biotin pull down assay as described [301].

For *in vitro* synthesis of biotinylated transcripts, 100 ng of rat liver cDNA, obtained as described before, were used as template for PCR with Platinum Taq DNA Polymerase High Fidelity (Invitrogen). Primers were designed with Primer 3 software in a way that all the cDNA sequences of *MAT1A* and *MAT2A* mRNAs were amplified in overlapping fragments. All forward oligonucleotides contained the T7 RNA polymerase promoter sequence (CCAAGCTTCTAACGACTCACTATAGGGAG) in the 5' region. Primer sequences (Table 5) were synthesized by Sigma-Aldrich. *GAPDH* 3'UTR biotinylated transcript was used as negative

control. PCR products were run on 2% agarose gel, extracted and purified using QIAquick Gel Extraction Kit (Qiagen) according to manufacturer's instructions, and sequenced to assess their fidelity.

1 µg of each purified T7-promoter-containing DNA was used as template for the synthesis of corresponding biotinylated RNAs using Maxi script T7 Kit (Ambion) and biotin-CTP. After 1 hour incubation at 37°C, 1 µl Turbo DNase (Ambion) was added and incubated for 15 minutes at 37 °C. The biotinylated transcripts obtained were purified using NucAway Spin Columns (Ambion) and the quality was assessed by electrophoresis in 1% agarose gel with ethidium bromide for visualization.

10 µl of paramagnetic streptavidin-conjugated Dynabeads (DYNAL) were prewashed twice with 200 µl of buffer A (0.1M NaOH, 0.05 M NaCl) and washed once with 200 µl of buffer B (0.1 M NaCl) by keeping beads in a magnet until beads get attached to the wall and buffer can be discarded. Beads were resuspended in 10 µl of 1x TENT binding buffer (10 mM Tris-HCl pH 8.0, 1 mM EDTA pH 8.0, 250 mM NaCl, 0.05% triton X-100) and kept on ice until the biotin pull-down assay.

Biotin pull-down assays were carried out by incubating 40 µg of cytoplasmic fractions with 1 µg of biotinylated transcripts in the presence of RNaseOUT and 2xTENT binding buffer for 30 minutes at room temperature. 10 µl of previously prepared Dynabeads were then added and incubated for another 30 minutes at RT to form beads-biotinylated transcripts complexes. Beads were then washed twice with ice cold 1x PBS, and, after discarding the supernatant, beads were resuspended in 10 µl SDS-PAGE sample buffer and boiled at 95 °C for 5 min. After spin centrifugation, supernatant was collected and loaded into SDS-PAGE acrylamide gel for Western blot analysis by using HuR or AUF1 antibodies.

4.11.2. Protein-Histidine affinity purification using nickel-nitriolotriacetic acid (Ni^{2+} -NTA) beads

MLP29 or SAMe-D cell lines were transfected with HuR-V5, H(K283R)V5, H(K313R)V5 or H(K326R)V5, in the presence/absence of Mdm2, together with His₆-NEDD8 or His₆-Ub, 36 hours after transfection, purification protocol was executed. For the UVC light experiments, 20 hours after transfection, cells were exposed to UVC light, as described above, and 6 hours later purification protocol was performed.

His₆-NEDDylated or His₆-Ubiquitinated proteins were purified as previously described [302]. Cells were lysed in 6 M guanidinium-HCl, 0.1 M Na₂HPO₄/NaH₂PO₄, 0.01 M Tris-HCl pH 8, plus 10 mM β-mercaptoethanol. After sonication, the lysates were centrifuged to eliminate cell debris, and lysates were mixed with 50 µl of low density Ni²⁺-NTA-agarose beads (ABT) precoated with BSA and prewashed with lysis buffer. Lysates were incubated with the beads for 2.5 hours at RT, successively washed first with lysis buffer, then with 8 M urea, 0.1 M Na₂HPO₄/NaH₂PO₄, 0.01 M Tris-HCl pH 8 plus 10 mM β-mercaptoethanol, and finally twice with 8 M urea, 0.1 M Na₂HPO₄/NaH₂PO₄, 0.01 M Tris-HCl pH 6.3 plus 10 mM β-mercaptoethanol. After last wash, the beads were eluted with 200 mM Imidazole in 5% SDS, 0.15 M Tris-HCl pH 6.7, 30% glycerol, 0.72 M β-mercaptoethanol. The eluates were subjected to SDS-PAGE and the proteins transferred to a nitrocellulose membrane for Western blotting against V5.

4.12. POLYSOME ANALYSIS

Untreated or SAMe treated rat hepatocytes (5 x 10⁶ cells) were cultured for 24 hours, then incubated with 0.1 mg/ml cycloheximide for 10 minutes. Cytoplasmic extracts were fractionated and collected through sucrose gradients. The RNA of each fraction was isolated with Trizol as described, and reverse transcription quantitative PCR analysis was performed. Protein from each fraction was precipitated with 10% trichloroacetic acid and resuspended in sample buffer for Western blotting.

4.13. IMMUNOSTAINING ASSAYS

4.13.1. Histology, immunohistochemistry and immunohistofluorescence

- For BrdU immunohistochemistry, frozen liver tissue sections were fixed with acetone for 1 minute at room temperature followed by treatment with 2 M HCl at 37 °C for 20 minutes. The sections were then neutralized with 0.1 M sodium borate for 10 minutes, and mouse monoclonal anti-BrdU antibody (Roche Diagnostics) was applied overnight at 4 °C, followed by goat anti-mouse rhodamine antibody (Cappel) and Hoechst nuclear dye. The number of BrdU-positive cells was counted in 10 microscope fields using a 40x objective in an Axiovert 200 microscope by two observers blinded to the animal's identity and treatment, and measured as a percentage of the number of BrdU-positive cells per field versus the total number of cell nuclei as visualized by Hoechst labeling.

- For the rest of stainings, paraffin-embedded sections (5 µm thick) of formalin-fixed liver samples were initially deparaffinized in xylene or xylene-substitute and rehydrated through graded alcohol solutions. Once hydrated, sections were subjected to the following stainings:

Hematoxylin & eosin: after deparaffinization and rehydration process, sections were subjected to conventional hematoxylin & eosin staining (http://www.ihcworld.com/_protocols/special_stains/h&e_ellis.htm).

Proliferating Cell Nuclear Antigen (PCNA) (Immunohistochemistry): rehydrated sections were

blocked with goat anti-mouse Fab fragment (Jackson Immunoresearch) (1 hour, RT, 1:10) and, then, stained with mouse monoclonal anti-PCNA primary antibody (1:400) (Santa Cruz Biotech), followed by peroxidase-labeled goat anti-mouse antibody Envision system (DAKO) at room temperature for 3 hours, stained with the peroxidase substrate 3,3' 2-diamino-bencidine chromogen (DAKO), and counterstained with hematoxylin.

HuR, methyl-HuR and AUF1 immunohistofluorescences: rehydrated sections were subjected to antigen retrieval with 10 mM sodium citrate buffer pH 6.0, and avidin-biotin blocked before overnight incubation with HuR (1:100, Santa Cruz Biotech), methyl-HuR (1:1000, [235]) and AUF1 (1:100; Millipore) primary antibodies followed by incubation with secondary antibodies. For quantification of immunofluorescence, images were acquired using 20x or 40x objectives with consistent exposure times for each section. The immunofluorescence intensity of approximately 50 cells from random fields for each sample was quantified using ImageJ software (<http://rsbweb.nih.gov/ij>) and expressed as relative immunofluorescence intensity. For minimizing variations in measurements, all specimens were immunolabeled at the same time under identical conditions.

HuR (Immunohistochemistry): rehydrated samples were unmasked with antigen retrieval solution (DAKO). Serial sections were blocked with goat anti-mouse Fab fragment (Jackson Immunoresearch) (1 hour, RT, 1:10), and incubated with primary HuR antibody (1:100) (Santa Cruz Biotech) overnight at 4°C and 30 minutes with anti-mouse Envision system (DAKO). Colorimetric detection was completed with Vector Vip purple substrate (Vector). Slides were counterstained with Mayer Hematoxylin. Samples were dehydrated through graded alcohol solutions and xylene-substitute and mounted in DPX mounting media. For the analysis, 12 images per colon carcinoma patient and five images from primary HCC patients were taken with a 40x objective from an upright light microscope (Carl Zeiss AG). Quantification of staining intensity in colon carcinoma metastasis was performed using ImageJ software (<http://rsbweb.nih.gov/ij>) and expressed as mean intensity and stained area percentage. For HCC samples, average sum of

intensities and stained area percentage of each patient was calculated using FRIDA software (<http://bui3.win.ad.jhu.edu/frida/>, Johns Hopkins University).

Mdm2 (Immunohistochemistry): rehydrated samples were unmasked with antigen retrieval solution (DAKO). Serial sections were blocked with goat anti-mouse Fab fragment (Jackson Immunoresearch) (1 hour, RT, 1:10) and incubated with primary Mdm2 antibody (1:100) (Calbiochem) overnight at 4°C and 30 minutes with anti-mouse Envision system (DAKO). Colorimetric detection was completed with Vector Vip purple substrate (Vector). Slides were counterstained with Mayer Hematoxylin. Dehydration, mounting, microscope analysis and quantification were performed as indicated for HuR.

4.13.2. Immunocytofluorescence

MLP29 cells were seeded over 12 mm coverslips (4.5×10^4 cells/coverslip). Cells were fixed with ethanol (for V5 antibody) or methanol (Mdm2) for 10 minutes and washed three times with 1x PBS. Cells were then blocked and permeabilized with 1x PBS containing 0.1% BSA, 10% horse serum and 0.1% Triton-X100 for 30 minutes at RT. After blocking step, cells were washed three times with 1x PBS and incubated overnight in a humid chamber with primary antibodies (V5 1:100, Mdm2 1:33) in blocking solution without Triton X-100. Cells were washed three times with 1x PBS and incubated for 1 hour at RT in blocking solution without Triton X-100 containing 1:100 (FITC)-conjugated secondary goat antibody to Mouse IgG (Cappel) or Cy3-conjugated secondary goat antibody to Mouse IgG (Jackson Immunoresearch). Images were taken using a Leica TCS-SP confocal laser microscope.

4.14. SAMe MEASUREMENT

Liver content of SAMe was measured in GNMT-KO mice and wild type mice before and 48 hours after PH. Measurements were performed in collaboration with OWL genomics. Approximately 30 mg fragments from snap-frozen livers were homogenized in ice-cold 1x PBS with the Precellys 24 (Bertin Technologies) homogenizer, and an aliquot was separated for protein quantification. Immediately, the rest of the sample was treated

with 0.8M perchloric acid on ice for 5 min and centrifuged at 3000g for 10 min at 4°C. The aqueous layer was transferred to HPLC vials and SAMe concentration was determined by LC/MS using a Waters ACQUITY-UPLC system coupled to a Waters Micromass LCT Premier Mass Spectrometer equipped with a Lockspray ionization source.

SAMe levels were calculated using standard curves and expressed in nmol SAMe/mg protein.

4.15. CASPASE-3 ACTIVITY MEASUREMENT

MLP29, SAMe-D, RKO and HepG2 cells were transfected with HuR-V5 and H(3KR)V5, or silenced with control siRNA or specific siRNAs for HuR or Mdm2, as described. In the case of HuR-V5 and H(3KR)V5 transfected cells, 8 hours after transfection cells were cultured in serum starvation conditions during 16 hours, and then UVC treated as described above.

Caspase-3 activity was measured in silenced or UVC treated cells as previously described [303]. After treatment, cells were lysed in caspase buffer (HEPES 10mM pH 7.4, 0.1% CHAPS, EDTA 2 mM, DTT 5 mM) and centrifuged for eliminating the debris. 20 µl of 25x reaction buffer (PIPES pH 7.4 250 mM, EDTA 50 mM, 2.5% CHAPS, DTT 125 mM) was mixed with 2.5 µl of fluorogenic caspase-3 substrate (Enzo Life Sciences) and with protein lysate in a total volume of 500 µl. This reaction mixture was divided into two duplicates. The kinetic assay was performed in 96 well plates, by using an Spectramax M3 spectrophotometer (Molecular Devices), during 2 hours at 37 °C (excitation wavelength 390 nm, emission wavelength 510 nm). Caspase-3 activity was normalized to the protein content, measured as described above.

4.16. CELL CYCLE ANALYSIS

Cell cycle distribution was determined by measuring the cellular DNA content using flow cytometry in MLP29, SAMe-D, RKO or HepG2 cells. After transfection with HuR-V5 and H(3KR)V5, or silencing with control siRNA or specific siRNAs for *HuR* or *Mdm2*, cells were synchronized in G0 phase by serum deprivation for

16 h and then were released from growth arrest by reexposure to 10% fetal bovine serum for 8 h. Then, cells were collected by trypsinization and washed with PBS. The collected cells were fixed in 70% ethanol. After the incubation with 10 mg/ml RNase A for 15 minutes at RT, the cells were resuspended in 0.5 ml 10 µg/ml propidium iodide solution (PI) for staining. The stained cells were monitored by a FACS Canto cytometer (Becton Dickinson). The percentage of cells in the S, G0/G1, and G2/M phases of the cell cycle was determined using the software FlowJo.

4.17. INVASIVENESS ASSAY (SOFT-AGAR)

MLP29 and HepG2 cells were seeded at a density of 1×10^4 cells per well in a 0.4% top agarose layer in DMEM supplemented with 10% FBS over a bottom agarose layer of 0.6%. 0.5 ml of fresh medium was added every four days. The number of colonies per well were revealed 21 days after the cultures were seeded, by using an inverted microscope Axiovert 200.

4.18. STATISTICAL ANALYSIS

All experiments were performed in triplicate unless different replicate number is indicated in the legends. Data of the graphs are expressed as means \pm SEM (standard error of the mean). Statistical significance was estimated with the Student's *t* test. For immunohistochemical analysis of human samples (Hepatitis C, ASH, NASH and control samples), logistic regression and Pearson's correlation coefficient were calculated by SPSS program. In all cases, values of $P > 0.05$ were considered statistically significant.

5. RESULTS

5. RESULTS

5.1. HuR/METHYL-HuR AND AUF1 REGULATE THE MAT EXPRESSED DURING LIVER PROLIFERATION, DIFFERENTIATION, AND CARCINOGENESIS.

Gastroenterology 2010;138:1943-1953

HGF, and also aminoimidazol carboxamide ribonucleotide (AICAR), both activators of the AMPK, exert a proliferative response in rat hepatocytes by translocating HuR to the cytosol and, thus, regulating the stability of cell cycle involved mRNAs, such as cyclin A2, D1 and D2 and increasing DNA synthesis (see section 2.2.5.1.) [152]. The treatment with SAMe avoids AMPK activation and, in consequence, blocks the HGF-induced hepatocyte proliferation and the HuR translocation and stabilization of *cyclin D1* and *D2* mRNAs [129]. Consequently, during liver regeneration, hepatic SAMe levels decrease, releasing the blockade imposed over the proliferation. This reduction in SAMe levels is due to the decrease in the expression of *MAT1A* together with an increase in *MAT2A* levels [98]. In accordance with this, the treatment with HGF up-regulates *MAT2A* mRNA levels, which is required for the liver proliferation process [304].

Until now, the up-regulation of *MAT2A* mRNA exerted by HGF, has been related at the transcriptional level with the increase of the acetylation of the histones H4 associated with *MAT2A* gene promoter, thus enhancing transcription factor binding to nucleosomes and increasing *MAT2A* gene transcription [107]. The transcription factors E2F and Sp1 were identified bound to *MAT2A* gene promoter, and particularly Sp1 seems to play a decisive role in *MAT2A* induction, binding the promoter when the gene is being actively transcribed [305].

Taking all these results in consideration, we investigated if there is any relation between the HGF-induced HuR translocation and the increase in *MAT2A* mRNA level during the proliferative process that can function together with the translational mechanisms described.

5.1.1. *MAT1A* and *MAT2A* mRNA levels are regulated by HuR and AUF1, respectively

We found that AICAR and HGF treatments in rat hepatocytes were able to upregulate the expression of *MAT2A* mRNA. This effect was completely blocked by the addition of SAMe (Figure 11A). Then, by using the transcriptional inhibitor Actinomycin D, we determined the half-life ($t_{1/2}$) of *MAT2A* mRNA after treating rat hepatocytes with AICAR alone or AICAR together with SAMe. The *MAT2A* half-life was increased by the treatment with AICAR ($t_{1/2} > 200$ min), compared with Actinomycin D alone ($t_{1/2} \approx 77$ min). The addition of SAMe together with AICAR, restricted the AICAR effect ($t_{1/2} \approx 173$ min) (Figure 11B, *upper graph*), suggesting that SAMe is able to destabilize *MAT2A* mRNA. These data are in accordance with previous reports showing that the addition of SAMe to an HCC cell line reduces the half-life of *MAT2A* mRNA [306].

When studying *MAT1A* mRNA expression during culture (Figure 11B, *bottom graph*), we could observe that, without treatment, *MAT1A* levels decrease, and the treatment with SAMe stabilizes *MAT1A* mRNA, what is in accordance with the published decrease of *MAT1A* during hepatocyte de-differentiation that is blocked by SAMe addition [101]. AICAR treatment had no significant effect on *MAT1A* mRNA levels (data not shown). Interestingly, the treatment with Actinomycin D increased *MAT1A* mRNA levels in comparison with the untreated condition, which can indicate that the inhibition of the transcription is reducing the expression levels of a factor implicated in the destabilization of *MAT1A* mRNA.

In order to directly assess the influence of the 3'UTR region in *MAT2A* mRNA stability, the 3'UTR was cloned into a plasmid expressing the GFP protein (pEGFP-C2). After transfecting the plasmid in the MLP29 mouse cell line, the expression of the GFP protein was reduced in the plasmid containing the 3'UTR of *MAT2A*, in comparison with the control plasmid. Moreover, the treatment with SAMe in the transfected cells reduced the expression of the GFP under the control of the *MAT2A* 3'UTR, but it presented no effect in the pEGFP-C2 control plasmid (Supplemental figure 1). These data suggest that the 3'UTR of *MAT2A*

is responsible of the destabilization of the GFP mRNA, and that SAMe is able to enhance the destabilizing effect that exerts. Thus, we hypothesize that *MAT2A* mRNA stability is under the control of its 3'UTR.

In silico analysis of the 3'UTR of *MAT1A* and *MAT2A* revealed the presence of a binding motif for the RNA binding protein AUF1 in the 3'UTR of *MAT1A* at position 3012, and a HuR binding site in

position 2200 in the 3'UTR of *MAT2A* (Figure 11C, scheme; the stars represent the predicted position of the motifs). No AUF1 or HuR motifs were found in the 3'UTR of *MAT2A* and *MAT1A*, respectively. In order to determine if the predicted binding motifs were functional, we used overlapping biotinylated probes corresponding with fragments of the mRNA of *MAT1A* and *MAT2A* (Figure 11C). The probes were incubated with cytoplasmic extracts from rat hepatocytes and purified with streptavidin. After

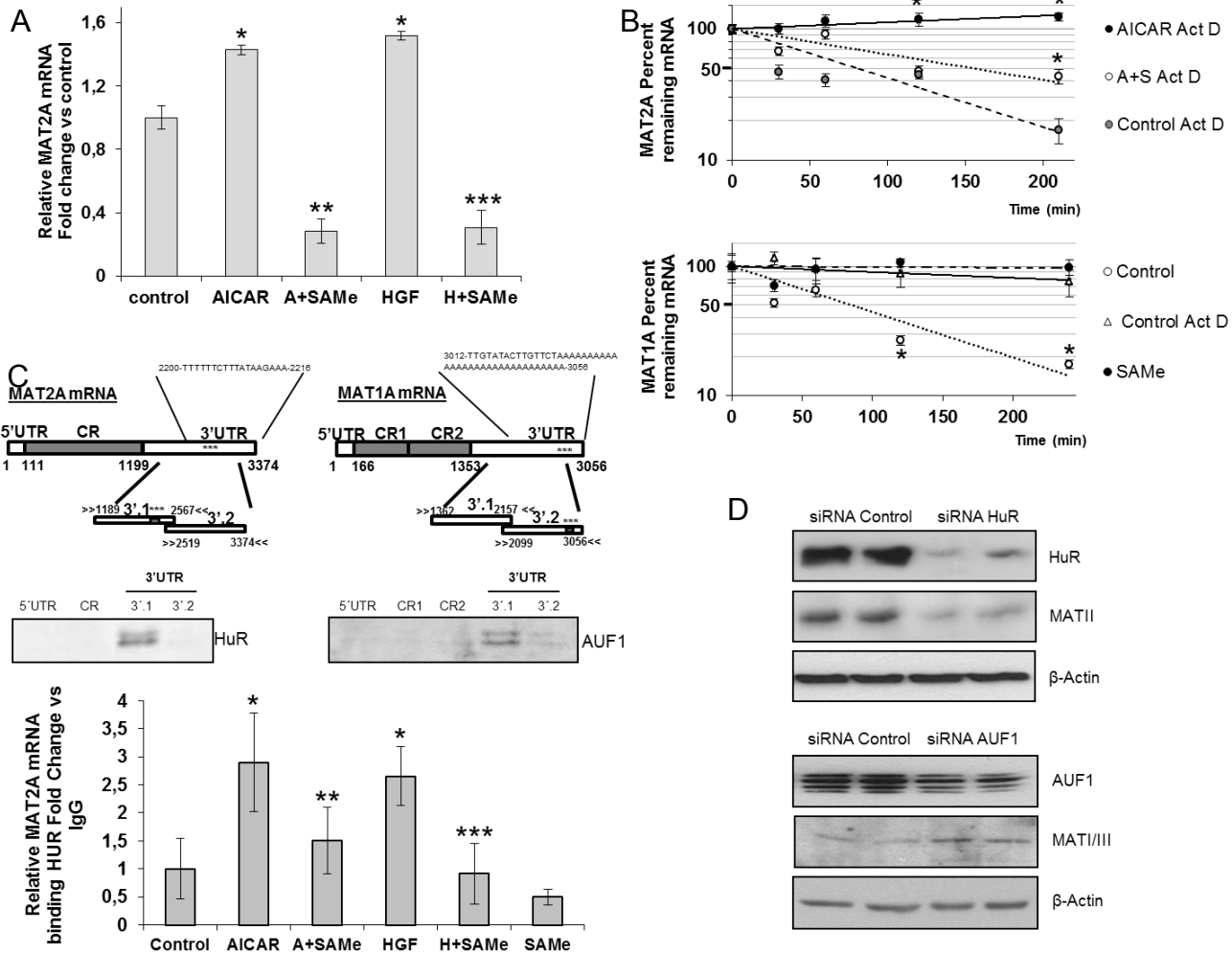


Figure 11. HuR stabilizes *MAT2A* mRNA and AUF1 destabilizes *MAT1A* mRNA. (A) Analysis of *MAT2A* mRNA from rat hepatocytes treated with AICAR (2 mmol/L), AICAR and SAMe (4 mmol/L), HGF (40 ng/mL), or HGF and SAMe for 4 hours. Treatments were performed in triplicate ($P < 0.05$, *AICAR or HGF vs. control, **SAMe and AICAR vs. AICAR, ***SAMe and HGF vs. HGF). (B) After AICAR, SAMe, or AICAR and SAMe treatments, rat hepatocytes were incubated with actinomycin D (Act D; 2 mcg/mL) for 4 hours. The levels of *MAT2A* and *MAT1A* mRNAs were normalized to GAPDH mRNA and represented on a semilogarithmic scale. Top graph, * $P < 0.05$, AICAR Act D or A and S Act D vs. Act D; bottom graph, * $P < 0.05$, SAMe vs. control. (C) Upper panel, *MAT2A* and *MAT1A* mRNA showing the biotinylated transcripts (5' UTR, coding region [CR], 3' UTR) and the predicted HuR and AUF1 motifs. Western blots show the association between HuR or AUF1 with biotinylated *MAT2A* and *MAT1A* fragments. Biotin pull-down assays were performed in triplicate using rat hepatocyte lysates. Bottom panel, RNP-IP analysis of *MAT2A* mRNA bound to HuR after SAMe, AICAR, AICAR and SAMe, HGF, and HGF and SAMe treatments. The enrichment was calculated from triplicate ($P < 0.05$, *AICAR or HGF vs. control, **SAMe and AICAR vs. AICAR, ***SAMe and HGF vs. HGF). (D) Three days after siRNA transfection, SAM-D and H4IIE cells were harvested to monitor the protein expression of HuR and *MAT2A*, or AUF1 and *MAT1A*, respectively. Western blots are representative of 3 independent experiments.

Western blot analysis, we found that HuR binds only to the 3'UTR of *MAT2A*, specifically with the fragment 3' (1) UTR-*MAT2A*. In the case of AUF1 the binding was just detected with the 3'UTR of *MAT1A*, in the fragment 3' (1) UTR-*MAT1A*, although the computational analysis predicted a binding site in the 3' (2) UTR-*MAT1A*. *In silico* predictions are not always biological hits, mainly due to a higher affinity of other RBPs to the predicted site. No interactions were observed for HuR in *MAT1A* mRNA or for AUF1 in *MAT2A* mRNA (not shown). For assuring the specificity of the technique, biotinylated GAPDH probes were used as negative control, and no signal was detected.

In this point, we inquired if the binding of HuR to *MAT2A* 3'UTR is modified by the treatment with AICAR, HGF and SAMe. For this, we performed a ribonucleoprotein immunoprecipitation (RNP-IP) assay by which we are able to immunoprecipitate HuR bound to its target mRNAs, and we obtain a cDNA library that we can analyze by quantitative PCR (qPCR). As shown in the Figure 11C (bottom graph), the qPCR analysis of the *MAT2A* mRNA bound to HuR, reveals that both AICAR and HGF significantly increased the binding of HuR to *MAT2A*, whereas SAMe treatment prevents the formation of this complex. Taking into account that HuR usually stabilizes its target mRNAs, this data correlates with the total *MAT2A* mRNA levels shown in the figure 11A.

Finally, the silencing of *HuR* and *AUF1* significantly reduced the expression of MAT II (66%) and increased MAT I/III (37%) proteins respectively, demonstrating the regulation of the *MAT2A* and *MAT1A* mRNAs (Figure 11D).

5.1.2. Coordinated expression of *MAT2A* and *MAT1A*, and their respective regulators, HuR and AUF1, during de-differentiation of cultured hepatocytes

As commented before, after isolating primary hepatocytes from the liver and culturing them, the hepatocytes de-differentiate losing their phenotype and acquiring a fibroblast-like phenotype. This de-differentiation is accompanied by a switch from *MAT1A* to *MAT2A*, an effect blocked by the supplementation of SAMe, which maintains the adult phenotype [101]. Studying the changes on *HuR* and *MAT2A* mRNAs during the de-

differentiation, we found that, similar to *MAT2A*, *HuR* levels also increased during culture. Both *MAT2A* and *HuR* in culture overexpressions were blocked by the addition of SAMe to the medium (Figure 12A, *upper* and *lower panels*). Previous reports have implicated the methylation of HuR on the arginine 217 in modulating HuR cytoplasmic levels and the affinity to the targets [235]. We studied HuR and methyl-HuR protein levels in cultured hepatocytes, with or without SAMe, and found that HuR levels remained unchanged at 6 and 12 hour independently of the addition of SAMe, and that HuR levels decrease at 24 hours after SAMe treatment. Methyl-HuR levels however, changed only slightly during de-differentiation process (Figure 12B).

To determine whether the two forms of HuR (methylated and unmethylated) bind to *MAT2A* mRNA differentially, RNP-IP assays were performed over time in the cultured hepatocytes, with the presence or absence of SAMe. As shown in the Figure 12C, *MAT2A* mRNA is enriched in HuR-IP compared with control IgG-IP, reaching a peak at 12 hours. Interestingly, the treatment with SAMe during the culture dramatically decreased the formation of the HuR-*MAT2A* RNP complexes (Figure 12C), corresponding with the decrease of the *MAT2A* mRNA level shown in Figure 12A. In contrast, methyl-HuR was bound to *MAT2A* mRNA only in the presence of SAMe (Figure 12D). Furthermore, we failed to detect *MAT2A* mRNA in AUF1 RNP-IP experiments performed on rat hepatocytes treated with SAMe, suggesting that AUF1 is not involved in the regulation of *MAT2A* mRNA stability.

These results suggest that HuR and methyl-HuR have opposite effects on *MAT2A* regulation: HuR stabilizes *MAT2A* mRNA during de-differentiation, but after the induction of the methylation of HuR by the addition of SAMe, methyl-HuR destabilizes *MAT2A* mRNA. According with our results, we propose that the ratio HuR/methyl-HuR functions as a sensor mechanism to control specific targets, such as *MAT2A* mRNA, during de-differentiation.

To address the functional role of methyl-HuR in the destabilization of *MAT2A* mRNA, a HuR mutant of the methylation site was generated by substituting the arginine 217 by a lysine. The binding of wild type HuR (*HuR(WT)-V5*) and

HuR(R217K)-V5 mutant to *MAT2A* mRNA was assayed in MLP29 cells transfected with plasmids containing WT or mutated HuR, in the presence of SAMe or not. Whereas HuR(WT)-V5 binding to *MAT2A* mRNA was decreased by the treatment with SAMe, the association of HuR(R217K)-V5 experimented no significant changes (Supplementary Figure 2). This indicates that the methylation of HuR is the mechanism by which the binding affinity to *MAT2A* mRNA changes in SAMe

treated hepatocytes.

Finally, hepatocytes cultured for 24 hours in the presence or absence of SAMe, were used to prepare a polysome gradient by sucrose fractionation. This technique separates polysomes by their molecular weight, which corresponds with the translational activity, from the non-translating light polysomes to the actively translating polysomes with higher molecular weight. After the separation, it is possible to analyze in each fraction

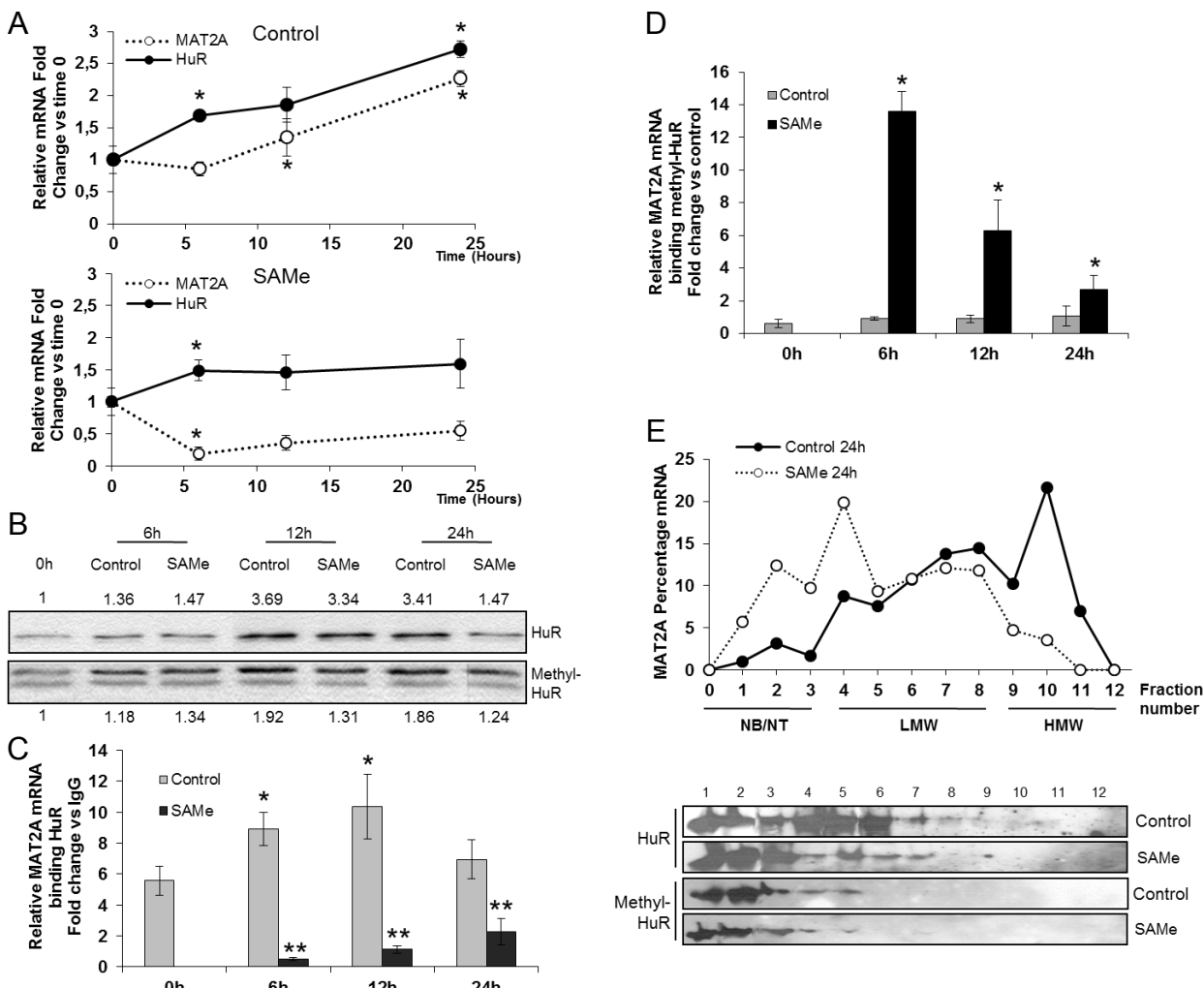


Figure 12. MAT2A expression during de-differentiation of cultured hepatocytes. (A) Expression of *MAT2A* mRNA over a time course in rat hepatocytes in the presence/absence of SAMe (4mM). * $P < 0.05$, time of treatment vs. previous time. (B) Representative Western blots of HuR and methyl-HuR in rat hepatocytes during de-differentiation. HuR vs. time 0 hours and methyl-HuR vs. time 0 ratios from densitometric analysis are presented; each assay was performed in triplicate. (C) The association of HuR with *MAT2A* was assayed by RNP-IP analysis using cytoplasmic fractions of rat hepatocytes. *MAT2A* mRNA was normalized to *GAPDH* mRNA in HuR-IPs, and results are represented as relative to the levels of *MAT2A* mRNA in control IgG-IPs. $P < 0.05$, *time of treatment vs. time 0 hours, **SAMe vs. control. (D) RNP-IP analysis of *MAT2A* mRNA bound to methyl-HuR; the enrichment was calculated from triplicate samples. * $P < 0.05$, SAME vs. control. (E) Polysome gradient analysis in rat hepatocytes cultured for 24 hours in the presence/absence of SAMe. *MAT2A* mRNA levels were plotted as a percentage of the total *MAT2A* mRNA levels. The translational activity of the polysomes is as follows: NB, not bound polysomes; NT, not translated; moderately translated (LMW, low molecular weight polysomes); and actively translated (HMW, high molecular weight polysomes) (upper panel). HuR and methyl-HuR protein in each fraction were analyzed by Western blot analysis (lower panel). Each assay was performed in triplicate.

the present mRNAs by qPCR and the proteins bound to the mRNAs by Western blotting. *MAT2A* mRNA was detected to be increased in the fractions corresponding to actively translating polysomes (fractions 7-11) in the control hepatocytes. After treatment with SAMe, *MAT2A* mRNA disappeared from the heavier fractions and it was detected increased in the fraction with limited translational activity (fractions 1-8) (Figure 12E, *upper panel*). When studying the presence of HuR and methyl-HuR proteins in the polysomes, we found that HuR was found in fractions 1-8, whereas after treatment with SAMe, HuR was more abundant in fractions 1-3, characterized by a limited translational activity. Methyl-HuR was present in the less translationally active polysomes, independently of SAMe treatment (Figure 12E, *lower panel*). Taken together, these results suggest that HuR-bound *MAT2A* mRNA is stabilized and actively translated during de-differentiation of the hepatocytes, whereas in the

presence of SAMe, only methyl-HuR co-localizes with untranslated *MAT2A* mRNA.

Once analyzed the relation between HuR and *MAT2A* during de-differentiation, we studied *MAT1A* mRNA and AUF1 regulation during this process. We found that, during hepatocyte de-differentiation, *MAT1A* mRNA levels decrease, together with an increase in the levels of the RBP AUF1, related usually with the destabilization of target mRNAs (Figure 13A, *upper panel*). The treatment with SAMe was able to maintain the level of *MAT1A* mRNA after 24 hours in culture similar to the levels at the initial time, and to block AUF1 increase (Figure 13A, *lower panel*). According with this, when studying MAT I/III and AUF1 proteins 24 hours after the culture, MAT I/III notably decreased compared with the initial culture time, together with the increase of the AUF1 protein. The treatment with SAMe reduced AUF1 level and increased the amount of MAT I/III protein

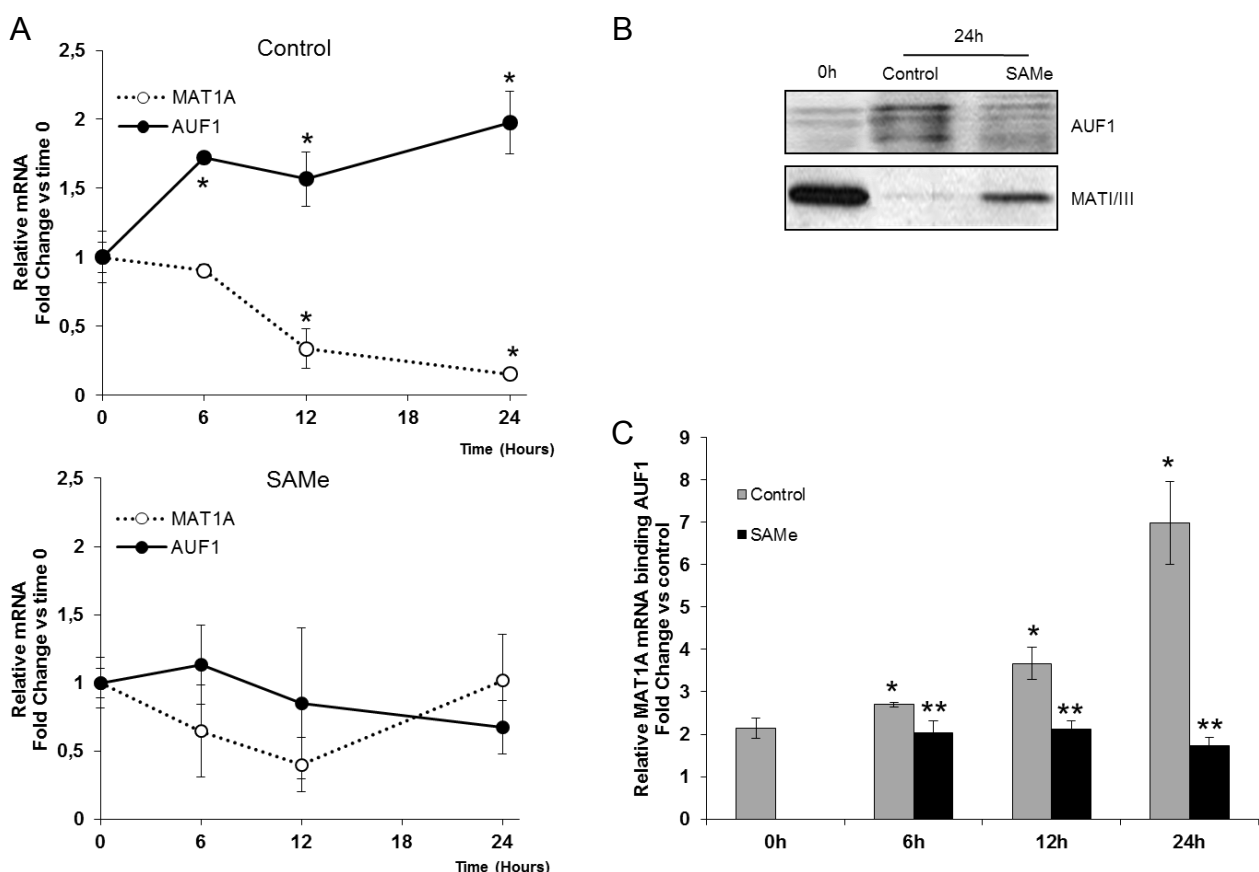


Figure 13. *MAT1A* expression during de-differentiation of cultured hepatocytes. (A) *MAT1A* and AUF1 mRNA expression in rat hepatocytes at the indicated times. * $P < 0.05$, culture time vs. time 0 hours. (B) Representative Western blot analysis of AUF1 and MAT I/III proteins in rat hepatocytes undergoing de-differentiation; data are representative of 3 independent experiments. (C) RNP-IP analysis of the association of AUF1 with *MAT1A* mRNA in cytoplasmic fractions of rat hepatocytes incubated as indicated. The enrichment of *MAT1A* mRNA in AUF1-IPs was calculated as described in Figure 2C. $P < 0.05$, *time of treatment vs. time 0 hours, **SAME vs. control.

(Figure 13B). The binding of AUF1 to *MAT1A* mRNA, assayed by RNP-IP, showed that during the culture AUF1 increases the binding to *MAT1A*, a process also abrogated by SAMe treatment (Figure 3C).

5.1.3. Role of HuR, methyl-HuR and AUF1 during liver development

The above-mentioned data involving HuR and AUF1 RBPs in the regulation of *MAT2A* and *MAT1A* mRNAs raise the question of whether they are also involved in liver differentiation. As explained in the introduction, *MAT1A* is expressed only in the adult liver, whereas *MAT2A* is found

predominantly in fetal liver, with a minimal expression in the adult liver [92]. During liver development from fetal stages to adult liver, it takes place a switch from *MAT2A* expression to *MAT1A* expression. We examined the expression levels of *MAT2A*, *MAT1A*, *HuR* and *AUF1* mRNAs in rat livers from embryonic days 16 and 18 (E16, E18), postnatal days 1 and 5 (P1, P5) and three month adult rats (Figure 14A and 14B). *MAT2A* and *HuR* levels decrease during liver development to minimal levels in adult livers (Figure 14A). In contrast, *MAT1A* reaches a maximum of expression in the adult liver, whereas *AUF1* mRNA decreases with the age of the rats (Figure 14B).

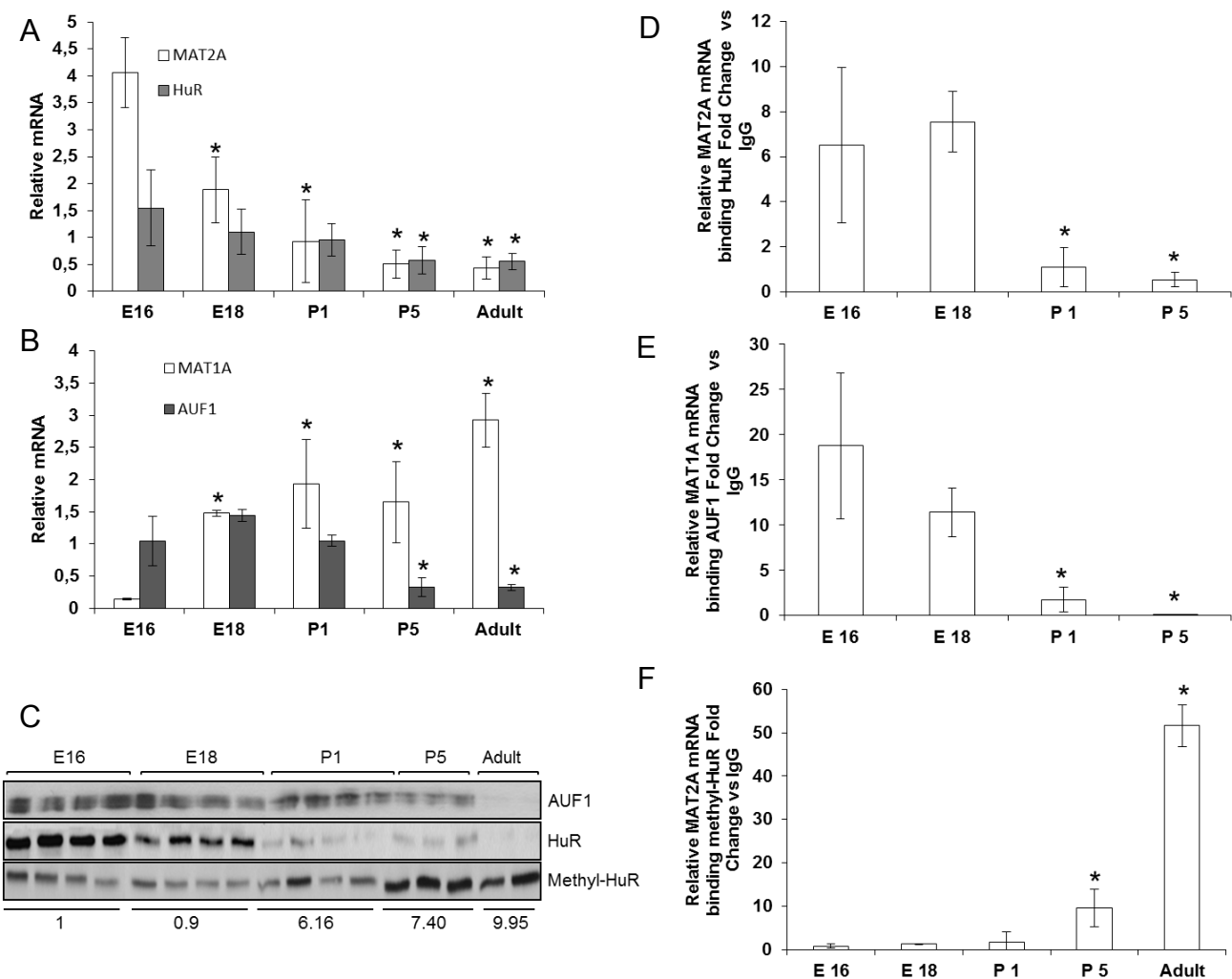


Figure 14. Role of HuR, methyl-HuR, and AUF1 during liver development. (A) mRNA expression of *MAT2A* and *HuR* in fetal livers (E16, E18), livers from pups (P1 and P5) and adult rats (3 months), normalized to *GAPDH* mRNA. **P* < 0.05, *ages of development vs. E16. (B) *MAT1A*, and *AUF1* mRNA levels during liver development. **P* < 0.05, *ages of development vs. E16. (C) Levels of HuR, methyl-HuR, and AUF1 proteins evaluated by Western blot analysis. Ponceau S staining was used as loading control (Supplementary Figure 3). The ratio of methyl-HuR/HuR was calculated. (D) Binding of HuR to *MAT2A* during liver development, as assessed by RNP-IP and real-time PCR analysis. **P* < 0.05, ages of development vs. E16. (E) RNP-IP showing the binding of AUF1 to *MAT1A* during liver development. **P* < 0.05, ages of development vs. E16. (F) RNP-IP analysis of *MAT2A* mRNA bound to methyl-HuR. **P* < 0.05, ages of development vs. E16. Enrichment represents the average from triplicate experiments.

At the protein level, both HuR and AUF1 decrease from E16 to adult livers, whereas methyl-HuR levels highly increase (Figure 14C). The methyl-HuR/HuR ratio also increases during liver development, correlating with the decrease in *MAT2A* mRNA levels.

We also studied the binding of HuR to *MAT2A* mRNA, finding a sharp decrease during liver development stages, which correlates with the decrease in the *MAT2A* mRNA levels (Figure 14D), and a marked decrease in the binding of AUF1 to *MAT1A* mRNA, in accordance with the decrease of *MAT1A* (Figure 14E). Finally, an increase in the binding of methyl-HuR to *MAT2A* mRNA was observed during liver development (Figure 14F), suggesting that methyl-HuR might destabilize *MAT2A* mRNA or inhibit its translation. Taken together these results strongly suggest that the balance between methyl-HuR, HuR and AUF1 is required to regulate the levels of *MAT2A* and *MAT1A* during liver development and differentiation.

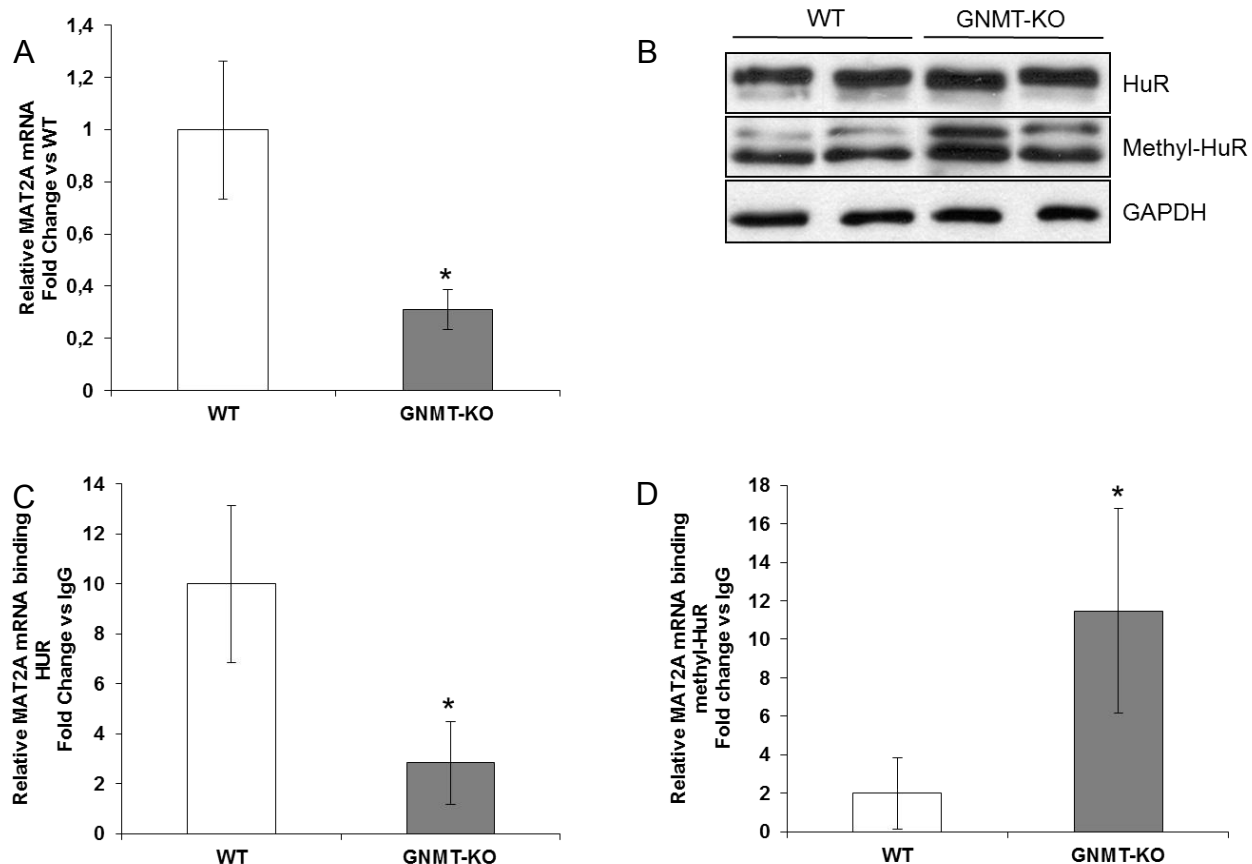


Figure 15. The levels of *MAT2A* mRNA are regulated by HuR in GNMT-KO mice. (A) *MAT2A* mRNA expression level in GNMT-KO mice expressed as fold-change vs. WT (* $P < 0.05$). (B) Levels of HuR, methyl-HuR and loading control GAPDH in total extracts. (C) RNP-IP analysis of HuR binding to *MAT2A* mRNA. (D) RNP-IP analysis of *MAT2A* mRNA bound to methyl-HuR, * $P < 0.05$, GNMT-KO vs. WT.

5.1.4. Regulation of *MAT2A* in an *in vivo* model of chronic excess of hepatic SAMe

As supported by our results, the methyl-HuR/HuR ratio regulates the expression of *MAT2A* in a SAMe-dependent manner. In order to further study this effect, we analyze the regulation of *MAT2A* mRNA in the mouse model of GNMT-KO (see Introduction section 2.2.7.2.). In these mice, SAMe levels are chronically elevated, and spontaneously develop steatosis, fibrosis and HCC.

The GNMT-KO mice present a significantly lower expression of *MAT2A* mRNA (Figure 15A), corresponding with an increased level of methyl-HuR protein compared with WT animals (Figure 15B). In contrast, although SAMe levels are high, GNMT-KO mice did not show reduced HuR levels, possibly due to the highly proliferative status of the livers in these mice [49]. In addition, the binding of HuR to *MAT2A* mRNA is lower in the GNMT-KO mouse compared to the WT mouse (Figure 15C), and the methyl-HuR-*MAT2A* mRNA RNP

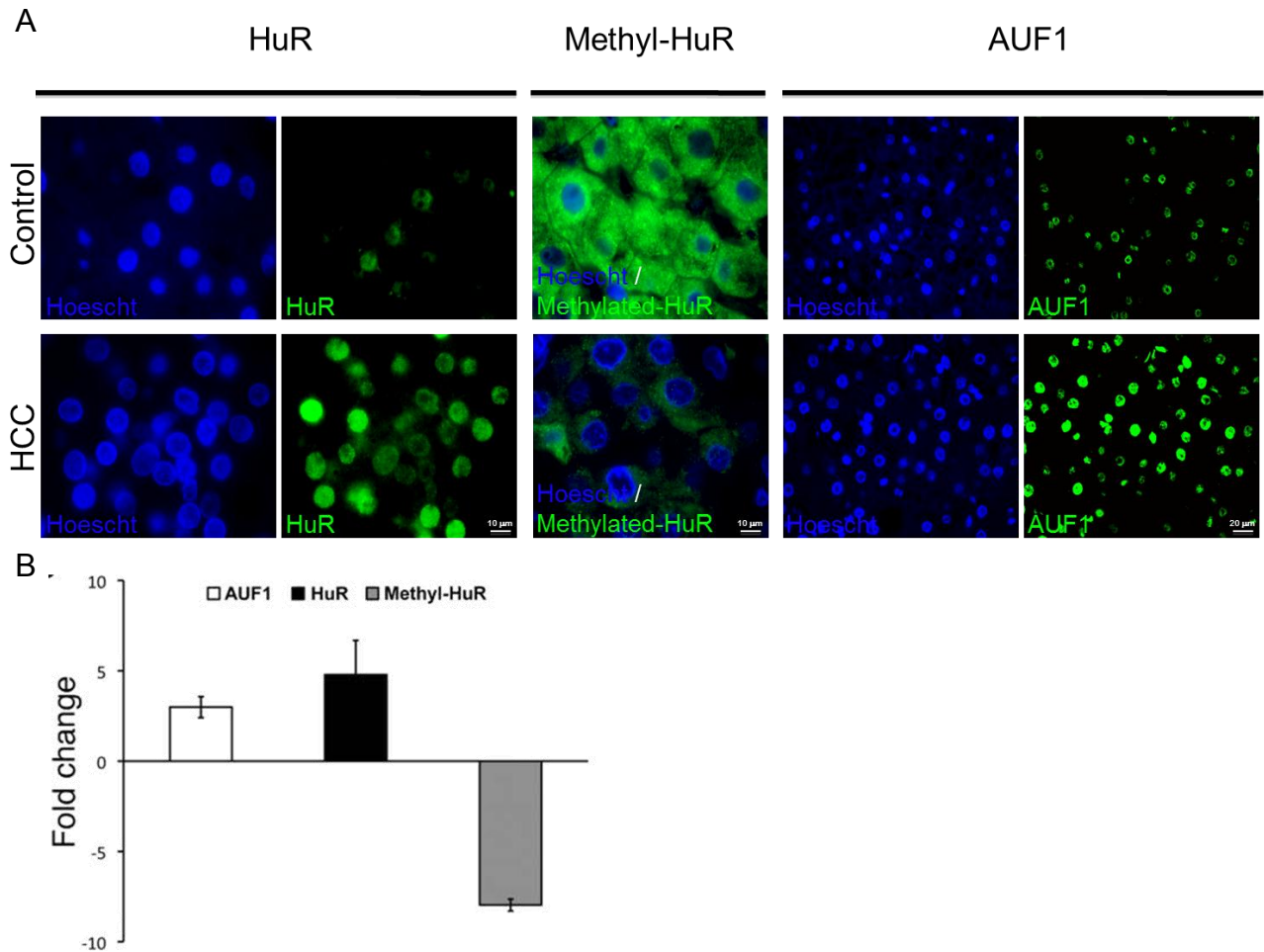


Figure 16. HuR, methyl-HuR and AUF1 detection in human HCC. (A) Representative immunofluorescence analysis of HuR, methyl-HuR and AUF1 protein in normal and human HCC samples. (B) The relative immunofluorescence in cancer tissues was calculated using Image J software and expressed as fold-change of the relative immunofluorescence intensity in normal tissues. Data are representative of experiments realized in 22 HCC patients and 4 normal biopsies, and fold-change are significantly different ($P < 0.05$).

complexes are increased in the KO animals (Figure 15D). In summary, the low levels of *MAT2A* mRNA in the GNMT-KO mouse can be due to the increase in the ratio methyl-HuR/HuR, the reduction of the HuR-MAT2A mRNA complexes, and the enhanced levels of methyl-HuR-MAT2A mRNA RNP complexes, corresponding with the results obtained in the models of de-differentiation and liver development.

The liver regeneration of the GNMT-KO mouse model, where the SAMe levels are impaired, will be studied in the section Results 5.2.

5.1.5. HuR and AUF1 levels in human HCC

The switch between *MAT1A* and *MAT2A* genes during de-differentiation has also been

investigated in human hepatoma cell lines and in tissues resected from patients of HCC and cirrhosis [47]. In order to assess the levels of HuR, methyl-HuR and AUF1 in human HCC, we performed immunofluorescence analysis of healthy and cancerous human livers. As shown in Figure 16, AUF1 and HuR are expressed at higher level in the HCC samples compared to the control livers, whereas methyl-HuR was found decreased in the liver tumors. These results are in accordance with the high *MAT2A* and low *MAT1A* mRNA levels characteristic of the HCC.

5.2. IMPAIRED LIVER REGENERATION IN MICE LACKING GLYCINE N-METHYLTRANSFERASE.

Hepatology 2009; 50(2):443-452

As described in the previous section, the GNMT-KO mouse, with chronically elevated levels of SAMe, presents a dysregulation in the methylation of HuR that leads to a decrease in MAT2A levels. Together with this, total HuR levels are elevated, corresponding with the high proliferative status of GNMT-KO liver that leads to spontaneously develop HCC (Introduction section 2.2.7.2.). In addition, high SAMe levels inactivate HuR cytoplasmic translocation, involved in the stabilization of cell cycle and proliferation mRNAs during hepatocyte proliferation, in response to LKB1/AMPK/eNOS pathway activation (see Introduction section 2.2.5.1.). Taking in consideration all these points, we studied whether the excess of hepatic SAMe in the GNMT-KO mouse impairs the liver regeneration after partial hepatectomy (PH) by blocking the LKB1/AMPK/eNOS pathway and HuR translocation.

5.2.1. Increased mortality in GNMT knockout mice during liver regeneration

Three-month old male GNMT-KO mice and age-matched WT animal were subjected to PH. Attending to the mortality in the first 48 hours after PH, no wild type animals died, whereas 38% of GNMT-KO mice did not survive Figure 17A. Together with the high mortality, also the apoptotic response was markedly increased in the GNMT-KO mice compared to the wild type, as evidenced by the high poly (ADP-ribose) polymerase (PARP) cleavage present before partial hepatectomy and maintained in the surviving animals (Figure 17B).

The cellular proliferation after PH was assessed by PCNA staining and BrdU incorporation. PCNA is an auxiliary protein of DNA polymerase delta, with a cell cycle-dependent expression, being detected in late G₁ phase, during all S phase and in the early postreplicative G₂ period [307]. BrdU is a thymidine analog that is incorporated during DNA synthesis (S phase) [307]. Thus, unless both are markers of cellular proliferation, only BrdU is specific of the S phase. As shown in Figure 18A and 18B, at baseline PCNA staining was higher in GNMT-KO compared

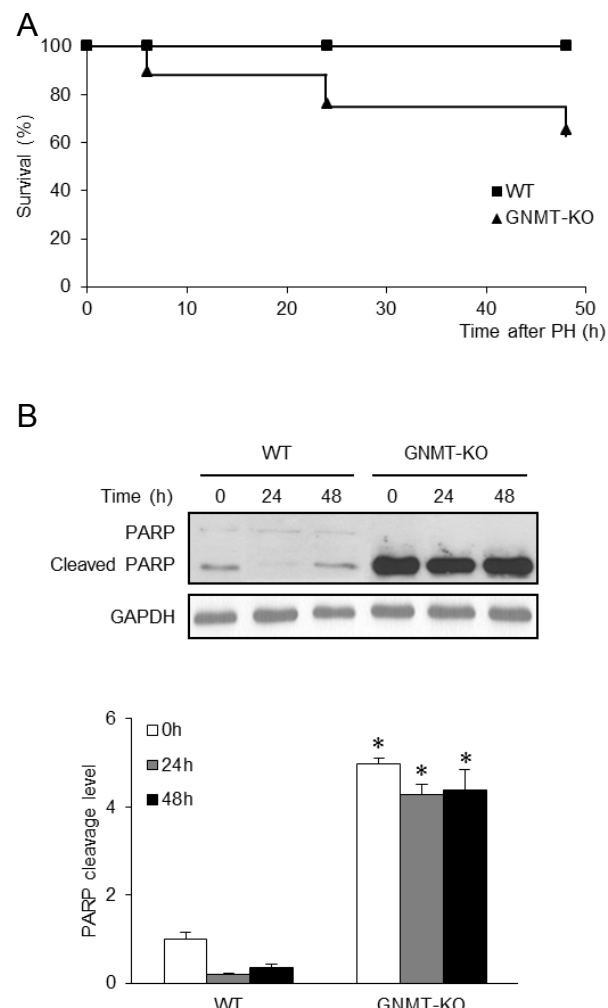


Figure 17. Mortality and PARP activation in WT and GNMT-KO mice after PH. (A) Cumulative survival of the WT ($n = 37$) and GNMT-KO ($n = 31$) mice after PH. The difference between the groups was statistically significant ($P < 0.05$). (B) PARP cleavage in WT and GNMT-KO after PH. *Upper panel:* Liver samples from WT and GNMT-KO mice were obtained at 0, 24 and 48 hours after PH and analyzed by Western blotting. Data are representative of an experiment performed five times. *Lower panel:* Graphical representation (mean \pm standard error of the mean [SEM]) of the densitometry changes of PARP cleavage in liver samples obtained at 0, 24, and 48 hours after PH from WT and GNMT-KO mice. * $P < 0.05$ GNMT-KO versus WT mice at the same time point.

with wild type animals, whereas BrdU-positive hepatocytes are similar. Following PH, the number of BrdU-positive and PCNA positive cells increased similarly in the controls and in the GNMT-KO mice (Figure 18 A, B). These results indicate that the increase in mortality in GNMT-KO mice after PH is not due to an inhibition of DNA

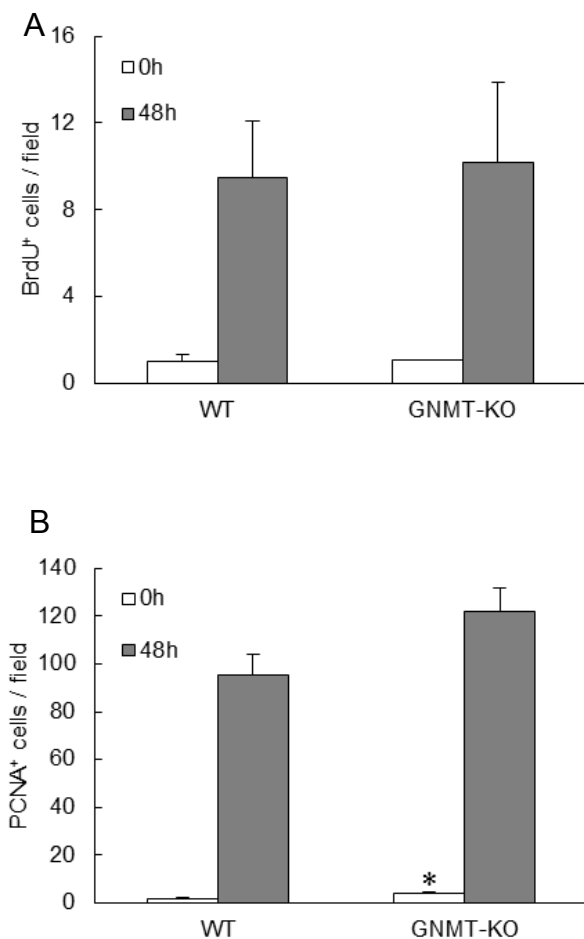


Figure 18. Hepatocyte proliferation after PH as assessed by BrdU incorporation and PCNA staining. (A) The number of BrdU-positive cells at 0 hours and 48 hours after PH were calculated and expressed as the number of positive cells per field in liver specimens from WT and GNMT-KO mice. (B) The number of PCNA-positive cells at 0 hours and 48 hours after PH were counted and expressed as the number of positive cells per field in liver specimens from WT and GNMT-KO mice. In both cases the number of positive cells was counted in 10 microscope fields using a $\times 40$ objective and a $\times 10$ eyepiece with a Zeiss AX10 microscope. Data are the average of five experiments performed independently. *P < 0.05 GNMT-KO versus WT mice at the same time point.

synthesis, but probably to increased liver apoptosis.

5.2.2. GNMT-KO mice are able to progress into cell cycle S phase

GNMT-KO mice are known to develop liver steatosis at 3 month of age, and multifocal HCC at 8 month of age. These injuries are in part due to aberrant DNA and histone methylation, resulting in

epigenetic modulation of critical carcinogenesis pathways [49]. Consistently with this, 3-month-old GNMT-KO mice present, at baseline, increased phosphorylation of STAT3, and increased cyclin D1 and cyclin A (Figure 19A, B). After partial hepatectomy, whereas wild type animals increase the phosphorylation of STAT3 (involved in the *priming phase* of the liver regeneration, section 2.2.5.1), in GNMT-KO mice dramatically decrease. The cyclin D1 and cyclin A failed to increase after PH in GNMT-KO animals, as occurs in the wild type (Figure 19A, B). Cyclin E increases after PH, but does not reach the same levels than in the control mice, and the inhibitor of cyclin A, p27 protein, decreased in wild type animals but increased in GNMT-KO (Figure 19B). These results, together with the previously shown ability of GNMT-KO mice hepatocytes to stimulate DNA synthesis, suggest that these hepatocytes are not arrested in G₁ phase of the cell cycle, being able to progress into the S phase.

5.2.3. LKB1/AMPK/eNOS pathway and HuR cytoplasmic translocation are inhibited during liver regeneration in GNMT-KO mice

The AMPK/LKB1/eNOS pathway is activated in response to HGF during hepatocyte proliferation, and, importantly, is inhibited by SAMe treatment prior PH. Accordingly, we studied the phosphorylation of LKB1 and AMPK after PH in GNMT-KO and control animals. We found that prior to PH, at baseline, both LKB1 and AMPK phosphorylation is reduced in GNMT-KO compared to the wild type animals (Figure 20A). We also found that LKB1 and AMPK are activated in the wild type mice 30 minutes after PH, whereas in the GNMT-KO there is no activation (Figure 20A). This agrees with the observation that the hepatic content of SAMe is about 50-fold higher in the GNMT-KO mice than in the controls [176], and with the present finding that, whereas in WT mice, as expected, SAMe levels decrease about half following PH, in the GNMT-KO mice SAMe levels fail to decrease (Table 6).

As commented before, after HGF treatment, wild type hepatocytes experiment an increased phosphorylation of LKB1 and AMPK. This process is inhibited by the addition of SAMe [132, 152]. In the GNMT-KO mice, the lack of activation of LKB1 and AMPK after PH can be explained by the high SAMe content in the liver, which would prevent the

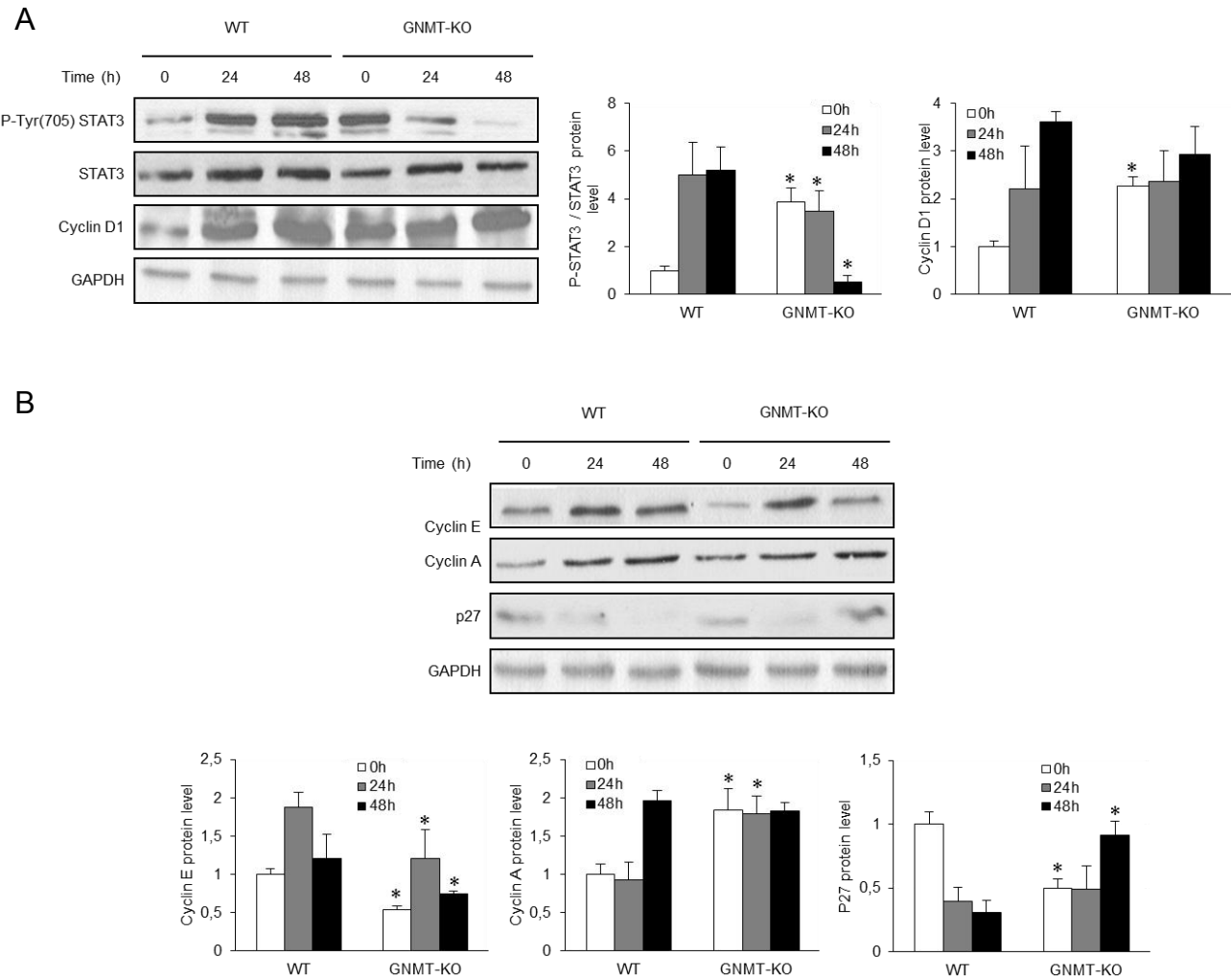


Figure 19. Phosphorylation of STAT3 and protein expression of cyclin D1, cyclin E, cyclin A, and p27 in WT and GNMT-KO mice following PH. (A) Left panel: Liver samples from WT and GNMT-KO mice were obtained at 0, 24, and 48 hours after PH and analyzed by Western blotting. Data are representative of an experiment performed five times. Right panels: Graphical representation of the densitometric changes of STAT3 phosphorylation and cyclin D1 protein content in liver samples from WT and GNMT-KO mice after PH. (B) Upper panel: liver samples from WT and GNMT-KO mice were obtained at 0, 24, and 48 hours after PH and analyzed by Western blotting. Data are representative of an experiment performed five times. Lower panel: Graphical representation of the densitometric changes of cyclin E, cyclin A, and p27 protein content in liver samples from WT and GNMT-KO mice after PH. *P <0.05 GNMT-KO versus WT mice at the same time point.

HGF-dependent phosphorylation of LKB1 and AMPK. In order to test this hypothesis, we measured LKB1 and AMPK phosphorylation in hepatocytes isolated from GNMT-KO mice. As shown in the Supplemental Figure 4, in the knockout hepatocytes HGF failed to induce the phosphorylation of both LKB1 and AMPK.

In addition to its function as energy sensor, hepatic AMPK is also involved in the phosphorylation and activation of eNOS, a key step for the activation of iNOS and NO synthesis in the liver, which is crucial in hepatocyte proliferation

and in the decrease of SAMe level (see Introduction section 2.2.5.1). We found that at baseline, eNOS phosphorylation was reduced in GNMT-KO mice as compared to the wild type animals (Figure 20A). After partial hepatectomy, eNOS is activated in WT animals, but in the GNMT-KO mice eNOS fails to increase its phosphorylation (Figure 20A).

The activation of AMPK in wild type hepatocytes is also responsible of the translocation of HuR from the nucleus to the cytoplasm, thus stabilizing cell cycle and

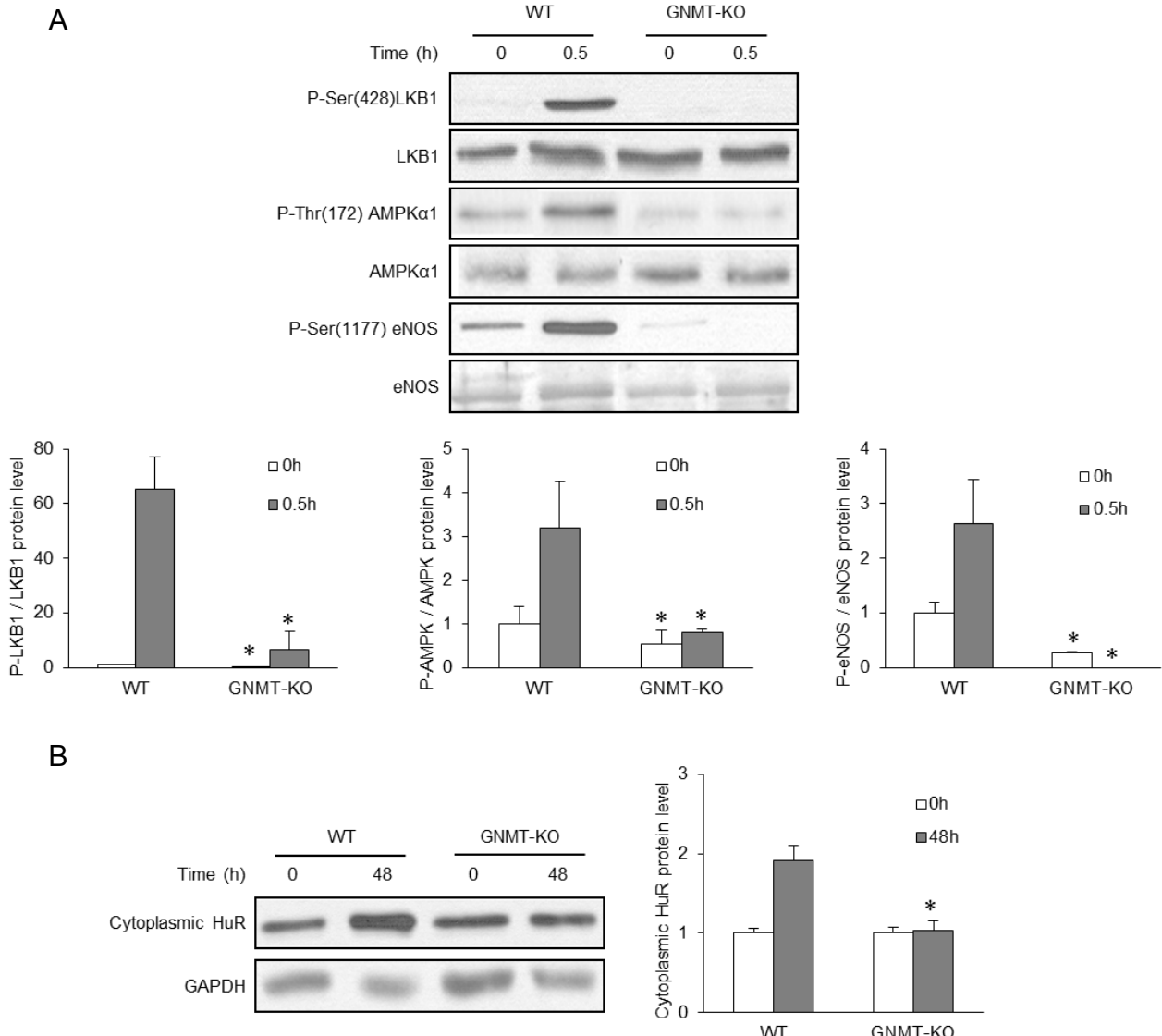


Figure 20. Phosphorylation of LKB1, AMPK and eNOS and cytoplasmic HuR content in WT and GNMT-KO mice during liver regeneration after PH. (A) *Upper panel*: Liver samples were obtained before and 30 minutes after PH and analyzed by Western blot. Data are representative of an experiment performed five times. *Lower panel*: Densitometry of LKB1, AMPK, and eNOS phosphorylation in liver samples from WT and GNMT-KO mice after PH. (B) *Left panel*: Representative Western blot of cytoplasmic HuR from liver samples before and 48 hours after PH. *Right panel*: Densitometry of cytoplasmic HuR protein levels in liver samples from WT and GNMT-KO mice after PH. *P < 0.05 GNMT-KO versus WT mice at the same time point.

proliferation genes such as cyclin D1, cyclin A2, etc. The treatment with SAMe blocks HuR translocation blocking cell cycle progression. As previously explained, in the GNMT-KO mice, total HuR levels at baseline are similar to the wild type (Figure 15B), and also the cytoplasmic HuR levels are similar (Figure 20B). 48 hours after PH, the cytoplasmic levels of HuR in the wild type mice increase, due to the translocation of HuR from the nucleus, whereas in the GNMT-KO animals the levels are maintained unchanged (Figure 20B). This anomalous regulation of HuR subcellular

localization can modify the binding to its targets, thus failing to stabilize mRNAs involved in cell cycle progression, proliferation, etc. Between these genes we can find cyclin D1 and cyclin A2, according with the lack of increase previously found (Figure 19).

Because GNMT-KO mice show at baseline steatosis and hypermethylation of multiple genes, the impairment in liver regeneration could be due in part to these abnormalities. In order to check this point, we analyzed the effect of GNMT

knockdown on HGF-induced cyclin D1 in isolated rat hepatocytes. Compared with control cells, hepatocytes transfected with siRNA specific for *GNMT* showed a marked decrease in *GNMT* mRNA without significantly affecting *MAT1A* mRNA (Figure 21A). When analyzing cyclin D1 overexpression after HGF treatment, we found a reduction of 60% in *GNMT* silenced cells compared with control cells (Figure 21B). These data point towards the dysregulation of the HGF-induced hepatocyte proliferating response.

We next silenced *GNMT* *in vivo* in WT mice to examine the effect of *GNMT* knockdown on liver regeneration after PH. As shown in Figure 22A and 22B, mice treated with *GNMT*-specific siRNA presented a 2-fold reduction in hepatic *GNMT* mRNA and protein as compared with control mice. The silencing of *GNMT* led to a marked reduction in cyclin D1 and A mRNA and protein after PH compared with control mice (Figure 22C and 22D). Also, the HuR cytoplasmic accumulation after PH is blocked in the mice treated with siRNA for *GNMT* (Figure 22D). This situation resembles that found in *GNMT*-KO mice after PH, where cyclin D1 and A expression, and cytoplasmic HuR remain unchanged (Figures 19 and 20), supporting the role of *GNMT* during liver regeneration after PH.

5.2.4. Inhibition of AMPK induces NF κ B activation in hepatocytes

Given that NF κ B activation and the induction of iNOS expression play an important role in liver regeneration [125, 154], we determined these two parameters in *GNMT* knockout and wild type mice after partial hepatectomy. The results are displayed in the Figure 23. At baseline, liver NF κ B activation was higher in the *GNMT*-KO mice compared to the wildtype, as evidenced by the nuclear accumulation of total and nuclear Ser(536) phosphorylated p65 (Figure 23A). However, 30 minutes after PH this situation drastically changes, and whereas in the WT mice the typical

regenerative response led to a marked increase of the nuclear p65, in the *GNMT*-KO animals the nuclear content of p65 remained constant and below the levels observed in the wild type (Figure 23A). Consistently with this abnormal pattern of NF κ B signaling, we observed that iNOS, which is a target of NF κ B, was significantly higher in *GNMT*-KO mice than in the control animals before PH, whereas after PH iNOS expression failed to increase in the *GNMT*-KO mice (Figure 23B). Moreover, *iNOS* mRNA is also stabilized by HuR, and thus the lack of HuR cytoplasmic accumulation after PH (Figure 20B) can also be involved in the misregulation of iNOS after PH.

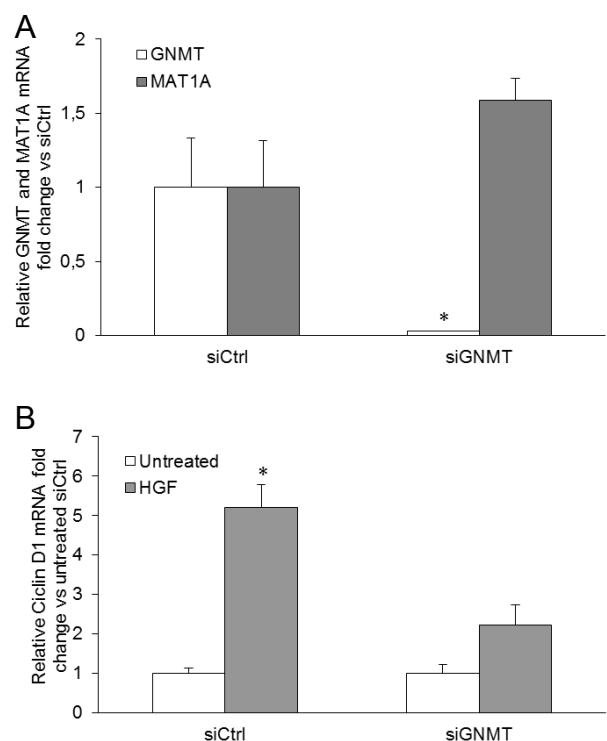


Figure 21. Knockdown of *GNMT* with siRNA reduces HGF-induced cyclin D1 expression. Freshly isolated rat hepatocytes were transfected with *GNMT* specific siRNA or control siRNA by electroporation using the rat hepatocyte Nucleofector® Kit from Amaxa. Two hours after attachment, the culture medium was replaced by MEM supplemented with 5% FBS and triamcinolone (100 nM). 24 hours after electroporation, hepatocytes were treated with HGF (25 ng/mL) for another 24 hours. mRNA was then isolated. (A) Real-time PCR analysis of *GNMT* and *MAT1A* mRNA expression in hepatocytes transfected with siCtrl or siGNMT. (*P < 0.05 siGNMT vs. siCtrl). (B) Real-time PCR analysis of cyclin D1 mRNA expression of hepatocytes transfected with siCtrl or siGNMT and treated with HGF during 24 hours. Each bar represents the mean ± SD of at least quadruplicate experiments (*P < 0.05 HGF vs. untreated). Values were normalized with 18S ribosomal RNA expression.

Table 6. Hepatic SAMe content in wild type (WT) and *GNMT*-KO mice before and 48 hours after PH

SAMe nmol/mg protein	0 hours	48 hours
WT	0.47±0.03	0.25±0.03*
<i>GNMT</i> -KO	21.73±0.88	20.64±0.97

Liver samples were obtained before (0 hours) and 48 hours after PH and the content of SAMe was determined. *P < 0.05, 48h vs. 0h

RESULTS

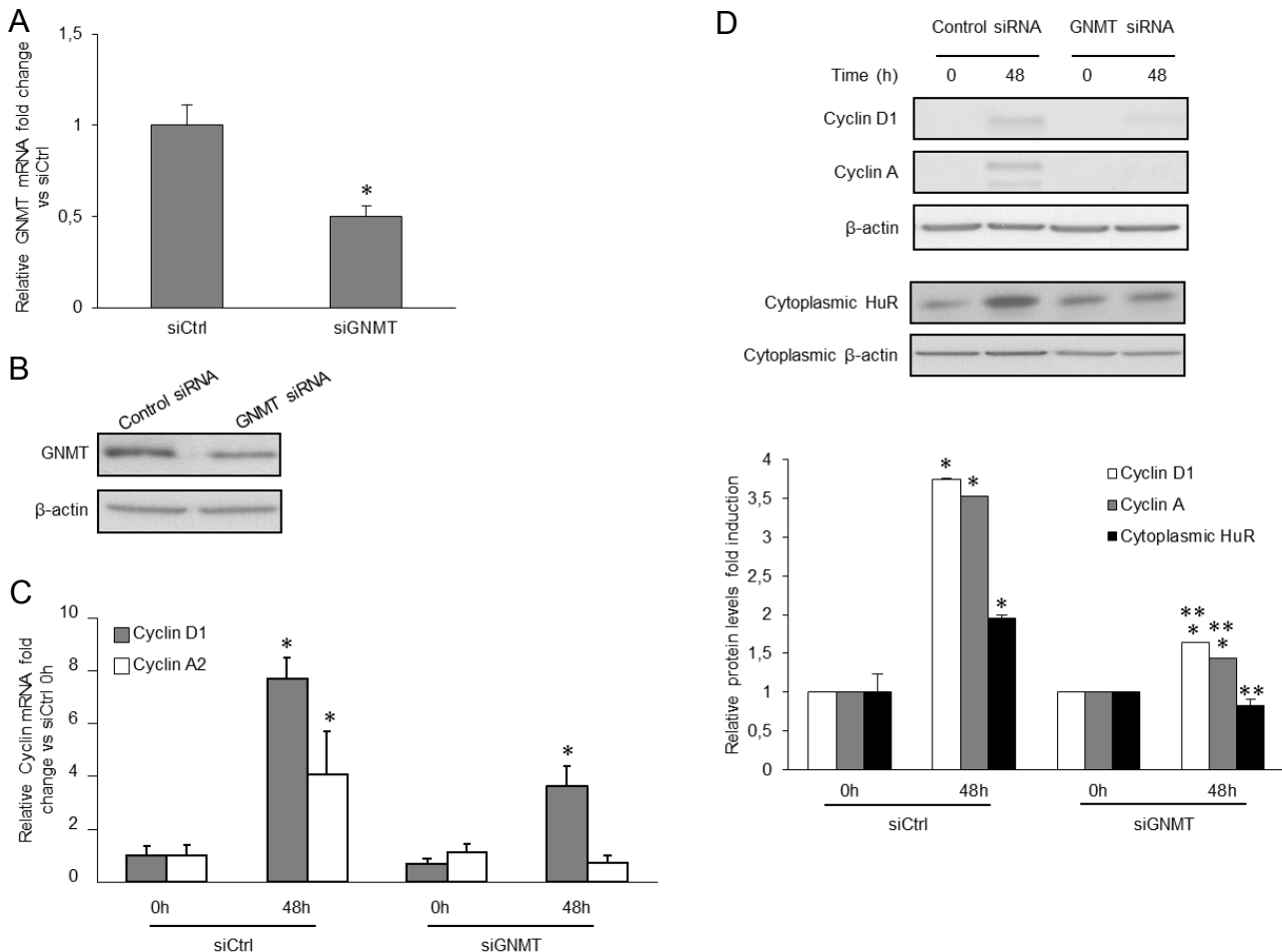


Figure 22. Knockdown of GNMT reduces cyclin A and D1 expression and cytoplasmic HuR accumulation in livers after partial hepatectomy. Three month-old male WT mice were injected intravenously in the tail vein (200 μ l of a 60 μ M solution) with GNMT specific siRNA or control siRNA 24 hours and 2 hours before PH. Livers were then removed during PH (time 0 hours) and 48 hours after PH, and mRNA and protein extracted. (A) Real-time PCR analysis of GNMT mRNA expression 24 hours after siRNA injection (time 0 hours) (* $P < 0.05$ siGNMT vs. siCtrl). Values of mRNA expression were normalized with 18S ribosomal RNA expression. (B) Western blot analysis of GNMT protein levels 24 hours after siRNA injection (time 0 hours). (C) Real-time PCR analysis of cyclin D1 and A2 mRNA expression levels in livers from mice injected with GNMT specific siRNA or control siRNA, 24 hours after the injection (time 0 hours) and 48 hours after the PH. Each bar represents the mean \pm SD of quadruplicate experiments (* $P < 0.05$ 48h vs. 0h). Values of mRNA expression were normalized with 18S ribosomal RNA expression. (D) Western blot analysis and densitometry of cyclin D1 and A and cytoplasmic HuR protein levels in livers from mice injected with GNMT specific siRNA or control siRNA, 24 hours after the injection (time 0 hours) and 48 hours after the PH. (* $P < 0.05$ 48h vs. 0h; ** $P < 0.05$ siGNMT vs. siCtrl at the same time point).

Because we found that in GNMT-KO mice liver AMPK phosphorylation is inhibited and NF κ B activated, we tried to find any relation between them. We analyzed the phosphorylation of AMPK and the activation of NF κ B in hepatocytes isolated from WT mice incubated with a specific inhibitor of AMPK (Compound C). As shown in Figure 24A, treatment of hepatocytes with Compound C (CC) inhibited AMPK phosphorylation, increased the phosphorylation and degradation of I κ B α , and induced the phosphorylation and translocation of p65 from the cytosol to the nucleus. In addition, the treatment with CC induced the cleavage of PARP (Figure 24A). Pretreatment of the

hepatocytes with CC for 2 hours prevented the activation of NF κ B in response to TNF α (Figure 24B), and blocked TNF α -induced iNOS expression (Figure 24C). These experiments reveal a previously unexpected relationship between AMPK phosphorylation, NF κ B activation and PARP cleavage.

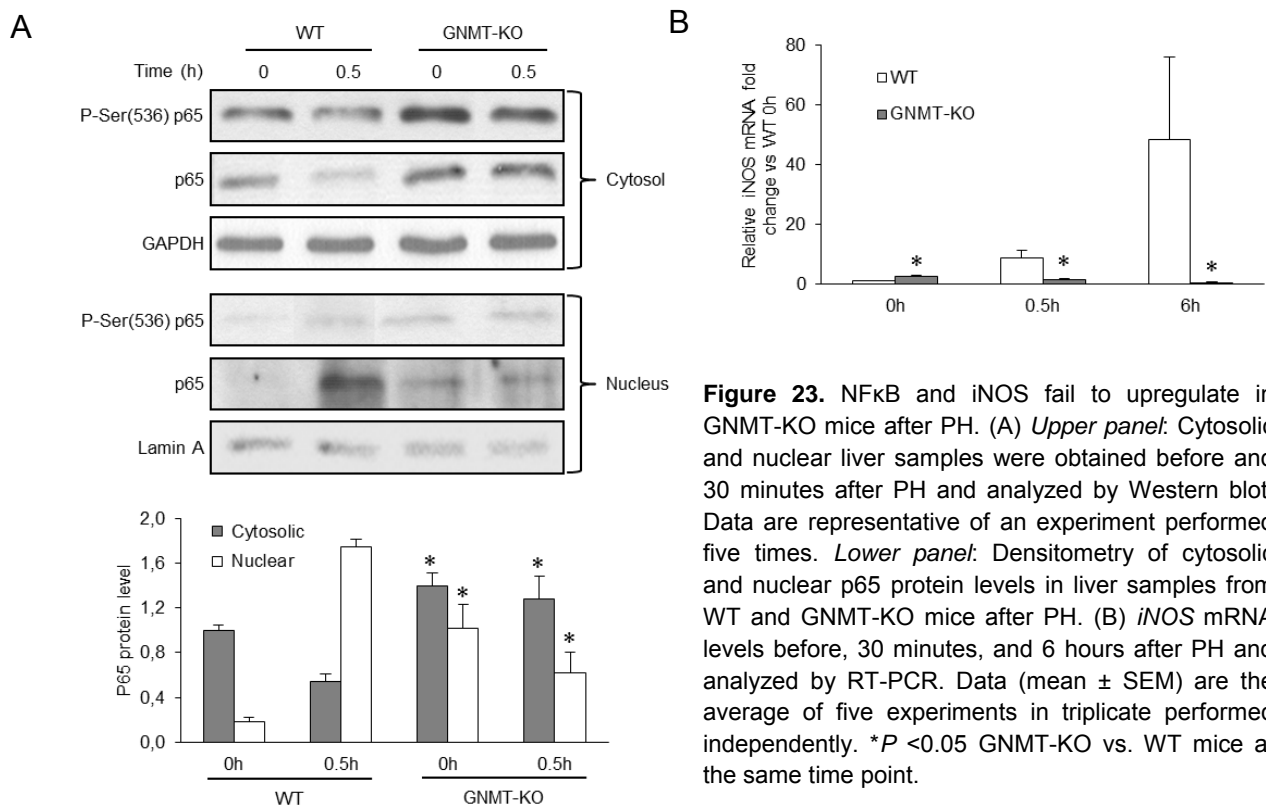


Figure 23. NF κ B and iNOS fail to upregulate in GNMT-KO mice after PH. (A) *Upper panel*: Cytosolic and nuclear liver samples were obtained before and 30 minutes after PH and analyzed by Western blot. Data are representative of an experiment performed five times. *Lower panel*: Densitometry of cytosolic and nuclear p65 protein levels in liver samples from WT and GNMT-KO mice after PH. (B) iNOS mRNA levels before, 30 minutes, and 6 hours after PH and analyzed by RT-PCR. Data (mean \pm SEM) are the average of five experiments in triplicate performed independently. *P < 0.05 GNMT-KO vs. WT mice at the same time point.

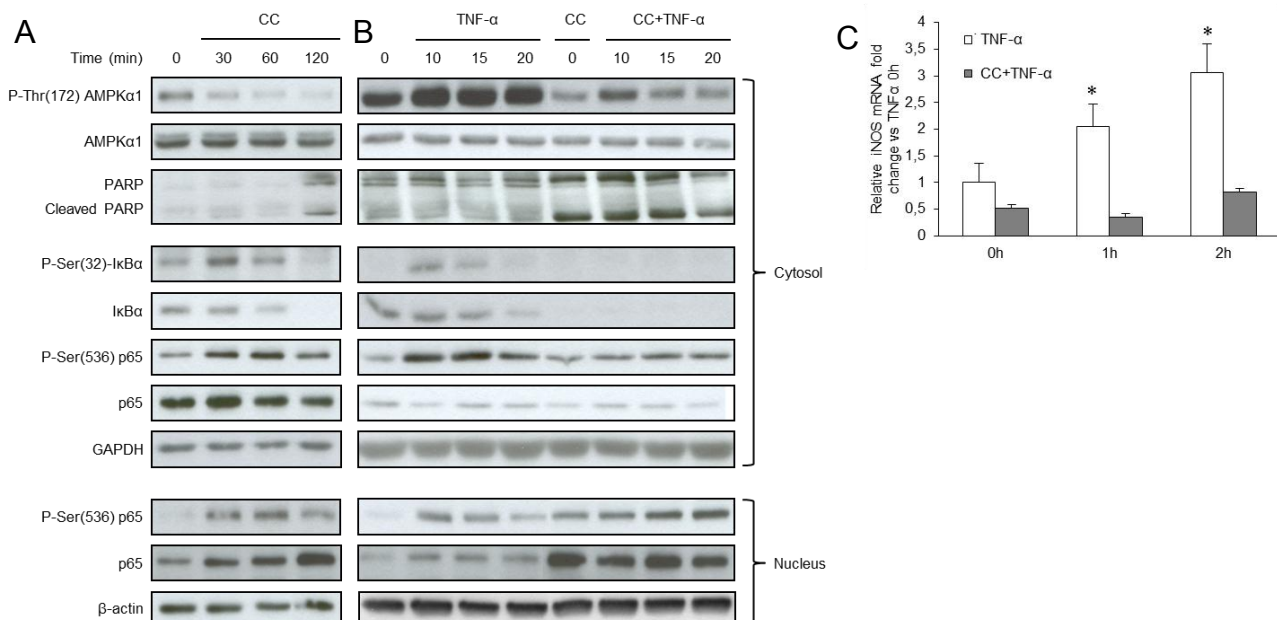


Figure 24. Effect of CC on basal and TNF- α -induced AMPK phosphorylation, NF κ B activation and iNOS expression in isolated mouse hepatocytes. (A) Phosphorylation of AMPK, PARP cleavage, and activation of NF κ B by removal of the inhibitory I κ B α through phosphorylation and translocation of p65 to the nucleus was analyzed by Western blot with the indicated antibodies in isolated hepatocytes before, 30, 60, and 120 minutes after the addition of CC (40 μ M). (B) Western blot analysis showing phosphorylation of AMPK, PARP cleavage, and activation of NF κ B by removal of the inhibitory I κ B α through phosphorylation and translocation of p65 to the in isolated hepatocytes before, 10, 15, and 20 minutes after the addition of TNF- α (10 ng/mL). Hepatocytes were incubated in the presence or absence of CC (40 μ M) during 120 minutes prior the addition of TNF- α . Results are representative of four independent experiments. (C) iNOS expression was analyzed by RT-PCR in isolated hepatocytes incubated in the presence or absence of CC (40 μ M) during 120 minutes prior the addition of TNF- α (10 ng/mL). Data are the average of four experiments in triplicate performed independently. *P < 0.05, time point vs. time 0 hours.

5.3. MURINE DOUBLE MINUTE 2 REGULATES HU ANTIGEN R STABILITY IN HUMAN LIVER AND COLON CANCER THROUGH NEDDYLATION.

Hepatology 2012;55(4):1237-1248
Comment in: Nat Rev Gastroenterol Hepatol. 2011 Dec 13;9(1):4

As previously shown, HuR is a key factor in liver differentiation, proliferation and HCC, regulating the *MAT2A* to *MAT1A* switch during liver development and the *MAT1A* to *MAT2A*

switch during hepatocyte de-differentiation and malignant transformation, being also fundamental during liver regeneration. Many aspects of HuR regulation have been described (see Introduction section 2.3.1.3), but although HuR has been shown to be degraded by ubiquitination-dependent proteasome degradation, the mechanisms leading to enhanced HuR protein stability remain unknown. In this section we discover a new HuR protein stability regulation involving Mdm2-mediated NEDDylation.

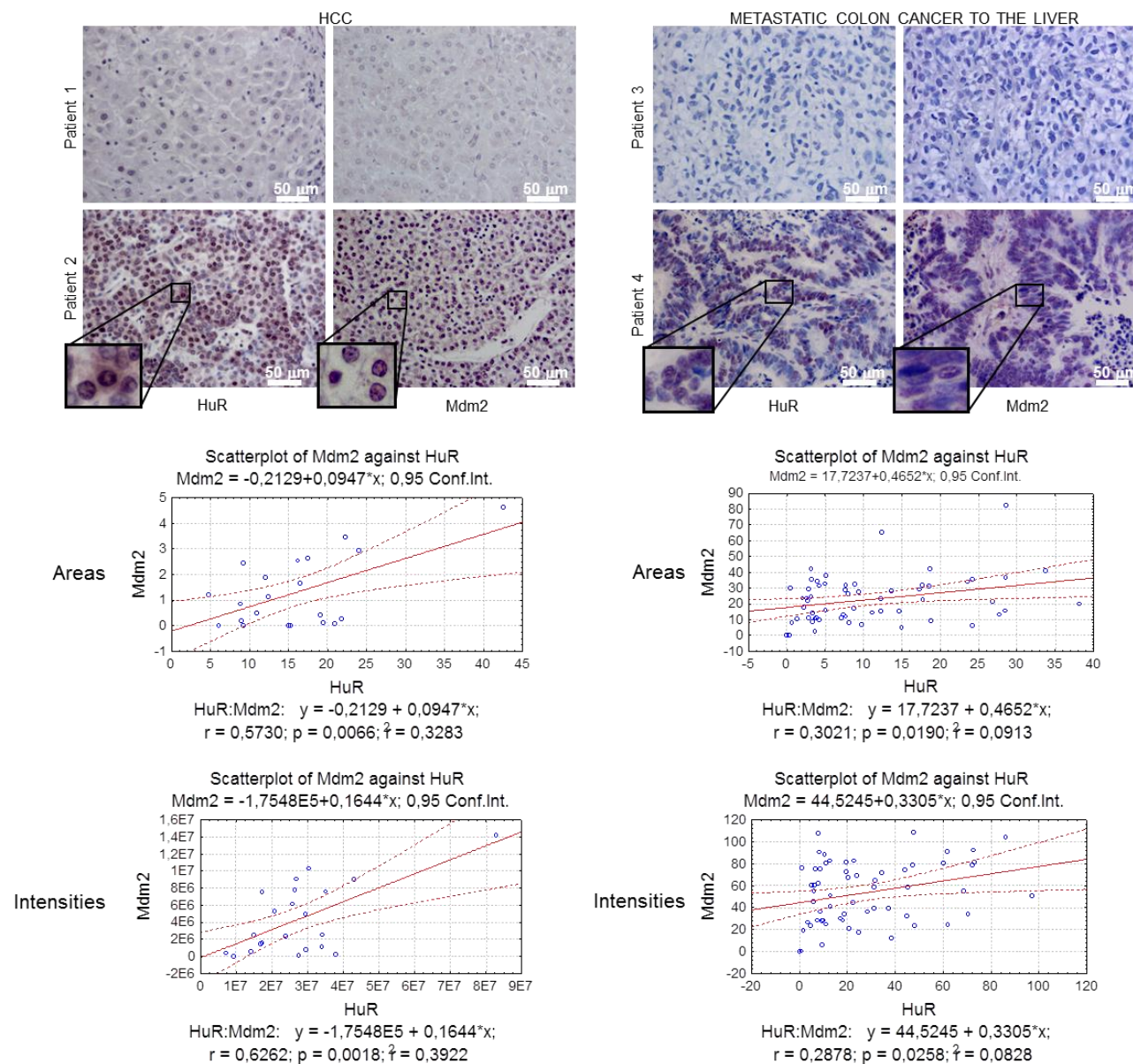


Figure 25. Mdm2 and HuR protein levels in human HCCs and metastatic colon cancer to the liver. *Upper panel:* representative tissue sections immunostainings from HCC (patient 1 ASH etiology and patient 2 hepatitis C etiology) and metastatic colon cancer to the liver, using HuR and Mdm2 antibodies. Original magnification, 40x; scale bar 50 μm. Magnified images are shown as insets. *Lower panel:* scatterplots for intensity and area staining of Mdm2 against HuR in tumors. Pearson correlation tests results are shown.

5.3.1. HuR and Mdm2 are overexpressed in hepatoma and colon cancer cells and in human HCC and colon carcinoma

Recent studies have shown that the expression levels of the RBP HuR are elevated in many types of cancer [201], and also that the E3 ligase Mdm2 levels are significantly higher in malignant than in benign lung and gastric tumors [308]. Whereas in normal liver tissues there was no significant expression of HuR (Figure 16A) and Mdm2 (Supplemental Figure 5A), in a cohort of primary human HCC and metastatic colon cancer to the liver we found a positive correlation between HuR and Mdm2 levels by analyzing their immunostaining intensity (Figure 25). When studying the HCC samples analyzed categorized by etiology (hepatitis C, ASH and NASH), a positive and significant correlation was found for the patients of HCC derived from hepatitis C virus infection (Supplemental Figure 5B).

Taking into account this correlation between HuR and Mdm2 levels, we studied the levels of these proteins in primary mouse hepatocytes, MLP29 cell line and SAMe-D cell line. As shown in Figure 26A, MLP29 cells and SAMe-D cells compared with hepatocytes, which is in accordance with the increased levels correlating with the transformation status.

In order to study the possible regulation of HuR level by Mdm2, we overexpressed Mdm2 in MLP29 cell line and in the human colon cancer cell line RKO. The overexpression of Mdm2 led to an increase in the levels of endogenous HuR protein in both cell lines (Figure 26B), and also in the levels of an exogenous V5-tagged wild type HuR (HuR-V5) transfected into the cells (Figure 26C).

We studied the ablation of HuR in terms of cell response (apoptosis and cell cycle progression) in MLP29, SAMe-D and RKO cell lines, and in the human hepatoma cell line HepG2.

Figure 26 (next page). Mdm2-dependent increased expression of HuR contributes to oncogenicity. (A) Western blotting of Mdm2, HuR, and its targets in primary mouse hepatocytes, MLP29, and SAMe-D cell lines. (B) Western blotting and densitometric analysis of endogenous HuR in control and Mdm2-overexpressing MLP29 and RKO cells. (* $P < 0.05$, Mdm2 transfected versus control). (C) MLP29 cells immunofluorescence, and western blotting of MLP29 and RKO cells transfected with HuR-V5 (alone or with Mdm2). (D) Left and right panels: caspase-3 activity assay and representative flow cytometry plots and histograms for cell cycle of cell lines transiently transfected with control or HuR-directed siRNAs. *Fold changes are statistically significant; $P < 0.05$. (E) Western blotting for MLP29, SAMe-D and RKO cell lines transfected with control or Mdm2-directed siRNAs. (F) Left and right panels: caspase-3 activity assay and representative flow cytometry plots and histograms for cell cycle of cell lines transiently transfected with control or Mdm2-directed siRNAs. *Fold changes are statistically significant; $P < 0.05$.

HuR silencing induced a strong activation of caspase-3, and flow cytometry showed a lower percentage of cells entering into S phase in all these cell lines (Figure 26D). Thus, this data suggest that HuR ablation promotes cell apoptosis and cell-cycle arrest.

Furthermore, Mdm2 silencing in MLP29, SAMe-D and RKO cells led to a decrease in the levels of HuR protein, and also in its cell cycle-related target cyclin A (Figure 26E). Moreover, 48 hours silencing of Mdm2 in RKO cells produced the increase of the caspase-3 activity (9.7 times) (Figure 26F, left graphs), whereas no changes were detected at this time in MLP29, SAMe-D and HepG2 (not shown). In these cell lines, 72 hours of Mdm2 silencing was necessary for obtaining a significant increase in caspase-3 activation and cell-cycle arrest (Figure 26F).

All these data suggest a cross-talk between HuR and Mdm2 in which Mdm2 levels regulate HuR protein levels. According with these observations, the oncogenic effects of Mdm2 could be, at least in part, mediated by HuR functionality.

5.3.2. NEDDylation is linked to HuR stability

Mdm2 can act as an E3 Ub ligase targeting substrates, and itself, for proteasomal degradation, regulating its own stability [289]. As explained in section 2.4.2.2., Mdm2 is also able to act as an E3 NEDD8 ligase, promoting p53 and ribosomal protein L11 stability. Taking into account the previous results in which the silencing of Mdm2 induced a down regulation in HuR protein levels, we examined whether this occurred by NEDDylation. To this end, we first overexpressed Mdm2 and NEDD8 in the MLP29 cell line. After immunoprecipitating HuR, high molecular weight bands immunoreactive to HuR antibody appeared in the presence of either Mdm2 or NEDD8 (Figure 27A).

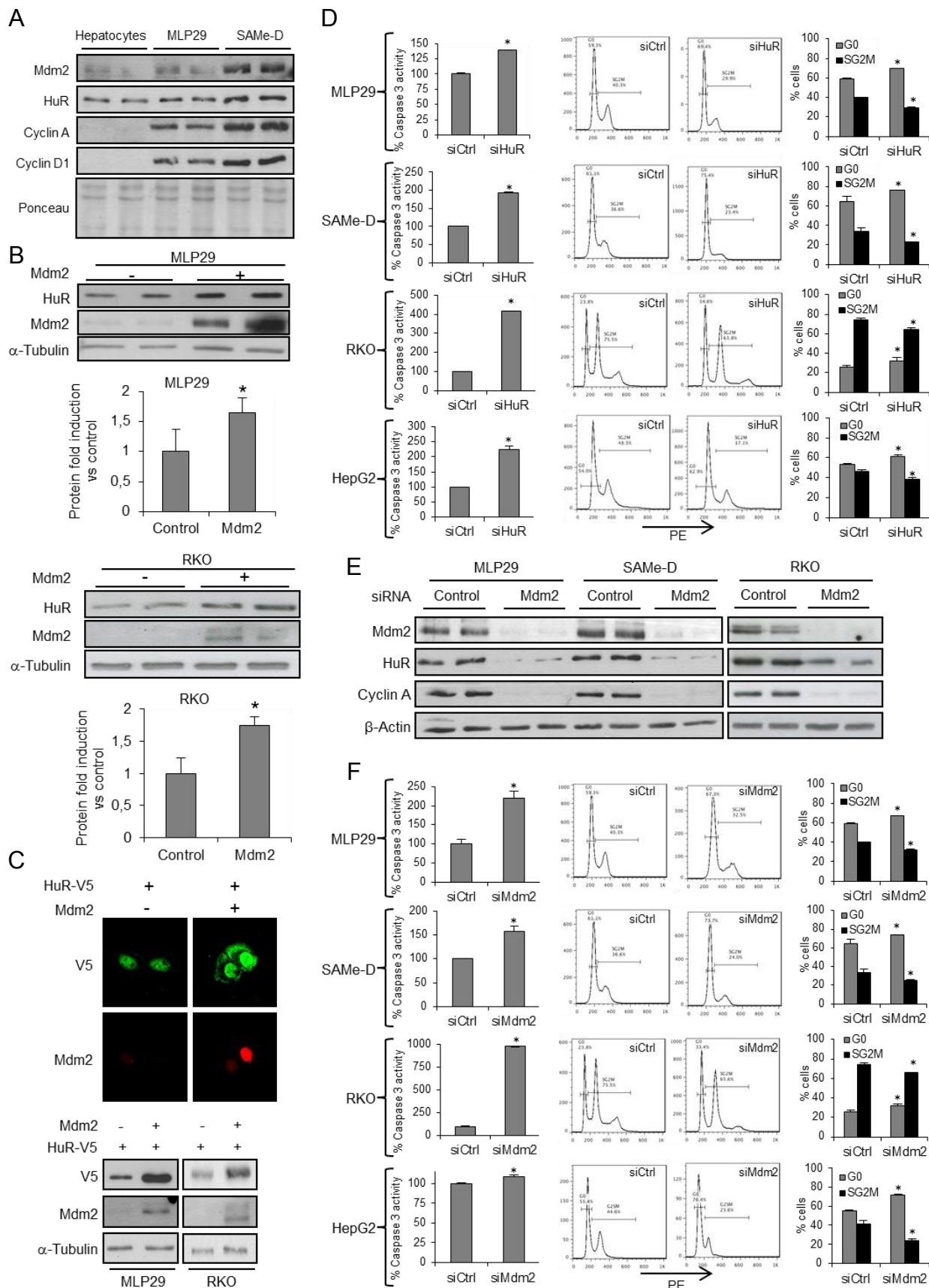


Figure 26 (legend in previous page)

To gain insight about the potential regulation of NEDDylation in HuR regulation, MLP29 cells were transfected with a plasmid expressing HuR-V5, together with Mdm2 and His₆-tagged NEDD8 (His₆-NEDD8). After histidine purification, we were able to recover the proteins conjugated to His₆-NEDD8. By Western blotting we detected NEDDylated HuR-V5 bands, which were increased by the overexpression of Mdm2 (Figure 27B), suggesting that Mdm2 plays a pivotal role in HuR NEDDylation.

In order to examine the influence of

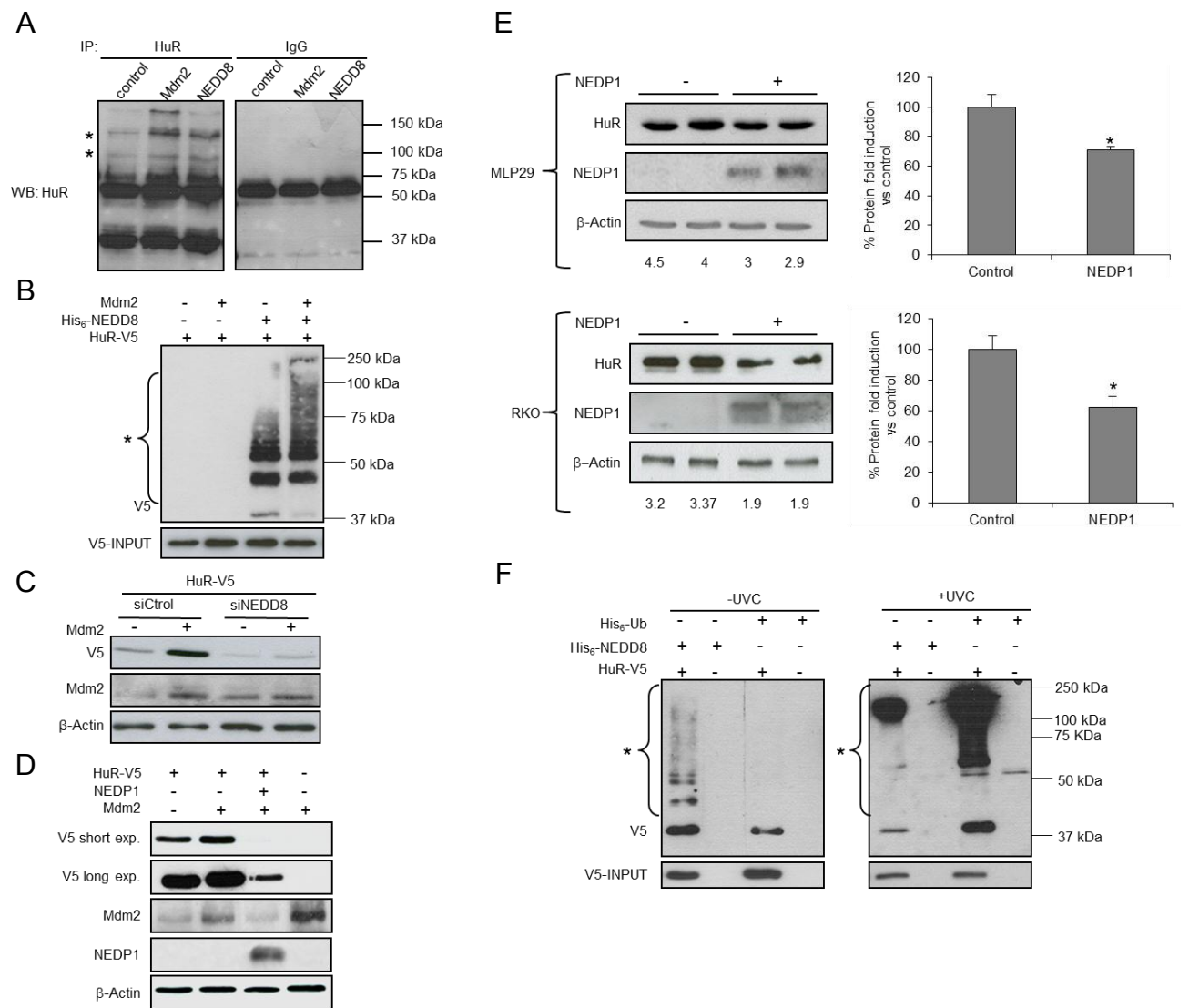


Figure 27. NEDDylation of endogenous HuR is dependent on Mdm2. (A) Western blotting analysis of endogenous HuR in IP reactions after overexpression of Mdm2 or NEDD8 in MLP29 cells. (B) V5-immunoreactive proteins in MLP29 cells expressing HuR-V5 and His₆-NEDD8 and/or Mdm2. (C) V5 and Mdm2 in MLP29 cells silenced with siControl or siNEDD8 twice, transfected with HuR-V5 and with or without Mdm2. (D) Western blotting analysis from MLP29 cells transfected with HuR-V5 and/or Mdm2 and/or NEDP1. (E) NEDP1 overexpression in MLP29 and RKO cells. Numbers represent the HuR protein quantification normalized by β-actin. Graphs show quantification of endogenous HuR protein levels ($P < 0.05$; NEDP1 transfected versus control). (F) SAME-D cells were transfected HuR-V5, His₆-Ub, and/or His₆-NEDD8 plasmids; 24 hours later, cells were irradiated with 20 J/m² of UVC, and V5-containing proteins were purified using Ni²⁺-NTA and were detected by western blotting. In (B) and (F), lower blots show the input of the transfected HuR-V5. In (A), (B), and (F), asterisk indicates the localization of post-translational modifications.

NEDDylation on HuR stabilization, we used siRNA to knockdown the expression of NEDD8. Sequential transfections during 48 hours completely destabilized HuR, even blocking Mdm2-dependent stabilization (Figure 27C). To further show the importance of the NEDD8 conjugation to HuR, we cotransfected HuR and Mdm2 together with the deNEDDylating cysteine protease NEDP1, able to remove NEDD8 chains from the proteins. Whereas Mdm2 is able to stabilize HuR, inducing its accumulation, the cotransfection with NEDP1 was able to not only

block this accumulation, but also completely destabilize HuR protein (Figure 27D). In agreement with this, the overexpression of NEDP1 induced the destabilization of endogenous HuR in MLP29 and RKO cells (Figure 27E).

The stability and the abundance of HuR has been shown to be regulated by Ub-mediated proteolysis, after stress stimulus [222] (see section 2.3.1.3.). After determining that HuR is NEDDylated by Mdm2, we examined whether the NEDDylation is affected by a stress signal, such as UVC. As shown in Figure 27F, after cotransfection of HuR-V5 with His₆-NEDD8 or His₆-Ub, cells were UVC treated. The subsequent histidine purification allowed isolating the NEDDylated and ubiquitinated proteins, showing by Western blot

that whereas in absence of UVC stimulus HuR appears NEDDylated, UVC treatment induced a switch to ubiquitinated HuR, in concordance with the decrease in total HuR levels.

In summary, the results indicate that Mdm2 regulates HuR NEDDylation and therefore its stability.

5.3.3. Lysines 283, 313 and 326 are important sites for HuR NEDDylation and stability

After determining that HuR is NEDDylated by Mdm2, we performed seven lysine-to-arginine mutants within the HuR region more abundant in lysines, the RRM3 and the C-terminus (Supplemental Figure 6).

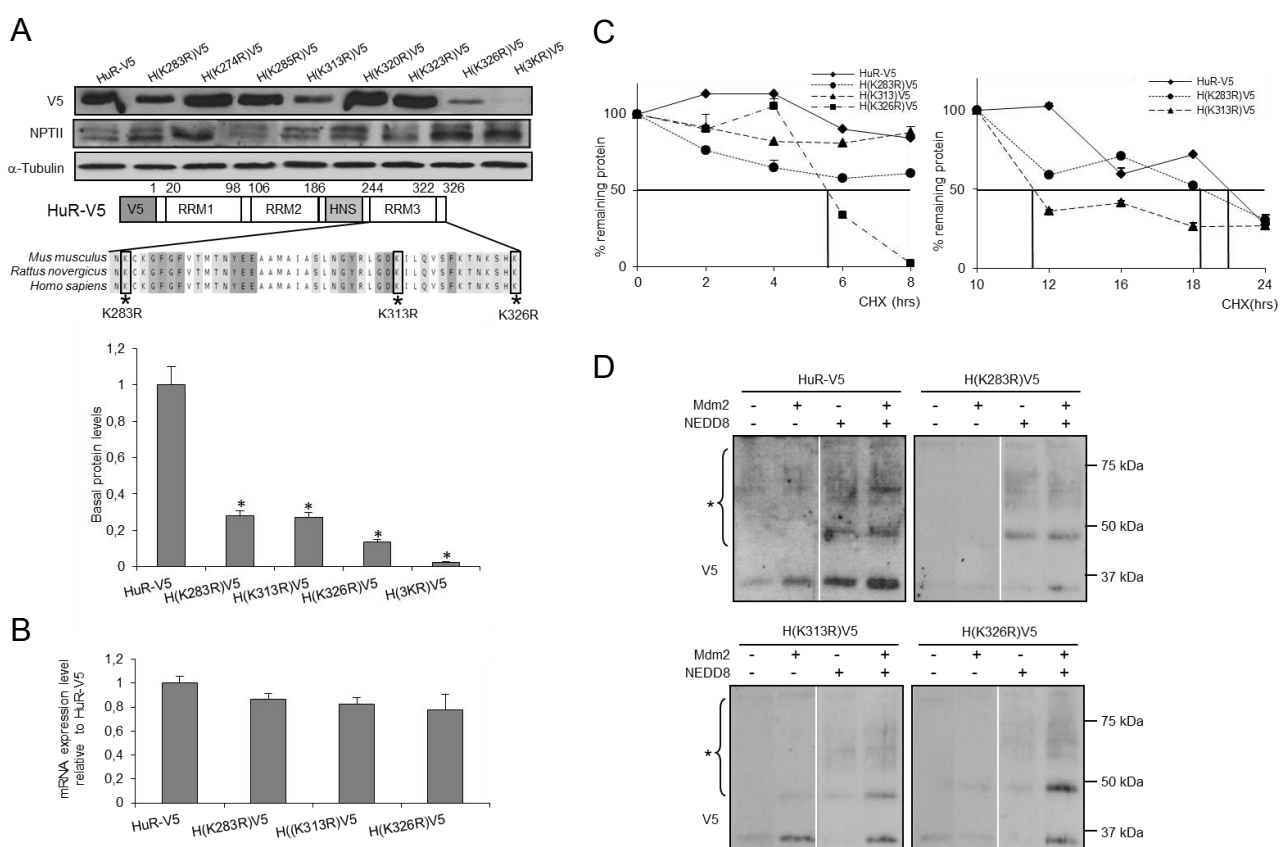


Figure 28. Identification of HuR residues involved in NEDDylation. (A) *Upper panel:* protein expression for HuR mutants after 24 hours of transfection in MLP29 cells using the expression of the NPTII as the transfection efficiency control. *Middle panel:* schematic representation of the HuR-V5 unstable mutants. Scheme displays the HuR-V5 protein, RRM1, 2, and 3, and HNS (HuR nucleocytoplasmic shuttling sequence). *Lower panel:* densitometric analysis of the expression of HuR-V5, H(K283R)V5, H(K313R)V5, H(K326R)V5 and H(3KR)V5 (B) mRNA levels of HuR-V5 and mutants 24 hours after transient transfection of plasmids in MLP29 cells. (C) Stability of HuR-V5, H(K283R)V5, H(K313R)V5, and H(K326R)V5 proteins as the percentage of protein level remaining after treated with CHX. 18 hours after transfection, MLP29 cells were treated with CHX (50 μ g/ml) and lysed during 24 hours for Western blotting analysis. Densitometric analysis was obtained from Western blotting data. Left graphic: HuR-V5 and mutant protein levels at different time points between 0 and 8 hours after CHX treatment. Right graphic: HuR-V5, H(K283R)V5, and H(K313R)V5 protein levels at different time points between 10 and 24 hours after CHX treatment. Vertical bars are indicative of the calculated half-life for every protein. (D) Ni²⁺-NTA purification in MLP29 cells transfected with HuR-V5 and mutants and/or His₆-NEDD8 and/or Mdm2. Western blotting was performed using an anti-V5 antibody. *Indicates post-translational modifications.

Among the seven mutants performed, we selected the mutation in lysines 283, 313 and 326, which exhibited effect in reducing HuR stability (Figure 28A), particularly lysine 326. These three residues are conserved between species (Figure 28A). Importantly, the combination of the three mutants in the triple mutant H(3KR)V5 (K283R/K313R/K326R), rendered a highly

unstable protein (Figure 28A). The mRNA levels of the mutants were comparable to the wild type HuR, thus discarding an effect at the transcriptional level (Figure 28B). All three mutants showed a decrease in their half-life compared to the HuR-V5, particularly marked in the H(K326R)V5, as assessed by cycloheximide (CHX) treatment (Figure 28C).

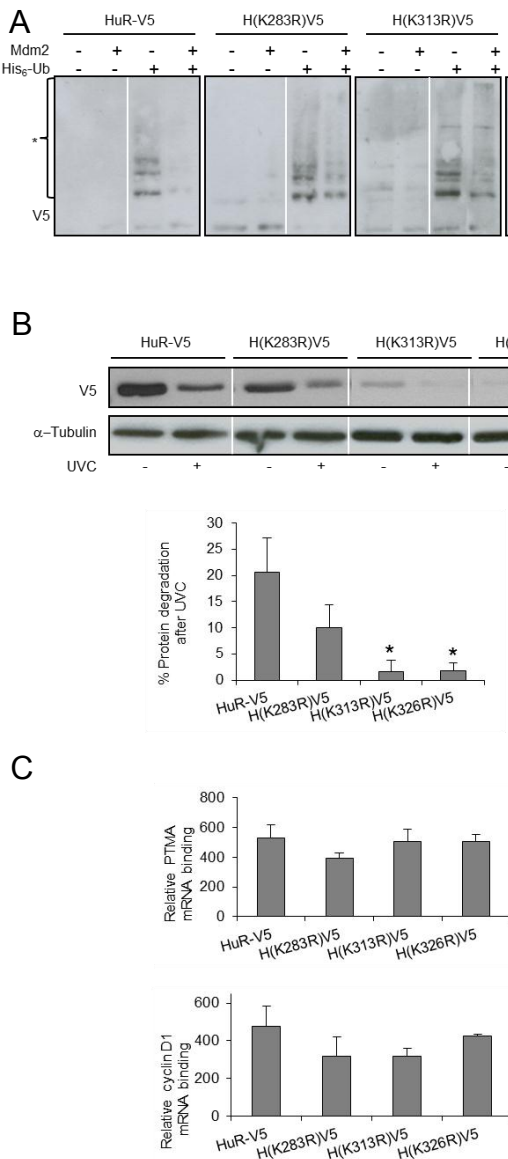
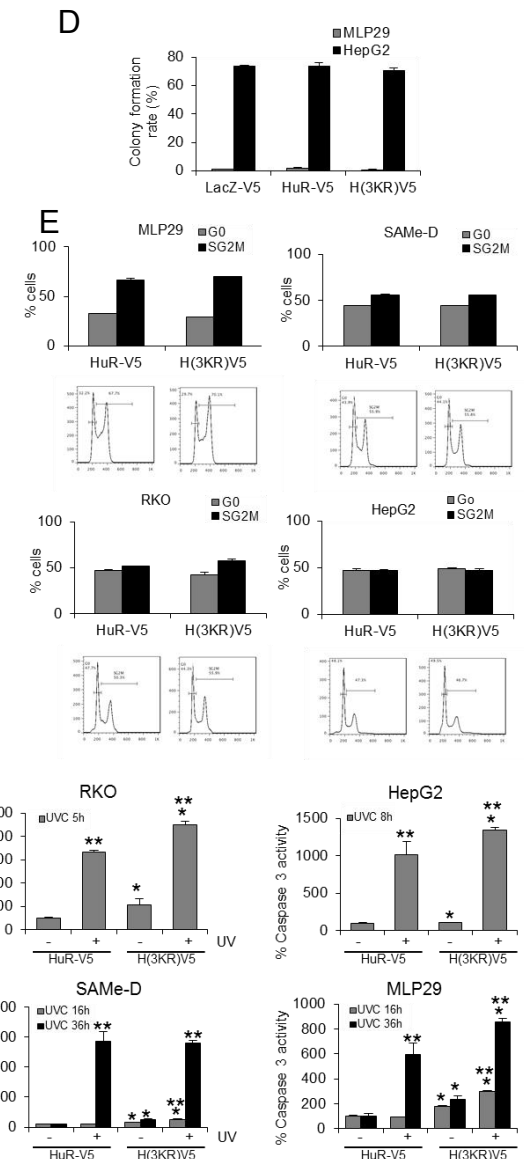


Figure 29. Characterization of HuR-V5 NEDDylation mutants. (A) HuR-V5 and mutants were transfected in MLP29 cells with or without His₆-Ubi and/or Mdm2. His₆-ubiquinated proteins were purified as described before. Asterisk indicates the localization of post-translational modifications. (B) *Upper panel*: After transfection of the MLP29 cell line with HuR-V5, H(K283R)V5, H(K313R)V5, and H(K326R)V5, cells were UVC-irradiated and, after 6 hours, lysed. *Bottom panel*: Densitometric analysis shows the percentage of protein degradation 6 hours after UVC; *P < 0.05, mutant vs. HuR-V5. (C) Activity of HuR-V5 and mutants was analyzed by RNP-IP. (D) Colony formation assays in soft agar plates. The colony formation rate (%) is shown for both MLP29 and HepG2 cell lines stably overexpressing HuR-V5 or H(3KR)V5. The data were obtained from two independent experiments. (E) Histograms and plots obtained by flow cytometry show cell cycle of MLP29, SAMe-D, HepG2 and RKO cell lines overexpressing HuR-V5 or H(3KR)V5 construct. The percentage of cells in G0 and SG2M was similar between cells expressing both proteins. (F) Caspase-3 activity assay for cell lines transfected with HuR-V5 or H(3KR)V5 and UVC (20 J/m²)-irradiated. *Differences between different constructs with the same UVC (+) or non-UVC (-) treatment (P < 0.05). **Differences between UVC (+) versus non-UVC (-) treatment for the same construct (P < 0.05).



These data suggest that the lysine residues 283, 313 and mainly 326 are important for the regulation of HuR stability. To further test if this stability regulation is due to the NEDDylation, we cotransfected HuR-V5 and mutants with His₆-NEDD8 and Mdm2, and a purification of the NEDDylated proteins was carried out. As shown in the Figure 28D, the intensity of the high molecular weight bands present in the wild type HuR after NEDD8 cotransfection decrease in the mutants, with a stronger reduction in the mutant H(K326R)V5. The addition of Mdm2 to the transfection increased the modification, probably by NEDDylating other residues. Finally, NEDD8 knockdown notably reduced the levels of HuR-V5 and H(K326R)V5 even in the presence of Mdm2 (Supplemental Figure 7).

We explored the susceptibility of HuR NEDDylation mutants to ubiquitination. After cotransfecting mutants with His₆-Ub and Mdm2 and purifying the ubiquitinated proteins, we observed that HuR-V5 and mutants present ubiquitinated bands, even more intense in the H(K263R)V5 and H(K313R)V5. The overexpression of Mdm2 decreased the ubiquitination of HuR-V5, whereas the reduction in H(K263R)V5 and H(K313R)V5 was less pronounced, and in the case of H(K326R)V5 Mdm2 increased the ubiquitination (Figure 29A). In accordance with this capacity to be ubiquitinated, the blocking of the proteasome by MG132 induced the accumulation of high molecular weight modified forms in HuR-V5 and in the three mutants (Supplemental Figure 8A). This excludes the possibility that these mutations are blocking ubiquitination sites. Endogenous HuR is degraded after UVC light exposure, with the presence of modified bands, presumably ubiquitinated forms (Supplemental Figure 8B). In the same way, the UVC light induced HuR degradation in HuR-V5 and mutants. This degradation was higher in the HuR-V5 than in the mutants, probably because of the high instability intrinsic to these mutants (Figure 29B).

NEDDylation of proteins, such as p53, is able to affect protein functionality [274]. Thus, by using RNP-IP assay, we tested if the mutants present differences in the binding affinity to the HuR proliferation-related targets *PTMA* (*prothymosin α*) and *cyclin D1* mRNA. The Figure 29C shows no differences between HuR-V5 and HuR mutants,

suggesting that lysine mutation of HuR did not interfere in its RNA binding function.

In accordance with the maintenance of mutated HuR binding to proliferation mRNAs, different cell lines transfected with HuR-V5 and H(3KR)V5 presented a lack of response in the colony formation rate in soft agar and in the cell-cycle progression (Figures 29D and 29E). In terms of apoptotic response, even at basal levels, H(3KR)V5 mutant sensitizes the different cell lines to apoptosis, as shown by the increased caspase-3 activity (Figure 29F). After UVC treatment, in the more sensible RKO and HepG2 cell lines, a robust caspase-3 activity increase was found at 5 hours and 8 hours after the treatment respectively, in the presence of H(3KR)V5 in comparison to HuR-V5 (Figure 29F). Similar results were found in SAMeD cells after 16 hours of UVC treatment, and in MLP29 cells after 16 and 36 hours (Figure 29F). The data highlight the proapoptotic phenotype associated with the H(3KR)V5 mutant, and therefore to the lack of HuR NEDDylation.

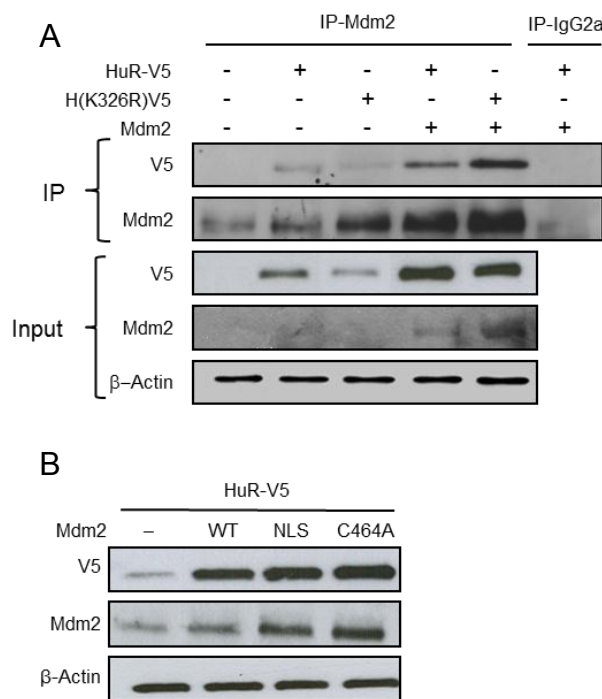


Figure 30. Mdm2 NEDDylates HuR in the cytoplasm. (A) IP of Mdm2 in whole cell lysates from MLP29 cells overexpressing HuR-V5 or H(K326R)V5. (B) Western blotting of HuR protein from MLP29 cells after cotransfection with HuR-V5, together with Mdm2-WT, Mdm2-NLS, or Mdm2(C464A).

5.3.4. Cytoplasmic NEDDylation of HuR is mediated by Mdm2

To further explore the mechanism by which HuR gets NEDDylated, we examined the interaction between HuR and Mdm2 by immunoprecipitation. As shown in Figure 30A, Mdm2 interacts with both HuR-V5 and H(K326R)V5 mutant. Also, HuR-V5 was cotransfected with wild type Mdm2 and two Mdm2

mutants: Mdm2-NLS and Mdm2(C464A). Mdm2-NLS lacks its nuclear localization signal, thus being characterized by its exclusively cytoplasmic localization [293, 309], and produced the same stabilization than wild type Mdm2, suggesting that Mdm2-mediated HuR stabilization takes place in the cytoplasm (Figure 30B). The Mdm2(C464A), which has mutated a cysteine residue required for Mdm2 function as an E3 Ub ligase [310], had the

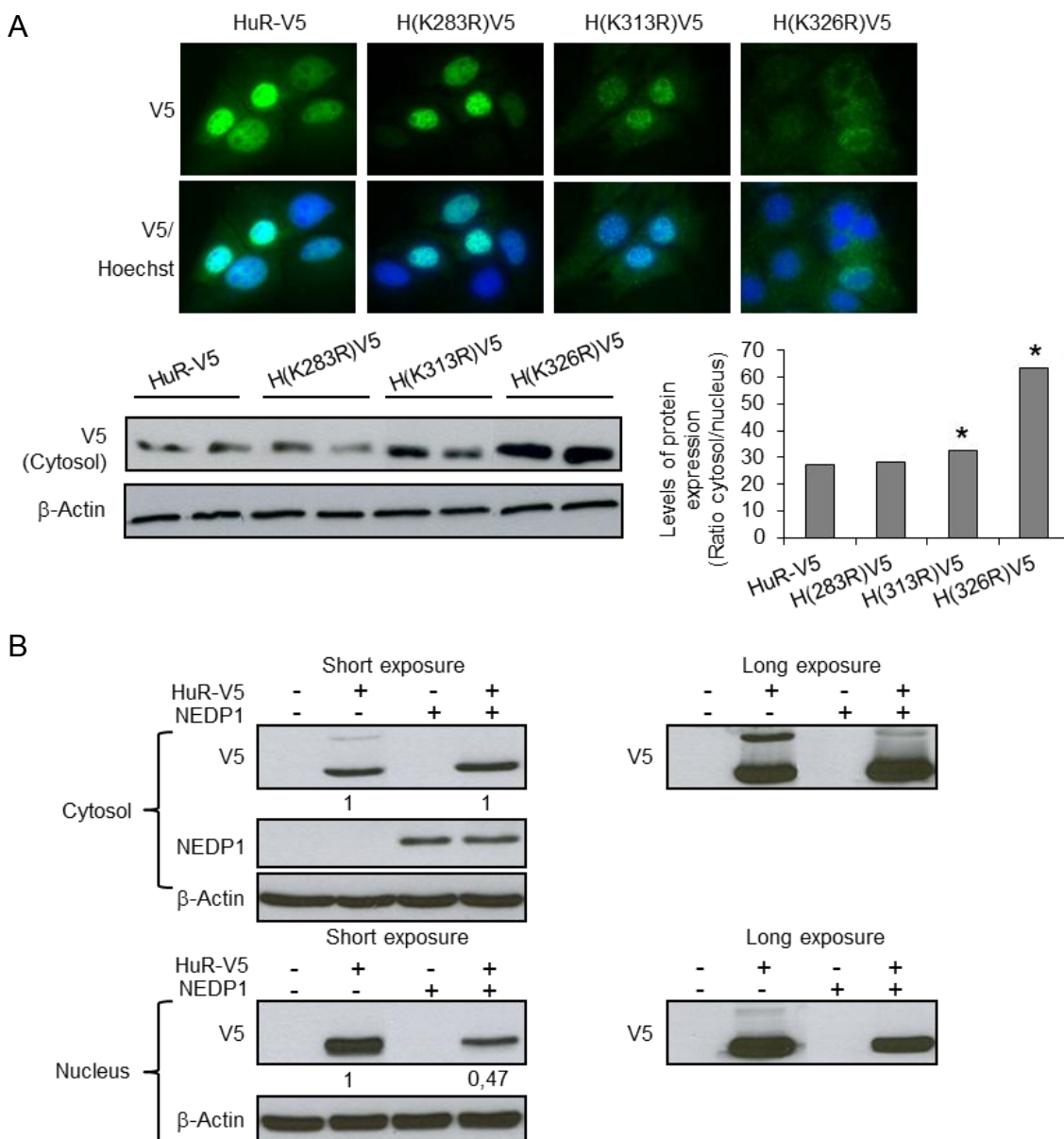


Figure 31. HuR nuclear localization is regulated by NEDDylation. (A) Localization of HuR WT and mutants. *Upper panel:* representative images of the localization of HuR-V5, H(K283R)V5, H(K313R)V5, and H(K326R)V5 by immunofluorescence in MLP29 cells. DNA quantities were adjusted to obtain similar expression levels: HuR-V5 (0.1 µg), H(K283R)V5, H(K313R)V5, and H(K326R)V5 (5 µg). *Lower panel:* cytoplasmic localization of HuR after HuR-V5 and mutant transfection by western blotting and densitometry. *Fold changes are statistically significant. (B) MLP29 cells were transfected with HuR-V5 and/or NEDP1 plasmids. Western blotting and densitometry using anti-V5 and anti-NEDP1 antibodies from cytosolic and nuclear proteins were developed. Two different exposures are presented.

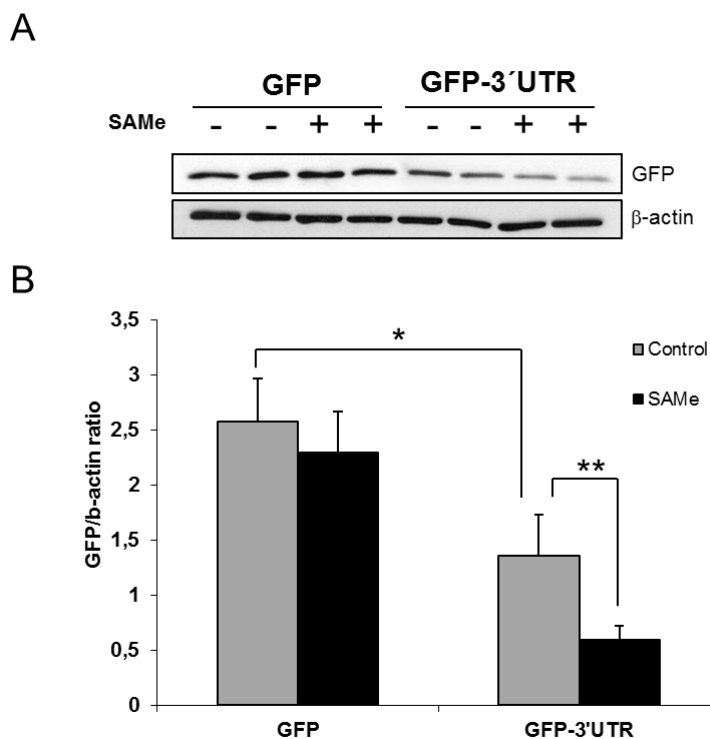
same effect as WT Mdm2 (Figure 30B).

In summary, these data indicate that Mdm2 interacts with HuR in the cytoplasm and participates in its stabilization independently of Mdm2 Ub ligase activity.

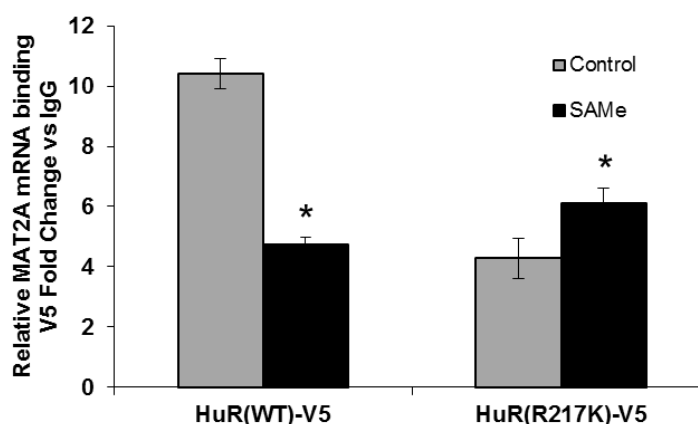
5.3.5. NEDDylation controls nuclear localization of HuR

HuR is predominantly a nuclear protein, but its subcellular localization is known to be regulated by phosphorylation of some kinases (see Introduction section 2.3.1.3.). Using immunofluorescence, we observed that HuR-V5 is localized mainly in the nucleus, similar to the endogenous protein, whereas HuR mutants had a more diffuse expression, with a predominantly cytoplasmic localization in the case of H(K326R)V5 (Figure 31A, upper panel). These results were confirmed by Western blot (Figure 31A, lower panel). Interestingly, the cysteine protease NEDP1, which removes NEDD8 molecules conjugated to the proteins, reduced by approximately 50% the nuclear amount of HuR-V5, having no effect on cytoplasmic content (Figure 31B). These data emphasize the role of NEDDylation in HuR nuclear localization.

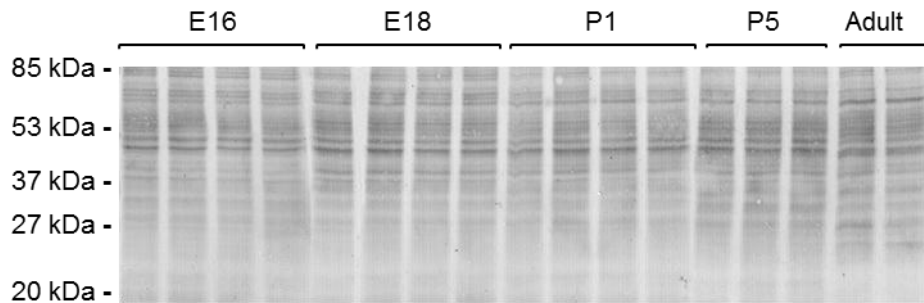
5.4. SUPPLEMENTAL FIGURES



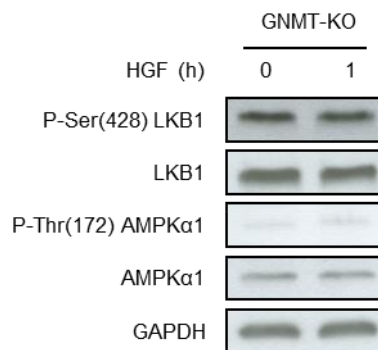
Supplemental Figure 1. The 3'UTR confers instability to GFP mRNA. The 3'UTR of MAT2A was cloned into the expression vector pEGFP-C2, and the resulting construct (pEGFP-C2-3'UTR) was transfected in the MLP29 cell line. Cells were treated with SAMe (4mM) for 4 hours. (A) Western blot analysis of the GFP expression. (B) Quantification of the expression levels of GFP and GFP-3'UTR, normalized to the loading control β -actin. There was no difference between SAMe treated and non-treated cells for the GFP expression. The expression of GFP-3'UTR was significantly reduced compared with the GFP control (* P<0.05), and the treatment with SAMe reduced the expression of GFP-3'UTR compared to the non-treated (** P<0.01).



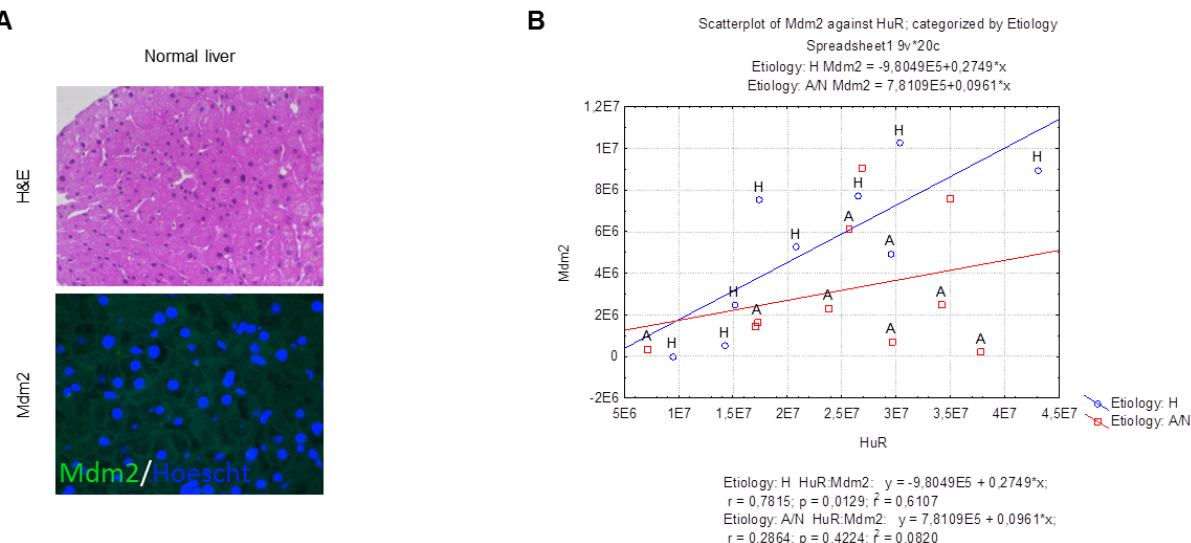
Supplemental Figure 2. HuR(R217K)-V5 binding to MAT2A mRNA is not altered in presence of SAMe. The binding of HuR(WT)-V5 and HuR(R217K)-V5 to MAT2A was assayed by RNP-IP in transfected MLP29 cells treated with or without SAMe (4mM). The levels of MAT2A mRNA were first normalized to the levels of the housekeeping GAPDH mRNA, and expressed as relative to the levels of MAT2A mRNA in IgG-IPs. * P<0.05, SAMe vs. control.



Supplemental Figure 3. Ponceau S staining of fetal liver extracts. Ponceau S staining of the nitrocellulose membranes was performed to ensure equal loading of protein samples in fetal liver Western blot experiments.



Supplemental Figure 4. HGF has no effect on LKB1 and AMPK phosphorylation in hepatocytes isolated from GNMT-KO mice. LKB1 and AMPK phosphorylation was analyzed via Western blotting with the indicated antibodies in GNMT-KO hepatocytes before and 1 hour after the addition of HGF (25 ng/ml). Results are representative of three independent experiments.



Supplemental Figure 5. Normal liver and HCC samples analysis. (A) Mdm2 immunostaining. Routine hematoxylin-eosin (H&E) staining and immunofluorescence analysis of Mdm2 were performed in liver samples from normal patients. (B) Representative plots for intensity staining of Mdm2 and HuR in the HCC samples. Pearson tests and scatter plots for the obtained data were developed. H means Hepatitis C patients and A/N means ASH/NASH patients.

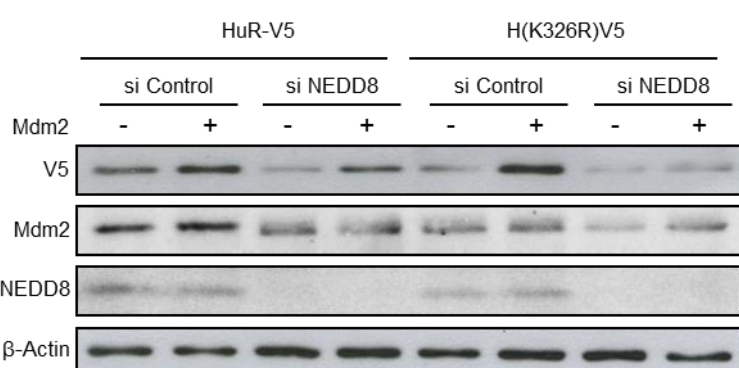
Schematic representation of HuR mutants with C-terminal K to R changes

HuR (326 aa):

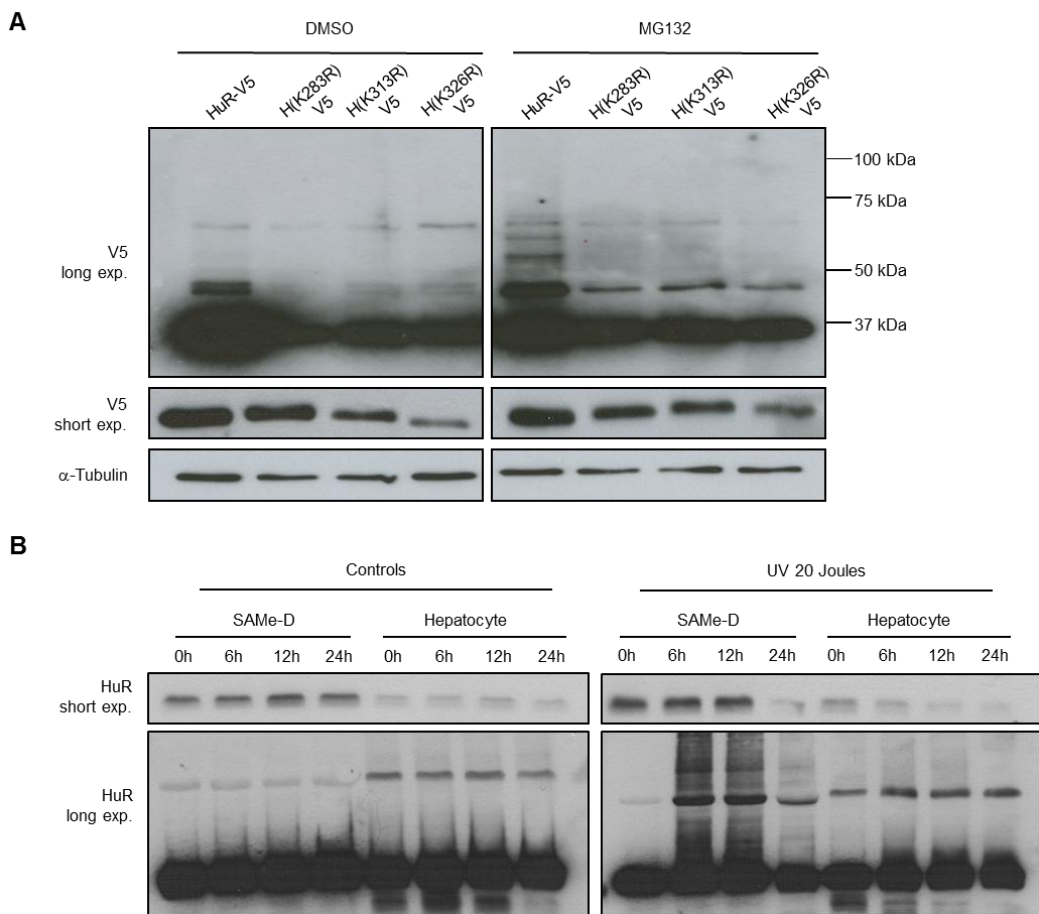
MSNGYEDHMAEDCRDDIGRTNLIVNLPQNMTQEELRSLFSSIGEVESAKLIRDKVAGHSLGYGFVNVTAKDAERAISTNLGLRQSKTIKVSYARPSSEVIKDANLYISG
LPRTMTQKDVEDMFSRFGRINSRVLDQTTGLSRGVAFIRFDKRSEAAEITSFNGHKPPGSSEPTVKFAANPNQKNMALLSQLYHSPARRFGGPVHHQAQRFRFSP
MGVDHMSGISGVNVPGNASSGWCIFYNLGQDADEGILWQMFGPFGAVTNVKVIRDFNTNKCKGFGVFTMTNYEEAAMAIASLNGYRLGDKILQVFKTNKSHK



Supplemental Figure 6. Representation of HuR NEDDylation mutants. Schematic representation of HuR mutants. To explore the HuR NEDDylation, seven K residues were mutated to R in the RRM3 and C-terminal of the HuR protein.



Supplemental Figure 7. NEDD8 knockdown reduces H(K326R)V5 stability. Thirty-six hours after transfecting MLP29 cells with NEDD8 siRNA, plasmids expressing HuR-V5 and H(K326R)V5 were transfected alone or cotransfected with Mdm2. Nine hours later, Western blot analysis was used to detect V5, Mdm2, NEDD8, and loading control β-actin.



Supplemental Figure 8. HuR is degraded by proteasome. A) Proteasome inhibition promotes accumulation of HuR mutants. MLP29 cell line was transfected with HuR-V5, H(K283R)V5, H(K313R)V5 and H(K326R)V5 for 24 hours. MG132 or DMSO was added and Western blot of the RIPA lysates was performed against V5. A long and a short exposition of the 37 kDa HuR protein is shown. α -Tubulin is showed as loading control. B) Degradation of HuR protein levels after UVC treatment in hepatocytes and SAMe-D cell line. Mouse primary hepatocytes and SAMe-D cell line were exposed at +/-20J UVC and RIPA extracts were obtained at different time points. Western blot against endogenous HuR was developed.

6. DISCUSSION

6. DISCUSSION

The chronic liver disease is one of the main causes of mortality in humans [2, 3], including different illnesses with several etiologies such as hepatitis B and C virus infection, toxins, alcohol and drugs consumption, autoimmune and hereditary diseases and non-alcoholic fatty liver disease (NAFLD) [1]. NAFLD has become one of the main chronic liver disease conditions, particularly in developed countries [6, 7]. NAFLD is associated with the metabolic syndrome risk factors (obesity, insulin resistance, dyslipidemia and hypertension) and includes a spectrum of alterations from steatosis to non-alcoholic steatohepatitis (NASH), in some cases accompanied by fibrosis [6, 7, 9, 11].

NAFLD can progress through a series of steps: starting from the usually benign liver steatosis, 10% of the patients develop NASH, which can usually be reversed. About 25% of NASH patients lead into cirrhosis, and, finally, liver failure or hepatocellular carcinoma (HCC). The mechanisms by which maintained steatosis progresses to NASH and HCC are not well understood [20–23].

In humans, liver tumors are an important cause of mortality worldwide, being HCC one of the most common lesions. HCC is the most prevalent cancer in the population with a poor prognosis, even in the developed countries. HCC represents the third leading cause of cancer related deaths, and the leading cause of death among patients with cirrhosis [27]. Multiple signaling pathways converge in HCC pathology, together with a wide variety of risk factors, among which we can find HBV and HCV infection, alcoholism and aflatoxin B1. Also NAFLD, as commented before, appears as a relevant and emerging risk factor.

Although the molecular factors linked to the progression of NAFLD to HCC have not been completely elucidated, oxidative stress, methionine metabolism and p53 impairment have been shown to play an essential role in the molecular bases of NAFLD-related HCC. In particular, the methionine metabolism impairment in the liver produces inflammation and lipid peroxidation, and in cirrhotic patients a decrease in the hepatic metabolism of methionine into S-adenosylmethionine (SAMe)

has been found. In fact, the reduction in SAMe levels has been detected in many types of liver diseases [46, 47].

SAMe is the main biological methyl donor in the cell, and the liver is the principal responsible of its homeostasis [70]. SAMe molecule participates in many biological reactions, such as transmethylation (constituting the universal methyl donor), transsulfuration (being a precursor of the antioxidant glutathione) and aminopropylation (taking part in polyamine synthesis). As biological functions, SAMe is a crucial regulator of hepatocyte proliferation, and is also able to promote the apoptotic response in HCC cells [166].

Taking into account the importance of SAMe in the liver, its levels are tightly regulated by the combined action of methionine adenosyltransferase (MAT) and glycine N-methyltransferase (GNMT) enzymes, which are responsible of the anabolism and catabolism of SAMe, respectively. In order to study the implications of the impairment of SAMe regulation in the liver, two knockout models were developed, MAT1A-KO and GNMT-KO.

The MAT1A-KO model lacks *MAT1A* gene, which codifies for MAT I and MAT III, the main enzymes involved in SAMe synthesis, which are expressed in the adult and differentiated liver. Those knockout mice are characterized by chronic deficiency in SAMe, increased serum methionine levels and decreased GSH content. MAT1A-KO mice present an upregulation of genes related with cell growth and proliferation, cell death and development. In addition there is an altered expression of genes involved in acute phase response, oxidative stress and lipid and carbohydrate metabolism. In relation with the oxidative stress, there is an increased expression of cytochrome P450 2E1 (CYP2E1) and uncoupling protein 2 (UCP-2), both involved in the production of ROS. Thus, this increased oxidative stress, together with the depletion in GSH content results in the predisposition of MAT1A-KO to liver injury after CCl₄ and ethanol treatment, and to the impairment of the regenerative response. As a consequence of the misregulation of these processes, the MAT1A-KO mice spontaneously

develop steatosis and NASH at 8 month, and HCC at 18 month [48, 174].

The GNMT-KO mice are deficient for the main enzyme responsible of SAMe catabolism, the glycine N-methyltransferase (GNMT). This enzyme catalyzes the transmethylation reaction by which SAMe transfers its methyl group to glycine. It is present in large amounts in liver, and it has been observed to be highly reduced in liver and prostate tumors [117, 118]. It has also been found that individuals with *GNMT* mutations spontaneously develop liver disease [72, 73]. GNMT enzyme regulates the SAMe to SAH ratio, which is considered the index of the transmethylation potential of the cell [121, 122]. The impairment of this ratio can result into aberrant methylation patterns. As consequence of the absence of GNMT enzyme, the GNMT-KO mice present chronically elevated SAMe levels and spontaneously develop steatosis, fibrosis and HCC [49]. The increased SAMe content present in the liver makes of these mice an epigenetic model characterized by global hypermethylation of the DNA. Particularly, SAMe chronic excess promotes the methylation of the promoters of some members of RASSF and SOCS family, inhibitors of Ras and JAK/STAT signaling pathways which leads to chronic activation of these pathways, as observed in human HCCs [49].

In the healthy liver, SAMe is able to inhibit the mitogenic effect of the hepatocyte growth factor (HGF), by inhibiting the activation of the LKB1/AMPK/eNOS pathway, and thus avoiding the translocation of the RNA binding protein HuR, which is involved in the stabilization of cycle progression, proliferation, stress and apoptosis mRNAs [132, 152]. SAMe administration during liver regeneration after partial hepatectomy (PH) is also known to inhibit LKB1/AMPK/eNOS pathway, preventing DNA synthesis and decreasing the proliferation, thus leading to impairment in the regenerative response [132]. When administered to HCC cells, SAMe is able to promote the apoptotic response, by increasing the proapoptotic protein Bcl-x_S [167], and by impairing the homocysteine metabolism, which results in endoplasmic reticulum stress and apoptosis [169].

As commented before, MAT enzymes are responsible of SAMe synthesis. In mammals, MAT enzymes are codified by two genes, *MAT1A* and

MAT2A. *MAT1A* codifies for the catalytic subunit α1, which associates into dimers or tetramers to conform the MAT III and MAT I enzymes, respectively. *MAT2A* codifies for the catalytic subunit α2 that conforms the tetramer MAT II [81, 83]. Together with the catalytic subunits there is a regulatory β subunit that associates with MAT II enzyme. The expression of *MAT1A* and *MAT2A* genes is dependent of the specific tissue and the developmental state. *MAT1A* is expressed in the adult and differentiated liver, whereas *MAT2A* is expressed in fetal and proliferating liver, and in extrahepatic tissues [70, 89]. During liver development, *MAT1A* expression increases progressively from fetal liver reaching a maximum in the adulthood, whereas *MAT2A* decreases during liver differentiation [92]. On the contrary, during liver proliferation after PH and de-differentiation of cultured hepatocytes, *MAT1A* levels decrease together with an increase of *MAT2A* levels [98, 101]. *MAT1A* expression is also blocked in HCC, which is characterized by an increased *MAT2A* mRNA expression [95]. It has been found that this regulation of *MAT1A* and *MAT2A* expression is related, among other mechanisms, with their promoters methylation status and the acetylation of the histones associated with their promoters [70].

As mentioned, SAMe levels in the liver must be tightly regulated, and, thus, *MAT1A* and *MAT2A* mRNA levels must be regulated. The regulation of their expression based on the promoter methylation and histone acetylation does not completely explain the complex changes between *MAT1A* and *MAT2A* during important biological processes. In addition, it is known that methionine conversion into SAMe regulates *MAT2A* mRNA turnover [100], which can indicate the involving of RNA binding proteins (RBPs) that bind to mRNAs regulating their turnover. The RBPs can enhance or diminish mRNA stability or translation. In the first group we can find HuR which is known to be involved in hepatocyte proliferation by AMPK-dependent translocation [152]. HuR, predominantly nuclear, mainly exerts mRNA stabilizing and translation modulation functions after translocating to the cytoplasm [194]. HuR is implicated in the regulation of cancer traits, enhancing cell proliferation and survival, increasing angiogenesis, helping to evade the immune system and promoting metastasis [201]. The regulation of HuR function is related with the regulation of its

localization, phosphorylation, methylation and HuR protein abundance [186]. In this point, HuR degradation is known to be regulated by ubiquitination, but the mechanisms leading to HuR stability, for example in tumors, are not known. A good candidate for enhancing HuR stability would be the post-translational modification NEDD8, which covalently binds to target proteins enhancing their stability [268]. NEDDylation is linked with cancer, as many of NEDD8 substrates (cullins, p53, Mdm2, p73, EGFR...) are related with tumorigenesis [270].

In the group of RBPs that destabilize mRNAs, we can find AUF1, which is one of the best characterized. Unless one of the main functions of AUF1 is to destabilize mRNAs, it can also be involved in mRNA stabilization and enhancement of translation. AUF1 is regulated by alternative splicing, obtaining different isoforms, by subcellular localization and by post-translational modifications. AUF1 regulates the expression of many key players in cancer, including proto-oncogenes, regulators of apoptosis and cell cycle and proinflammatory cytokines, appearing upregulated in some kind of tumors [264].

In the present work, we studied the role of HuR and AUF1 binding proteins in the regulation of *MAT1A* and *MAT2A* mRNAs, and we also in-depth studied the liver regeneration impairment in the GNMT-KO mice, which presents HuR and *MAT2A* misregulation. Finally, we studied the mechanisms by which HuR protein abundance is enhanced in liver and colon malignancies, involving the post-translational modification by NEDD8.

6.1. HuR/METHYL-HuR AND AUF1 REGULATE THE MAT EXPRESSED DURING LIVER PROLIFERATION, DIFFERENTIATION, AND CARCINOGENESIS.

Gastroenterology 2010;138:1943-1953

As explained, the control of SAMe level mediated by MAT I/III and MAT II is fundamental during hepatic processes related with proliferation, differentiation, dedifferentiation and malignant

transformation. The activity of MAT I/III is directly regulated by the production of NO after the HGF-dependent activation of the LKB1/AMPK/eNOS pathway [132], which blocks SAMe production after proliferative stimulus. Together with this, in the proliferating processes in the liver and during HCC development there is a change from MAT I/III to MAT II, accompanied by a switch from *MAT1A* to *MAT2A* expression [95, 97, 98]. In the liver development the switch occurs as opposite, from *MAT2A* in fetal liver to *MAT1A* in the adulthood [92]. The regulation of this expression has been related with the methylation of the promoters of *MAT1A* and *MAT2A* and the acetylation of the histones associated to these promoters [70]. In the case of *MAT2A*, HGF-induced histones H4 acetylation in its promoter allows the binding of transcription factors such as E2F and Sp1 [107, 305]. Although this regulation at the transcriptional level partially explains *MAT1A* and *MAT2A* regulation, other studies show SAMe-induced decrease of *MAT2A* mRNA half-life, thus pointing towards a post-transcriptional regulation of the mRNA [100, 306].

All these data, together with the high importance of the HuR RNA binding protein during hepatocyte proliferation led us to ask whether *MAT1A* and *MAT2A* are post-transcriptionally regulated through the modification of the turnover of their mRNAs. Our results support the existence of a post-transcriptional regulation of *MAT1A* and *MAT2A* involving two RBPs, AUF1 and HuR, respectively. The abundance of AUF1 and HuR implies the modification of the levels of *MAT1A* and *MAT2A* mRNAs. In addition, the balance between HuR and the post-translationally modified methyl-HuR is controlled by SAMe abundance, and is able to modulate the *MAT2A* mRNA level. For this reason we propose that methylation of HuR modulates its function, leading the RBP to function as *MAT2A* destabilizer, and influencing hepatocyte proliferation.

There is great interest in understanding the genetic changes that occur in the liver during malignant transformation, which in part are similar to those occurring *in vitro* during hepatocyte dedifferentiation and HGF-dependent induction of the proliferation, and *in vivo* during liver proliferation after partial hepatectomy. In all these processes it takes place an increase of *MAT2A* mRNA accompanied by the decrease of *MAT1A* mRNA

levels. The treatment of cultured hepatocytes with HGF and AICAR, activators of AMPK, allow the translocation of HuR from the nucleus to the cytosol, thus enhancing hepatocyte proliferation [152]. Together with this, there is an increase in *MAT2A* mRNA levels [304] and in its half-life that can be blocked by high levels of SAMe, which also enhances *MAT1A* levels and its half-life. Our data show the existence of a binding of HuR to *MAT2A* mRNA and AUF1 to *MAT1A* mRNA, which regulates their turnover. The RNA binding protein HuR, develops several functions in the regulation of the mRNA stability and translation, being the best described the stabilization of its targets [186, 200], and AUF1 is mainly described as a mRNA destabilizer [246]. According with this, HuR binds to *MAT2A* mRNA stabilizing it, and AUF1 binding to *MAT1A* mRNA promotes its degradation. These findings were tested in two models in which SAMe levels and *MAT1A* and *MAT2A* levels are tightly regulated: de-differentiation of cultured hepatocytes and differentiation of fetal liver.

After isolation of primary hepatocytes from healthy rat livers and in culture maintenance, hepatocytes start a de-differentiation process by which they lose hepatocyte phenotype and characteristics, including the expression of the liver-specific markers, acquiring a fibroblast phenotype and recapitulating certain features of the malignant transformation. Between the liver markers that are lost over culture time, we can find albumin, transferrin, haptoglobin, hemopexin, glutathione peroxidase, tyrosine aminotransferase, tryptophan oxygenase, liver gap junction protein and cytochrome P-450 [103]. During this de-differentiation and loss of hepatocyte characteristics, there is also a decrease in SAMe levels, accompanied by the switch from *MAT1A* to *MAT2A* expression. Importantly, the addition of SAMe is able to maintain the levels of *MAT1A* high and prevents the de-differentiation process [101].

Our findings show that *HuR* and *AUF1* mRNAs increase in a time dependent manner during de-differentiation process together with the binding affinity to *MAT2A* and *MAT1A* respectively. This correlates with the increase in *MAT2A* and decrease in *MAT1A* mRNA levels. The treatment with SAMe is able to abrogate the increase of both RBPs and their binding affinity, thus blocking the up-regulation of *MAT2A* and the diminution of

MAT1A. Together with the blockade in *HuR* upregulation, the treatment with SAMe promotes the methylation of HuR. Methyl-HuR presents high affinity to *MAT2A* mRNA and is localized within the polysome fraction that corresponds with the lower translational activity. Previously, the methylation of HuR has been related with changes in its subcellular localization and in the affinity to the targets [235]. In accordance with our results, methyl-HuR binds to *MAT2A* mRNA promoting its decay or inhibiting its translation, a function that has been previously reported [211–213]. In some cases, the inhibition of the translation exerted by HuR implicates the recruitment of other RNA-binding proteins or micro RNAs [311, 312]. As AUF1 is also known to be involved in the inhibition of translation and is related with *MAT1A* mRNA degradation we checked if methyl-HuR collaborates with AUF1 for *MAT2A* decrease after SAMe treatment, but RNP-IP analysis showed no interaction between AUF1 and *MAT2A* mRNA.

Although many aspects of the regulation exerted by HuR and methyl-HuR remain to be elucidated, we propose a model in which the ratio between HuR and methyl-HuR is able to modulate the stabilization of *MAT2A* mRNA. HuR promotes the accumulation of *MAT2A* mRNA, whereas methyl-HuR avoids it. In the presence of high levels of SAMe, the balance between methylated and un-methylated HuR determines the abundance of *MAT2A* mRNA. The importance of this mechanism lies in the effect that its misregulation would exert in the hepatocytes, promoting the de-differentiation of the hepatocytes, impairing the MAT homeostasis and thus the liver function, and even promoting malignant transformation in the liver.

The second model for the study of the regulation of *MAT1A* and *MAT2A* mRNA corresponds with the liver development, from fetal liver to the adulthood. Contrarily of the previous model, this consists in the differentiation of the liver, and it corresponds with a switch from *MAT2A* in the fetal liver, when it is actively proliferating, to *MAT1A* in the adult liver [92]. The regulation is inverse to the one found during hepatocyte de-differentiation. In the fetal highly-proliferating liver, HuR level is upregulated, corresponding with high *MAT2A* mRNA abundance and low SAMe level, which prevents HuR methylation. On the other hand, *MAT1A* level is maintained low,

corresponding with high AUF1 abundance. Over time, as liver develops, proliferation is progressively reduced, and the liver obtains the differentiated status and markers. During liver development, *MAT2A* abundance is progressively reduced together with a decrease in HuR protein level and increase in methyl-HuR amount and binding to the mRNA. At the same time, *MAT1A* expression is enhanced when leaving the immature phenotype, which is accompanied by a reduction in the AUF1 level and binding affinity to *MAT1A*. In summary, these results suggest a mechanism in which the relative abundance of HuR, methyl-HuR and AUF1 can drive the differentiation of the hepatocytes, in a process dependent on SAMe levels. The correct functionality of this process during liver differentiation is fundamental, because assures the preservation of MAT I activity in the adult liver, and, thus, liver function. The malfunction of this regulation could lead to a non-differentiated hepatic phenotype with a high proliferating status and susceptible to malignant transformation.

The observation that during both hepatocyte

differentiation and de-differentiation the levels of HuR and AUF1 vary coordinately arises the question about which is the regulatory mechanism underlying this expression dependent of the differentiation status. Both HuR and AUF1 expression appears modulated at mRNA and protein levels, indicating that at least there should be a transcriptional or post-transcriptional regulation. In the case of HuR, it has been shown to be transcriptionally regulated by the NF κ B transcription factor in gastric tumors [214], in a mechanism dependent of PI3K/AKT signaling pathway. In the liver it is known that NF κ B activates in response to TNF α and IL6 during hepatocyte proliferation and liver regeneration [124, 154], and also NF κ B activation appears as a key factor in HCC development [313, 314]. Thus, in the highly proliferating developing liver and during the hepatocyte de-differentiation it is possible that NF κ B enhances HuR transcription. Together with this, at the post-transcriptional level, HuR mRNA is the target for the miRNAs miR-519 and miR-125a that reduce HuR expression [218, 219, 221]. We hypothesize that these or other

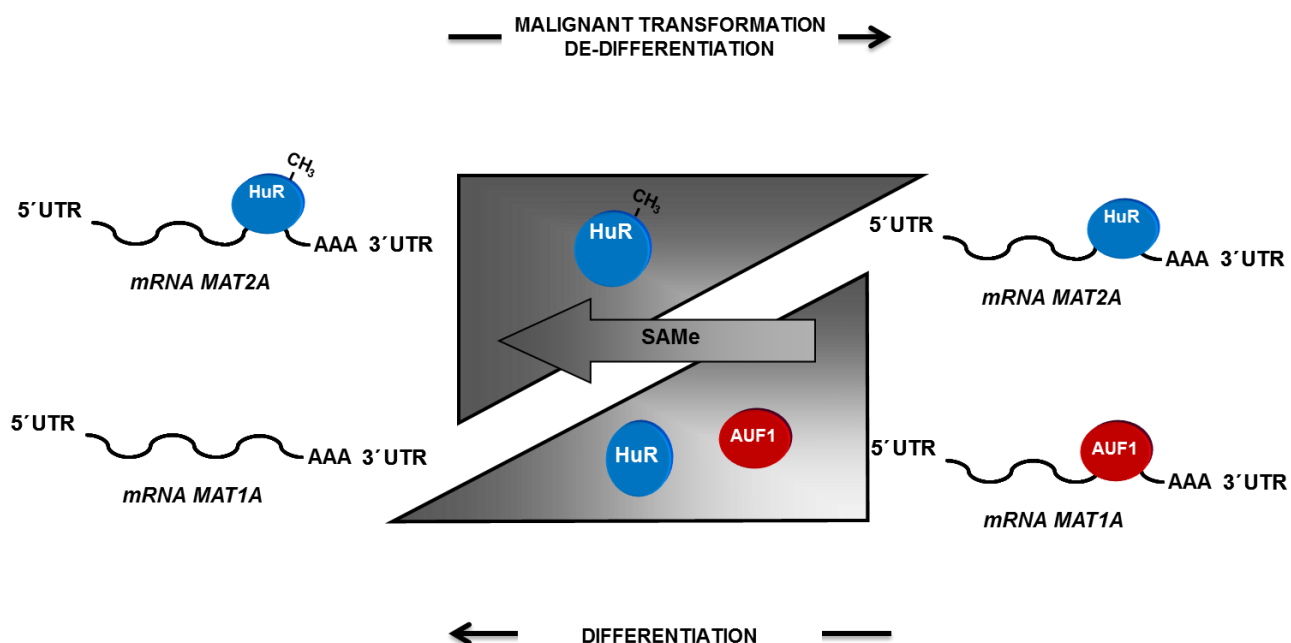


Figure 32. Diagram of *MAT2A* and *MAT1A* mRNAs, and their posttranslational regulators HuR, methyl-HuR, and AUF1 during hepatocyte de-differentiation, liver development, and malignant transformation. Mature hepatocytes express high levels of *MAT1A* mRNA and low levels of AUF1 protein, whereas *MAT2A* mRNA presents low abundance owing to its negative regulator, methyl-HuR. During de-differentiation, the levels of AUF1 protein in hepatocytes increase and the ratio of methyl-HuR/HuR decreases. This leads to a switch from *MAT1A* to *MAT2A* mRNA expression. SAMe treatment of hepatocytes prevents these changes. Malignant transformation of hepatocytes is accompanied by similar expression patterns for AUF1, HuR, and methyl-HuR, as well as for *MAT1A* and *MAT2A* mRNAs. During liver development, the opposite is observed, with decreased AUF1 levels and increased methyl-HuR/HuR ratios, which leads to decrease of *MAT2A* mRNA levels and increase of *MAT1A* mRNA levels.

miRNAs can be expressed at different levels during liver development, proliferation and de-differentiation, also contributing to HuR expression. In the case of AUF1, its regulation at the transcriptional and post-transcriptional levels appears unclear, but considering the HuR and AUF1 coordinated expression during liver differentiation and de-differentiation, the same or a close mechanism could be responsible of both RBPs expression in those processes. Finally, HuR protein abundance is also influenced by ubiquitination [222] and by a novel mechanism involving Mdm2-dependent NEDDylation, that will be described in the discussion section 6.3. The ubiquitinated and NEDDylated status of the liver appears regulated during liver development and in the GNMT-KO and MAT1A-KO mice models (data not shown, unpublished results). Also the NEDDylation level is reduced by SAMe treatment (data not shown, unpublished results). In conclusion, the mechanisms involving ubiquitination and NEDDylation of HuR could participate in HuR abundance during liver development, hepatocyte proliferation and malignant transformation.

Taking into account that the balance between HuR and methyl-HuR, regulated by SAMe level, has a high importance to the regulation of *MAT2A* mRNA abundance and, as a consequence, appears as fundamental to the differentiation, de-differentiation and malignant transformation processes, we studied this regulation in a model with high chronic SAMe levels, the GNMT-KO mice [176]. In these mice, the loss of the main enzyme involved in SAMe catabolism, GNMT, increases 35-fold the hepatic SAMe levels, promoting the spontaneous development of steatosis, fibrosis and hepatocellular carcinoma [49]. These mice also present oxidative stress, inflammation and lipid metabolism impairment [177], and show a hyperactivated Ras/MEK/ERK pathway, conferring proliferative and survival advantage [49]. Compared with the wild type mice, the GNMT-KO presents a lower *MAT2A* mRNA level that correlates with a high methyl-HuR level that actively binds to *MAT2A* mRNA. Thus, the high SAMe level methylates HuR, regulating *MAT2A* level. Contrary of expected, the high SAMe level does not reduce HuR level, probably because of the influence that the highly activated Ras and JAK/STAT pathways exerts over the proliferating status of the liver [49]. Additionally,

although HuR levels are elevated, its functionality after a stimulus such as partial hepatectomy is impaired, as we will see in the next section of the Discussion.

Finally, we studied the level of HuR, methyl-HuR and AUF1 in a cohort of human HCC compared with healthy livers. In human HCC, there is a switch from *MAT1A* to *MAT2A* mRNA expression that enhances cancer cell growth. A transcriptional regulation for this switch in HCC has been proposed, involving the transcription factors Sp1 and c-Myb which would upregulate *MAT2A* gene transcription [315]. Our results suggest the existence of a post-transcriptional regulation involving AUF1, HuR and methyl-HuR in HCC. Both HuR and AUF1 are involved in many types of cancers, as explained in the Introduction sections 2.3.1. and 2.3.2. We were able to detect the presence of both HuR and AUF1 in resected samples from HCC patients, whereas methyl-HuR, consistently, was found in low abundance. By contrast, in the healthy sample HuR and AUF1 were found at low levels and methyl-HuR was increased. According with our results, we postulate that increased levels of HuR and AUF1 and reduced HuR methylation observed in surgically resected HCC might be the hallmarks of the transformation of hepatocytes into cancer cells. The imbalance between HuR/methyl-HuR and AUF1 in the hepatocytes can underlie the deregulation of *MAT2A* and *MAT1A* homeostasis, the decrease of SAMe levels and the transformation into liver cancer cells.

In conclusion, our results provide a model for the post-translational regulation of *MAT1A* and *MAT2A* mRNAs, in a SAMe-dependent manner, involving the RBPs HuR/methyl-HuR and AUF1, during essential biological processes such as hepatocyte de-differentiation, liver development and malignant transformation (Figure 32). According with our model, differentiated adult hepatocytes present high levels of *MAT1A* mRNA and low levels of *MAT2A* mRNA, together with low HuR and AUF1 content and high SAMe levels that methylate HuR. During hepatocyte de-differentiation and malignant transformation, SAMe levels decrease, promoting HuR and AUF1 levels increase and HuR de-methylation, which renders the overexpression of *MAT2A* and the decay of *MAT1A* mRNA. There is a similar temporal distribution of both RBPs, suggesting that they

regulate cell growth and differentiation through their opposing functions. The mechanisms underlying the coordinated regulation of HuR and AUF1 abundance are not known, and further studies are needed to elucidate if they involve transcription factors such as NF κ B, microRNAs or post-translational modifications as ubiquitination and NEDDylation. Finally, the observation that methyl-HuR binds to *MAT2A* mRNA in correlation with its enhanced decay constitutes a novel finding that points to a mechanism by which SAMe may regulate liver functionality.

These results are significant because they reveal critical new insight into the molecular mechanisms underlying the switch between *MAT1A* and *MAT2A* expression, which is observed consistently during hepatic malignant transformation, and facilitates the development and progression of HCC.

6.2. IMPAIRED LIVER REGENERATION IN MICE LACKING GLYCINE N-METHYLTRANSFERASE.

Hepatology 2009; 50(2):443-452

Adult hepatocytes are normally quiescent, in G₀ phase, but have great replicative capacity and are capable of repopulating the liver when a loss in hepatic mass occurs, for example after partial hepatectomy [125, 154]. Many studies have emphasized the activation of the Ras/ERK/MAPK pathway in HGF-induced hepatocyte proliferation and liver regeneration after PH. In addition, the alternative non-canonical pathway LKB1/AMPK/eNOS that we recently discovered, is activated in response to HGF and is blocked by high SAMe levels [132]. This pathway appears to be critical during hepatocyte proliferation after partial hepatectomy, as its blockade diminishes the mitogenic effect of HGF in hepatocytes. The potential mechanism for this inhibition of the proliferation involves the ability of AMPK to translocate HuR from the nucleus to the cytoplasm [152]. The inactivation of AMPK by SAMe avoids HuR translocation in response to HGF, and as a consequence HuR is unable to stabilize target mRNAs involved in cell cycle progression, such as cyclin A and cyclin D1, as well as other mRNAs

that play an important role in liver regeneration after PH, such as iNOS [186, 316]. The production of NO is fundamental for the liver regeneration [125, 154], participating in the inactivation of MAT I/III and protecting hepatocytes from cytokine-induced apoptosis. Mice lacking either iNOS or eNOS present an abnormal liver regeneration after PH [132, 317]. In fact another mechanism by which AMPK inactivation can regulate hepatocyte proliferation during liver regeneration may be through its capacity for stimulating eNOS phosphorylation and NO production [132, 151]. As AMPK is also the energy sensor in the cell, coordinating catabolic and anabolic processes, it provides a link between cellular metabolism and hepatocyte proliferation during liver regeneration.

As commented, the production of NO during liver regeneration inactivates MAT I/III enzymes by nitrosylation of a single cysteine residue [113], which together with the increase in AUF1 RBP that destabilizes *MAT1A* mRNA leads to the decrease in SAMe content in the hepatocyte. This fall in SAMe content is an early event after PH that precedes DNA synthesis [98], and releases the inhibitory effect that SAMe exerts over the HGF-induced LKB1/AMPK/eNOS pathway, the HuR translocation to the nucleus and, finally, over the mitogenic effects [129, 132, 152]. The correct SAMe regulation is fundamental for the success of the regenerative process. The MAT1A-KO mouse model that is characterized for a chronic reduced hepatic SAMe content presents an impaired liver regeneration. This mouse lacks MAT I/III enzyme, which leads to an overexpression of MAT II, which is not subject to inactivation by NO [70]. Consequently with the low SAMe level, the LKB1/AMPK/eNOS pathway is hyperactivated, which results in loss of responsiveness to mitogenic signals, impaired regenerative response after PH, increased hepatic growth and spontaneous development of HCC [132, 174, 175]. Consistent with these findings, we hypothesize that, in the GNMT-KO mouse, the chronic increase in hepatic SAMe content will prevent the LKB1/AMPK/eNOS cascade and the HuR translocation to the nucleus after PH, leading to an impaired regenerative response.

According to our results, after PH in the GNMT-KO mice, the proliferation and the DNA synthesis, determined by PCNA and BrdU positive hepatocytes, are comparable between wild type

and KO mice, suggesting that in the GNMT-KO mice, the hepatocytes progress normally through the S phase of the cell cycle. This agrees with the observation that upstream signaling pathways required for the G₁/S transition, such as cyclin D1 and cyclin A, are activated in the knockout mice both at baseline and after PH. In spite of this normal DNA synthesis, the mortality of the GNMT-KO mice 48 hours after PH reaches nearly 40%, thus demonstrating the existence of an impaired liver regeneration. According with this increased mortality, the liver reveals the existence of a high level of apoptotic response both before and after the PH, as determined by the PARP cleavage.

As expected, the LKB1/AMPK/eNOS pathway fails to activate after partial hepatectomy, together with the HuR translocation. This lack in HuR

translocation from the nucleus to the cytosol is probably related with the absence of increase of cyclin D1, cyclin A and cyclin E after partial hepatectomy. Also iNOS, which is a target of HuR, fails to overexpress after partial hepatectomy. In addition, STAT3 is not phosphorylated and NF κ B does not translocate to the nucleus. The loss of induction of iNOS would reduce the production of NO and, consequently, the protection NO exerts against the cytokine-induced apoptosis. The high PARP cleavage observed in the liver of the GNMT-KO mice could be in part consequence of the lack of this protective mechanism.

It has been previously shown that, after partial hepatectomy, DNA synthesis is impaired in wild type mice treated with SAMe [132]. Our results from the GNMT-KO mice contrast with those

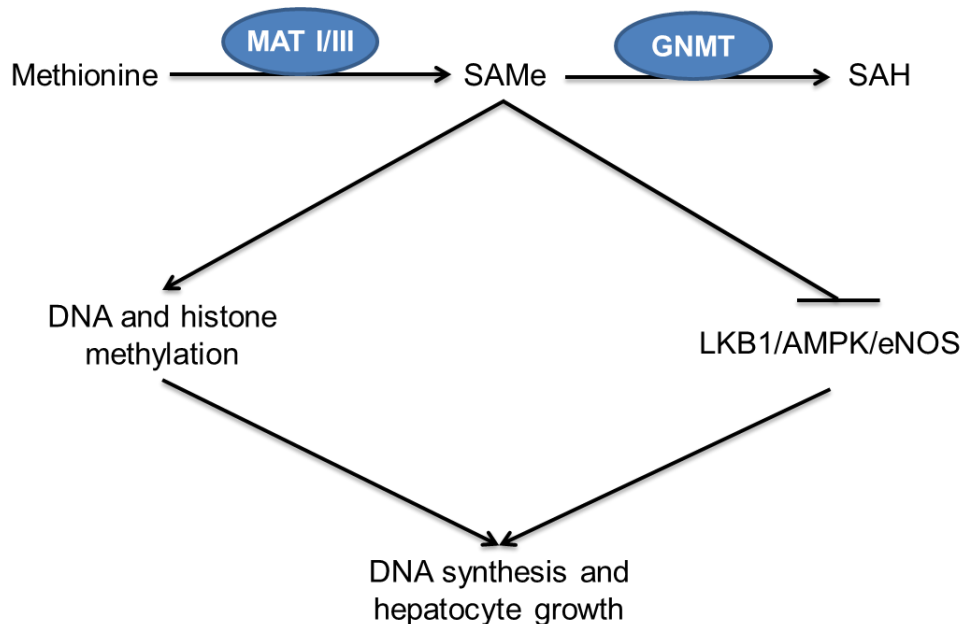


Figure 33. MAT I/III and GNMT control DNA synthesis and hepatocyte growth. Hepatic SAMe content is maintained constant by the combined action of MAT I/III and GNMT enzymes. SAMe induces DNA and histone methylation, as well as the inactivation of the LKB1/AMPK/eNOS pathway. Under normal conditions, liver SAMe content is low enough not to induce spontaneous DNA and histone hypermethylation that results in epigenetic modulation of critical carcinogenesis pathways, such as the Ras and JAK/STAT pathways, but is sufficiently elevated to avoid the spontaneous activation of the LKB1/AMPK/eNOS cascade resulting in uncontrolled DNA synthesis and hepatocyte growth. During liver regeneration following PH, SAMe content transiently decreases releasing its inhibitory effect on the LKB1/AMPK/eNOS cascade, which contributes to normal DNA synthesis and hepatocyte proliferation. In MATI/III-deficient mice, SAMe content is chronically reduced, resulting in the activation of the LKB1/AMPK/eNOS cascade, increased DNA synthesis and hepatocyte growth, together with impaired liver regeneration after PH. In SAMe-treated mice the fall in hepatic SAMe content and the activation of the LKB1/AMPK/eNOS cascade following PH are prevented but without inducing DNA and histone hypermethylation, resulting in the inhibition of DNA synthesis and blockade of the hepatocyte growth. In GNMT-KO, SAMe content is chronically elevated about 50-fold compared with WT animals, resulting in inhibition of the LKB1/AMPK/eNOS cascade. We have demonstrated that in GNMT-KO mice, liver DNA and histones are hypermethylated, leading to the activation of the Ras and JAK/STAT pathways. After PH, activation of the Ras and JAK/STAT cascades facilitates DNA synthesis and hepatocyte growth, although the inhibition of multiple pathways playing a critical role in liver regeneration, such as the activation of the LKB1/AMPK/eNOS cascade, the cytoplasmic translocation of HuR, iNOS activation, and STAT3 phosphorylation impair this process.

observations, as in the present model, DNA synthesis is stimulated in the knockout mice in a similar manner than the wild type. These differences can be explained (Figure 33) by the difference in the SAMe content. In the SAMe-treated mice liver, SAMe level transiently increases about 2-fold compared with the non-treated wild-type mice, but in the case of the GNMT-KO, the hepatic SAMe content is chronically elevated about 50-fold higher than in the wild type mice [176]. As a consequence of this chronic supra-physiological elevation of SAMe levels, there exist an aberrant methylation of the DNA in the liver. These aberrant methylations affect the promoters and histones associated with Ras and JAK/STAT inhibitors (RASSF1, RASSF4, SOCS 1-3 and CIS). This constitutes an epigenetic regulation of the expression of those tumor suppressor genes, leading to the activation of the Ras and JAK/STAT pathways and facilitating DNA synthesis after partial hepatectomy. Although these proliferative pathways are active, the LKB1/AMPK/eNOS pathway is blocked following PH, which results in impaired liver regeneration. On the contrary, in the mice treated with SAMe, the fall in hepatic SAMe content is prevented together with the activation of the LKB1/AMPK/eNOS cascade, but without inducing the activation of the Ras and JAK/STAT pathways (Varela-Rey, Martínez-Chantar and Mato, unpublished results). This results in the inhibition of the DNA synthesis and the impairment in the liver regeneration.

As previously commented, the study of the GNMT-KO mice liver regeneration also revealed a hyperactivation of the NF κ B transcription factor under basal conditions. Our results support a link between the inactivation of AMPK phosphorylation and the NF κ B activation, confirmed in vitro by the inactivation of AMPK by the specific inhibitor compound C (CC). The treatment with CC recapitulates the effect of GNMT ablation on basal hepatic NF κ B activation and also PARP cleavage. Moreover, we also found that the inactivation of AMPK with CC inhibits TNF α -induced NF κ B activation and iNOS expression. These results suggest that under physiological conditions basal AMPK activity prevents hepatocytes from spontaneous but not from TNF α -induced NF κ B activation. In the GNMT-KO mice, inactivation of AMPK by an excess of SAMe leads to NF κ B activation and PARP cleavage under normal

conditions, but renders insensitive hepatocytes to TNF α -induced NF κ B activation and iNOS expression.

Our model presents some limitations for the study of the role of GNMT during liver regeneration. The steatosis and hypermethylation of many genes [49], intrinsic characteristics of the GNMT-KO mice, could be partially responsible of the impaired liver regeneration. Due to this limitation, common to many other knockout models developed to study the importance of a specific gene in liver regeneration, our results need to be validated in a time-specific GNMT-KO mouse model. However, the finding that hepatocytes transfected with a specific GNMT siRNA present reduced expression of cyclin D1 in response to HGF, together with the observation that the knockdown of GNMT in wild type mice reduces the expression of cyclin D1 and cyclin A, as well as the accumulation of cytoplasmic HuR after partial hepatectomy, supports the hypothesis that GNMT plays an important role in liver regeneration.

In conclusion, GNMT appears as a key factor in the hepatocyte proliferation and liver regeneration. This impairment in the proliferation could lead to abnormal proliferation and HCC development, as occurs spontaneously in the GNMT-KO mice. Moreover, the study of the liver regeneration in the GNMT-KO mouse model has relevance because of the existence of patients with GNMT mutations who spontaneously develop liver disease [71–73].

Given the importance of HuR in the posttranscriptional regulation of many critical proteins involved in hepatocyte proliferation and differentiation, liver regeneration and malignant transformation, in the next section we will discuss the new post-translational mechanism involved in the overexpression of HuR, particularly in HCC and colon cancer.

6.3. MURINE DOUBLE MINUTE 2 REGULATES HU ANTIGEN R STABILITY IN HUMAN LIVER AND COLON CANCER THROUGH NEDDYLATION.

Hepatology 2012;55(4):1237-1248

Comment in: Nat Rev Gastroenterol Hepatol. 2011 Dec 13;9(1):4

The RBP HuR is a key factor in the post-transcriptional regulation of the mRNAs. Its specific binding to target mRNAs is able to stabilize them, thus increasing the abundance of genes related with cell cycle progression, apoptosis, etc. Together with this mRNA stabilization function, HuR has also been found to either upregulate or repress mRNA translation, often interfering with repressor RBPs or micro RNAs, or recruiting them [186]. In the case of cancer, HuR acts over mRNAs related with the enhancing of the cell proliferation and cell survival, the elevation of the local angiogenesis, the evasion of the immune response, and the invasion and metastasis [201]. In the liver, as discussed in the previous sections, HuR is involved in the regulation of *MAT2A* mRNA abundance during hepatocyte differentiation and dedifferentiation, liver development and liver regeneration after partial hepatectomy. HuR is also found to be elevated in human HCC, and, recently, a relationship between HuR and cirrhosis was described, involving the activation of the hepatic stellate cells [237].

The regulation of HuR function occurs at many levels: subcellular localization, phosphorylation and methylation, and regulation of HuR abundance. The localization of HuR is mainly nuclear, but the best characterized functions occur in the cytoplasm; in consequence, the nucleocytoplasmic shuttling is important for its function. The phosphorylation and methylation of HuR proteins affects the subcellular localization and the binding affinity of HuR for its targets. Finally, the abundance of HuR is regulated by the transcription factor NF κ B, by autoregulation, being able to bind to its own mRNA, by the binding of microRNAs, by caspase mediated cleavage, and by ubiquitin-dependent proteasomal degradation [186]. Unless HuR degradation is regulated by ubiquitination, the mechanisms involved in the enhancing of HuR protein stability are not known.

Here we provide a new mechanism involving the post-translational modification NEDD8 that explains the overexpression of HuR in HCC and colon cancer.

Our results show the existence of a strong and positive correlation between the levels of HuR and Mdm2 in a cohort of human HCC and metastatic colon cancer to the liver. This correlation is corroborated by the finding that, according with the transformation status of the cells, the levels of both HuR and Mdm2 increase from primary hepatocytes to HCC cell lines. Consequently with this correlation, the overexpression and knockdown of Mdm2 is able to increase or decrease HuR level, respectively. The decrease in HuR levels after Mdm2 silencing also regulates the abundance of the HuR target cyclin A. Cyclin A is a central regulator of cell cycle progression in S phase, and its overexpression is implicated as a driving feature in various types of cancer [318, 319]. In relation with this, both HuR and Mdm2 silencing reduces the entering into S phase, and also increases the apoptosis, thus suggesting that part of the oncogenic features linked to Mdm2 could be due to its influence over HuR abundance.

The protein Mdm2, which is implicated in many human cancers, can act as an E3 NEDD8 ligase, stabilizing protein targets by NEDDylation. Many of the NEDDylated proteins seem to be either NEDDylated or ubiquitinated, revealing an intriguing relationship between ubiquitination and NEDDylation. Good examples are p53 and its relative p73, which are both NEDDylated and ubiquitinated by the RING-domain protein Mdm2 [290]. We observed that under basal conditions, HuR-V5 is NEDDylated, but after UVC treatment there is a switch to ubiquitinated forms, which is accompanied by a decrease in HuR-V5 levels. In addition, endogenous HuR was also a target for NEDDylation conjugation and Mdm2 was demonstrated to increase its stabilization due to a robust enrichment in this posttranslational modification.

HuR protein is composed of three conserved RNA recognition motifs (RRM) and the hinge region (HR) lying between RRM2 and RRM3 [192]. We performed several K→R single mutations in the RRM3 and C-terminal region of HuR. Our results demonstrate that there are three lysines

(K283, K313, K326), that showed a role in the regulation of HuR stabilization, in particular K326. Those residues are conserved among species from mouse to human. The analysis of those mutants revealed the same basal levels of mRNA, but the protein expression and their stability were lower than the control HuR-V5. In addition, those mutants did not show any particular differences in their capability to bind mRNA targets such as *PTMA* or *cyclin D1*, suggesting that this modification did not alter the functionality of HuR. The combination of the three mutants rendered a triple mutant, H(3KR)V5, that presents the lower stability. This triple mutant showed a clear proapoptotic phenotype, suggesting that although the binding capacity is not affected, the mutation of the lysines modifies some of the HuR targets.

NEDD8 silencing drastically reduced the levels of HuR, and NEDDylation experiments showed that specially H(K326R)V5 is deficient for NEDD8 conjugation compared to the wild type

HuR-V5, corresponding to increased destabilization of the mutant. In addition, this specific mutant showed an increase in the abundance of ubiquitinated forms in the presence of Mdm2 and ubiquitin after His purification, highlighting the role of K326 as a specific site for NEDDylation process. These results suggest that the suppression of NEDDylation renders HuR protein more susceptible to the ubiquitination pathway.

One of the possible mechanism by which H(K326R)V5 showed this characteristic behavior could be its uncommon localization. As commented, HuR is a nuclear protein that shuttles from this cellular compartment to the cytoplasm in response to specific stimuli. However the localization of these mutants differed from the wild type HuR-V5 and consequently H(K326R)V5 was mostly cytoplasmic. It has been previously reported that NEDD8 play a role in the correct nuclear localization of L11. This is the mechanism

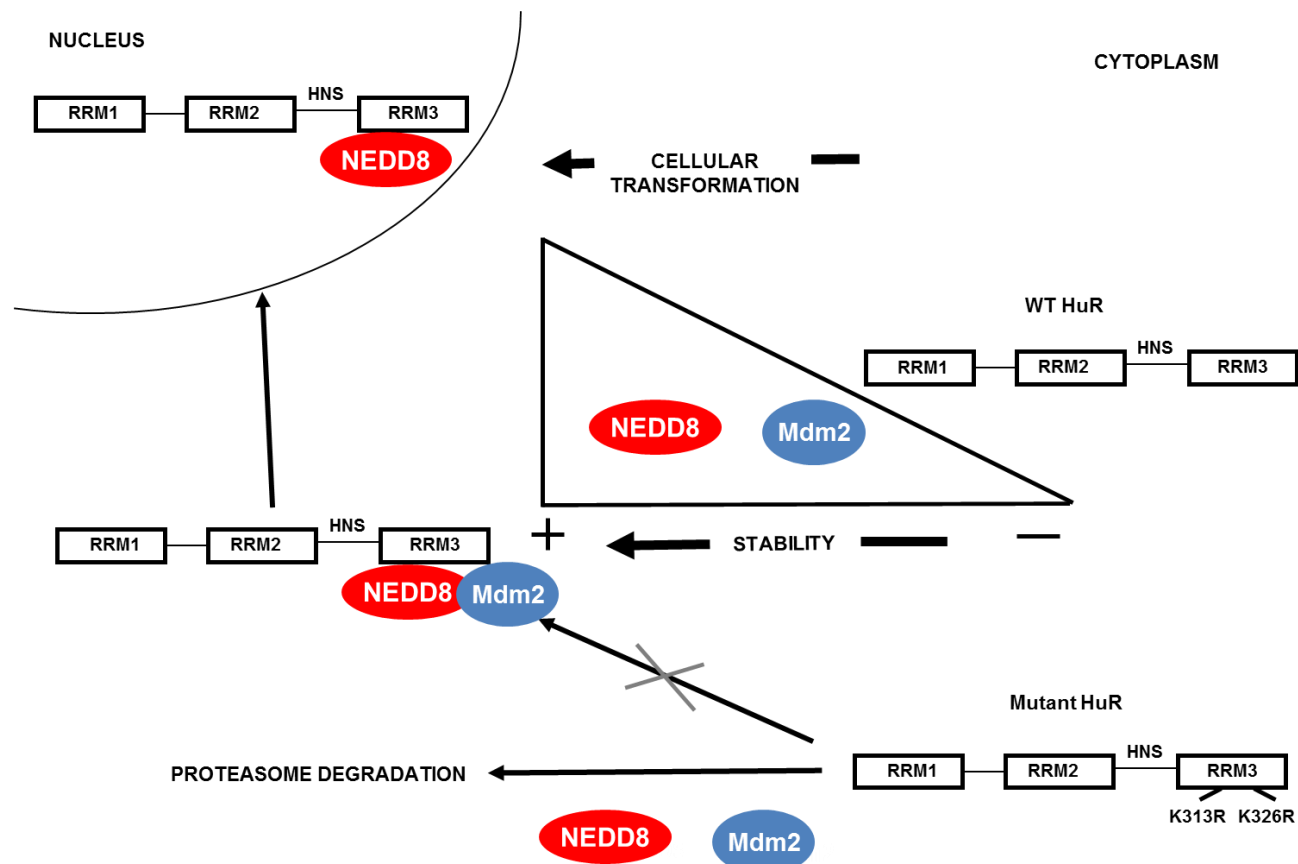


Figure 34. Model for HuR NEDDylation. Mdm2 acts as an E3 NEDD8 ligase promoting HuR NEDDylation and stabilization. HuR NEDDylation occurs in the cytoplasm and is required for the correct localization of HuR in the nucleus. This post-translational modification maintains HuR out of the ubiquitination pathway. In the case of mutated HuR, NEDDylation does not occur, and, thus, proteasomal degradation is able to reduce HuR abundance.

by which NEDDylation protects L11 from destabilization [293]. Our data demonstrated that, in addition to the unusual HuR mutant localization, NEDP1 transfection induced a reduction in nuclear but not in the cytoplasmic content of HuR-V5. Taking in consideration that K313R and K326R mutants are located in the RRM3 and C-terminal of HuR and considering that the RRM3 has been implicated in the interaction with other nuclear cargos (pp32, SETa, SETb and APRIL) [228] and bears sequences, which confer the nuclear export of Hu proteins, we suggest that NEDDylation plays a role in HuR nuclear localization. As HuR export to the cytoplasm is related with its proteasomal degradation after UVC treatment, and HuR mutants are degraded by the proteasome in the cytoplasm, we propose that the NEDDylation of HuR promotes its nuclear localization protecting HuR from cytoplasmic ubiquitination and degradation. To gain insight in the functionality of HuR NEDDylation, we identified that Mdm2-NLS mutant, which is localized exclusively in the cytoplasm, was able to promote HuR stabilization at comparable levels to wild type Mdm2. Comparable results were obtained with Mdm2 mutation in C464, previously identified as a residue involved in Mdm2 auto-ubiquitination as well as ubiquitination of other targets. These results further support the idea that HuR NEDDylation occurs in the cytoplasm and due to the E3 NEDD8 ligase and independently of its ubiquitination activity.

In summary, a general model is shown in Figure 34. Mdm2 acts as an E3 NEDD8 ligase stabilizing HuR protein levels. This NEDDylation takes place in the cytoplasm and is required for the correct localization of HuR in the nucleus. This post-translational modification maintains HuR out of the ubiquitination pathway. The mutants described in this paper, particularly K313 and K326, are not likely to be NEDDylated and are degraded through the action of the proteasome in the cytoplasm. These findings pointed out that NEDDylation and ubiquitination are important mechanisms that could be affecting HuR cellular localization and therefore its functionality. These results are in agreement with the cytoplasmic localization of p53 mediated by NUB1 where cooperation between NEDD8 and ubiquitin was observed [291].

In addition, our results show the importance of the Mdm2-NEDD8 network in HuR overexpression detected during malignant transformation, supporting the role of HuR in tumorigenesis. The potential of antitumor activity for the NEDD8-activating enzyme (NAE) inhibitor MLN4924 has been shown in human colon and lung tumor xenograft models in immunocompromised mice [270, 320]. Taken together, HuR is a new target for NEDDylation, and NEDD8-dependent regulation plays a crucial role as a principal conductor of a new regulatory mechanism. Our findings might represent a useful tool to uncover new therapeutic strategies for HCC and colon cancer. In closing, our results show that NEDDylation is a novel mechanism for HuR regulation, which broadly reveals its influence on the cellular post-transcriptional regulatory machinery.

Summarizing, this study accomplishes with the objective of identifying new mechanisms implicated in the hepatocyte proliferation, differentiation and de-differentiation, liver regeneration and malignant transformation. Taking into consideration the importance of the SAMe levels homeostasis in the liver, we go in depth into the molecular regulation underlying the processes in which SAMe levels modification is needed. In particular, the SAMe level is known to decrease during the proliferating stages of the hepatocyte, including liver regeneration after PH or damage, de-differentiation of cultured primary hepatocytes and malignant transformation. On the contrary, during the liver development from embryos to adults, hepatic SAMe amount progressively increases to reach the level that allows the liver to perform 85% of all methylation reactions.

The reduction of SAMe levels during hepatocyte proliferation releases the blockade that this molecule exerts over the LKB1/AMPK/eNOS pathway, which is fundamental for the correct liver regeneration and hepatocyte proliferation. This reduction is due to the HGF-dependent eNOS activation, which produces NO that nitrosylates MAT I /III enzyme inactivating it. The activation of the LKB1/AMPK/eNOS pathway also allows the translocation of HuR from the nucleus to the cytoplasm, where it can exert the functions stabilizing mRNAs related with cell cycle progression and proliferation. Together with this,

there is also an increase in the levels of MAT II during the hepatocyte proliferation. During liver development the process occurs conversely, with a progressive increase of MAT I/III and a decrease of the proliferation-related MAT II enzyme.

This regulation of MAT I/III and MAT II during the hepatocyte differentiation and de-differentiation also occurs at the mRNA level. Here we demonstrate that *MAT1A* and *MAT2A* mRNA levels are regulated post-transcriptionally by the RNA binding proteins AUF1 and HuR, respectively, during liver development and hepatocyte de-differentiation. AUF1 binds to *MAT1A* mRNA destabilizing it during hepatocyte de-differentiation together with a stabilization of *MAT2A* mRNA by HuR. In the case of the liver differentiation, HuR is methylated by SAMe becoming a destabilizer for *MAT2A* mRNA, and AUF1 decreases allowing *MAT1A* mRNA to increase. These results intensifies the relation of SAMe with the regulation of hepatocyte proliferation, not only blocking the LKB1/AMPK/eNOS pathway and the HuR translocation, but also avoiding the stabilization of *MAT2A* mRNA, which is highly related with the liver proliferation. This relation is confirmed with the model of the GNMT-KO mice that is characterized by chronically elevated SAMe levels. These GNMT-KO mice corresponds with an epigenetic model of aberrant DNA and histone methylations that renders a hyper-activated Ras and JAK/STAT pathways, which provide proliferative and survival advantages, and finally HCC development. Despite this high proliferating status under basal conditions, the GNMT-KO mice present impairment in the liver regeneration after PH, which can be explained because of the incapacity to activate the LKB1/AMPK/eNOS pathway and to translocate HuR to the cytoplasm. Moreover, HuR appears methylated, promoting the destabilization of *MAT2A* mRNA.

The study of the GNMT-KO mice also provided another interesting relation between SAMe and hepatocyte proliferation. According with our findings, the chronic inactivation of AMPK by SAMe excess promotes the hyperactivation of

NF κ B, but makes hepatocytes insensitive to the TNF α -dependent activation of NF κ B and iNOS expression. Thus, SAMe blocks a fundamental pathway for the proliferation during liver regeneration.

The impairment of SAMe regulation can lead to HCC progression. This occurs both in cases of excess SAMe, as in the GNMT-KO mice, and low levels of SAMe, as in the MAT1A-KO mice. In humans, the low level of SAMe has been detected in many types of liver diseases, including cirrhosis and HCC. Our results show that in human HCC, the levels of HuR and AUF1 are increased, together with a low methylation status of HuR, which according with the mechanism we propose, correlates with high *MAT2A* and low *MAT1A* mRNA levels. In fact, HuR appears elevated in many types of cancers, correlating with their prognosis, and, as explained, is also fundamental for the hepatocyte proliferation, liver regeneration and liver development. The mechanism by which HuR levels are elevated is not well understood. Here we propose a new way for HuR protein stabilization in HCC and colon cancer, involving Mdm2-dependent NEDDylation. Our study demonstrates that HuR and Mdm2 levels correlate in human HCC and metastatic colon cancer to the liver, and also in hepatoma and colon cancer cell lines, according with their transformation status. Moreover, we found that Mdm2 acts over HuR as an E3 NEDD8 ligase, NEDDylating and promoting its nuclear localization, thus avoiding the proteasomal degradation. This mechanism can be important for the development and progression of the HCC, considering that HuR promotes hepatocyte proliferation, and that its impairment can lead to uncontrolled cell division.

In conclusion, in this study we uncovered different mechanism for the hepatocyte proliferation, differentiation and malignant transformation, discovering new potential targets for therapy in liver diseases such as HCC. In particular, the HuR NEDDylation could be targeted with the NEDD8-activating enzyme MLN4924, which has proved its antitumoral properties in other types of cancers.

7. CONCLUSIONS

7. CONCLUSIONS

7.1. HuR/METHYL-HuR AND AUF1 REGULATE THE MAT EXPRESSED DURING LIVER PROLIFERATION, DIFFERENTIATION, AND CARCINOGENESIS.

1. HuR and AUF1 are important regulators of the liver development, de-differentiation and proliferation.
2. HuR promotes the accumulation of *MAT2A* mRNA, and methyl-HuR functions as destabilizer of *MAT2A* mRNA. The ratio methyl-HuR/HuR is regulated by SAMe abundance.
3. AUF1 promotes the destabilization of *MAT1A* mRNA.
4. The relative abundance of HuR, methyl-HuR and AUF1 can drive the differentiation and de-differentiation of hepatocytes in a process dependent on SAMe levels.
5. The increase in HuR and AUF1, and the reduced methylation of HuR might be hallmarks of the transformation of hepatocytes into HCC cells.
6. We propose a new model for HuR, methyl-HuR and AUF1 function on the post-transcriptional regulation of *MAT2A* and *MAT1A* mRNAs in a SAMe-dependent manner during hepatocyte differentiation, de-differentiation and malignant transformation.

7.2. IMPAIRED LIVER REGENERATION IN MICE LACKING GLYCINE N-METHYLTRANSFERASE.

1. Liver regeneration is impaired in the GNMT-KO mice, characterized by chronic increase in hepatic SAMe level.
2. Chronic high SAMe level in the GNMT-KO mice blocks LKB1/AMPK/eNOS pathway activation, HuR cytoplasmic translocation, nuclear translocation of NF κ B, STAT3 phosphorylation and iNOS expression after partial hepatectomy.
3. AMPK inactivation promotes basal hepatic activation of NF κ B.
4. AMPK inactivation by high SAMe levels inhibits TNF α -dependent NF κ B activation and iNOS expression, and increases the apoptotic response.

7.3. MURINE DOUBLE MINUTE 2 REGULATES HU ANTIGEN R STABILITY IN HUMAN LIVER AND COLON CANCER THROUGH NEDDYLATION.

1. Mdm2 NEDDylates HuR protein in the cytoplasm promoting its stabilization, independently of the ubiquitin ligase activity.
2. HuR NEDDylation is linked to lysine residues K283, K313 and, particularly, K326.
3. HuR NEDDylation promotes its nuclear localization, protecting it from proteasomal degradation.
4. HuR and Mdm2 expression cooperatively influences tumor cell growth by controlling the expression of cell cycle regulators.
5. Mdm2-dependent NEDDylation of HuR promotes its overexpression during malignant transformation, supporting the role of HuR in tumorigenesis.
6. HuR NEDDylation represents a new therapeutic target for HCC and colon cancer, through the NEDD8-activating enzyme inhibitor MLN4924.

8. BIBLIOGRAPHY

8. BIBLIOGRAPHY

- [1] T. R. Riley 3rd and A. M. Bhatti, "Preventive strategies in chronic liver disease: part I. Alcohol, vaccines, toxic medications and supplements, diet and exercise," *Am Fam Physician*, vol. 64, no. 9, pp. 1555–1560, Nov. 2001.
- [2] S. L. Murphy, "Deaths: final data for 1998," *Natl Vital Stat Rep*, vol. 48, no. 11, pp. 1–105, Jul. 2000.
- [3] D. L. Hoyert, E. Arias, B. L. Smith, S. L. Murphy, and K. D. Kochanek, "Deaths: final data for 1999," *Natl Vital Stat Rep*, vol. 49, no. 8, pp. 1–113, Sep. 2001.
- [4] A. Propst, T. Propst, G. Zangerl, D. Ofner, G. Judmaier, and W. Vogel, "Prognosis and life expectancy in chronic liver disease," *Dig. Dis. Sci.*, vol. 40, no. 8, pp. 1805–1815, Aug. 1995.
- [5] G. Vernon, A. Baranova, and Z. M. Younossi, "Systematic review: the epidemiology and natural history of non-alcoholic fatty liver disease and non-alcoholic steatohepatitis in adults," *Alimentary Pharmacology & Therapeutics*, vol. 34, no. 3, pp. 274–285, 2011.
- [6] L. A. Adams, P. Angulo, and K. D. Lindor, "Nonalcoholic fatty liver disease," *CMAJ*, vol. 172, no. 7, pp. 899–905, Mar. 2005.
- [7] L. A. Adams and K. D. Lindor, "Nonalcoholic fatty liver disease," *Ann Epidemiol*, vol. 17, no. 11, pp. 863–869, Nov. 2007.
- [8] E. M. Brunt, "Pathology of nonalcoholic steatohepatitis," *Hepatol. Res.*, vol. 33, no. 2, pp. 68–71, Oct. 2005.
- [9] M. R. Teli, O. F. W. James, A. D. Burt, M. K. Bennett, and C. P. Day, "The natural history of nonalcoholic fatty liver: A follow-up study," *Hepatology*, vol. 22, no. 6, pp. 1714–1719, 1995.
- [10] P. Angulo and K. D. Lindor, "Non-alcoholic fatty liver disease," *Journal of Gastroenterology and Hepatology*, vol. 17, pp. S186–S190, 2002.
- [11] A. B. Siegel and A. X. Zhu, "Metabolic syndrome and hepatocellular carcinoma," *Cancer*, vol. 115, no. 24, pp. 5651–5661, 2009.
- [12] L. W. Cho, "Metabolic syndrome," *Singapore Med J*, vol. 52, no. 11, pp. 779–785, Nov. 2011.
- [13] E. Vanni, E. Bugianesi, A. Kotronen, S. De Minicis, H. Yki-Järvinen, and G. Svegliati-Baroni, "From the metabolic syndrome to NAFLD or vice versa?," *Dig Liver Dis*, vol. 42, no. 5, pp. 320–330, May 2010.
- [14] K. M. Flegal, M. D. Carroll, R. J. Kuczmarski, and C. L. Johnson, "Overweight and obesity in the United States: prevalence and trends, 1960–1994," *Int. J. Obes. Relat. Metab. Disord.*, vol. 22, no. 1, pp. 39–47, Jan. 1998.
- [15] A. J. McCullough, "Update on nonalcoholic fatty liver disease," *J. Clin. Gastroenterol.*, vol. 34, no. 3, pp. 255–262, Mar. 2002.
- [16] A. Del Gaudio, L. Boschi, G.-A. Del Gaudio, L. Mastrangelo, and D. Munari, "Liver damage in obese patients," *Obes Surg*, vol. 12, no. 6, pp. 802–804, Dec. 2002.
- [17] P. Gupte, D. Amarapurkar, S. Agal, R. Baijal, P. Kulshrestha, S. Pramanik, N. Patel, A. Madan, A. Amarapurkar, and Hafeezunnisa, "Non-alcoholic steatohepatitis in type 2 diabetes mellitus," *Journal of Gastroenterology and Hepatology*, vol. 19, no. 8, pp. 854–858, 2004.
- [18] S. Bellentani, F. Scaglioni, M. Marino, and G. Bedogni, "Epidemiology of non-alcoholic fatty liver disease," *Dig Dis*, vol. 28, no. 1, pp. 155–161, 2010.
- [19] D. Preiss and N. Sattar, "Non-alcoholic fatty liver disease: an overview of prevalence, diagnosis, pathogenesis and treatment considerations," *Clinical Science*, vol. 115, no. 5, p. 141, Sep. 2008.
- [20] F. Marra, A. Gastaldelli, G. Svegliati Baroni, G. Tell, and C. Tiribelli, "Molecular basis and mechanisms of progression of non-alcoholic steatohepatitis," *Trends in Molecular Medicine*, vol. 14, no. 2, pp. 72–81, Feb. 2008.
- [21] G. C. Farrell and C. Z. Larter, "Nonalcoholic fatty liver disease: From steatosis to cirrhosis," *Hepatology*, vol. 43, no. S1, pp. S99–S112, 2006.
- [22] Y. Falck-Ytter, Z. M. Younossi, G. Marchesini, and A. J. McCullough, "Clinical features and natural history of nonalcoholic steatosis syndromes," *Semin. Liver Dis.*, vol. 21, no. 1, pp. 17–26, 2001.

- [23] X.-Y. Duan, L. Qiao, and J.-G. Fan, "Clinical features of nonalcoholic fatty liver disease-associated hepatocellular carcinoma," *HPBD INT*, vol. 11, no. 1, pp. 18–27, Feb. 2012.
- [24] A. Jemal, F. Bray, M. M. Center, J. Ferlay, E. Ward, and D. Forman, "Global cancer statistics," *CA Cancer J Clin*, vol. 61, no. 2, pp. 69–90, Apr. 2011.
- [25] D. M. Parkin, P. Pisani, and J. Ferlay, "Global cancer statistics," *CA Cancer J Clin*, vol. 49, no. 1, pp. 33–64, 1, Feb. 1999.
- [26] A. J. Sanyal, S. K. Yoon, and R. Lencioni, "The Etiology of Hepatocellular Carcinoma and Consequences for Treatment," *The Oncologist*, vol. 15, no. Supplement 4, pp. 14–22, Nov. 2010.
- [27] Y. Fong, R. L. Sun, W. Jarnagin, and L. H. Blumgart, "An Analysis of 412 Cases of Hepatocellular Carcinoma at a Western Center," *Ann Surg*, vol. 229, no. 6, p. 790, Jun. 1999.
- [28] R. S. Finn, "Development of molecularly targeted therapies in hepatocellular carcinoma: where do we go now?," *Clin. Cancer Res.*, vol. 16, no. 2, pp. 390–397, Jan. 2010.
- [29] C. Frenette and R. Gish, "Targeted systemic therapies for hepatocellular carcinoma: Clinical perspectives, challenges and implications," *World J Gastroenterol*, vol. 18, no. 6, pp. 498–506, Feb. 2012.
- [30] J. M. Llovet and J. Bruix, "Systematic review of randomized trials for unresectable hepatocellular carcinoma: Chemoembolization improves survival," *Hepatology*, vol. 37, no. 2, pp. 429–442, 2003.
- [31] A. X. Zhu, "Systemic Therapy of Advanced Hepatocellular Carcinoma: How Hopeful Should We Be?," *The Oncologist*, vol. 11, no. 7, pp. 790–800, Jul. 2006.
- [32] D. H. Van Thiel and G. Ramadori, "Non-Viral Causes of Hepatocellular Carcinoma," *J Gastrointest Cancer*, vol. 42, no. 4, pp. 191–194, Dec. 2011.
- [33] M.-F. Yuen and C.-L. Lai, "Hepatitis B virus genotypes: natural history and implications for treatment," *Expert Rev Gastroenterol Hepatol*, vol. 1, no. 2, pp. 321–328, Dec. 2007.
- [34] E. Szabó, C. Páska, P. Kaposi Novák, Z. Schaff, and A. Kiss, "Similarities and differences in hepatitis B and C virus induced hepatocarcinogenesis," *Pathol. Oncol. Res.*, vol. 10, no. 1, pp. 5–11, 2004.
- [35] M. A. Feitelson, "Hepatitis B virus in hepatocarcinogenesis," *Journal of Cellular Physiology*, vol. 181, no. 2, pp. 188–202, 1999.
- [36] M. Malaguarnera, M. Di Rosa, F. Nicoletti, and L. Malaguarnera, "Molecular mechanisms involved in NAFLD progression," *J. Mol. Med.*, vol. 87, no. 7, pp. 679–695, Jul. 2009.
- [37] D. Pessayre, A. Berson, B. Fromenty, and A. Mansouri, "Mitochondria in steatohepatitis," *Semin. Liver Dis.*, vol. 21, no. 1, pp. 57–69, 2001.
- [38] M. A. Tirmenstein, F. A. Nicholls-Grzemski, J. G. Zhang, and M. W. Fariss, "Glutathione depletion and the production of reactive oxygen species in isolated hepatocyte suspensions," *Chem. Biol. Interact.*, vol. 127, no. 3, pp. 201–217, Jul. 2000.
- [39] K. Schulze-Osthoff, A. C. Bakker, B. Vanhaesebroeck, R. Beyaert, W. A. Jacob, and W. Fiers, "Cytotoxic activity of tumor necrosis factor is mediated by early damage of mitochondrial functions. Evidence for the involvement of mitochondrial radical generation.," *J. Biol. Chem.*, vol. 267, no. 8, pp. 5317–5323, Mar. 1992.
- [40] M. Curzio, H. Esterbauer, G. Poli, F. Biasi, G. Cecchini, C. Di Mauro, N. Cappello, and M. U. Dianzani, "Possible role of aldehydic lipid peroxidation products as chemoattractants," *Int J Tissue React*, vol. 9, no. 4, pp. 295–306, 1987.
- [41] K. S. Lee, M. Buck, K. Houglum, and M. Chojkier, "Activation of hepatic stellate cells by TGF alpha and collagen type I is mediated by oxidative stress through c-myb expression.," *J Clin Invest*, vol. 96, no. 5, pp. 2461–2468, Nov. 1995.
- [42] I. A. Leclercq, G. C. Farrell, J. Field, D. R. Bell, F. J. Gonzalez, and G. R. Robertson, "CYP2E1 and CYP4A as microsomal catalysts of lipid peroxides in murine nonalcoholic steatohepatitis," *J Clin Invest*, vol. 105, no. 8, pp. 1067–1075, Apr. 2000.
- [43] C. H. Best, J. M. Hershey, and M. E. Huntsman, "The effect of lecithine on fat deposition in the liver of the normal rat," *J Physiol*, vol. 75, no. 1, pp. 56–66, May 1932.
- [44] L. W. KINSELL and H. A. HARPER, "Rate of disappearance from plasma of intravenously administered methionine in patients with liver damage," *Science*, vol. 106, no. 2763, p. 589, Dec. 1947.

- [45] L. W. Kinsell, H. A. Harper, H. C. Barton, M. E. Hutchin, and J. R. Hess, "STUDIES IN METHIONINE AND SULFUR METABOLISM. I. THE FATE OF INTRAVENOUSLY ADMINISTERED METHIONINE, IN NORMAL INDIVIDUALS AND IN PATIENTS WITH LIVER DAMAGE 12," *J Clin Invest*, vol. 27, no. 5, pp. 677–688, Sep. 1948.
- [46] A. M. Duce, P. Ortiz, C. Cabrero, and J. M. Mato, "S-adenosyl-L-methionine synthetase and phospholipid methyltransferase are inhibited in human cirrhosis," *Hepatology*, vol. 8, no. 1, pp. 65–68, 1988.
- [47] M. A. Avila, C. Berasain, L. Torres, A. Martín-Duce, F. J. Corrales, H. Yang, J. Prieto, S. C. Lu, J. Caballería, J. Rodés, and J. M. Mato, "Reduced mRNA abundance of the main enzymes involved in methionine metabolism in human liver cirrhosis and hepatocellular carcinoma," *Journal of Hepatology*, vol. 33, no. 6, pp. 907–914, Dec. 2000.
- [48] S. C. Lu, L. Alvarez, Z.-Z. Huang, L. Chen, W. An, F. J. Corrales, M. A. Avila, G. Kanel, and J. M. Mato, "Methionine adenosyltransferase 1A knockout mice are predisposed to liver injury and exhibit increased expression of genes involved in proliferation," *PNAS*, vol. 98, no. 10, pp. 5560–5565, May 2001.
- [49] M. L. Martínez-Chantar, M. Vázquez-Chantada, U. Ariz, N. Martínez, M. Varela, Z. Luka, A. Capdevila, J. Rodríguez, A. M. Aransay, R. Matthiesen, H. Yang, D. F. Calvisi, M. Esteller, M. Fraga, S. C. Lu, C. Wagner, and J. M. Mato, "Loss of the glycine N-methyltransferase gene leads to steatosis and hepatocellular carcinoma in mice," *Hepatology*, vol. 47, no. 4, pp. 1191–1199, 2008.
- [50] A. J. Levine and M. Oren, "The first 30 years of p53: growing ever more complex," *Nat Rev Cancer*, vol. 9, no. 10, pp. 749–758, Oct. 2009.
- [51] J. T. Zilfou and S. W. Lowe, "Tumor Suppressive Functions of p53," *Cold Spring Harb Perspect Biol*, vol. 1, no. 5, Nov. 2009.
- [52] N. Yahagi, H. Shimano, T. Matsuzaka, M. Sekiya, Y. Najima, S. Okazaki, H. Okazaki, Y. Tamura, Y. Iizuka, N. Inoue, Y. Nakagawa, Y. Takeuchi, K. Ohashi, K. Harada, T. Gotoda, R. Nagai, T. Kadokami, S. Ishibashi, J. Osuga, and N. Yamada, "p53 Involvement in the Pathogenesis of Fatty Liver Disease," *J. Biol. Chem.*, vol. 279, no. 20, pp. 20571–20575, May 2004.
- [53] A. Panasiuk, J. Dzieciol, B. Panasiuk, and D. Prokopowicz, "Expression of p53, Bax and Bcl-2 proteins in hepatocytes in non-alcoholic fatty liver disease," *World J. Gastroenterol.*, vol. 12, no. 38, pp. 6198–6202, Oct. 2006.
- [54] G. C. Farrell, C. Z. Larter, J. Y. Hou, R. H. Zhang, M. M. Yeh, J. Williams, A. Dela Peña, R. Francisco, S. R. Osvath, J. Brooking, N. Teoh, and L. M. Sedger, "Apoptosis in experimental NASH is associated with p53 activation and TRAIL receptor expression," *Journal of Gastroenterology and Hepatology*, vol. 24, no. 3, pp. 443–452, 2009.
- [55] K. Tomita, T. Teratani, T. Suzuki, T. Oshikawa, H. Yokoyama, K. Shimamura, K. Nishiyama, N. Mataki, R. Irie, T. Minamino, Y. Okada, C. Kurihara, H. Ebinuma, H. Saito, I. Shimizu, Y. Yoshida, R. Hokari, K. Sugiyama, K. Hatsuse, J. Yamamoto, T. Kanai, S. Miura, and T. Hibi, "p53/p66Shc-mediated signaling contributes to the progression of nonalcoholic steatohepatitis in humans and mice," *Journal of Hepatology*, May 2012.
- [56] N. Martínez-López, M. Varela-Rey, D. Fernández-Ramos, A. Woodhoo, M. Vázquez-Chantada, N. Embade, L. Espinosa-Hevia, F. J. Bustamante, L. A. Parada, M. S. Rodriguez, S. C. Lu, J. M. Mato, and M. L. Martínez-Chantar, "Activation of LKB1-Akt pathway independent of phosphoinositide 3-kinase plays a critical role in the proliferation of hepatocellular carcinoma from nonalcoholic steatohepatitis," *Hepatology*, vol. 52, no. 5, pp. 1621–1631, Nov. 2010.
- [57] J. M. Llovet and J. Bruix, "Novel advancements in the management of hepatocellular carcinoma in 2008," *J. Hepatol.*, vol. 48 Suppl 1, pp. S20–37, 2008.
- [58] S. Ryder, "Guidelines for the diagnosis and treatment of hepatocellular carcinoma (HCC) in adults," *Gut*, vol. 52, no. Suppl 3, pp. iii1–iii8, May 2003.
- [59] R. Wong and C. Frenette, "Updates in the Management of Hepatocellular Carcinoma," *Gastroenterol Hepatol (N Y)*, vol. 7, no. 1, pp. 16–24, Jan. 2011.
- [60] A. J. Sheen, G. J. Poston, and D. J. Sherlock, "Cryotherapeutic ablation of liver tumours," *British Journal of Surgery*, vol. 89, no. 11, pp. 1396–1401, 2002.

- [61] Y. S. Chang, J. Adnane, P. A. Trail, J. Levy, A. Henderson, D. Xue, E. Bortolon, M. Ichetovkin, C. Chen, A. McNabola, D. Wilkie, C. A. Carter, I. C. A. Taylor, M. Lynch, and S. Wilhelm, "Sorafenib (BAY 43-9006) inhibits tumor growth and vascularization and induces tumor apoptosis and hypoxia in RCC xenograft models," *Cancer Chemother. Pharmacol.*, vol. 59, no. 5, pp. 561–574, Apr. 2007.
- [62] S. M. Wilhelm, C. Carter, L. Tang, D. Wilkie, A. McNabola, H. Rong, C. Chen, X. Zhang, P. Vincent, M. McHugh, Y. Cao, J. Shujath, S. Gawlak, D. Eveleigh, B. Rowley, L. Liu, L. Adnane, M. Lynch, D. Auclair, I. Taylor, R. Gedrich, A. Voznesensky, B. Riedl, L. E. Post, G. Bollag, and P. A. Trail, "BAY 43-9006 Exhibits Broad Spectrum Oral Antitumor Activity and Targets the RAF/MEK/ERK Pathway and Receptor Tyrosine Kinases Involved in Tumor Progression and Angiogenesis," *Cancer Res.*, vol. 64, no. 19, pp. 7099–7109, Oct. 2004.
- [63] H. Huynh, K. H. P. Chow, K. C. Soo, H. C. Toh, S. P. Choo, K. F. Foo, D. Poon, V. C. Ngo, and E. Tran, "RAD001 (everolimus) inhibits tumour growth in xenograft models of human hepatocellular carcinoma," *J. Cell. Mol. Med.*, vol. 13, no. 7, pp. 1371–1380, Jul. 2009.
- [64] A. Villanueva, D. Y. Chiang, P. Newell, J. Peix, S. Thung, C. Alsinet, V. Tovar, S. Roayaie, B. Minguez, M. Sole, C. Battiston, S. van Laarhoven, M. I. Fiel, A. Di Feo, Y. Hoshida, S. Yea, S. Toffanin, A. Ramos, J. A. Martignetti, V. Mazzaferro, J. Bruix, S. Waxman, M. Schwartz, M. Meyerson, S. L. Friedman, and J. M. Llovet, "Pivotal Role of mTOR Signaling in Hepatocellular Carcinoma," *Gastroenterology*, vol. 135, no. 6, pp. 1972–198411, Dec. 2008.
- [65] J.-F. Zhang, J.-J. Liu, M.-Q. Lu, C.-J. Cai, Y. Yang, H. Li, C. Xu, and G.-H. Chen, "Rapamycin inhibits cell growth by induction of apoptosis on hepatocellular carcinoma cells in vitro," *Transpl. Immunol.*, vol. 17, no. 3, pp. 162–168, Apr. 2007.
- [66] H. Huynh, V. C. Ngo, H. N. Koong, D. Poon, S. P. Choo, C. H. Thng, P. Chow, H. S. Ong, A. Chung, and K. C. Soo, "Sorafenib and rapamycin induce growth suppression in mouse models of hepatocellular carcinoma," *J. Cell. Mol. Med.*, vol. 13, no. 8B, pp. 2673–2683, Aug. 2009.
- [67] C. J. McClain, D. B. Hill, Z. Song, R. Chawla, W. H. Watson, T. Chen, and S. Barve, "S-Adenosylmethionine, cytokines, and alcoholic liver disease," *Alcohol*, vol. 27, no. 3, pp. 185–192, Jul. 2002.
- [68] C. S. Lieber, A. Casini, L. M. DeCarli, C. I. Kim, N. Lowe, R. Sasaki, and M. A. Leo, "S-adenosyl-L-methionine attenuates alcohol-induced liver injury in the baboon," *Hepatology*, vol. 11, no. 2, pp. 165–172, Feb. 1990.
- [69] J. M. Mato, J. Cámaras, J. F. de Paz, L. Caballería, S. Coll, A. Caballero, L. García-Buey, J. Beltrán, V. Benita, J. Caballería, R. Solà, R. Moreno-Otero, F. Barrao, A. Martín-Duce, J. A. Correa, A. Parés, E. Barrao, I. García-Magaz, J. L. Puerta, J. Moreno, G. Boissard, P. Ortiz, and J. Rodés, "S-Adenosylmethionine in alcoholic liver cirrhosis: a randomized, placebo-controlled, double-blind, multicenter clinical trial," *Journal of Hepatology*, vol. 30, no. 6, pp. 1081–1089, Jun. 1999.
- [70] J. M. Mato, F. J. Corrales, S. C. Lu, and M. A. Avila, "S-Adenosylmethionine: a control switch that regulates liver function," *FASEB J.*, vol. 16, no. 1, pp. 15–26, Jan. 2002.
- [71] S. H. Mudd, R. Cerone, M. C. Schiaffino, A. R. Fantasia, G. Minniti, U. Caruso, R. Lorini, D. Watkins, N. Matiaszuk, D. S. Rosenblatt, B. Schwahn, R. Rozen, L. LeGros, M. Kotb, A. Capdevila, Z. Luka, J. D. Finkelstein, A. Tangerman, S. P. Stabler, R. H. Allen, and C. Wagner, "Glycine N-methyltransferase deficiency: a novel inborn error causing persistent isolated hypermethioninaemia," *J. Inherit. Metab. Dis.*, vol. 24, no. 4, pp. 448–464, Aug. 2001.
- [72] Z. Luka, R. Cerone, J. A. Phillips 3rd, H. S. Mudd, and C. Wagner, "Mutations in human glycine N-methyltransferase give insights into its role in methionine metabolism," *Hum. Genet.*, vol. 110, no. 1, pp. 68–74, Jan. 2002.
- [73] P. Augoustides-Savvopoulou, Z. Luka, S. Karyda, S. P. Stabler, R. H. Allen, K. Patsiaoura, C. Wagner, and S. H. Mudd, "Glycine N-methyltransferase deficiency: A new patient with a novel mutation," *Journal of Inherited Metabolic Disease*, vol. 26, no. 8, pp. 745–759, 2003.
- [74] T.-L. Tseng, Y.-P. Shih, Y.-C. Huang, C.-K. Wang, P.-H. Chen, J.-G. Chang, K.-T. Yeh, Y.-M. A. Chen, and K. H. Buetow, "Genotypic and Phenotypic Characterization of a Putative Tumor Susceptibility Gene, GNMT, in Liver Cancer," *Cancer Res.*, vol. 63, no. 3, pp. 647–654, Feb. 2003.

- [75] G. L. Cantoni, "Activation of Methionine for Transmethylation," *J. Biol. Chem.*, vol. 189, no. 2, pp. 745–754, Apr. 1951.
- [76] G. L. Cantoni, "Methylation of Nicotinamide with a Soluble Enzyme System from Rat Liver," *J. Biol. Chem.*, vol. 189, no. 1, pp. 203–216, Mar. 1951.
- [77] G. L. Cantoni, "S-ADENOSYLMETHIONINE; A NEW INTERMEDIATE FORMED ENZYMATICALLY FROM I-METHIONINE AND ADENOSINETRIPHOSPHATE," *J. Biol. Chem.*, vol. 204, no. 1, pp. 403–416, Sep. 1953.
- [78] S. H. Mudd and J. R. Poole, "Labile methyl balances for normal humans on various dietary regimens," *Metab. Clin. Exp.*, vol. 24, no. 6, pp. 721–735, Jun. 1975.
- [79] J. D. Finkelstein, "Methionine metabolism in mammals," *J. Nutr. Biochem.*, vol. 1, no. 5, pp. 228–237, May 1990.
- [80] S. C. Lu, "S-Adenosylmethionine," *Int. J. Biochem. Cell Biol.*, vol. 32, no. 4, pp. 391–395, Apr. 2000.
- [81] J. M. Mato, L. Alvarez, P. Ortiz, and M. A. Pajares, "S-adenosylmethionine synthesis: molecular mechanisms and clinical implications," *Pharmacol. Ther.*, vol. 73, no. 3, pp. 265–280, 1997.
- [82] C. S. Lieber and L. Packer, "S-Adenosylmethionine: molecular, biological, and clinical aspects—an introduction," *Am J Clin Nutr*, vol. 76, no. 5, p. 1148S–1150S, Nov. 2002.
- [83] M. Kotb, S. H. Mudd, J. M. Mato, A. M. Geller, N. M. Kredich, J. Y. Chou, and G. L. Cantoni, "Consensus nomenclature for the mammalian methionine adenosyltransferase genes and gene products," *Trends in Genetics*, vol. 13, no. 2, pp. 51–52, Feb. 1997.
- [84] F. Schlenk, "Methylthioadenosine," *Adv. Enzymol. Relat. Areas Mol. Biol.*, vol. 54, pp. 195–265, 1983.
- [85] M. A. Avila, E. R. García-Trevijano, S. C. Lu, F. J. Corrales, and J. M. Mato, "Methylthioadenosine," *The International Journal of Biochemistry & Cell Biology*, vol. 36, no. 11, pp. 2125–2130, Nov. 2004.
- [86] H. Ogawa, T. Gomi, F. Takusagawa, and M. Fujioka, "Structure, function and physiological role of glycine N-methyltransferase," *The International Journal of Biochemistry & Cell Biology*, vol. 30, no. 1, pp. 13–26, Mar. 1998.
- [87] H. H. Richards, P. K. Chiang, and G. L. Cantoni, "Adenosylhomocysteine hydrolase. Crystallization of the purified enzyme and its properties," *J. Biol. Chem.*, vol. 253, no. 12, pp. 4476–4480, Jun. 1978.
- [88] J. D. Finkelstein, "Metabolic regulatory properties of S-adenosylmethionine and S-adenosylhomocysteine," *Clinical Chemical Laboratory Medicine*, vol. 45, no. 12, pp. 1694–1699, Jan. 2007.
- [89] S. C. Lu and J. M. Mato, "S-Adenosylmethionine in cell growth, apoptosis and liver cancer," *J Gastroenterol Hepatol*, vol. 23, no. Suppl 1, pp. S73–S77, Mar. 2008.
- [90] S. C. Lu, "Regulation of hepatic glutathione synthesis: current concepts and controversies," *FASEB J*, vol. 13, no. 10, pp. 1169–1183, Jul. 1999.
- [91] A. Prudova, Z. Bauman, A. Braun, V. Vitvitsky, S. C. Lu, and R. Banerjee, "S-adenosylmethionine stabilizes cystathione β -synthase and modulates redox capacity," *Proc Natl Acad Sci U S A*, vol. 103, no. 17, pp. 6489–6494, Apr. 2006.
- [92] B. Gil, M. Casado, M. A. Pajares, L. Bosca, J. M. Mato, P. Martin-Sanz, and L. Alvarez, "Differential expression pattern of S-adenosylmethionine synthetase isoenzymes during rat liver development," *Hepatology*, vol. 24, no. 4, pp. 876–881, 1996.
- [93] H. L. LeGros, A.-B. Halim, A. M. Geller, and M. Kotb, "Cloning, Expression, and Functional Characterization of the β Regulatory Subunit of Human Methionine Adenosyltransferase (MAT II)," *J. Biol. Chem.*, vol. 275, no. 4, pp. 2359–2366, Jan. 2000.
- [94] H. YANG, A. I. ARA, N. MAGILNICK, M. XIA, K. RAMANI, H. CHEN, T. D. LEE, J. M. MATO, and S. C. LU, "Expression Pattern, Regulation, and Functions of Methionine Adenosyltransferase 2 β Splicing Variants in Hepatoma Cells," *Gastroenterology*, vol. 134, no. 1, pp. 281–291, Jan. 2008.
- [95] J. Cai, W. Sun, J. Hwang, S. C. Stain, and S. C. Lu, "Changes in S-adenosylmethionine synthetase in human liver cancer: Molecular characterization and significance," *Hepatology*, vol. 24, no. 5, pp. 1090–1097, 1996.

- [96] T. D. Lee, M. R. Sadda, M. H. Mendler, T. Bottiglieri, G. Kanel, J. M. Mato, and S. C. Lu, "Abnormal Hepatic Methionine and Glutathione Metabolism in Patients With Alcoholic Hepatitis," *Alcoholism: Clinical and Experimental Research*, vol. 28, no. 1, pp. 173–181, 2004.
- [97] S. C. Lu, Z.-Z. Huang, H. Yang, J. M. Mato, M. A. Avila, and H. Tsukamoto, "Changes in methionine adenosyltransferase and S-adenosylmethionine homeostasis in alcoholic rat liver," *Am J Physiol Gastrointest Liver Physiol*, vol. 279, no. 1, pp. G178–G185, Jul. 2000.
- [98] Z.-Z. Huang, Z. Mao, J. Cai, and S. C. Lu, "Changes in methionine adenosyltransferase during liver regeneration in the rat," *Am J Physiol Gastrointest Liver Physiol*, vol. 275, no. 1, pp. G14–G21, Jul. 1998.
- [99] J. Cai, Z. Mao, J.-J. Hwang, and S. C. Lu, "Differential Expression of Methionine Adenosyltransferase Genes Influences the Rate of Growth of Human Hepatocellular Carcinoma Cells," *Cancer Res*, vol. 58, no. 7, pp. 1444–1450, Apr. 1998.
- [100] M. L. Martínez-Chantar, E. R. García-Trevijano, M. U. Latasa, A. Martín-Duce, P. Fortes, J. Caballería, M. A. Avila, and J. M. Mato, "Methionine adenosyltransferase II beta subunit gene expression provides a proliferative advantage in human hepatoma," *Gastroenterology*, vol. 124, no. 4, pp. 940–948, Apr. 2003.
- [101] E. R. García-Trevijano, M. U. Latasa, M. V. Carretero, C. Berasain, J. M. Mato, and M. A. Avila, "S-Adenosylmethionine regulates MAT1A and MAT2A gene expression in cultured rat hepatocytes: a new role for S-adenosylmethionine in the maintenance of the differentiated status of the liver," *FASEB J*, vol. 14, no. 15, pp. 2511–2518, Dec. 2000.
- [102] J. M. Caron, "Induction of albumin gene transcription in hepatocytes by extracellular matrix proteins," *Mol Cell Biol*, vol. 10, no. 3, pp. 1239–1243, Mar. 1990.
- [103] E. G. Schuetz, D. Li, C. J. Omiecinski, U. Muller-Eberhard, H. K. Kleinman, B. Elswick, and P. S. Guzelian, "Regulation of gene expression in adult rat hepatocytes cultured on a basement membrane matrix," *Journal of Cellular Physiology*, vol. 134, no. 3, pp. 309–323, 1988.
- [104] L. Torres, M. A. Ávila, M. V. Carretero, M. U. Latasa, J. Caballería, G. López-Rodas, A. Boukaba, S. C. Lu, L. Franco, and J. M. Mato, "Liver-specific methionine adenosyltransferase MAT1A gene expression is associated with a specific pattern of promoter methylation and histone acetylation: implications for MAT1A silencing during transformation," *FASEB J*, vol. 14, no. 1, pp. 95–102, Jan. 2000.
- [105] L. Torres, G. López-Rodas, M. U. Latasa, M. V. Carretero, A. Boukaba, J. L. Rodríguez, L. Franco, J. M. Mato, and M. A. Avila, "DNA methylation and histone acetylation of rat methionine adenosyltransferase 1A and 2A genes is tissue-specific," *The International Journal of Biochemistry & Cell Biology*, vol. 32, no. 4, pp. 397–404, Apr. 2000.
- [106] H. Yang, Z.-Z. Huang, Z. Zeng, C. Chen, R. R. Selby, and S. C. Lu, "Role of promoter methylation in increased methionine adenosyltransferase 2A expression in human liver cancer," *Am J Physiol Gastrointest Liver Physiol*, vol. 280, no. 2, pp. G184–G190, Feb. 2001.
- [107] M. U. Latasa, A. Boukaba, E. R. García-Trevijano, L. Torres, J. L. Rodríguez, J. Caballería, S. C. Lu, G. López-Rodas, L. Franco, J. M. Mato, and M. A. Avila, "Hepatocyte growth factor induces MAT2A expression and histone acetylation in rat hepatocytes: role in liver regeneration," *FASEB J*, Mar. 2001.
- [108] S. C. Lu and J. M. Mato, "Role of methionine adenosyltransferase and S-adenosylmethionine in alcohol-associated liver cancer," *Alcohol*, vol. 35, no. 3, pp. 227–234, Apr. 2005.
- [109] D. M. Sullivan and J. L. Hoffman, "Fractionation and kinetic properties of rat liver and kidney methionine adenosyltransferase isozymes," *Biochemistry*, vol. 22, no. 7, pp. 1636–1641, Mar. 1983.
- [110] A.-B. Halim, L. LeGros, A. Geller, and M. Kotb, "Expression and Functional Interaction of the Catalytic and Regulatory Subunits of Human Methionine Adenosyltransferase in Mammalian Cells," *J. Biol. Chem.*, vol. 274, no. 42, pp. 29720–29725, Oct. 1999.
- [111] H. L. LeGros, A. M. Geller, and M. Kotb, "Differential Regulation of Methionine Adenosyltransferase in Superantigen and Mitogen Stimulated Human T Lymphocytes," *J. Biol. Chem.*, vol. 272, no. 25, pp. 16040–16047, Jun. 1997.

- [112] M. A. Avila, J. Mingorance, M. L. Martínez-Chantar, M. Casado, P. Martín-Sanz, L. Boscá, and J. M. Mato, "Regulation of rat liver S-adenosylmethionine synthetase during septic shock: Role of nitric oxide," *Hepatology*, vol. 25, no. 2, pp. 391–396, 1997.
- [113] F. Ruiz, F. J. Corrales, C. Miqueo, and J. M. Mato, "Nitric oxide inactivates rat hepatic methionine adenosyltransferase in vivo by S-nitrosylation," *Hepatology*, vol. 28, no. 4, pp. 1051–1057, 1998.
- [114] I. Pérez-Mato, C. Castro, F. A. Ruiz, F. J. Corrales, and J. M. Mato, "Methionine Adenosyltransferase S-Nitrosylation Is Regulated by the Basic and Acidic Amino Acids Surrounding the Target Thiol," *J. Biol. Chem.*, vol. 274, no. 24, pp. 17075–17079, Jun. 1999.
- [115] E. J. Yeo and C. Wagner, "Tissue distribution of glycine N-methyltransferase, a major folate-binding protein of liver," *Proc Natl Acad Sci U S A*, vol. 91, no. 1, pp. 210–214, Jan. 1994.
- [116] Z. Luka, S. H. Mudd, and C. Wagner, "Glycine N-Methyltransferase and Regulation of S-Adenosylmethionine Levels," *J Biol Chem*, vol. 284, no. 34, pp. 22507–22511, Aug. 2009.
- [117] Y.-C. Huang, C.-M. Lee, M. Chen, M.-Y. Chung, Y.-H. Chang, W. J.-S. Huang, D. M.-T. Ho, C.-C. Pan, T. T. Wu, S. Yang, M.-W. Lin, J.-T. Hsieh, and Y.-M. A. Chen, "Haplotypes, Loss of Heterozygosity, and Expression Levels of Glycine N-Methyltransferase in Prostate Cancer," *Clin Cancer Res*, vol. 13, no. 5, pp. 1412–1420, Mar. 2007.
- [118] J. E. Heady and S. J. Kerr, "Alteration of Glycine N-Methyltransferase Activity in Fetal, Adult, and Tumor Tissues," *Cancer Res*, vol. 35, no. 3, pp. 640–643, Mar. 1975.
- [119] N. Suzuki and C. Wagner, "Purification and characterization of a folate binding protein from rat liver cytosol," *Arch. Biochem. Biophys.*, vol. 199, no. 1, pp. 236–248, Jan. 1980.
- [120] S. J. Kerr, "Competing Methyltransferase Systems," *J. Biol. Chem.*, vol. 247, no. 13, pp. 4248–4252, Jul. 1972.
- [121] G. L. Cantoni, "S-adenosyl amino acids thirty years later: 1951–1981. Usdin, E. Borchardt, R. T. Creveling, C. R. eds.," in *The Biochemistry of S-Adenosylmethionine and Related Compounds*, Macmillan Press London, U.K., 1982, pp. 3–10.
- [122] G. L. Cantoni and P. K. Chiang, "The role of S-adenosylhomocysteine hydrolase in the control of biological methylations. Cavallini, D. Gaull, G. E. Zappia, V. eds.," in *Natural Sulfur Compounds*, Plenum Press New York, NY., 1980, pp. 67–80.
- [123] M. J. Rowling, M. H. McMullen, D. C. Chipman, and K. L. Schalinske, "Hepatic Glycine N-Methyltransferase Is Up-Regulated by Excess Dietary Methionine in Rats," *J. Nutr.*, vol. 132, no. 9, pp. 2545–2550, Sep. 2002.
- [124] N. Fausto, "Liver regeneration," *J. Hepatol.*, vol. 32, no. 1 Suppl, pp. 19–31, 2000.
- [125] G. K. Michalopoulos and M. C. DeFrances, "Liver regeneration," *Science*, vol. 276, no. 5309, pp. 60–66, Apr. 1997.
- [126] C.-G. Huh, V. M. Factor, A. Sánchez, K. Uchida, E. A. Conner, and S. S. Thorgeirsson, "Hepatocyte growth factor/c-met signaling pathway is required for efficient liver regeneration and repair," *Proc Natl Acad Sci U S A*, vol. 101, no. 13, pp. 4477–4482, Mar. 2004.
- [127] C. Ponzetto, A. Bardelli, Z. Zhen, F. Maina, P. dalla Zonca, S. Giordano, A. Graziani, G. Panayotou, and P. M. Comoglio, "A multifunctional docking site mediates signaling and transformation by the hepatocyte growth factor/scatter factor receptor family," *Cell*, vol. 77, no. 2, pp. 261–271, Apr. 1994.
- [128] R. Paumelle, D. Tulasne, Z. Kherrouche, S. Plaza, C. Leroy, S. Reveneau, B. Vandenbunder, V. Fafeur, D. Tulasne, and S. Reveneau, "Hepatocyte growth factor/scatter factor activates the ETS1 transcription factor by a RAS-RAF-MEK-ERK signaling pathway," *Oncogene*, vol. 21, no. 15, pp. 2309–2319, Apr. 2002.
- [129] E. R. García-Trevijano, M. L. Martínez-Chantar, M. U. Latasa, J. M. Mato, and M. A. Avila, "NO sensitizes rat hepatocytes to proliferation by modifying S-adenosylmethionine levels," *Gastroenterology*, vol. 122, no. 5, pp. 1355–1363, May 2002.
- [130] H. Talarmin, C. Rescan, S. Cariou, D. Glaise, G. Zanninelli, M. Bilodeau, P. Loyer, C. Guguen-Guillouzo, and G. Baffet, "The Mitogen-Activated Protein Kinase Kinase/Extracellular Signal-Regulated Kinase Cascade Activation Is a Key Signalling Pathway Involved in the Regulation of G1 Phase Progression in Proliferating Hepatocytes," *Mol Cell Biol*, vol. 19, no. 9, pp. 6003–6011, Sep. 1999.

- [131] P. Loyer, S. Cariou, D. Glaise, M. Bilodeau, G. Baffet, and C. Guguen-Guilhouzo, "Growth Factor Dependence of Progression through G and S Phases of Adult Rat Hepatocytes in Vitro EVIDENCE OF A MITOGEN RESTRICTION POINT IN MID-LATE G," *J. Biol. Chem.*, vol. 271, no. 19, pp. 11484–11492, May 1996.
- [132] M. Vázquez-Chantada, U. Ariz, M. Varela-Rey, N. Embade, N. Martínez-Lopez, D. Fernández-Ramos, L. Gómez-Santos, S. Lamas, S. C. Lu, M. L. Martínez-Chantar, and J. M. Mato, "Evidence for LKB1/AMP-activated protein kinase/ endothelial nitric oxide synthase cascade regulated by hepatocyte growth factor, S-adenosylmethionine, and nitric oxide in hepatocyte proliferation," *Hepatology*, vol. 49, no. 2, pp. 608–617, Feb. 2009.
- [133] G. R. Steinberg and B. E. Kemp, "AMPK in Health and Disease," *Physiol Rev*, vol. 89, no. 3, pp. 1025–1078, Jul. 2009.
- [134] B. E. Kemp, D. Stapleton, D. J. Campbell, Z.-P. Chen, S. Murthy, M. Walter, A. Gupta, J. J. Adams, F. Katsis, B. van Denderen, I. G. Jennings, T. Iseli, B. J. Michell, and L. A. Witters, "AMP-activated protein kinase, super metabolic regulator," *Biochem. Soc. Trans.*, vol. 31, no. Pt 1, pp. 162–168, Feb. 2003.
- [135] D. G. Hardie, I. P. Salt, S. A. Hawley, and S. P. Davies, "AMP-activated protein kinase: an ultrasensitive system for monitoring cellular energy charge.," *Biochem J*, vol. 338, no. Pt 3, pp. 717–722, Mar. 1999.
- [136] M. J. Sanders, P. O. Grondin, B. D. Hegarty, M. A. Snowden, and D. Carling, "Investigating the mechanism for AMP activation of the AMP-activated protein kinase cascade," *Biochem J*, vol. 403, no. Pt 1, pp. 139–148, Apr. 2007.
- [137] S. A. Hawley, M. Davison, A. Woods, S. P. Davies, R. K. Beri, D. Carling, and D. G. Hardie, "Characterization of the AMP-activated Protein Kinase Kinase from Rat Liver and Identification of Threonine 172 as the Major Site at Which It Phosphorylates AMP-activated Protein Kinase," *J. Biol. Chem.*, vol. 271, no. 44, pp. 27879–27887, Nov. 1996.
- [138] R. J. Shaw, K. A. Lamia, D. Vasquez, S.-H. Koo, N. Bardeesy, R. A. DePinho, M. Montminy, and L. C. Cantley, "The Kinase LKB1 Mediates Glucose Homeostasis in Liver and Therapeutic Effects of Metformin," *Science*, vol. 310, no. 5754, pp. 1642–1646, Dec. 2005.
- [139] K. Imai, K. Inukai, Y. Ikegami, T. Awata, and S. Katayama, "LKB1, an upstream AMPK kinase, regulates glucose and lipid metabolism in cultured liver and muscle cells," *Biochem. Biophys. Res. Commun.*, vol. 351, no. 3, pp. 595–601, Dec. 2006.
- [140] S. A. Hawley, D. A. Pan, K. J. Mustard, L. Ross, J. Bain, A. M. Edelman, B. G. Frenguelli, and D. G. Hardie, "Calmodulin-dependent protein kinase kinase-β is an alternative upstream kinase for AMP-activated protein kinase," *Cell Metabolism*, vol. 2, no. 1, pp. 9–19, Jul. 2005.
- [141] R. L. Hurley, K. A. Anderson, J. M. Franzone, B. E. Kemp, A. R. Means, and L. A. Witters, "The Ca²⁺/Calmodulin-dependent Protein Kinase Kinases Are AMP-activated Protein Kinase Kinases," *J. Biol. Chem.*, vol. 280, no. 32, pp. 29060–29066, Aug. 2005.
- [142] M. Momcilovic, S.-P. Hong, and M. Carlson, "Mammalian TAK1 Activates Snf1 Protein Kinase in Yeast and Phosphorylates AMP-activated Protein Kinase in Vitro," *J. Biol. Chem.*, vol. 281, no. 35, pp. 25336–25343, Sep. 2006.
- [143] M. Xie, D. Zhang, J. R. B. Dyck, Y. Li, H. Zhang, M. Morishima, D. L. Mann, G. E. Taffet, A. Baldini, D. S. Khoury, and M. D. Schneider, "A pivotal role for endogenous TGF-β-activated kinase-1 in the LKB1/AMP-activated protein kinase energy-sensor pathway," *Proc Natl Acad Sci U S A*, vol. 103, no. 46, pp. 17378–17383, Nov. 2006.
- [144] X. Fu, S. Wan, Y. L. Lyu, L. F. Liu, and H. Qi, "Etoposide Induces ATM-Dependent Mitochondrial Biogenesis through AMPK Activation," *PLoS ONE*, vol. 3, no. 4, Apr. 2008.
- [145] S. Singh and T. W. Evans, "Nitric oxide, the biological mediator of the decade: fact or fiction?," *Eur Respir J*, vol. 10, no. 3, pp. 699–707, Mar. 1997.
- [146] L. McNaughton, L. Puttagunta, M. A. Martinez-Cuesta, N. Kneteman, I. Mayers, R. Moqbel, Q. Hamid, and M. W. Radomski, "Distribution of nitric oxide synthase in normal and cirrhotic human liver," *Proc Natl Acad Sci U S A*, vol. 99, no. 26, pp. 17161–17166, Dec. 2002.
- [147] J. E. Saavedra, T. R. Billiar, D. L. Williams, Y. M. Kim, S. C. Watkins, and L. K. Keefer, "Targeting nitric oxide (NO) delivery in vivo. Design of a liver-selective NO donor prodrug that blocks tumor necrosis factor-alpha-induced apoptosis and toxicity in the liver," *J. Med. Chem.*, vol. 40, no. 13, pp. 1947–1954, Jun. 1997.

- [148] J. A. Reihill, M.-A. Ewart, D. G. Hardie, and I. P. Salt, "AMP-activated protein kinase mediates VEGF-stimulated endothelial NO production," *Biochem Biophys Res Commun*, vol. 354, no. 4, pp. 1084–1088, Mar. 2007.
- [149] Z.-P. Chen, K. I. Mitchelhill, B. J. Michell, D. Stapleton, I. Rodriguez-Crespo, L. A. Witters, D. A. Power, P. R. Ortiz de Montellano, and B. E. Kemp, "AMP-activated protein kinase phosphorylation of endothelial NO synthase," *FEBS Letters*, vol. 443, no. 3, pp. 285–289, Jan. 1999.
- [150] V. A. Morrow, F. Foufelle, J. M. C. Connell, J. R. Petrie, G. W. Gould, and I. P. Salt, "Direct Activation of AMP-activated Protein Kinase Stimulates Nitric-oxide Synthesis in Human Aortic Endothelial Cells," *J. Biol. Chem.*, vol. 278, no. 34, pp. 31629–31639, Aug. 2003.
- [151] F. Gobeil, T. Zhu, S. Brault, A. Geha, A. Vazquez-Tello, A. Fortier, D. Barbaz, D. Checchin, X. Hou, M. Nader, G. Bkaily, J.-P. Gratton, N. Heveker, A. Ribeiro-da-Silva, K. Peri, H. Bard, A. Chorvatova, P. D'Orléans-Juste, E. J. Goetzl, and S. Chemtob, "Nitric Oxide Signaling via Nuclearized Endothelial Nitric-oxide Synthase Modulates Expression of the Immediate Early Genes iNOS and mPGES-1," *J. Biol. Chem.*, vol. 281, no. 23, pp. 16058–16067, Jun. 2006.
- [152] M. L. Martínez-Chantar, M. Vázquez-Chantada, M. Garnacho, M. U. Latasa, M. Varela-Rey, J. Dotor, M. Santamaría, L. A. Martínez-Cruz, L. A. Parada, S. C. Lu, and J. M. Mato, "S-adenosylmethionine regulates cytoplasmic HuR via AMP-activated kinase," *Gastroenterology*, vol. 131, no. 1, pp. 223–232, Jul. 2006.
- [153] A. Z. Khan and S. S. Mudan, "LIVER REGENERATION: MECHANISMS, MYSTERIES AND MORE," *ANZ Journal of Surgery*, vol. 77, no. 1–2, pp. 9–14, 2007.
- [154] N. Fausto, J. S. Campbell, and K. J. Riehle, "Liver regeneration," *Hepatology*, vol. 43, no. S1, pp. S45–S53, 2006.
- [155] A. Zimmermann, "Regulation of liver regeneration," *Nephrology Dialysis Transplantation*, vol. 19, no. suppl_4, pp. iv6–iv10, Jul. 2004.
- [156] R. Taub, "Liver regeneration: from myth to mechanism," *Nat. Rev. Mol. Cell Biol.*, vol. 5, no. 10, pp. 836–847, Oct. 2004.
- [157] A. K. Greene and M. Puder, "Partial hepatectomy in the mouse: technique and perioperative management," *J Invest Surg*, vol. 16, no. 2, pp. 99–102, Apr. 2003.
- [158] Y. Yamada, I. Kirillova, J. J. Peschon, and N. Fausto, "Initiation of liver growth by tumor necrosis factor: Deficient liver regeneration in mice lacking type I tumor necrosis factor receptor," *Proc Natl Acad Sci U S A*, vol. 94, no. 4, pp. 1441–1446, Feb. 1997.
- [159] C. W. Strey, M. Markiewski, D. Mastellos, R. Tudoran, L. A. Spruce, L. E. Greenbaum, and J. D. Lambris, "The Proinflammatory Mediators C3a and C5a Are Essential for Liver Regeneration," *J Exp Med*, vol. 198, no. 6, pp. 913–923, Sep. 2003.
- [160] L. Yang, S. T. Magness, R. Bataller, R. A. Rippe, and D. A. Brenner, "NF-κB activation in Kupffer cells after partial hepatectomy," *Am J Physiol Gastrointest Liver Physiol*, vol. 289, no. 3, pp. G530–G538, Sep. 2005.
- [161] S. H. Gregory, E. J. Wing, K. L. Danowski, N. van Rooijen, K. F. Dyer, and D. J. Tweardy, "IL-6 Produced by Kupffer Cells Induces STAT Protein Activation in Hepatocytes Early During the Course of Systemic Listerial Infections," *J Immunol*, vol. 160, no. 12, pp. 6056–6061, Jun. 1998.
- [162] S. Hortelano, B. Dewez, A. M. Genaro, M. J. M. Díaz-Guerra, and L. Boscá, "Nitric oxide is released in regenerating liver after partial hepatectomy," *Hepatology*, vol. 21, no. 3, pp. 776–786, 1995.
- [163] M. Zeini, S. Hortelano, P. G. Través, A. G. Gómez-Valadés, A. Pujol, J. C. Perales, R. Bartrons, and L. Boscá, "Assessment of a dual regulatory role for NO in liver regeneration after partial hepatectomy: protection against apoptosis and retardation of hepatocyte proliferation," *FASEB J*, Mar. 2005.
- [164] Y.-M. Kim, R. V. Talanian, and T. R. Billiar, "Nitric Oxide Inhibits Apoptosis by Preventing Increases in Caspase-3-like Activity via Two Distinct Mechanisms," *J. Biol. Chem.*, vol. 272, no. 49, pp. 31138–31148, Dec. 1997.
- [165] L. Kohoutek, Z. Cervinková, O. Kucera, T. Rousar, T. Garnol, J. Siller, and H. Lotková, "Effect of S-adenosylmethionine on liver regeneration induced by partial hepatectomy," *Gen. Physiol. Biophys.*, vol. 29, no. 1, pp. 72–78, Mar. 2010.

- [166] E. Ansorena, E. R. García-Trevijano, M. L. Martínez-Chantar, Z.-Z. Huang, L. Chen, J. M. Mato, M. Iraburu, S. C. Lu, and M. A. Avila, "S-adenosylmethionine and methylthioadenosine are antiapoptotic in cultured rat hepatocytes but proapoptotic in human hepatoma cells," *Hepatology*, vol. 35, no. 2, pp. 274–280, 2002.
- [167] H. Yang, M. R. Sadda, M. Li, Y. Zeng, L. Chen, W. Bae, X. Ou, M. T. Runnegar, J. M. Mato, and S. C. Lu, "S-adenosylmethionine and its metabolite induce apoptosis in HepG2 cells: Role of protein phosphatase 1 and Bcl-xS," *Hepatology*, vol. 40, no. 1, pp. 221–231, 2004.
- [168] L. H. Boise, M. González-García, C. E. Postema, L. Ding, T. Lindsten, L. A. Turka, X. Mao, G. Nuñez, and C. B. Thompson, "bcl-x, a bcl-2-related gene that functions as a dominant regulator of apoptotic cell death," *Cell*, vol. 74, no. 4, pp. 597–608, Aug. 1993.
- [169] X. Ou, H. Yang, K. Ramani, A. I. Ara, H. Chen, J. M. Mato, and S. C. Lu, "Inhibition of human betaine–homocysteine methyltransferase expression by S-adenosylmethionine and methylthioadenosine," *Biochem J*, vol. 401, no. Pt 1, pp. 87–96, Jan. 2007.
- [170] J. M. Mato and S. C. Lu, "Homocysteine, the bad thiol," *Hepatology*, vol. 41, no. 5, pp. 976–979, May 2005.
- [171] C. García-Ruiz, A. Morales, A. Colell, A. Ballesta, J. Rodés, N. Kaplowitz, and J. C. Fernández-Checa, "Feeding S-adenosyl-L-methionine attenuates both ethanol-induced depletion of mitochondrial glutathione and mitochondrial dysfunction in periportal and perivenous rat hepatocytes," *Hepatology*, vol. 21, no. 1, pp. 207–214, 1995.
- [172] R. M. Pascale, M. M. Simile, M. R. De Miglio, A. Nufris, L. Daino, M. A. Seddaiu, P. M. Rao, S. Rajalakshmi, D. S. Sarma, and F. Feo, "Chemoprevention by S-adenosyl-L-methionine of rat liver carcinogenesis initiated by 1,2-dimethylhydrazine and promoted by orotic acid," *Carcinogenesis*, vol. 16, no. 2, pp. 427–430, Feb. 1995.
- [173] J. Li, K. Ramani, Z. Sun, C. Zee, E. G. Grant, H. Yang, M. Xia, P. Oh, K. Ko, J. M. Mato, and S. C. Lu, "Forced Expression of Methionine Adenosyltransferase 1A in Human Hepatoma Cells Suppresses in Vivo Tumorigenicity in Mice," *Am J Pathol*, vol. 176, no. 5, pp. 2456–2466, May 2010.
- [174] M. L. Martínez-Chantar, F. J. Corrales, L. A. Martínez-Cruz, E. R. García-Trevijano, Z.-Z. Huang, L. Chen, G. Kanel, M. A. Avila, J. M. Mato, and S. C. Lu, "Spontaneous oxidative stress and liver tumors in mice lacking methionine adenosyltransferase 1A," *FASEB J*, Jun. 2002.
- [175] L. Chen, Y. Zeng, H. Yang, T. D. Lee, S. W. French, F. J. Corrales, E. R. García-Trevijano, M. A. Avila, J. M. Mato, and S. C. Lu, "Impaired liver regeneration in mice lacking methionine adenosyltransferase 1A," *FASEB J*, Mar. 2004.
- [176] Z. Luka, A. Capdevila, J. M. Mato, and C. Wagner, "A Glycine N-methyltransferase knockout mouse model for humans with deficiency of this enzyme," *Transgenic Res*, vol. 15, no. 3, pp. 393–397, Jun. 2006.
- [177] M. Varela-Rey, N. Martínez-López, D. Fernández-Ramos, N. Embade, D. F. Calvisi, A. Woodhoo, J. Rodríguez, M. F. Fraga, J. Julve, E. Rodríguez-Millán, I. Frades, L. Torres, Z. Luka, C. Wagner, M. Esteller, S. C. Lu, M. L. Martínez-Chantar, and J. M. Mato, "Fatty liver and fibrosis in glycine N-methyltransferase knockout mice is prevented by nicotinamide," *Hepatology*, vol. 52, no. 1, pp. 105–114, Jul. 2010.
- [178] J. Ross, "mRNA stability in mammalian cells," *Microbiol Rev*, vol. 59, no. 3, pp. 423–450, Sep. 1995.
- [179] A. M. Zubiaga, J. G. Belasco, and M. E. Greenberg, "The nonamer UUAUUUAUU is the key AU-rich sequence motif that mediates mRNA degradation," *Mol Cell Biol*, vol. 15, no. 4, pp. 2219–2230, Apr. 1995.
- [180] D. Beisang and P. R. Bohjanen, "Perspectives on the ARE as it turns 25 years old," *Wiley Interdisciplinary Reviews. RNA*, Jun. 2012.
- [181] E. Carballo, W. S. Lai, and P. J. Blackshear, "Feedback inhibition of macrophage tumor necrosis factor-alpha production by tristetraprolin," *Science*, vol. 281, no. 5379, pp. 1001–1005, Aug. 1998.
- [182] W. S. Lai, E. Carballo, J. R. Strum, E. A. Kennington, R. S. Phillips, and P. J. Blackshear, "Evidence that Tristetraprolin Binds to AU-Rich Elements and Promotes the Deadenylation and Destabilization of Tumor Necrosis Factor Alpha mRNA," *Mol Cell Biol*, vol. 19, no. 6, pp. 4311–4323, Jun. 1999.

- [183] C.-Y. Chen, R. Gherzi, S.-E. Ong, E. L. Chan, R. Raijmakers, G. J. M. Pruijn, G. Stoecklin, C. Moroni, M. Mann, and M. Karin, "AU Binding Proteins Recruit the Exosome to Degrade ARE-Containing mRNAs," *Cell*, vol. 107, no. 4, pp. 451–464, Nov. 2001.
- [184] G. Stoecklin, M. Colombi, I. Rainieri, S. Leuenberger, M. Mallaun, M. Schmidlin, B. Gross, M. Lu, T. Kitamura, and C. Moroni, "Functional cloning of BRF1, a regulator of ARE-dependent mRNA turnover," *EMBO J*, vol. 21, no. 17, pp. 4709–4718, Sep. 2002.
- [185] K. Abdelmohsen, Y. Kuwano, H. H. Kim, and M. Gorospe, "Posttranscriptional gene regulation by RNA-binding proteins during oxidative stress: implications for cellular senescence," *Biological Chemistry*, vol. 389, no. 3, pp. 243–255, Jan. 2008.
- [186] S. Srikantan, "HuR function in disease," *Frontiers in Bioscience*, vol. 17, no. 1, p. 189, 2012.
- [187] W. Zhang, B. J. Wagner, K. Ehrenman, A. W. Schaefer, C. T. DeMaria, D. Crater, K. DeHaven, L. Long, and G. Brewer, "Purification, characterization, and cDNA cloning of an AU-rich element RNA-binding protein, AUF1.," *Mol Cell Biol*, vol. 13, no. 12, pp. 7652–7665, Dec. 1993.
- [188] A. Gouble, S. Grazide, F. Meggetto, P. Mercier, G. Delsol, and D. Morello, "A New Player in Oncogenesis: AUF1/hnRNPD Overexpression Leads to Tumorigenesis in Transgenic Mice," *Cancer Res*, vol. 62, no. 5, pp. 1489–1495, Mar. 2002.
- [189] B. C. Blaxall, L. D. Dwyer-Nield, A. K. Bauer, T. J. Bohlmeier, A. M. Malkinson, and J. D. Port, "Differential expression and localization of the mRNA binding proteins, AU-rich element mRNA binding protein (AUF1) and Hu antigen R (HuR), in neoplastic lung tissue," *Mol. Carcinog.*, vol. 28, no. 2, pp. 76–83, Jun. 2000.
- [190] J. Deschênes-Furry, N. Perrone-Bizzozero, and B. J. Jasmin, "The RNA-binding protein HuD: a regulator of neuronal differentiation, maintenance and plasticity," *Bioessays*, vol. 28, no. 8, pp. 822–833, Aug. 2006.
- [191] A. Pascale, M. Amadio, and A. Quattrone, "Defining a neuron: neuronal ELAV proteins," *Cell. Mol. Life Sci.*, vol. 65, no. 1, pp. 128–140, Jan. 2008.
- [192] W.-J. Ma, S. Cheng, C. Campbell, A. Wright, and H. Furneaux, "Cloning and Characterization of HuR, a Ubiquitously Expressed Elav-like Protein," *J. Biol. Chem.*, vol. 271, no. 14, pp. 8144–8151, Apr. 1996.
- [193] C. M. Brennan and J. A. Steitz*, "HuR and mRNA stability," *Cellular and Molecular Life Sciences*, vol. 58, no. 2, pp. 266–277, Feb. 2001.
- [194] M. N. Hinman and H. Lou, "Diverse molecular functions of Hu proteins," *Cell Mol Life Sci*, vol. 65, no. 20, pp. 3168–3181, Oct. 2008.
- [195] P. J. Good, "A conserved family of elav-like genes in vertebrates.," *Proc Natl Acad Sci U S A*, vol. 92, no. 10, pp. 4557–4561, May 1995.
- [196] H. J. Okano and R. B. Darnell, "A Hierarchy of Hu RNA Binding Proteins in Developing and Adult Neurons," *J. Neurosci.*, vol. 17, no. 9, pp. 3024–3037, May 1997.
- [197] Y. Wakamatsu and J. a. Weston, "Sequential expression and role of Hu RNA-binding proteins during neurogenesis," *Development*, vol. 124, no. 17, pp. 3449–3460, Sep. 1997.
- [198] X. C. Fan and J. A. Steitz, "HNS, a nuclear-cytoplasmic shuttling sequence in HuR," *Proc Natl Acad Sci U S A*, vol. 95, no. 26, pp. 15293–15298, Dec. 1998.
- [199] N. Mukherjee, D. L. Corcoran, J. D. Nusbaum, D. W. Reid, S. Georgiev, M. Hafner, M. Ascano, T. Tuschl, U. Ohler, and J. D. Keene, "Integrative regulatory mapping indicates that the RNA-binding protein HuR (ELAVL1) couples pre-mRNA processing and mRNA stability," *Mol Cell*, vol. 43, no. 3, pp. 327–339, Aug. 2011.
- [200] S. Srikantan and M. Gorospe, "UneCLIPsing HuR Nuclear Function," *Molecular Cell*, vol. 43, no. 3, pp. 319–321, Aug. 2011.
- [201] K. Abdelmohsen and M. Gorospe, "Posttranscriptional regulation of cancer traits by HuR," *Wiley Interdiscip Rev RNA*, vol. 1, no. 2, pp. 214–229, Oct. 2010.
- [202] J. S. Butler, "The yin and yang of the exosome," *Trends Cell Biol.*, vol. 12, no. 2, pp. 90–96, Feb. 2002.
- [203] D. Mukherjee, M. Gao, J. P. O'Connor, R. Raijmakers, G. Pruijn, C. S. Lutz, and J. Wilusz, "The mammalian exosome mediates the efficient degradation of mRNAs that contain AU-rich elements," *EMBO J*, vol. 21, no. 1–2, pp. 165–174, Jan. 2002.

- [204] R. Gherzi, K.-Y. Lee, P. Briata, D. Wegmüller, C. Moroni, M. Karin, and C.-Y. Chen, "A KH Domain RNA Binding Protein, KSRP, Promotes ARE-Directed mRNA Turnover by Recruiting the Degradation Machinery," *Molecular Cell*, vol. 14, no. 5, pp. 571–583, Jun. 2004.
- [205] T. EYSTATHIOY, A. JAKYMIW, E. K. L. CHAN, B. SÉRAPHIN, N. COUGOT, and M. J. FRITZLER, "The GW182 protein colocalizes with mRNA degradation associated proteins hDcp1 and hLSm4 in cytoplasmic GW bodies," *RNA*, vol. 9, no. 10, pp. 1171–1173, Oct. 2003.
- [206] N. Kedersha, G. Stoecklin, M. Ayodele, P. Yacono, J. Lykke-Andersen, M. J. Fritzler, D. Scheuner, R. J. Kaufman, D. E. Golan, and P. Anderson, "Stress granules and processing bodies are dynamically linked sites of mRNP remodeling," *J Cell Biol*, vol. 169, no. 6, pp. 871–884, Jun. 2005.
- [207] D. Durie, S. M. Lewis, U. Liwak, M. Kisilewicz, M. Gorospe, and M. Holcik, "RNA-binding protein HuR mediates cytoprotection through stimulation of XIAP translation," *Oncogene*, vol. 30, no. 12, pp. 1460–1469, Mar. 2011.
- [208] K. Mazan-Mamczarz, S. Galbán, I. L. de Silanes, J. L. Martindale, U. Atasoy, J. D. Keene, and M. Gorospe, "RNA-binding protein HuR enhances p53 translation in response to ultraviolet light irradiation," *Proc Natl Acad Sci U S A*, vol. 100, no. 14, pp. 8354–8359, Jul. 2003.
- [209] S. N. Bhattacharyya, R. Habermacher, U. Martine, E. I. Closs, and W. Filipowicz, "Relief of microRNA-Mediated Translational Repression in Human Cells Subjected to Stress," *Cell*, vol. 125, no. 6, pp. 1111–1124, Jun. 2006.
- [210] T. Kawai, A. Lal, X. Yang, S. Galban, K. Mazan-Mamczarz, and M. Gorospe, "Translational Control of Cytochrome c by RNA-Binding Proteins TIA-1 and HuR," *Mol Cell Biol*, vol. 26, no. 8, pp. 3295–3307, Apr. 2006.
- [211] M. Kullmann, U. Göpfert, B. Siewe, and L. Hengst, "ELAV/Hu proteins inhibit p27 translation via an IRES element in the p27 5'UTR," *Genes Dev*, vol. 16, no. 23, pp. 3087–3099, Dec. 2002.
- [212] Z. Meng, N. L. Jackson, H. Choi, P. H. King, P. D. Emanuel, and S. W. Blume, "Alterations in RNA-binding activities of IRES-regulatory proteins as a mechanism for physiological variability and pathological dysregulation of IGF-IR translational control in human breast tumor cells," *Journal of Cellular Physiology*, vol. 217, no. 1, pp. 172–183, 2008.
- [213] H. H. Kim, Y. Kuwano, S. Srikantan, E. K. Lee, J. L. Martindale, and M. Gorospe, "HuR recruits let-7/RISC to repress c-Myc expression," *Genes Dev*, vol. 23, no. 15, pp. 1743–1748, Aug. 2009.
- [214] M.-J. Kang, B.-K. Ryu, M.-G. Lee, J. Han, J.-H. Lee, T.-K. Ha, D.-S. Byun, K.-S. Chae, B.-H. Lee, H. S. Chun, K. Y. Lee, H.-J. Kim, and S.-G. Chi, "NF-kappaB activates transcription of the RNA-binding factor HuR, via PI3K-AKT signaling, to promote gastric tumorigenesis," *Gastroenterology*, vol. 135, no. 6, pp. 2030–2042, 2042.e1–3, Dec. 2008.
- [215] R. Pullmann, H. H. Kim, K. Abdelmohsen, A. Lal, J. L. Martindale, X. Yang, and M. Gorospe, "Analysis of Turnover and Translation Regulatory RNA-Binding Protein Expression through Binding to Cognate mRNAs," *Mol Cell Biol*, vol. 27, no. 18, pp. 6265–6278, Sep. 2007.
- [216] W. Al-Ahmadi, M. Al-Ghamdi, L. Al-Haj, M. Al-Saif, and K. S. A. Khabar, "Alternative polyadenylation variants of the RNA binding protein, HuR: abundance, role of AU-rich elements and auto-Regulation," *Nucleic Acids Res*, vol. 37, no. 11, pp. 3612–3624, Jun. 2009.
- [217] J. Yi, N. Chang, X. Liu, G. Guo, L. Xue, T. Tong, M. Gorospe, and W. Wang, "Reduced nuclear export of HuR mRNA by HuR is linked to the loss of HuR in replicative senescence," *Nucl. Acids Res.*, vol. 38, no. 5, pp. 1547–1558, Mar. 2010.
- [218] K. Abdelmohsen, M. M. Kim, S. Srikantan, E. M. Mercken, S. E. Brennan, G. M. Wilson, R. de Cabo, and M. Gorospe, "miR-519 suppresses tumor growth by reducing HuR levels," *Cell Cycle*, vol. 9, no. 7, pp. 1354–1359, Apr. 2010.
- [219] K. Abdelmohsen, S. Srikantan, Y. Kuwano, and M. Gorospe, "miR-519 reduces cell proliferation by lowering RNA-binding protein HuR levels," *Proc Natl Acad Sci U S A*, vol. 105, no. 51, pp. 20297–20302, Dec. 2008.
- [220] B. S. Marasa, S. Srikantan, J. L. Martindale, M. M. Kim, E. K. Lee, M. Gorospe, and K. Abdelmohsen, "MicroRNA profiling in human diploid fibroblasts uncovers miR-519 role in replicative senescence," *Aging (Albany NY)*, vol. 2, no. 6, pp. 333–343, Jun. 2010.
- [221] X. Guo, Y. Wu, and R. Hartley, "MicroRNA-125a represses cell growth by targeting HuR in breast cancer," *RNA Biology*, vol. 6, no. 5, pp. 575–583, Nov. 2009.

- [222] K. Abdelmohsen, S. Srikantan, X. Yang, A. Lal, H. H. Kim, Y. Kuwano, S. Galban, K. G. Becker, D. Kamara, R. de Cabo, and M. Gorospe, "Ubiquitin-mediated proteolysis of HuR by heat shock," *The EMBO Journal*, vol. 28, no. 9, pp. 1271–1282, Mar. 2009.
- [223] R. Mazroui, S. Di Marco, E. Clair, C. von Roretz, S. A. Tenenbaum, J. D. Keene, M. Saleh, and I.-E. Gallouzi, "Caspase-mediated cleavage of HuR in the cytoplasm contributes to pp32/PHAP-I regulation of apoptosis," *J Cell Biol*, vol. 180, no. 1, pp. 113–127, Jan. 2008.
- [224] C. von Roretz and I.-E. Gallouzi, "Protein Kinase RNA/FADD/Caspase-8 Pathway Mediates the Proapoptotic Activity of the RNA-binding Protein Human Antigen R (HuR)," *J Biol Chem*, vol. 285, no. 22, pp. 16806–16813, May 2010.
- [225] P. Beauchamp, C. Nassif, S. Hillock, K. van der Giessen, C. von Roretz, B. J. Jasmin, and I.-E. Gallouzi, "The cleavage of HuR interferes with its transportin-2-mediated nuclear import and promotes muscle fiber formation," *Cell Death Differ.*, vol. 17, no. 10, pp. 1588–1599, Oct. 2010.
- [226] S. Güttinger, P. Mühlhäuser, R. Koller-Eichhorn, J. Brennecke, and U. Kutay, "Transportin2 functions as importin and mediates nuclear import of HuR," *Proc Natl Acad Sci U S A*, vol. 101, no. 9, pp. 2918–2923, Mar. 2004.
- [227] A. REBANE, A. AAB, and J. A. STEITZ, "Transportins 1 and 2 are redundant nuclear import factors for hnRNP A1 and HuR," *RNA*, vol. 10, no. 4, pp. 590–599, Apr. 2004.
- [228] C. M. Brennan, I.-E. Gallouzi, and J. A. Steitz, "Protein Ligands to HuR Modulate Its Interaction with Target Mrnas in Vivo," *J Cell Biol*, vol. 151, no. 1, pp. 1–14, Oct. 2000.
- [229] K. Abdelmohsen, R. Pullmann, A. Lal, H. H. Kim, S. Galban, X. Yang, J. Blethrow, M. Walker, J. Shubert, D. A. Gillespie, H. Furneaux, and M. Gorospe, "Phosphorylation of HuR by Chk2 regulates SIRT1 expression," *Mol Cell*, vol. 25, no. 4, pp. 543–557, Feb. 2007.
- [230] H. H. Kim, K. Abdelmohsen, A. Lal, R. Pullmann, X. Yang, S. Galban, S. Srikantan, J. L. Martindale, J. Blethrow, K. M. Shokat, and M. Gorospe, "Nuclear HuR accumulation through phosphorylation by Cdk1," *Genes Dev*, vol. 22, no. 13, pp. 1804–1815, Jul. 2008.
- [231] A. Doller, A. Huwiler, R. Müller, H. H. Radeke, J. Pfeilschifter, and W. Eberhardt, "Protein Kinase C δ -dependent Phosphorylation of the mRNA-stabilizing Factor HuR: Implications for Posttranscriptional Regulation of Cyclooxygenase-2," *Mol Biol Cell*, vol. 18, no. 6, pp. 2137–2148, Jun. 2007.
- [232] A. Doller, E.-S. Akool, A. Huwiler, R. Müller, H. H. Radeke, J. Pfeilschifter, and W. Eberhardt, "Posttranslational Modification of the AU-Rich Element Binding Protein HuR by Protein Kinase C δ Elicits Angiotensin II-Induced Stabilization and Nuclear Export of Cyclooxygenase 2 mRNA," *Mol Cell Biol*, vol. 28, no. 8, pp. 2608–2625, Apr. 2008.
- [233] A. Doller, K. Schlepckow, H. Schwalbe, J. Pfeilschifter, and W. Eberhardt, "Tandem Phosphorylation of Serines 221 and 318 by Protein Kinase C δ Coordinates mRNA Binding and Nucleocytoplasmic Shutting of HuR," *Mol Cell Biol*, vol. 30, no. 6, pp. 1397–1410, Mar. 2010.
- [234] V. Lafarga, A. Cuadrado, I. Lopez de Silanes, R. Bengoechea, O. Fernandez-Capetillo, and A. R. Nebreda, "p38 Mitogen-Activated Protein Kinase- and HuR-Dependent Stabilization of p21Cip1 mRNA Mediates the G1/S Checkpoint," *Mol Cell Biol*, vol. 29, no. 16, pp. 4341–4351, Aug. 2009.
- [235] H. Li, S. Park, B. Kilburn, M. A. Jelinek, A. Henschen-Edman, D. W. Aswad, M. R. Stallcup, and I. A. Laird-Offringa, "Lipopolysaccharide-induced Methylation of HuR, an mRNA-stabilizing Protein, by CARM1," *J. Biol. Chem.*, vol. 277, no. 47, pp. 44623–44630, Nov. 2002.
- [236] I. L. de Silanes, J. Fan, X. Yang, A. B. Zonderman, O. Potapova, E. S. Pizer, and M. Gorospe, "Role of the RNA-binding protein HuR in colon carcinogenesis," *Oncogene*, vol. 22, no. 46, pp. 7146–7154, 2003.
- [237] A. Woodhoo, M. Iruarrizaga-Lejarreta, N. Beraza, J. L. García-Rodríguez, N. Embade, D. Fernández-Ramos, N. Matinez-Lopez, V. Gutiérrez, B. Arteta, J. Caballeria, S. C. Lu, J. M. Mato, M. Varela-Rey, and M. L. Martinez-Chantar, "HuR contributes to Hepatic Stellate Cell activation and liver fibrosis," *Hepatology (Baltimore, Md.)*, May 2012.
- [238] G. Brewer, "An A + U-rich element RNA-binding factor regulates c-myc mRNA stability in vitro.," *Mol Cell Biol*, vol. 11, no. 5, pp. 2460–2466, May 1991.

- [239] B. J. Wagner, C. T. DeMaria, Y. Sun, G. M. Wilson, and G. Brewer, "Structure and genomic organization of the human AUF1 gene: alternative pre-mRNA splicing generates four protein isoforms," *Genomics*, vol. 48, no. 2, pp. 195–202, Mar. 1998.
- [240] B. Trojanowicz, H. Dralle, and C. Hoang-Vu, "AUF1 and HuR: possible implications of mRNA stability in thyroid function and disorders," *Thyroid Res*, vol. 4, no. Suppl 1, p. S5, Aug. 2011.
- [241] M. Suzuki, M. Iijima, A. Nishimura, Y. Tomozoe, D. Kamei, and M. Yamada, "Two separate regions essential for nuclear import of the hnRNP D nucleocytoplasmic shuttling sequence," *FEBS Journal*, vol. 272, no. 15, pp. 3975–3987, 2005.
- [242] L. A. Dempsey, M. J. Li, A. DePace, P. Bray-Ward, and N. Maizels, "The human HNRPD locus maps to 4q21 and encodes a highly conserved protein," *Genomics*, vol. 49, no. 3, pp. 378–384, May 1998.
- [243] K. Mazan-Mamczarz, Y. Kuwano, M. Zhan, E. J. White, J. L. Martindale, A. Lal, and M. Gorospe, "Identification of a signature motif in target mRNAs of RNA-binding protein AUF1," *Nucleic Acids Res*, vol. 37, no. 1, pp. 204–214, Jan. 2009.
- [244] C.-Y. A. CHEN, N. XU, W. ZHU, and A.-B. SHYU, "Functional dissection of hnRNP D suggests that nuclear import is required before hnRNP D can modulate mRNA turnover in the cytoplasm," *RNA*, vol. 10, no. 4, pp. 669–680, Apr. 2004.
- [245] A. Lapucci, M. Donnini, L. Papucci, E. Witort, A. Tempestini, A. Bevilacqua, A. Nicolin, G. Brewer, N. Schiavone, and S. Capaccioli, "AUF1 Is a bcl-2 A + U-rich Element-binding Protein Involved in bcl-2 mRNA Destabilization during Apoptosis," *J. Biol. Chem.*, vol. 277, no. 18, pp. 16139–16146, May 2002.
- [246] C. T. DeMaria and G. Brewer, "AUF1 Binding Affinity to A+U-rich Elements Correlates with Rapid mRNA Degradation," *J. Biol. Chem.*, vol. 271, no. 21, pp. 12179–12184, May 1996.
- [247] G. Brewer, S. Saccani, S. Sarkar, A. Lewis, and S. Pestka, "Increased interleukin-10 mRNA stability in melanoma cells is associated with decreased levels of A + U-rich element binding factor AUF1," *J. Interferon Cytokine Res.*, vol. 23, no. 10, pp. 553–564, Oct. 2003.
- [248] X. Y. Wang, P. E. Hoyle, and J. A. McCubrey, "Characterization of proteins binding the 3' regulatory region of the IL-3 gene in IL-3-dependent and autocrine-transformed hematopoietic cells," *Leukemia*, vol. 12, no. 4, pp. 520–531, Apr. 1998.
- [249] K. Masuda, B. Marasa, J. L. Martindale, M. K. Halushka, and M. Gorospe, "Tissue- and age-dependent expression of RNA-binding proteins that influence mRNA turnover and translation," *Aging (Albany NY)*, vol. 1, no. 8, pp. 681–698, Jul. 2009.
- [250] F. M. Gratacós and G. Brewer, "The role of AUF1 in regulated mRNA decay," *Wiley Interdiscip Rev RNA*, vol. 1, no. 3, pp. 457–473, Dec. 2010.
- [251] K. C. M. Moraes, A. J. C. Quaresma, K. Maehnss, and J. Kobarg, "Identification and characterization of proteins that selectively interact with isoforms of the mRNA binding protein AUF1 (hnRNP D)," *Biol. Chem.*, vol. 384, no. 1, pp. 25–37, Jan. 2003.
- [252] A. Sela-Brown, J. Silver, G. Brewer, and T. Naveh-Many, "Identification of AUF1 as a Parathyroid Hormone mRNA 3'-Untranslated Region-binding Protein That Determines Parathyroid Hormone mRNA Stability," *J. Biol. Chem.*, vol. 275, no. 10, pp. 7424–7429, Mar. 2000.
- [253] M. Kiledjian, C. T. DeMaria, G. Brewer, and K. Novick, "Identification of AUF1 (heterogeneous nuclear ribonucleoprotein D) as a component of the alpha-globin mRNA stability complex," *Mol Cell Biol*, vol. 17, no. 8, pp. 4870–4876, Aug. 1997.
- [254] B. Liao, Y. Hu, and G. Brewer, "Competitive binding of AUF1 and TIAR to MYC mRNA controls its translation," *Nat. Struct. Mol. Biol.*, vol. 14, no. 6, pp. 511–518, Jun. 2007.
- [255] P. Loflin, C.-Y. A. Chen, and A.-B. Shyu, "Unraveling a cytoplasmic role for hnRNP D in the in vivo mRNA destabilization directed by the AU-rich element," *Genes Dev*, vol. 13, no. 14, pp. 1884–1897, Jul. 1999.
- [256] N. Xu, C.-Y. A. Chen, and A.-B. Shyu, "Versatile Role for hnRNP D Isoforms in the Differential Regulation of Cytoplasmic mRNA Turnover," *Mol Cell Biol*, vol. 21, no. 20, pp. 6960–6971, Oct. 2001.

- [257] I. Raineri, D. Wegmueller, B. Gross, U. Certa, and C. Moroni, "Roles of AUF1 isoforms, HuR and BRF1 in ARE-dependent mRNA turnover studied by RNA interference," *Nucleic Acids Res.*, vol. 32, no. 4, pp. 1279–1288, 2004.
- [258] G. M. Wilson, Y. Sun, J. Sellers, H. Lu, N. Penkar, G. Dillard, and G. Brewer, "Regulation of AUF1 Expression via Conserved Alternatively Spliced Elements in the 3' Untranslated Region," *Mol Cell Biol.*, vol. 19, no. 6, pp. 4056–4064, Jun. 1999.
- [259] L. Banihashemi, G. M. Wilson, N. Das, and G. Brewer, "Upf1/Upf2 Regulation of 3' Untranslated Region Splice Variants of AUF1 Links Nonsense-Mediated and A+U-Rich Element-Mediated mRNA Decay," *Mol Cell Biol.*, vol. 26, no. 23, pp. 8743–8754, Dec. 2006.
- [260] B. Sarkar, J.-Y. Lu, and R. J. Schneider, "Nuclear Import and Export Functions in the Different Isoforms of the AUF1/Heterogeneous Nuclear Ribonucleoprotein Protein Family," *J. Biol. Chem.*, vol. 278, no. 23, pp. 20700–20707, Jun. 2003.
- [261] G. M. Wilson, J. Lu, K. Sutphen, Y. Sun, Y. Huynh, and G. Brewer, "Regulation of A + U-rich Element-directed mRNA Turnover Involving Reversible Phosphorylation of AUF1," *J. Biol. Chem.*, vol. 278, no. 35, pp. 33029–33038, Aug. 2003.
- [262] G. M. Wilson, J. Lu, K. Sutphen, Y. Suarez, S. Sinha, B. Brewer, E. C. Villanueva-Feliciano, R. M. Ysla, S. Charles, and G. Brewer, "Phosphorylation of p40AUF1 Regulates Binding to A + U-rich mRNA-destabilizing Elements and Protein-induced Changes in Ribonucleoprotein Structure," *J. Biol. Chem.*, vol. 278, no. 35, pp. 33039–33048, Aug. 2003.
- [263] G. Laroia and R. J. Schneider, "Alternate exon insertion controls selective ubiquitination and degradation of different AUF1 protein isoforms," *Nucleic Acids Res.*, vol. 30, no. 14, pp. 3052–3058, Jul. 2002.
- [264] B. E. Zucconi and G. M. Wilson, "Modulation of neoplastic gene regulatory pathways by the RNA-binding factor AUF1," *Front. Biosci.*, vol. 17, pp. 2307–2325, 2012.
- [265] B. Trojanowicz, L. Brodauf, C. Sekulla, K. Lorenz, R. Finke, H. Dralle, and C. Hoang-Vu, "The role of AUF1 in thyroid carcinoma progression," *Endocr Relat Cancer*, vol. 16, no. 3, pp. 857–871, Sep. 2009.
- [266] S. Kumar, Y. Tomooka, and M. Noda, "Identification of a set of genes with developmentally down-regulated expression in the mouse brain," *Biochem. Biophys. Res. Commun.*, vol. 185, no. 3, pp. 1155–1161, Jun. 1992.
- [267] T. Kamitani, K. Kito, H. P. Nguyen, and E. T. H. Yeh, "Characterization of NEDD8, a Developmentally Down-regulated Ubiquitin-like Protein," *J. Biol. Chem.*, vol. 272, no. 45, pp. 28557–28562, Nov. 1997.
- [268] G. Rabut and M. Peter, "Function and regulation of protein neddylation. 'Protein Modifications: Beyond the Usual Suspects' Review Series," *EMBO Rep.*, vol. 9, no. 10, pp. 969–976, Oct. 2008.
- [269] D. P. Xirodimas, A. Sundqvist, A. Nakamura, L. Shen, C. Botting, and R. T. Hay, "Ribosomal proteins are targets for the NEDD8 pathway," *EMBO reports*, vol. 9, no. 3, pp. 280–286, Mar. 2008.
- [270] I. R. Watson, M. S. Irwin, and M. Ohh, "NEDD8 Pathways in Cancer, Sine Quibus Non," *Cancer Cell*, vol. 19, no. 2, pp. 168–176, Feb. 2011.
- [271] W. M. Abida, A. Nikolaev, W. Zhao, W. Zhang, and W. Gu, "FBXO11 Promotes the Neddylation of p53 and Inhibits Its Transcriptional Activity," *J. Biol. Chem.*, vol. 282, no. 3, pp. 1797–1804, Jan. 2007.
- [272] T. Kamura, M. N. Conrad, Q. Yan, R. C. Conaway, and J. W. Conaway, "The Rbx1 subunit of SCF and VHL E3 ubiquitin ligase activates Rub1 modification of cullins Cdc53 and Cul2," *Genes Dev.*, vol. 13, no. 22, pp. 2928–2933, Nov. 1999.
- [273] S. Oved, Y. Mosesson, Y. Zwang, E. Santonicò, K. Shtiegman, M. D. Marmor, B. S. Kochupurakkal, M. Katz, S. Lavi, G. Cesareni, and Y. Yarden, "Conjugation to Nedd8 Instigates Ubiquitylation and Down-regulation of Activated Receptor Tyrosine Kinases," *J. Biol. Chem.*, vol. 281, no. 31, pp. 21640–21651, Aug. 2006.
- [274] D. P. Xirodimas, M. K. Saville, J.-C. Bourdon, R. T. Hay, and D. P. Lane, "Mdm2-Mediated NEDD8 Conjugation of p53 Inhibits Its Transcriptional Activity," *Cell*, vol. 118, no. 1, pp. 83–97, Jul. 2004.

- [275] T. Kurz, N. Ozlü, F. Rudolf, S. M. O'Rourke, B. Luke, K. Hofmann, A. A. Hyman, B. Bowerman, and M. Peter, "The conserved protein DCN-1/Dcn1p is required for cullin neddylation in *C. elegans* and *S. cerevisiae*," *Nature*, vol. 435, no. 7046, pp. 1257–1261, Jun. 2005.
- [276] H. M. Mendoza, L. Shen, C. Botting, A. Lewis, J. Chen, B. Ink, and R. T. Hay, "NEDP1, a Highly Conserved Cysteine Protease That deNEDDylates Cullins," *J. Biol. Chem.*, vol. 278, no. 28, pp. 25637–25643, Jul. 2003.
- [277] Y. Chan, J. Yoon, J.-T. Wu, H.-J. Kim, K.-T. Pan, J. Yim, and C.-T. Chien, "DEN1 deneddylates non-cullin proteins in vivo," *J Cell Sci*, vol. 121, no. 19, pp. 3218–3223, Oct. 2008.
- [278] N. H. Stickle, J. Chung, J. M. Klco, R. P. Hill, W. G. Kaelin, and M. Ohh, "pVHL Modification by NEDD8 Is Required for Fibronectin Matrix Assembly and Suppression of Tumor Development," *Mol Cell Biol*, vol. 24, no. 8, pp. 3251–3261, Apr. 2004.
- [279] F. Gao, J. Cheng, T. Shi, and E. T. H. Yeh, "Neddylation of a breast cancer-associated protein recruits a class III histone deacetylase that represses NFκB-dependent transcription," *Nat. Cell Biol.*, vol. 8, no. 10, pp. 1171–1177, Oct. 2006.
- [280] T. Li, R. Santocky, R.-F. Shen, E. Tekle, G. Wang, D. C. H. Yang, and P. B. Chock, "A general approach for investigating enzymatic pathways and substrates for ubiquitin-like modifiers," *Arch. Biochem. Biophys.*, vol. 453, no. 1, pp. 70–74, Sep. 2006.
- [281] I. R. Watson, A. Blanch, D. C. C. Lin, M. Ohh, and M. S. Irwin, "Mdm2-mediated NEDD8 Modification of TAp73 Regulates Its Transactivation Function," *J. Biol. Chem.*, vol. 281, no. 45, pp. 34096–34103, Nov. 2006.
- [282] J. Herrmann, L. O. Lerman, and A. Lerman, "Ubiquitin and Ubiquitin-Like Proteins in Protein Regulation," *Circulation Research*, vol. 100, no. 9, pp. 1276–1291, May 2007.
- [283] A. Sarikas, T. Hartmann, and Z.-Q. Pan, "The cullin protein family," *Genome Biol*, vol. 12, no. 4, p. 220, 2011.
- [284] J. D. Oliner, K. W. Kinzler, P. S. Meltzer, D. L. George, and B. Vogelstein, "Amplification of a gene encoding a p53-associated protein in human sarcomas," *Nature*, vol. 358, no. 6381, pp. 80–83, Jul. 1992.
- [285] J. Momand, D. Jung, S. Wilczynski, and J. Niland, "The MDM2 gene amplification database.," *Nucleic Acids Res*, vol. 26, no. 15, pp. 3453–3459, Aug. 1998.
- [286] Y. Haupt, R. Maya, A. Kazaz, and M. Oren, "Mdm2 promotes the rapid degradation of p53," *Nature*, vol. 387, no. 6630, pp. 296–299, May 1997.
- [287] J. Chen, V. Marechal, and A. J. Levine, "Mapping of the p53 and mdm-2 interaction domains.," *Mol Cell Biol*, vol. 13, no. 7, pp. 4107–4114, Jul. 1993.
- [288] A. M. Bode and Z. Dong, "Post-translational modification of p53 in tumorigenesis," *Nat. Rev. Cancer*, vol. 4, no. 10, pp. 793–805, Oct. 2004.
- [289] J. M. Stommel and G. M. Wahl, "Accelerated MDM2 auto-degradation induced by DNA-damage kinases is required for p53 activation," *EMBO J*, vol. 23, no. 7, pp. 1547–1556, Apr. 2004.
- [290] C. Dohmesen, M. Koeppel, and M. Dobbelstein, "Specific inhibition of Mdm2-mediated neddylation by Tip60," *Cell Cycle*, vol. 7, no. 2, pp. 222–231, Jan. 2008.
- [291] G. Liu and D. P. Xirodimas, "NUB1 promotes cytoplasmic localization of p53 through cooperation of the NEDD8 and ubiquitin pathways," *Oncogene*, vol. 29, no. 15, pp. 2252–2261, Apr. 2010.
- [292] I. R. Watson, B. K. Li, O. Roche, A. Blanch, M. Ohh, and M. S. Irwin, "Chemotherapy induces NEDP1-mediated destabilization of MDM2," *Oncogene*, vol. 29, no. 2, pp. 297–304, Jan. 2010.
- [293] A. Sundqvist, G. Liu, A. Mirsaliotis, and D. P. Xirodimas, "Regulation of nucleolar signalling to p53 through NEDDylation of L11," *EMBO Rep*, vol. 10, no. 10, pp. 1132–1139, Oct. 2009.
- [294] X.-X. Sun, Y.-G. Wang, D. P. Xirodimas, and M.-S. Dai, "Perturbation of 60 S Ribosomal Biogenesis Results in Ribosomal Protein L5- and L11-dependent p53 Activation," *J Biol Chem*, vol. 285, no. 33, pp. 25812–25821, Aug. 2010.
- [295] T. A. Soucy, L. R. Dick, P. G. Smith, M. A. Milhollen, and J. E. Brownell, "The NEDD8 Conjugation Pathway and Its Relevance in Cancer Biology and Therapy," *Genes Cancer*, vol. 1, no. 7, pp. 708–716, Jul. 2010.

- [296] B. Higgins and R. Andersen, "Experimental pathology of liver: restoration of liver of the white rat following partial surgical removal," *Arch Pathol.*, vol. 12, pp. 186–202, 1931.
- [297] H. L. Leffert, K. S. Koch, T. Moran, and M. Williams, "Liver cells," *Meth. Enzymol.*, vol. 58, pp. 536–544, 1979.
- [298] E. Medico, A. M. Mongiovi, J. Huff, M. A. Jelinek, A. Follenzi, G. Gaudino, J. T. Parsons, and P. M. Comoglio, "The tyrosine kinase receptors Ron and Sea control 'scattering' and morphogenesis of liver progenitor cells in vitro," *Mol. Biol. Cell*, vol. 7, no. 4, pp. 495–504, Apr. 1996.
- [299] S. Rozen and H. Skaletsky, "Primer3 on the WWW for general users and for biologist programmers," *Methods Mol. Biol.*, vol. 132, pp. 365–386, 2000.
- [300] J. Fan, F. T. Ishmael, X. Fang, A. Myers, C. Cheadle, S.-K. Huang, U. Atasoy, M. Gorospe, and C. Stellato, "Chemokine Transcripts as Targets of the RNA-Binding Protein HuR in Human Airway Epithelium," *J Immunol*, vol. 186, no. 4, pp. 2482–2494, Feb. 2011.
- [301] I. L. de Silanes, M. Zhan, A. Lal, X. Yang, and M. Gorospe, "Identification of a target RNA motif for RNA-binding protein HuR," *PNAS*, vol. 101, no. 9, pp. 2987–2992, Mar. 2004.
- [302] M. S. Rodriguez, J. M. Desterro, S. Lain, C. A. Midgley, D. P. Lane, and R. T. Hay, "SUMO-1 modification activates the transcriptional response of p53..," *EMBO J*, vol. 18, no. 22, pp. 6455–6461, Nov. 1999.
- [303] N. Beraza, T. Lüdde, U. Assmus, T. Roskams, S. Vander Borght, and C. Trautwein, "Hepatocyte-specific IKK gamma/NEMO expression determines the degree of liver injury," *Gastroenterology*, vol. 132, no. 7, pp. 2504–2517, Jun. 2007.
- [304] C. Pañeda, I. Gorospe, B. Herrera, T. Nakamura, I. Fabregat, and I. Varela-Nieto, "Liver cell proliferation requires methionine adenosyltransferase 2A mRNA up-regulation," *Hepatology*, vol. 35, no. 6, pp. 1381–1391, 2002.
- [305] J. L. Rodríguez, A. Boukaba, J. Sandoval, E. I. Georgieva, M. U. Latasa, E. R. García-Trevijano, G. Serviddio, T. Nakamura, M. A. Ávila, J. Sastre, L. Torres, J. M. Mato, and G. López-Rodas, "Transcription of the MAT2A gene, coding for methionine adenosyltransferase, is up-regulated by E2F and Sp1 at a chromatin level during proliferation of liver cells," *The International Journal of Biochemistry & Cell Biology*, vol. 39, no. 4, pp. 842–850, 2007.
- [306] M. L. Martínez-Chantar, M. U. Latasa, M. Varela-Rey, S. C. Lu, E. R. García-Trevijano, J. M. Mato, and M. A. Avila, "L-Methionine Availability Regulates Expression of the Methionine Adenosyltransferase 2A Gene in Human Hepatocarcinoma Cells ROLE OF S-ADENOSYL METHIONINE," *J. Biol. Chem.*, vol. 278, no. 22, pp. 19885–19890, May 2003.
- [307] N. Assy and G. Y. Minuk, "Liver regeneration: methods for monitoring and their applications," *J. Hepatol.*, vol. 26, no. 4, pp. 945–952, Apr. 1997.
- [308] S. P. Deb, "Function and dysfunction of the human oncoprotein MDM2," *Front. Biosci.*, vol. 7, pp. d235–243, Jan. 2002.
- [309] D. P. Xirodimas, C. W. Stephen, and D. P. Lane, "Cocompartmentalization of p53 and Mdm2 is a major determinant for Mdm2-mediated degradation of p53," *Exp. Cell Res.*, vol. 270, no. 1, pp. 66–77, Oct. 2001.
- [310] S. Fang, J. P. Jensen, R. L. Ludwig, K. H. Vousden, and A. M. Weissman, "Mdm2 Is a RING Finger-dependent Ubiquitin Protein Ligase for Itself and p53," *J. Biol. Chem.*, vol. 275, no. 12, pp. 8945–8951, Mar. 2000.
- [311] V. Katsanou, O. Papadaki, S. Milatos, P. J. Blackshear, P. Anderson, G. Kollias, and D. L. Kontoyiannis, "HuR as a Negative Posttranscriptional Modulator in Inflammation," *Molecular Cell*, vol. 19, no. 6, pp. 777–789, Sep. 2005.
- [312] E. A. Suswam, L. B. Nabors, Y. Huang, X. Yang, and P. H. King, "IL-1beta induces stabilization of IL-8 mRNA in malignant breast cancer cells via the 3' untranslated region: Involvement of divergent RNA-binding factors HuR, KSRP and TIAR," *Int. J. Cancer*, vol. 113, no. 6, pp. 911–919, Mar. 2005.
- [313] G. He and M. Karin, "NF-κB and STAT3 – key players in liver inflammation and cancer," *Cell Res.*, vol. 21, no. 1, pp. 159–168, Jan. 2011.
- [314] W. Wu, D.-F. Yao, L.-W. Qiu, W.-L. Sai, J.-J. Shen, H.-B. Yu, X.-H. Wu, Y.-M. Li, Y.-L. Wang, and W.-J. Gu, "Characteristics of hepatic nuclear-transcription factor-kappa B expression

- and quantitative analysis in rat hepatocarcinogenesis," *HBPD INT*, vol. 8, no. 5, pp. 504–509, Oct. 2009.
- [315] H. Yang, Z.-Z. Huang, J. Wang, and S. C. Lu, "The role of c-Myb and Sp1 in the up-regulation of methionine adenosyltransferase 2A gene expression in human hepatocellular carcinoma," *FASEB J*, vol. 15, no. 9, pp. 1507–1516, Jul. 2001.
- [316] W. Wang, M. C. Caldwell, S. Lin, H. Furneaux, and M. Gorospe, "HuR regulates cyclin A and cyclin B1 mRNA stability during cell proliferation," *EMBO J*, vol. 19, no. 10, pp. 2340–2350, May 2000.
- [317] R. M. Rai, F. Y. J. Lee, A. Rosen, S. Q. Yang, H. Z. Lin, A. Koteish, F. Y. Liew, C. Zaragoza, C. Lowenstein, and A. M. Diehl, "Impaired liver regeneration in inducible nitric oxide synthasedeficient mice," *Proc Natl Acad Sci U S A*, vol. 95, no. 23, pp. 13829–13834, Nov. 1998.
- [318] K. Jürchott, S. Bergmann, U. Stein, W. Walther, M. Janz, I. Manni, G. Piaggio, E. Fietze, M. Dietel, and H.-D. Royer, "YB-1 as a Cell Cycle-regulated Transcription Factor Facilitating Cyclin A and Cyclin B1 Gene Expression," *J. Biol. Chem.*, vol. 278, no. 30, pp. 27988–27996, Jul. 2003.
- [319] D. M. Bortner and M. P. Rosenberg, "Overexpression of cyclin A in the mammary glands of transgenic mice results in the induction of nuclear abnormalities and increased apoptosis," *Cell Growth Differ.*, vol. 6, no. 12, pp. 1579–1589, Dec. 1995.
- [320] T. A. Soucy, P. G. Smith, M. A. Milholen, A. J. Berger, J. M. Gavin, S. Adhikari, J. E. Brownell, K. E. Burke, D. P. Cardin, S. Critchley, C. A. Cullis, A. Doucette, J. J. Garnsey, J. L. Gaulin, R. E. Gershman, A. R. Lublinsky, A. McDonald, H. Mizutani, U. Narayanan, E. J. Ohava, S. Peluso, M. Rezaei, M. D. Sintchak, T. Talreja, M. P. Thomas, T. Traore, S. Vyskocil, G. S. Weatherhead, J. Yu, J. Zhang, L. R. Dick, C. F. Claiborne, M. Rolfe, J. B. Bolen, and S. P. Langston, "An inhibitor of NEDD8-activating enzyme as a new approach to treat cancer," *Nature*, vol. 458, no. 7239, pp. 732–736, Apr. 2009.

9. SUPPORT

9. SUPPORT

This work was supported by:

- NIH grants: AT-1576 (to Shelly C. Lu, M. Luz Martínez Chantar and José M. Mato) and AT004896 (to Shelly C. Lu and José M. Mato)
- Plan Nacional de I+D: SAF 2005-00855 and SAF 2008-04800 (to M. Luz Martínez Chantar and José M. Mato)
- HEPADIP-EULSHM-CT-205 (to M. Luz Martínez Chantar and José M. Mato)
- ETORTEK 2008, 2009 and 2011 (to M. Luz Martínez Chantar and José M. Mato)
- Fundación “La Caixa” (to M. Luz Martínez Chantar)
- CIBERehd, funded by the Instituto de Salud Carlos III
- Sanidad del Gobierno Vasco 2009 (to M. Luz Martínez Chantar)
- Educación Gobierno Vasco 2011 (to M. Luz Martínez Chantar)
- FIS PI11/01588 (to M. Luz Martínez Chantar)

